DESIGN AND CHARACTERISATION OF NOVEL BLENDS OF POLY(LACTIC ACID)

By

SUKUNYA JUIKHAM

Doctor of Philosophy

ASTON UNIVERSITY

Department of Chemical Engineering and Applied Chemistry

September 2011

THESIS SUMMARY

ASTON UNIVERSITY

DESIGN AND CHARACTERISATION OF NOVEL BLENDS OF POLY(LACTIC ACID)

SUKUNYA JUIKHAM

Submitted for the Degree of Doctor of Philosophy September 2011

This thesis is concerned with the effect of polymer structure on miscibility of the three component blends based on poly(lactic acid) (PLA) with using blending techniques. The examination of novel PLA homologues (pre-synthesised poly(α-esters)), including a range of aliphatic and aromatic poly(α-esters) is an important aspect of the work. Because of their structural simplicity and similarity to PLA, they provide an ideal system to study the effect of polyester structures on the miscibility of PLA polymer blends. The miscibility behaviour of the PLA homologues is compared with other aliphatic polyesters (e.g. poly(ε-caprolactone) (PCL), poly(hydroxybutyrate hydroxyvalerate) (P(HB-HV)), together with a series of cellulose-based polymers (e.g. cellulose acetate butyrate (CAB)).

The work started with the exploration the technique used for preliminary observation of the miscibility of blends referred to as “a rapid screening method” and then the miscibility of binary blends was observed and characterised by percent transmittance together with the Coleman and Painter miscibility approach. However, it was observed that symmetrical structures (e.g. α1(dimethyl), α2(diethyl)) promote the well-packing which restrict their chains from intermingling into poly(L-lactide) (PLLA) chains and leads the blends to be immiscible, whereas, asymmetrical structures (e.g. α4(cyclohexyl)) behave to the contrary. α6(chloromethyl-methyl) should interact well with PLLA because of the polar group of chloride to form interactions, but it does not. It is difficult to disrupt the helical structure of PLLA. PLA were immiscible with PCL, P(HB-HV), or compatibiliser (e.g. G40, LLA-co-PCL), but miscible with CAB which is a hydrogen-bonded polymer. However, these binary blends provided a useful indication for the exploration the novel three component blends.

In summary, the miscibility of the three-component blends are miscible even if only two polymers are miscible. This is the benefit for doing the three components blend in this thesis, which is not an attempt to produce a theoretical explanation for the miscibility of three components blend system.

Keywords: Poly(lactic acid) (PLA); Poly(α-ester) homologues; Characterisation; Blends; Miscibility; Compatibilisers; Degree of crystallinity

FOR

MY FAMILY

Acknowledgements

First of all, I would like to express my sincere thankfulness to my brilliant supervisor Professor Brian Tighe for all his continuous support and encouragement during my pleasurable year here to do Ph.D study since July 2007. It has been a great privilege to work and learn from someone who is so respected and admired in his field. I could not have imagined having a better advisor and mentor for my Ph.D study.

I would like to express my thanks to all the people at the Biomaterials Research Unit who made me being there very enjoyable for all their hospitality extended to me, in particular Dr. Val Franklin, for making the unit run smoothly. Sincere thanks and appreciation are also extended to Dr. Robert Molloy for providing the opportunity to do this Ph.D here with a brilliant supervisor, for his help in the initial stage of my Ph.D study, and his continuous encouragement, to Dr. Paul Topham for his help with an X-ray diffraction analysis and his advice, and to Dr. Mike Perry for his help and assistance with the NMR analysis.

My deep-felt gratitude to the lovely Dr. Gareth Ross for his patience and dedication in the first correcting my thesis grammar, all his support, and being with me to fulfill my life during study. Special thanks are also to my best friends - Sararat Mahasaranon and Surangkanar Rawangyot - for all their supports and encouragements, and to my family for giving me a tremendous amount of support.

A special thanks goes to the Ministry of Science and Technology (Bangkok, Thailand), and Naresuan University (Phitsanulok, Thailand), for their financial support for the duration of my work.

And finally, many thanks go to all people who helped for experimental analysis and my friends to make my Ph.D study so enjoyable.

TABLE OF CONTENTS

Page

TABLE OF CONTENTS (continued)

Page

TABLE OF CONTENTS (continued)

TABLE OF CONTENTS (continued)

Page

CHAPTER 7:

CHAPTER 8:

CHAPTER 9:

LIST OF FIGURES

LIST OF FIGURES (continued)

Page

LIST OF FIGURES (continued)

Page

LIST OF FIGURES (continued)

Page

LIST OF FIGURES (continued)

LIST OF TABLES

Page

LIST OF TABLES (continued)

CHAPTER 1

INTRODUCTION

Chapter 1

Introduction

1.1 Overview

This thesis examines two novel approaches to study the miscibility of polymer blends based on poly(lactic acid) (PLA) in a search for useful materials and also to increase understanding. The first novel approach is the use of three component blends. The second novel approach is to study of the homologues of poly(lactic acid) and their miscibility and their potential as compatibilisers. Because the poly(lactic acid) homologues (pre-synthesised poly(α-ester) homologues) are available only in milligram quantities, the work also required the design of a new method based on solvent blending. This is a "rapid screening method" and requires only very small (mg-range) quantities of polymers. This project is not a theoretical project but involves experiment and theory together, using the interpretive approaches developed by Coleman and Painter [1]. Therefore, the Coleman and Painter principles were compared with experimental observations of blend miscibility to observe if the approach can be used to predict on understand blend miscibility. This introductory chapter deals with published background information on poly(lactic acid) and previous attempts to use blending techniques to produce materials with a wider range of properties than the base polymers.

1.2 Poly(L-lactide) (PLLA) and biodegradable polymers

This section describes the reasons for the choice of PLLA in this study and background information on polyesters. This includes details about biodegradable polymers that are frequently used, such as poly(lactic acid) or polylactide (PLA), poly(glycolic acid) or polyglycolide (PGA), poly(ε-caprolactone) (PCL), poly(3-hydroxybutyrate) (PHB) and other poly(hydroxyalkanoates).

1.2.1 Reasons to use PLLA

Poly(L-lactide) (PLLA) is one of the most widely used materials in the manufacture of disposable and biodegradable plastic products. It is produced from cassava, corn, rice-derived dextrose or from bacterially-fermented starch obtained from food waste, such as potato peelings. PLLA is more expensive than many polymers based on petroleum, however, PLLA using corn has become cheaper as the scale of production increases due to the higher demand [2]. In addition, PLLA would be a new business in an agricultural country like Thailand, which has a potential base to produce biomass plastic materials [3]. PLLA does have limitations, however, which are addressed in this project. It is a semi-crystalline polymer with a high (60-65 ^{o}C) glass transition temperature and limited thermal processing. This means that the polymer tends to be brittle and has a narrow window of melt processing conditions. Therefore, it can be concluded that the major reasons for using PLLA in this work are: PLLA can be produced from inexpensive agricultural plants; PLLA is biodegradable polyester widely used in many applications; PLLA is limited to use by its mechanical properties. These reasons make PLLA to be a good choice of biodegradable polymer to study miscibility by blending with other biodegradable polymers in this study.

1.2.2 Polyesters

In recent years, biodegradable polymer developments have been particularly focused on the environmental and social aspects and a range of biologically-based products, such as sutures, tissue-supporting scaffolds, drug delivery devices, biodegradable plastics and packaging materials that are produced from plants instead of petroleum. It is also of interest in many countries that have an industrial composting infrastructure in place. Polyesters are one of the most important biodegradable plastics being used in industry, due to their potentially hydrolysable ester bonds.

In general, polymers derived from nature are more biodegradable than synthetic polymers; especially those polymers containing ester functionality, which are called polyesters. Aliphatic polyesters have more potential to biodegrade than their aromatic counterparts. They are degraded by both microbial and hydrolytic processes. It is believed that biodegradation of these polymers proceeds by attack on the ester groups by non-specific esterases produced by ground microflora combined with hydrolytic attack. Their degradable products can be quickly metabolised by microorganisms [4]. The presence of ester linkages in the polyester backbones allows gradual hydrolytic degradation of polyesters. The initial degradation products are low-molecular weight polyesters, which are endogenous compounds and as such are non-toxic. When the cleavage of the ester linkages continues by water hydrolysis, the final products are carbon dioxide and water. For example, the hydrolytic degradation of PLLA is shown in Figure 1.1. Intramolecular degradation occurs by base attack on the carbonyl carbon of the ester group, followed by hydrolysis of the ester link, leading to low molecular weight polyester fragments. Finally, PLA is decomposed into carbon dioxide (CO_2) and water (H_2O).

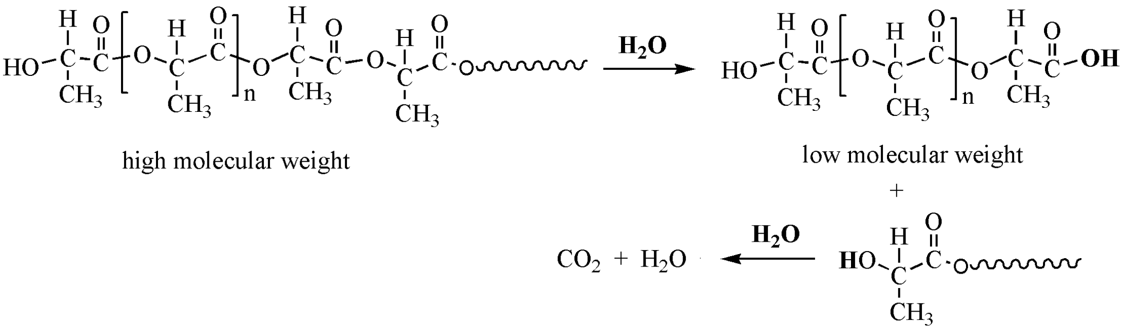

Figure 1.1 Hydolysis of poly(L-lactide).

The polyester family can be divided into two major groups, aliphatic and aromatic polyesters, as classified and shown in Figure 1.2. They are in the market place and are in commercial development. The aliphatic polyesters are: polyhydroxyalkanoates (PHA), which can be divided into polyhydroxybutyrate (PHB), polyhydroxyvalerate (PHV), polyhydroxyhexanoate (PHH), and their copolymers; polylactide (PLA); poly(ε-caprolactone) (PCL); polybutylenesuccinate (PBS) and its derivative poly(butylenesuccinate adipate) (PBSA). The aromatic polyesters are: modified poly(ethylene terephthalate) (PET) such as poly(butylene adipate/terephthalate) (PBAT) and poly(tetramethylene adipate-co-terephthalate) (PTMAT); and aliphatic-aromatic copolyesters (AAC). Aliphatic polyesters are completely biodegradable while aromatic polyesters are almost resistant to microbial attack. However, the mechanical properties of aliphatic polyesters are not very good for commercial applications.

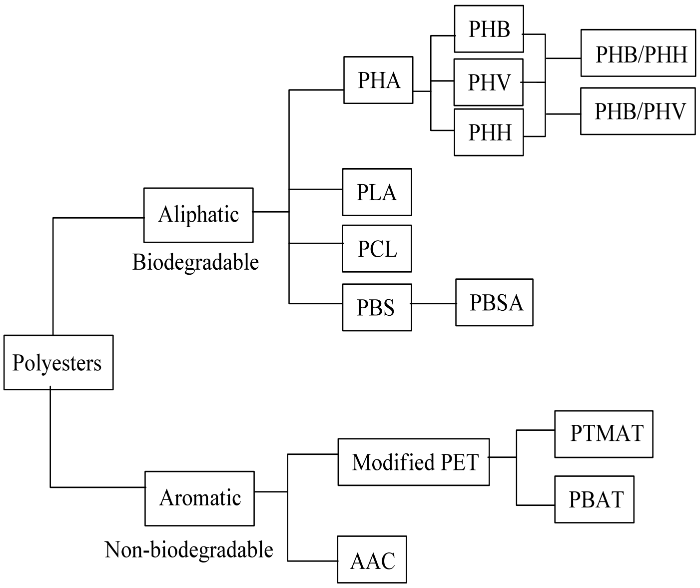

Figure 1.2 The classification of biodegradable polyesters.

Aliphatic polyesters, especially homo- and copolymers derived from glycolic acid, lactic acid, ε-caprolactone, and 3-hydroxybutyrate, have been known for a long time as materials in degradable drug delivery systems. As discussed, aliphatic polyesters degrade chemically by hydrolytic cleavage of the backbone ester bonds, catalysed by either acids or bases, or enzymatically. Carboxylic acid end groups are formed during chain scission, and this may enhance the rate of further hydrolysis. Degradation products are reabsorbed by the body with minimal reaction of the tissues [2].

The other poly(hydroxy acid)s have been synthesised by specialist groups [5, 6]. More details for the route of this synthesis of polymers used in this thesis are given in Chapter 2.

1.2.2.1 Polyglycolide or Poly(glycolic acid), PGA [2]

PGA is the simplest linear aliphatic and hydrolytically instable polyester. It is a hard, tough, crystalline polymer with a glass transition temperature of 35-40 ^{o}C and a melting temperature in the range of 225-230 ^{o}C. Unlike closely related polyesters, such as PLA, PGA is insoluble in almost all common organic solvents due to its high crystallinity and packing. However, it is soluble in highly fluorinated solvents like hexafluoroisopropanol (HFIP) and hexafluoroacetone sesquihydrate. A high molecular weight PGA is commonly obtained by ring-opening polymerisation of the cyclic ester glycolide. Ring-opening polymerisation of glycolide, which is shown in Figure 1.3, can be catalysed using different catalysts, including antimony compounds, such as antimony trioxide or antimony trihalides, zinc compounds (zinc lactate) and tin compounds like stannous octoate (tin(II) 2-ethylhexanoate) or tin alkoxides. Stannous octoate is the most commonly used initiator. The polymerisation is processed under a nitrogen atmosphere at 195 ^{o}C and allowed to proceed for about two hours, then raising the temperature to 230 ^{o}C for about half an hour before isolation of the high molecular weight PGA.

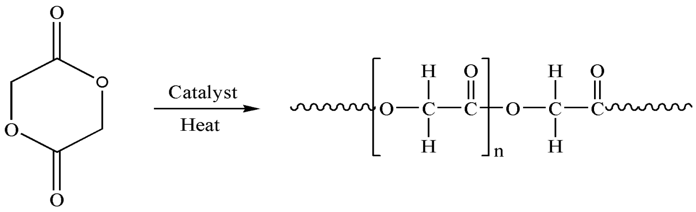

Figure 1.3 Ring-opening polymerisation of glycolide to polyglycolide.

PGA and its copolymers such as poly(lactic-co-glycolic acid) with lactic acid, poly(glycolide-co-caprolactone) with ε–caprolactone, and poly(glycolide-co-trimethylene carbonate) with trimethylene carbonate, are widely used as materials for the synthesis of absorbable sutures and are being evaluated in the biomedical field.

1.2.2.2 Polylactide or Poly(lactic acid), PLA [2, 3]

As discussed, PLA is a thermoplastic aliphatic polyester derived from renewable resources, such as corn starch, tapioca products, sugarcanes. The potential of PLA as a biodegradable polyester and non-toxic material was recognised. PLA has a wide range of applications, such as packaging applications, biomedical applications, and tissue engineering due to its biodegradability and biocompatibility in contact with living tissues. Copolymerisation and blending of PLA has been extensively investigated as a useful route to vary the chemical structure of the copolymer over a wide range to obtain a product with a particular combination of desirable properties. PLA can exist in three stereochemical forms: poly(L-lactide) (PLLA), poly(D-lactide) (PDLA), and poly(D, L-lactide) (PDLLA). The most commonly used isomer is the L-isomer and commercial poly(lactic acid) referred to as PLA is the L-isomer.

The polymerisation of lactic acid or 2-hydroxypropionic acid, a naturally-occuring organic acid, is used as a starting material to form PLA. It exists in two stereo-isomers, L- and D-lactic acid. Figure 1.4 illustrates these two forms. It has potential uses in food, textile, pharmaceutical, leather and chemical industries. It can be produced by chemical synthesis or bacterial fermentation of renewable resources. The petrochemical route produces D, L-lactic acid, while fermentation exists almost exclusively as L-lactic acid. The synthesis of PLA is a multistep process, which starts from the production of lactic acid and ends with its polymerisation.

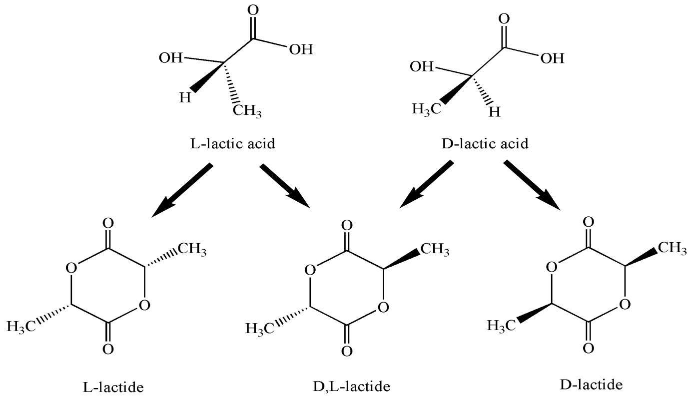

Figure 1.4 Stereochemical forms of lactides.

The existence of both a hydroxyl and a carboxyl group in lactic acid enables it to be converted directly into polyester via a polycondensation reaction. However, it cannot be directly polymerised to high molecular weight PLA because each polymerisation generates one molecule of water. Therefore, lactide (the diester of lactic acid) is generally used to synthesis PLA. Lactide has two asymmetric carbons and thus exists as the optically active L- and D- forms or as the racemic (or meso) lactide the 50/50 mixture of L- and D- lactic acid. Figure 1.4 shows the stereochemical forms of those three lactides. Polymerisation of the pure enantiomeric L-lactide yields PLLA, and that of D-lactide yields PDLA, which are semi-crystalline polymers. While, polymerisation of the diastereo-isomer (D,L-lactide) or a racemic mixture of D,D-lactide/L,L-lactide produces amorphous PDLLA.

Figure 1.5 shows the three main routes to synthesise PLA. Lactic acid is polymerised by condensation to yield a low molecular weight, brittle polymer, which, for the most part, is unusable, unless external coupling agents are employed to increase its chain length. The second route is the azeotropic dehydrative condensation of lactic acid. It can yield high molecular weight PLA without the use of chain extenders. The third and main process is ring-opening polymerisation of lactide to obtain higher molecular weight PLA which most commonly uses a stannous octoate catalyst. Finally, lactic acid units can be part of a more complex macromolecular architecture as found in copolymers.

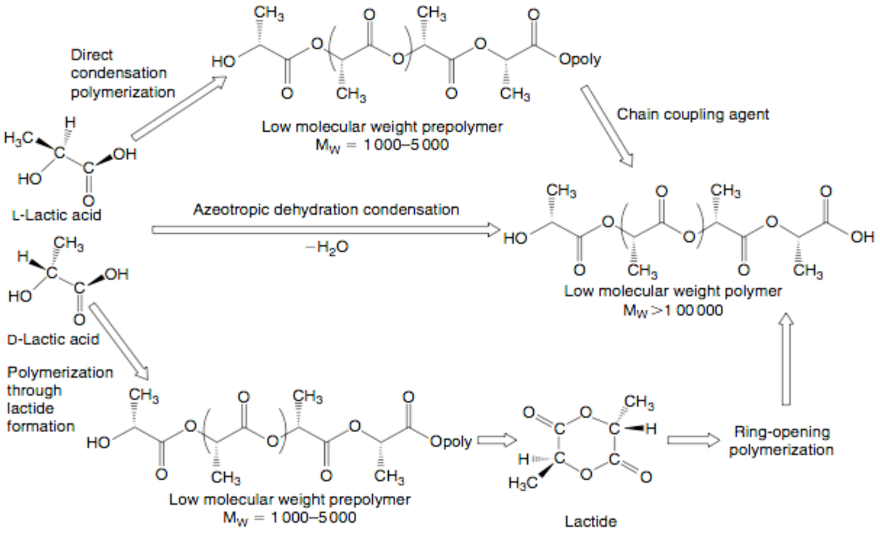

Figure 1.5 Synthetic methods for obtaining high molecular weight [7].

The properties of PLA depend on the component isomer, processing temperature, annealing time and molecular weight. PLLA is a semi-crystalline polymer, which has a crystallinity of around 37%, crystalline melting temperature (T_m) between 170-180 ^oC, and a glass transition temperature (T_g) between 60-67 ^oC. PLLA can be normally dissolved in halogenated hydrocarbons, such as chloroform, methylene chloride, 1,1,2-trichloroethane, and dichloroacetic acid, but is only partially soluble in ethyl benzene, toluene, acetone, and tetrahydrofuran. PDLLA is an amorphous polymer. It has a T_g in the region of 50-60 ^oC. Since polymers from lactic acids have T_g above body temperature, these matrices are stiff with little elasticity in the body and are somewhat brittle at room temperature.

1.2.2.3 Poly(ε-caprolactone), PCL

PCL is known as a flexible polymer, which is very relatively compatible with other polymers. It degrades predominantly through microbial agents. PCL shows a low T_g at -60 °C, which make PCL a rubbery material and exhibits high permeability to low molecular species at body temperature. With the regular structure and low T_m at 60 °C, PCL is a crystalline polymer. PCL is obtained by ring opening polymerisation of the 6-membered lactone called ε-caprolactone using a catalyst such as stannous octanoate, the reaction as shown in Figure 1.6.

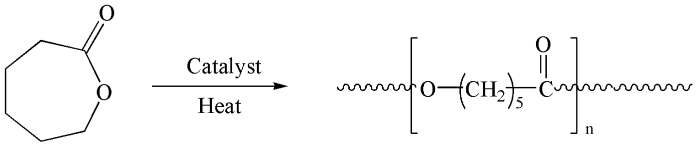

Figure 1.6 Ring opening polymerisation of ε-caprolactone to polycaprolactone (PCL).

As previously mentioned, PCL is widely used as an additive for other polymers to improve their processing characteristics and their end use properties (e.g. impact resistance) [2]. For example, PCL can be mixed with starch to lower its cost and increase biodegradability. Blends of PCL with other degradable polymers also have a great potential for drug delivery applications.

1.2.2.4 Poly(3-hydroxybutyrate), PHB and other poly(hydroxyalkanoates)

PHB belongs to the group of polyhydroxyalkanoate (PHA) polymers and is an aliphatic beta-polyester. There are many other polymers in the PHA class, which are produced by a variety of organisms. Examples include poly(4-hydroxybutyrate) (P4HB), polyhydroxyvalerate (PHV), polyhydroxyhexanoate (PHH), polyhydroxyoctanoate) (PHO) and their copolymers. Figure 1.7 shows chemical structure of PHB, PHV and their copolymer PHBV.

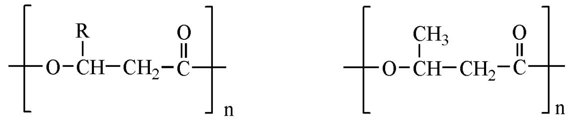

$\left[-O-\overset{R}{\overset{|}{C}H}-CH_2-\overset{O}{\overset{\|}{C}}- \right]_n$ $\left[-O-\overset{CH_3}{\overset{|}{C}H}-CH_2-\overset{O}{\overset{\|}{C}}- \right]_n$

PHA:polyhydroxyalkanoate PHB: poly(3-hydroxybutyrate)

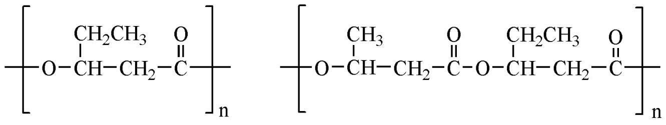

$\left[-O-\overset{CH_2CH_3}{\overset{|}{C}H}-CH_2-\overset{O}{\overset{\|}{C}}- \right]_n$ $\left[-O-\overset{CH_3}{\overset{|}{C}H}-CH_2-\overset{O}{\overset{\|}{C}}-O-\overset{CH_2CH_3}{\overset{|}{C}H}-CH_2-\overset{O}{\overset{\|}{C}}- \right]_n$

PHV: polyhydroxyvalerate PHBV: polyhydroxybutyratevalerate

Figure 1.7 Chemical structure of polyhydroxyalkanoate (PHA) class.

PHB has unusually high levels of crystallinity because of the remarkable stereo-regularity of the perfectly isotactic chain configuration. This high crystallinity results in a rather hard and brittle material, which is not very useful for many applications. PHB shows a T_g at 15 ^oC and T_m at 175 ^oC, which is close to the region of its thermal decomposition temperature. This makes PHB homopolymer difficult to handle using conventional plastic melt processing equipment. PHB is soluble in chloroform and other chlorinated hydrocarbons, water insoluble and relatively resistant to hydrolytic degradation which differentiates it from most biodegradable plastics. PHB is primarily a product of glucose or starch and is employed by a large number of bacteria (e.g., those present in soil or sewage) as a carbon source. The synthesis starts with the condensation of two molecules of acetyl-CoA to give acetoacetyl-CoA, which is subsequently reduced to hydroxybutyryl-CoA, used as a monomer that is polymerised to PHB. It is regarded as a biocompatible material, suitable for medical applications and has the trade name Biopol^{TM}. A number of PHB blends have been prepared with other polymeric materials to produce highly compatible composites called polymer alloys, especially those made from renewable resources, such as starch derivatives and PLA [2, 3, 8].

In order to improve the properties of PHB, copolymers incorporating other structural units such as PHBV have been produced. T_m of PHBV varies according to the hydroxyvalerate (HV) content in the repeating unit. For example, the incorporation of 12% HV gives rise to a T_m of 144 ^oC (compared to the T_m of 179 ^oC for 0% HV) [9]. This leads PHBV to be potentially more useful as a commercial thermoplastic than PHB homopolymer because its lower T_m makes it more processable. PHBV is, however, more costly to produce than PHB which limits its usefulness.

1.3 Polymer blends and miscibility

1.3.1 Definitions

A polymer blend is a macroscopically homogeneous mixture of two or more different polymers, which is can be binary, ternary, or quaternary depending on the number of constituents in the blend [10]. The method used to mix polymers together to create a new material with different physical properties is called polymer blending. There are a few blending techniques to prepare polymer blends, however, solvent blending and melt blending processes were used in this work. Polymer blends can be broadly divided into three categories; miscible polymer blends, immiscible polymer blends, and compatible polymer blends.

It is important to distinguish between the fundamental definition of a miscible polymer blend, which involves the criteria for true thermodynamic miscibility and experimental detection of apparent miscibility that is the identification of potentially useful blend combinations. To understand the terms immiscible, miscible, and compatible blend, the definition of the word "miscible" is defined by International Union of Pure and Applied Chemistry (IUPAC) [10]. Miscibility is defined as the capability of a mixture to form a single phase over certain ranges of temperature, pressure, and composition, subject to the details below.

1. Whether or not a single phase exists depends on the chemical structure, molar mass distribution, and molecular architecture of the components present.
2. The single phase in a mixture may be confirmed by light scattering, X-ray scattering, and neutron scattering.
3. For a two-component mixture, a necessary and sufficient condition for stable or metastable equilibrium of a homogeneous single phase is

$$\left(\frac{\partial^2 \Delta_{\text{mix}} G}{\partial \phi^2}\right)_{T,p} > 0,$$

where $\Delta_{\text{mix}}G$ is the Gibbs energy of mixing and φ the composition, where φ is usually taken as the volume fraction of one of the components. T and p are temperature and pressure, respectively. The system is unstable if the above second derivative is negative. The borderline (spinodal) between (meta) stable and unstable states is defined by the above second derivative equaling zero. If the compositions of two conjugate (coexisting) phases become identical upon a change of temperature or pressure, the third derivative also equals zero (defining a critical state).

4. If a mixture is thermodynamically metastable, it will demix if suitably nucleated. If a mixture is thermodynamically unstable, it will demix by spinodal decomposition or by nucleation and growth if suitably nucleated, provided there is minimal kinetic hindrance.

Therefore, the IUPAC definitions for miscible, compatible, and immiscible polymer blend are as follows:

A miscible polymer blend or homogeneous polymer blend is a polymer blend that exhibits miscibility. It can be defined into four descriptions:

(i) for a polymer blend to be miscible, it must satisfy the criteria of miscibility
(ii) miscibility is sometimes erroneously assigned on the basis that a blend exhibits a single T_g or optical clarity
(iii) a miscible system can be thermodynamically stable or metastable
(iv) for components of chain structures that would be expected to be miscible, miscibility may not occur if molecular architecture is changed, *e.g.*, by crosslinking.

An immiscible polymer blend or heterogeneous polymer blend is a polymer blend that exhibits immiscibility.

A compatible polymer blend is an immiscible polymer blend that exhibits macroscopically uniform physical properties throughout its whole volume. The macroscopically uniform properties are usually caused by sufficiently strong interactions between the component polymers.

However, IUPAC's definition for polymer miscibility is based on thermo- dynamic theory, which is not a useful method of detection. Thus, people have often showed miscibility in terms of optical clarity and single T_g as methods of detection of miscibility under the conditions of the experiment. However, optical clarity and a single T_g maybe observed because they are just kinetically frozen in a state of apparent miscibility, which is not permanently miscible. So it is perfectly legitimate to observe clarity and T_g in order to make an experimentally based comment about the sample at that time but not to assume that the thermodynamic conditions for miscibility have been precisely met.

Immiscibility, miscibility, and compatibility, these three words are sometimes used interchangeably and given different meanings. Many research papers define immiscible as those polymer blends or heterogeneous polymer blends that separately show the glass transition temperature (T_g) of each polymer components, while, miscible polymer blends or homogeneous polymer blends show a single T_g from a single phase structure. Compatible polymer blends exhibit macroscopically uniform properties due to strong interactions between the polymer components [11].

Within this thesis, however, a useful experimental description of miscibility and immiscibility is given by percent transmittance (%T) and glass transition temperature (T_g). The polymer blend films will be catalogued into three types; optically clear, translucent, and opaque. The optically clear film shows %T more than 75% and a single T_g, which will be described as a miscible blend. The translucent film shows %T between 31-75% and will be denoted as a partially miscible blend. The opaque film shows %T between 0-30% and separate T_g of each homopolymer, which will be reserved as an immiscible blend. While, the requirement for a compatible blend will be defined in terms of the strong interaction of polymer phases and the toughness of polymer blend produced.

In addition, the miscibility guide by Coleman and Painter [1] which links theory to practical usefulness will be used to interpret the miscibility behaviour of polymer blends. This uses structural interaction factors, such as hydrogen bonding and polar interaction, as a means of explaining why polymer systems can show the symptoms of miscibility, although they are not perfectly matched in thermodynamic terms. Therefore, optical clarity, T_g, and the Coleman and Painter approach will be used as a preliminarily guide to detect apparent or temporary miscibility of the blends, whereas they do not predict that the system obeys the criteria for thermodynamic miscibility.

1.3.2 Introduction and background to the miscibility of blends

There are many objectives for using polymer blending processes depending on applications and properties of the polymer blends. First, to improve mechanical properties and fracture resistance, such as adding a rubber phase into the rigid polymers. Secondly, to achieve some specific performances, such as transparency, heat distortion, and barrier properties. Two-phase materials can be transparent if the refractive indices are matched closely enough or the phases are small enough. Improving the ability of a rigid polymer to function at elevated temperature by increasing its heat distortion temperature can lead to the formulation of commercially successful products. Thirdly, in order to reinforce neat plastics, a variety of reinforcing fillers or polymers are normally used to make polymer blends strong enough for specific required applications. Fourthly, to make elastomeric blends, a mixture of two or more elastomers is subsequently vulcanised using the traditional methods of rubber technology [11].

The miscibility of polymers is governed by the Flory-Huggins equation and the free energy of mixing (ΔG_m) and is written in equation 1.1. The polymer blends will be miscible when ΔG_m is negative; more details (such as what each symbol represents) are given in Chapter 7.

$$\frac{\Delta G_m}{RT} = \frac{\Phi_A}{M_A}\ln\Phi_A + \frac{\Phi_B}{M_B}\ln\Phi_B + \Phi_A\Phi_B\chi + \frac{\Delta G_H}{RT} \qquad \text{Eq. 1.1}$$

The factors that affect the miscibility of polymers blends are usually composition and temperature. There is a range of compositions of polymer blends resulting in either miscibility or immiscibility. Figure 1.8 shows an example of how polymer blend miscibility is affected by composition of another polymer (B). It can be seen that, in this example, polymer A/B blends will be miscible when polymer B is less than 30 %wt. and more than 70 % wt., while immiscible and showing phase separation when polymer B is between 30-70 % wt.

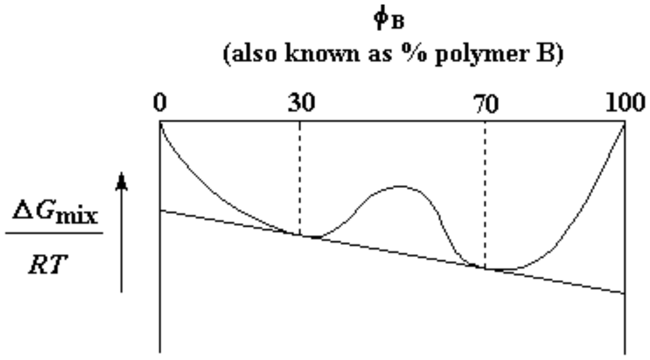

Figure 1.8 The free energy of mixing (ΔG_m) of polymer A and B versus % wt. of polymer B; the miscibility depending on composition [12].

However, the composition range for miscibility can be changed by temperature, as shown in Figure 1.9. For some polymer pairs, the components of a mixture are miscible when the temperature is below or at the critical point. This temperature is called lower critical solution temperature (LCST). This means that the range of miscibility increases with decreasing temperature. For other polymer pairs, the components of a mixture are miscible when the temperature is above the critical point, called upper critical solution temperature (UCST). This means the range of miscibility increases with increasing temperature. The LCST and UCST depend on pressure, degree of polymerisation, polydispersity and branching of polymers.

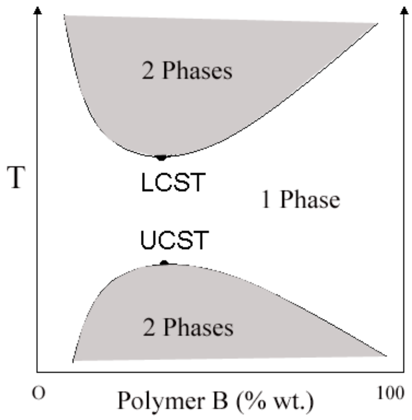

Figure 1.9 Polymer solution phase behavior showing LCST and UCST.

In general, polymer blends have physical and mechanical properties between those of the neat polymers used to blend. For example, the T_g of polymer blends will depend on the ratio of neat polymers. If two polymers have different T_g, one is low and another one is high, the T_g of the blend generally increases in a linear fashion when the composition of the polymer having high T_g increases. Sometimes the T_g will be higher than expected because the two polymers entangle more strongly to each other than to themselves, which causes lower chain mobility. The T_g affects other polymer properties, such as mechanical properties, chemical resistance, and heat resistance.

As mentioned in Section 1.3.1, there are two major methods for polymer blends, solvent blending and melt blending. Solvent blending involves dissolving polymers in a solvent, and then allowing the solvent to evaporate at the required temperature. This solvent blending method is normally used on the laboratory scale because of the limitation of the price, since it is very expensive to evaporate or recapture the solvent on an industrial scale. Additionally, the solvents themselves are expensive and the evaporating solvents will have an adverse effect on the environment. Thus, melt blending is regularly used in industry. The polymers used for blending are heated above their T_g and mixed together in machines such as extruders, two-roll mills, and internal mixers. The details of solvent and melt blending used in this work are discussed in Chapters 4 and 5, and 8, respectively.

1.3.3 Why use blends?

Many neat polymers have limited uses because of a lack of mechanical properties and/or physical properties; thus, polymer-blending techniques are used to remedy this shortcoming, instead of trying to synthesise a new polymer, which is more difficult. Polymer blends can have some of the properties of one polymer, and some of the properties of another. As discussed in the earlier section, these are the main reasons to use polymer-blending processes. However, another important reason for blending polymers is to lower the price. For example, PLLA/starch blends are economically suitable for certain applications because their price is less than neat PLLA [13-16]. Other reasons to use polymer blending are to improve processability, optical properties, and degradation. PLA is an important biodegradable polymer, which has been used in this work because it has some limitations for applications, as discussed in Section 1.2.1. Therefore, blending PLA with other polymers from renewable resources provides a good way to try and resolve this problem.

1.3.4 Guidelines for miscible polymer blends

The principles that govern the miscibility of polymers depend on their thermodynamics of mixing. If the energy required for mixing polymers together is less than to keep them separated, the two polymers will be miscible. This mainly depends on their structures and their solubility parameters. Choices of the right temperature and composition ranges for blending are also importance factors for obtaining miscible polymer blends because miscibility rarely extends to all compositions and temperatures for given polymer combinations.

However, most simple polymer blends are immiscible, but there are several ways to make them miscible. The well-known way is to use copolymers or compatibilisers. The first design strategy for compatibilising copolymers is to make one segment of the copolymer miscible with one of the polymers and another segment miscible with the second polymer, and then the two polymers will be miscible. In the second strategy, one segment of the copolymer is polar and another is non-polar, thus they do not like each other. If a polymer, which is immiscible with one of the segments of this copolymer, is used to form a blend, it can be a miscible blend because polymer will be in between the two segments of copolymer. This is because the two segments of copolymer avoid coming into contact with each other [17]. The Coleman and Painter approach [1] is used as a guide line for determination of the miscible or immiscible blends in this work. It is discussed with the results from solvent blending in Chapter 7.

1.4 Literature review of polymer blends based on PLA

PLA is one of the most interesting polyesters used in the market because it is produced from renewable resources and can be degraded by hydrolysis. Recently, Nampoothiri et al. [18] have reviewed the recent developments in PLA research, with sections on; lactic acid, polymerisation, copolymers and blends of PLA, degradation, applications, and PLA-challenges. Similarily, understanding of the degradation of PLA has recently been reviewed by Hirao et al. [19]. They studied the hydrolysis of PLA using microwave irradiation and showed that microwave irradiation could make the hydrolysis of PLLA dramatically faster than conventional heating. To attain a 45% yield of lactic acid from the hydrolysis of PLLA, it took only 120 minutes for microwave irradiation compared with 800 minutes for conventional heating. Moreover, the optical purity of L-lactic acid obtained from microwave irradiation was found to be higher than from conventional heating. They also proposed that microwave irradiation would be useful for the chemical recycling of all polyesters, and can be used industrially to improve the efficiency of chemical recycling.

As discussed earlier, PLA has limited applications because of its poor mechanical properties and because it is an expensive polymer. Therefore, a great number of investigations have been performed on PLA to improve its mechanical properties and to reduce its price for use in the market. To achieve these points, blending techniques by solvent or melting and also co-polymerisation have been widely investigated to modify the physical properties. However, the blending techniques are more significant for practical use than the synthesis of the new copolymers because they can be useful in the market. To synthesise new copolymers of PLA will be expensive to develop commercially on a large scale.

PLA has been blended with plasticisers and a number of candidate polymers. Examples of such polymers are: poly(ε-caprolactone) (PCL) [20-23], polyhydroxy butyrate (PHB) [24, 25], poly(butylene succinate) (PBS) [26], poly(butylene succinate adipate) (PBSA) [27], poly(ethylene terephthalate) (PET) [28], thermoplastic starch [29-31], petroleum-based polymers such as linear low density polyethylene (LLDPE) [32], polyurethane [33, 34]; and plasticisers, such as tributyl citrate (TBC) [35], poly(ethylene glycol) (PEG) [35-39] , poly(propylene glycol) (PPG) [40], and citrate esters [41, 42]. Copolymerising with a flexible polymer, such as PEG, PBS, and PCL, is one of many approaches to improve the toughness of PLA [43]. In addition, other factors such as composition ranges, molecular weight, thermal effect, and crystallinity, which affect the miscible or compatible blends, are studied.

Poly(ε-caprolactone) (PCL) has been the most popular polymer used to blend with PLA to increase impact strength and solve the brittleness problem. However, PLA/PCL blends still suffer from poor mechanical properties due to the phase separation and poor adhesion between the immiscible components of PLLA and PCL. Thus, many researchers have tried to improve the miscibility or the compatibility of PLA/PCL in different ways. Harada et al. [20] used PCL reactive blends with PLA by adding reactive processing agents, such as lysine triisocyanate (LTI), and lysine diisocyanate (LDI). The result indicated that isocyanate groups of LTI react with terminal hydroxyl or carboxyl groups of both PLA and PCL, and the compatibility of PLA/PCL blends improved. Todo et al. [21] studied the melted PLLA/PCL blends with various compositions of PCL and observed their fracture behaviour by polarising optical and scanning electron microscopy. It was found that the fracture behaviour was improved, with 5 wt% of PCL giving the greatest improvement. At higher levels of PCL (more than 5 wt%), phase separation was observed due to the incompatibility of PLLA and PCL and the size of the PCL phases increased with increasing PCL content.

Ramiro Dell'Erba et al. [22] synthesised a triblock PLLA-PCL-PLLA copolymer to use as a third component for PLLA/PCL reactive blending. The PLLA-PCL-PLLA copolymer acts at the phase boundary as an interfacial agent and produces a more homogeneous distribution of particle size and a lowering of the fraction of large domains. However, PLLA/PCL blends characterised by a fine dispersion of PCL domains can be obtained up to a 30 wt% of PCL. The PLLA crystallisation rate, both from the melt and the glassy state, was observed to be enhanced by the presence of PCL domains because of the increase in nucleation rate. Wang et al. [44] synthesised poly(D,L-lactide-co-ε-caprolactone) (PLCA) and poly(D,L-lactide-coglycolide) (PLGA) and blended PLCA/PLGA by solution blending. The authors observed that the blend was immiscible but compatible. Other copolymers of PLA with PCL have been synthesised as a means of extending the applications of PLA [45]. In one example, PLLA/PCL blends were blended for biodegradable filtration membranes. The membranes were formed via the thermally-induced phase separation process and were used to separate yeast cells from their suspension [46].

Poly(D,L-lactide) (PDLLA) has been used in blends with PLLA with and without the presence of compatibilisers because its amorphous structure is expected to reduce the brittleness of semi-crystalline PLLA. Bouapao et al. [47] studied the effect of solvent blending PDLLA with PLLA on the isothermal crystallisation, spherulite growth, and structure of blends. The DSC results showed that PLLA/PDLLA blend films were immiscible and phase-separated during crystallisation. Small-angle X-ray scattering indicated that for a crystallisation temperature of 130 ^{o}C, the long period associated with the lamellae stacks and the mean lamellar thickness values of PLLA and the blend films did not depend on the PDLLA content, and wide-angle X-ray scattering revealed that the crystalline form of PLLA did not vary in the presence of PDLLA. The presence of PDLLA is believed to disturb the diffusion of PLLA chains to the growth sites of PLLA crystallites. Chen et al. [39] solvent-blended PLLA with PDLLA in the presence of poly(ethylene oxide) (PEO) and poly(propylene oxide) (PPO) as compatibilisers. The DSC data showed that PLLA/PDLLA blends had two T_g's. This demonstrated that PLLA/PDLLA blend has poor miscibility, however, its miscibility was improved by adding PEO and PPO, depending on the composition used in blends. The DMA data showed that 40/60 PLLA/PDLLA is harder and tougher than pure PLLA and is more improved when 2% compatibilisers was added. These authors also blended PLLA and PCL with PEO or PPO as compatibilisers. The PLLA/PCL blends showed higher elongation than the PLLA/PDLLA blends.

Poly(3-hydroxybutyrate) (PHB) and poly(3-hydroxybutyrate-co-3-hydroxyvalerate) (P(HB-HV)) belong to the group of polyesters known as polyhydroxyalkanoates (PHAs). PHB is a beta-aliphatic polyester, which has been used to blend with PLA and to modify other polymers. For example, Noda et al. [24], who worked with Procter and Gamble in Ohio, USA, investigated a class of ductile plastic PHAs which they called Nodax, together with highly compatible blends or polymer alloys made of Nodax and PLA. The molecular structure of Nodax copolymer, where x = 0.01-0.50, and n = 2–14, as shown below.

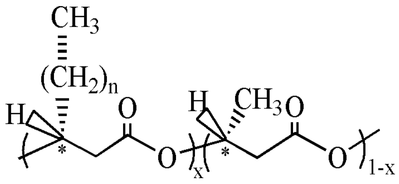

Two different types of Nodax or PHBHx copolymers, the copolymer comprised of 3-hydroxybutyrate (3HB) and 3-hydroxyhexanoate (3HHx), were prepared by bacterial fermentation; one is composed of 13 mole% 3HHx and another 5 mole%. PLA/PHBHx blends with different compositions were prepared by melt-mixing in a single-screw extruder. The results showed that the addition of a small amount of PHBHx - as little as 10 wt% - dramatically improved the toughness of PLA. Samples containing less than 20 wt% PHBHx are as clear and transparent as unmodified PLA, while more than 20 wt% produced translucent blends with levels of opacity increasing with the PHBHx content.

For the clear samples, clarity is thought to be either because PHBHx crystallites become so small that they no longer scatter light, or they are not crystallised at all in the PLA matrix when the PHBHx content is kept below 20 wt%. The IR spectroscopy results indicate that PHBHx dispersed in a PLA matrix at a relatively low level (below 20 wt%) does not significantly crystallise, even after being cooled well below their melting temperature. This is deduced from the absence of a sharp crystalline absorption band around 1720 cm^{-1} assignable exclusively to the crystalline contribution of PHBHx. A very fine dispersion of Nodax particles is created in blend systems with PHBHx content below 20 wt%. This favourable dispersibility is most likely due to the low interfacial energy between the highly compatible PLA and PHBHx. Using PHBHx at levels more than 20 wt% increases the particle size of the dispersed phase leading to rapid cystallisation of PHBHx, and to loss of optical clarity and toughness of the blends.

Domb [25] studied the degradable polymer blends and discussed them in terms of miscibility. One of the results relating to aliphatic polyester blends showed that both low and high molecular weight PLA and their copolymers with glycolic acid were miscible in several polymers including: P(HB-HV), PHB, PCL, poly(mandelic acid), and poly(propylene fumarate), both in melt and in solution. Zen et al. [26] synthesised a novel biodegradable multiblock poly(ester urethane), poly(L-lactide)-*block*-poly(butylene succinate) (PLLA-b-PBS), by a chain-extension reaction of dihydroxyl terminated PLLA (PLLA-OH) and PBS prepolymers (PBS-OH) using toluene-2,4-diisocyanate (TDI) as a chain extender. The molecular weight of the resultant PLLA-b-PBS increased with increasing PBS content. PLLA and PBS segments were generated compatible in the amorphous phase, and the crystallisation of PLLA-b-PBS was significantly increased by increasing the PBS block.

Poly(butylene succinate adipate) (PBSA) is a commercially available aliphatic polyester with high flexibility, excellent impact strength, melt processibility, chemical resistance, low melting point and is more readily biodegraded than PLA. Lee et al. [27] investigated thermal, rheological, morphological and mechanical properties of PLA/PBSA blends. The thermal study revealed that the T_g of PLA in the blends was slightly decreased with increasing PBSA content. At 80 wt% PBSA, the T_g decreased from 63 ^{o}C for pure PLA to 59 ^{o}C for composite blends due to active interaction between

PLA and PBSA chains, which is an indication of partial miscibility of PLA/PBSA blends. The stability of the blends at high temperature was lower than that of pure PLA and PBSA. The tensile strength and tensile modulus of the blends were decreased with PBSA content, however, the impact strength increased much higher than pure PLA at 20 wt.% PBSA. The early stage biodegradation rate of the blends was found to be highest at a level of 80 wt.% PBSA.

Poly(ethylene terephthalate) (PET) is a thermoplastic polymer of the polyester family used in synthetic fibers, beverage, food and other liquid containers, thermoforming applications, and engineering resins. Chen et al. [28] have studied non-isothermal crystallisation of PLA/PET blends, which had not previously been investigated in detail. PLA and PET were dissolved in hexafluoro-2-propanol with concentrations of about 10 wt.% of polymer, and then cast to form films. The DSC results showed a single T_g of the blends over the entire composition range of PET. This was taken as an indication that PET is completely miscible with PLA and produced a homogeneous amorphous phase structure. PET was found to crystallise in all amorphous or crystalline PLA forms in the blends, and its degree of crystallinity decreased as the PLA content increased. However, PLA can crystallise even in 30/70 PLA/PET blends when using amorphous PET, while PLA is hardly able to crystallise at all even when PET is crystalline.

Starch is an attractive blend component for PLA because it offers an advantage in terms of cost. PLA and starch are two apparently promising candidates for biodegradable polymer blends, but they are thermodynamically immiscible. PLA is hydrophobic, while starch is hydrophilic leading to poor adhesion between their blends. Therefore, a third type of component such as compatibilisers, plasticisers, and block copolymers are often added into PLA/starch blends to reduce the interfacial energy, to thereby improve dispersion, and consequently to enhance adhesion between binary polymer phases. Another way to improve PLA/starch blends is to use reactive blending, which can promote chemical reactions between the two polymers by adding a reactive third component with appropriate functional groups or a catalyst. Kozlowski et al. [29] blended potato starch with PLA using poly(ethylene glycol) as a plasticiser. The presence of starch worsened the mechanical properties of the blends. Wheat gluten is also blended with PLA for use in food plastic industries [48]. The presence of gluten reduced the number of cycles needed to change the PLA crystalline structure to a predo-minantly amorphous form.

Reactive blending is frequently used to enhance compatibility and miscibility by chemical reaction. Methylenediphenyl diisocyanate (MDI) is found to be one of the most efficient third components to improve mechanical properties of reactive blending of PLA/starch blends. It promoted a strong chemical linkage between the carboxyl from PLA and hydroxyl groups from starch although it is toxic. Maleic anhydride was then used as nontoxic reactive compatibiliser instead of MDI. Subsequently, Zhang and Sun [30] used dioctyl maleate, a derivative of maleic anhydride, as a reactive compatibiliser for PLA/starch blends. The tensile strength of PLA/starch blends was found to improve when using low concentrations of dioctyl maleate. Ke et al. [49] added triethyl citrate as a plasticiser into PLA/starch blends in a presence of methylenediphenyl diisocyanate (MDI). It was found that triethyl citrate increased the elongation at break and toughness but decreased the tensile strength and modulus of the blends. They have been many studies of PLA/starch blends, for example, with various compatibilisers [15] and using starch with various amylose contents [31]. Starch is also used to blend with PLLA for hybrid foams [16, 50].

Petroleum-based polymers and non-biodegradable polymers, such as polyethylene, polyurethane, and acrylonitrile-butadiene-styrene copolymers (ABS), have been used in blends with PLA aiming to improve the toughness of PLA. It is well known that PLA/PE are very immiscible, based on thermodynamic arguments as “like dissolves like”. Therefore, many researchers have tried to make them miscible. Wang and Hilmyer [32] blended PLLA/linear low-density polyethylene (LLDPE) by solution blending on a laboratory scale in the presence of a PLLA-PE block copolymer as a compatibiliser. The toughness of PLLA was improved. Subsequently, they studied the same blends of PLLA/LLDPE/PLLA-PE using the melt blending method [51]. The effect of the PLLA-PE block copolymer on the morphology and impact resistance was examined. The results showed that the toughening of amorphous PLA (PDLLA) was improved by adding the compatibiliser but this was not the case for semi-crystalline PLA (PLLA). In contrast, PLLA showed significantly better adhesion to LLDPE than PDLLA did. They proposed that tacticity effects on the entanglement molecular weight or miscibility of PLLA allow for the improved adhesion between PLLA and LLDPE.

Polyurethanes: Li and Shimizu [33] blended PLA with poly(ether)urethane elastomers, which has a unique combination of toughness, durability, flexibility, and biocompatibility. The soft segments of PU elastomers are mainly polyester or polyether, which are expected to have good compatibility with PLA. The results showed the toughening effects of the PU elastomer on PLA. Yuan and Ruckenstein [34] toughened PLA by introducing 5 wt% of a PCL diol- and triol- based PU network into the solution blend in toluene. Three kinds of PU were used with an OH mole ratio (diol and triol) between 10/0, 9/1 and 7/3, denoted as PU-0, PU-1 and PU-3, respectively. The toughness of PLA/PU-0 was not improved significantly, while PLA/PU-1 significantly improved; more so than PLA/PU-2. The adhesion between PLA and PU-0 was suggested to be poor because PU-0 is more polar than PLA and strong hydrogen bonding in the former stimulates self-aggregation. PLA interpenetrates the PU-1 to generate PU-PLA semi-interpenetrating networks leading to more compatible blends. The lower toughness of PLA/PU-3 is due to the increased stiffness of the semi-interpenetrating PU-PLA network leading to less intermingling between the PU-PLA networks and the PLA.

Other studies include the use of acrylonitrile-butadiene-styrene copolymers (ABS), which are non-biodegradable, melt-blended with PLLA, in the presence of a compatibiliser (styrene/acrylonitrile/glycidyl methacrylate copolymer (SAN-GMA)) and ethyl-triphenyl phosphonuium bromide (ETPB) catalyst [52].

It is clear that many attempts have recently been made to improve the mechanical properties of PLA through the blending with other polymers and compatibilisers. The underlying reason is to develop the properties of PLA for suitable application to use as a commercial polymer in the market place. As mentioned previously, PLA is currently used in a number of biomedical applications, bio-plastic film applications, and in tissue engineering.

Applications: in the past decade, there have been many researchers using plasticisers to modify the toughness of PLA films. For example, lactide monomer used as a plasticiser in PLA has shown a significant increase in thermal degradation during the processing and rapidly migrate into the end-product surface. Poly(ethylene glycol) (PEG) which is widely used as a plasticiser was found to be a good plasticiser but its migration to the surface over time results in an unstable PLA/PEG blend. Lemmouchi et al. [35] used tributyl citrate as a plasticiser to blend with PLA and also synthesised low molecular weight PLA-b-PEG block copolymers. They studied physical properties, mechanical properties, and degradation. They highlighted the reasons for using tributyl citrate and PLA-b-PEG as plasticisers for PLA: (a) tributyl citrate can reach high elongation at break values, whereas PLA-b-PEG copolymer will retain the high tensile strength of the blends; (b) using tributyl citrate together with PLA-b-PEG can reduce the amount of volatiles and degradation products of the blends; (c) PLA-b-PEG copolymer should enhance the interaction between PLA phase and copolymer because of their ester groups. The results showed that the blend films at 80/20 PLA/plasticisers show a glass-transition temperature below 30 ^{o}C, elongation at break more than 220%, and suitable tensile strength for packaging application. Tributyl citrate in association with the copolymer also has a beneficial effect in the increase of impact strength of PLA. For the biodegradation study, the results showed that PLA-b-PEG/ tributyl citrate enhances the degradation of the PLA matrix.

Hailin et al. [53] blended PLA with silk fibroin (SF) to widen the potential application of SF in the biomaterials field. The mechanical and thermal properties of the blend films were improved but surface hydrophilicity and swelling capacity decreased depending on PLA content. Chitosan was used as a polymeric matrix to produce films from renewable resources, which exhibit potential antifungal properties on mycotoxinogen strains, because of its good film-forming properties and its recognised antimicrobial activity. Thus, composite films for food packaging from chitosan and PLA in the presence of PEG as a plasticiser were prepared by solvent blending [54]. The results showed that it was difficult to produce miscible PLA/chitosan film forming solutions. However, this film did produce heterogeneous films with high water sensitivity. Peesan et al. [55] used hexanoyl chitosan (H-chitosan) containing hexanoyl group substitution along the chains to blend with PLA. However, the results showed no significant interaction between H-chitosan and PLA. Subsequently, they studied the effect of various casting solvents; chloroform, dichloromethane, and tetrahydrofuran, on the characteristics of H-chitosan/PLA blend films [56]. It was found that no significant effect from the type of the casting solvent on thermal degradation behaviour was observable. Casting of blend films in chloroform and dichloromethane showed extensive phase separation of H-chitosan and PLA, with the minor phase forming into discrete domains throughout the matrix.

Recently, novel antibacterial nanofibrous PLLA scaffolds for medical applications were prepared from PLLA/poly(lactide-co-glycolide) (PLGA) nanospheres [57]. The effect of surface-modified collagen on the adhesion, biocompatibility and differentiation of bone marrow stromal cells in PLLA/poly(lactide-co-glycolide) (PLGA)/chitosan scaffolds was studied [58]. PDLLA/PEG fibrous scaffolds were prepared by electrospinning for skin tissue engineering [59]. The blends with different ratios were dissolved in 3/1 v/v of acetone and dichloromethane. It was found that electrospun mats containing 30% PEG showed the best balance of properties, including a moderately hydrophilic surface, minimal dimensional changes, adaptable bulk biodegradation pattern and enhancement of cell penetration and growth within fibrous mats. PLLA/gelatin nanofibres for wound dressing were also fabricated by electrospining in aqueous acetic acid at room temperature [60]. Nanofibrous mats from PLLA/gelatin showed controlled evaporative water loss, promoted fluid drainage ability, and excellent biocompatibility, especially a potential application as wound dressing. For other usefulness of PLA, such as nanocomposites, PLA was used to blend with fumed silica nanoparticles (SiO2), montmorillonite (MMT) and oxidised multi-walled carbon nanotubes (o-MWCNTs), organoclay nanocomposites/PEG [61-63], and PLA/nanoclay [62, 63].

As reflected in earlier references in this chapter, amongst the large number of research related to PLA, reactive blending is an important technique in developing polymer blends suitable for commercial applications. Recently, Oyama [64] was successful in producing the super-tough PLA by reactive blending with poly(ethylene-glycidyl methacrylate). It is concluded that the epoxide group incorporated in poly(ethylene-glycidyl methacrylate) will react with both the carboxyl groups and the hydroxyl groups located at the PLA chain-ends during melt-mixing, resulting in the formation of graft copolymers at the interface. Natural fibres were used in reactive blending with PLA to produce biocomposites comparable to PP [65].

There also have been many researchers who have studied the degradation of PLA blends. For example, Tsuneizumi et al. [66] studied the degradation of PLLA/polyethylene and PLLA/poly(butylene succinate). The blends were degraded into repolymerisable oligomers using environmentally benign catalysts, clay catalysts and enzymes, with the objective of developing a selective chemical recycling process.

It can be seen that there are many pieces of research involving PLA binary blends, but not PLA ternary blends. Similarly, there has been no research involving blending or miscibility studies with PLA homologues other than PGA. These are two important aspects of the present work.

1.5 Aims and Objectives

There are many researchers attempting to improve the mechanical properties and physical properties of poly(lactic acid) for suitable applications, as discussed earlier. In addition, there are many reasons to use poly(lactic acid), a widely used biodegradable polyester, as mentioned in Section 1.2.1. For that reason, poly(lactic acid) was chosen for a laboratory scale study in this research using the techniques of solvent blending and melt blending.

The aim of this research is to design miscible or compatible blends either with polymers that are inherently miscible or using compatibilisers or compatibilising techniques. Both of these approaches would be expected to depend upon the identification of polymer species that interact strongly with each other. This work will concentrate on the effects of structure on miscibility and compatibility of two families of materials. The first is three component blends in which regions of mutual miscibility and compatibilities will be identified using ternary phase diagrams. The second family to be investigated are the homologues of poly(lactic acid) - that is other member of the poly(α-ester) series. Some of these polymers are available in this laboratory from earlier synthetic studied but have never been examined in terms of their miscibility or compatibilisation effects with poly(lactic acid). Since these materials are only available in small (mg) quantities and important part of the work will be the design of a small-scale technique for solvent blending studies.

The aim of this work is not an attempt to produce a theoretical explanation for the miscibility of polymer blend system but to detect composition regions where unusual phenomena of polymer miscibility appear to occur. It will be of importance, however, to use a theoretical model to attempt to explain and understand the results.

CHAPTER 2

MATERIALS
AND
EXPERIMENTAL METHODS

Chapter 2

Materials and Experimental Methods

2.1 Materials

Polymers and reagents were used from different sources. Table 2.1 shows synthesised materials in this laboratory. Table 2.2 shows commercial materials and reagents.

Table 2.1 Synthesised materials in this laboratory information.

Materials	Abbreviations in this work	Molecular Structure
Aliphatic Poly α-esters:		
Poly(2-hydroxy-2-methyl-propanoic acid) or Poly(α-hydroxy isobutyric acid)	α1(dimethyl)	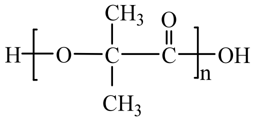 $H\left[O-\underset{CH_3}{\overset{CH_3}{C}}-\overset{O}{\overset{\|}{C}}\right]_n OH$
Poly(2-hydroxy-2-ethyl-butanoic acid)	α2(diethyl)	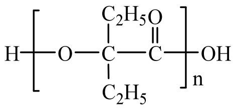 $H\left[O-\underset{C_2H_5}{\overset{C_2H_5}{C}}-\overset{O}{\overset{\|}{C}}\right]_n OH$
Poly(2-hydroxy-2-cyclopentyl-ethanoic acid)	α3(cyclopentyl)	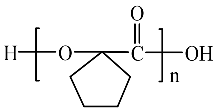
Poly(2-hydroxy-2-cyclohexyl-ethanoic acid)	α4(cyclohexyl)	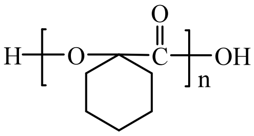
Poly(2-hydroxy-2-cycloheptyl-ethanoic acid)	α5(cycloheptyl)	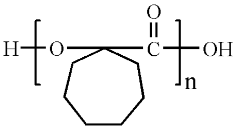

Table 2.1 Synthesised materials in this laboratory information. (Continued)

Materials	**Abbreviations in this work**	**Molecular Structure**
Poly(2-hydroxy-2-chloromethyl-propanoic acid)	α6 (chloromethyl-methyl)	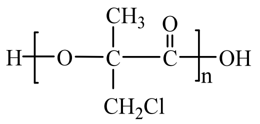 $\text{H}\left[\text{O}-\overset{\text{CH}_3}{\underset{\text{CH}_2\text{Cl}}{\text{C}}}-\overset{\text{O}}{\overset{\parallel}{\text{C}}}\right]_n\text{OH}$
Aromatic Poly α-esters:		
Poly(2-hydroxy-2-pentafluorophenyl propanoic acid)	ArS1 (pentafluorophenyl-methyl)	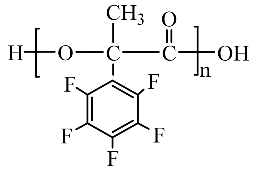
Poly(2-hydroxy-2-phenyl propanoic acid)	ArS2 (phenyl-methyl)	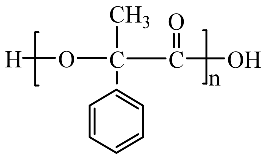
Poly(2-hydroxy-2-phenyl ethanoic acid)	ArS3 (phenyl)	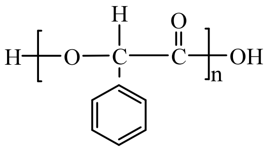
Copolymer of poly(2-hydroxy-2-pentafluorophenyl propanoic acid) and poly(2-hydroxy-2-phenyl ethanoic acid)	Copolymer of ArS1 and ArS3	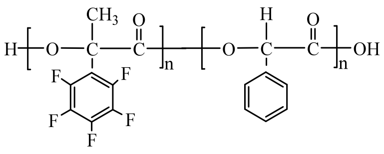
Copolymer of poly(2-hydroxy-2-pentafluoro phenyl propanoic acid) and poly(glycolic acid)	Copolymer of ArS1 and PGA(synthesised)	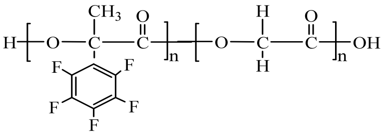
Poly(glycolic acid)	PGA (synthesised)	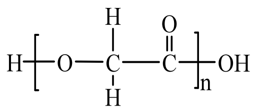 $\text{H}\left[\text{O}-\overset{\text{H}}{\underset{\text{H}}{\text{C}}}-\overset{\text{O}}{\overset{\parallel}{\text{C}}}\right]_n\text{OH}$

Table 2.1 Synthesised materials in this laboratory information. (Continued)

Materials	**Abbreviations in this work**	**Molecular Structure**
Poly(D,L-lactide)	PDLLA (synthesised)	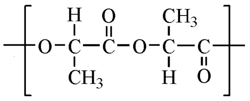 $-\left[O-\underset{CH_3}{\overset{H}{C}}-\overset{O}{C}-O-\underset{H}{\overset{CH_3}{C}}-\underset{O}{C}\right]-$
L-lactide-co-Poly(ε-caprolactone) copolymer	LLA-co-PCL (synthesised)	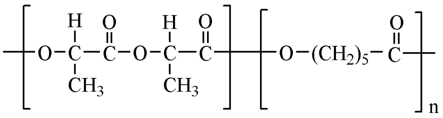 $-\left[O-\underset{CH_3}{\overset{H}{C}}-\overset{O}{C}-O-\underset{CH_3}{\overset{H}{C}}-\overset{O}{C}\right]-\left[O-(CH_2)_5-\overset{O}{C}\right]_n-$

Table 2.2 Commercial materials and reagents information.

Materials	**Abbreviations in this work**	**Suppliers**	**Other details**
Poly(L-lactide)	PLLA1	Cargill Dow, Inc.	M_n = 18,700 M_w =28,000
	PLLA2	Sigma-Aldrich Co., Inc, USA	M_n = 63,500 M_w = 94,800
Poly(ε-caprolactone)	PCL1	Sigma-Aldrich Co., Inc, USA	M_n = 7,500 M_w = 13,300
	PCL2	Sigma-Aldrich Co., Inc, USA	M_n = 57,800 M_w = 81,700
Cellulose acetate butyrate	CAB	Eastman Chemical	CAB-531-1 M_w= 40,000 Butylrate = 50%
Cellulose acetate propionate	CAP	Sigma-Aldrich Co., Inc, USA	M_n ~ 25,000 mp = 188-210 ^{o}C
Cellulose propionate	CP	Sigma-Aldrich Co., Inc, USA	M_n ~ 70,000 M_w ~ 130,000

Table 2.2 Commercial materials and reagents information. (Continued)

Materials	**Abbreviations in this work**	**Suppliers**	**Other details**
Poly(glycolic acid)	PGA	Sigma-Aldrich Co., Inc, USA	mp = 225-230 ^{o}C
Poly(propylene succinate)	PPS	Sigma-Aldrich Co., Inc, USA	-
Poly(1,4-butylene succinate) extended with 1,6-diisocyanatohexane	PBS	Sigma-Aldrich Co., Inc, USA	mp = 120^{o}C, d=1.3, MFI = 10
Poly(ethylene succinate)	PES	Sigma-Aldrich Co., Inc, USA	-
Poly(butylene succinate)	Bionolle 1020	Showa Highpolymer Co.Ltd	-
Poly(butylene succinate adipate)	Bionolle 3010	Showa Highpolymer Co.Ltd	-
Poly(ethylene glycol)	PEG	Sigma Chemical Co.Ltd	M_w ~10,000
Poly(ester adipate)	G40	Croxton and Garry Co.Ltd	-
Poly(hydroxybutyric-hydroxyvaleric acid)	P(HB-HV)	Sigma-Aldrich Co., Inc, USA	20.1 % HV
Thermoplastic polyurethane	TPU	B.F. Goodrich Co.,Ltd	Commercial name: Estane 5706 P
Chloroform	$CHCl_3$	Fluka Chemical Co.,Ltd	-
Hexafluoroiso-propanol	HFIP	Fluka Chemical Co.,Ltd	-
Tetrahydrofuran	THF	Fluka Chemical Co.,Ltd	-

2.2 Synthesis of PLA homologues

As mentioned in Chapter 1, poly α-esters have potential useful applications, and in addition because of their structural simplicity they provide an ideal system to study structure-property and structure-additive-property relationships. However, a general method for their preparation is not exactly known.

There are a number of potential methods to synthesise PLA homologues or poly(α-esters) having the general formula as shown in Figure 2.1a. The most common method of poly(α-ester) synthesis involves polymerisation of the cyclic glycolide (Figure 2.1b). The problem, however, is that polymerisation of the 6-membered diglycolide ring is restricted to cases in which R_1 is a hydrogen and increasing of the bulk of R_2 decreases polymerisability. In effect this limits the rate to polymers of glycolic (R_1=R_2=H) and lactic (R_1=H, R_2=CH_3) acids. The α-hydroxy acids, as shown in Figure 2.1c can also be used to synthesise aliphatic-α-polyesters by heating in an inert solvent in the presence of an acid catalyst. However, the molecular weights are shown to be low, and the same structural limitations that apply to glycolide polymerisation apply to the acid. Thus, the methods readily available for the preparation of poly(α-esters) are not numerous and often result in poor yields of polymer and low molecular weight. Therefore, the most convenient approach is to convert the α-hydroxy acid into the five-membered ring of α-hydroxycarboxylic acid anhydrosulphites or α-hydroxycarboxylic acid anhydrocarboxylate, the general formulae as shown in Figures 2.1d and e, respectively. The homologues series of PLA used in this work, in which the aliphatic and aromatic alpha-side chains play an important role of determining not only the physical properties but also the degradation characteristics of polymers, were synthesised from these monomers by previous workers in these laboratories [5, 67], and the details of their chemical structures are shown in Table 2.1.

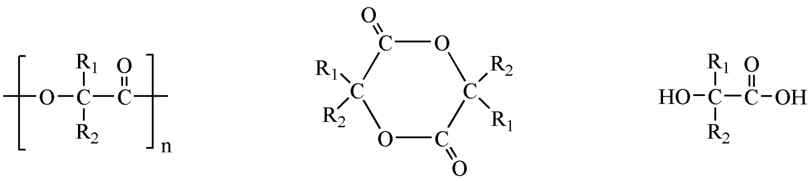

(a) Poly(α -ester) **(b) 6-membered diglycolide ring** **(c) α - hydroxy acid**

(d) α - hydroxy carboxylic acid anhydrosulphite **(e) α - hydroxy carboxylic acid anhydrocarboxylate**

Figure 2.1. The general formulae to synthesise poly(lactic acid) homologues.

2.3 Blending methods

Two types of blending methods, solvent blending and melt blending, were used to study the design and characterisation of the novel blends of poly(lactic acid) or polylactide. Solvent blending is used as a preliminary observation of the miscibility of polymer blends and then some compositions are selected to do melt blending.

2.3.1 Solvent blending process

The technique developed in this study called "a rapid screening method", as discussed in Section 4.1, was used for solvent blending both of binary and ternary blends. The polymer sample preparatory technique is shown in Figure 2.2. The polymer samples were dissolved in solvent at a concentration of 7 wt% by volume and then pipetted into the well plates. The total of this polymer solution volume used for blending was 100 μL and a further 100 μL solvent was then added. Samples were then left to evaporate slowly at room temperature.

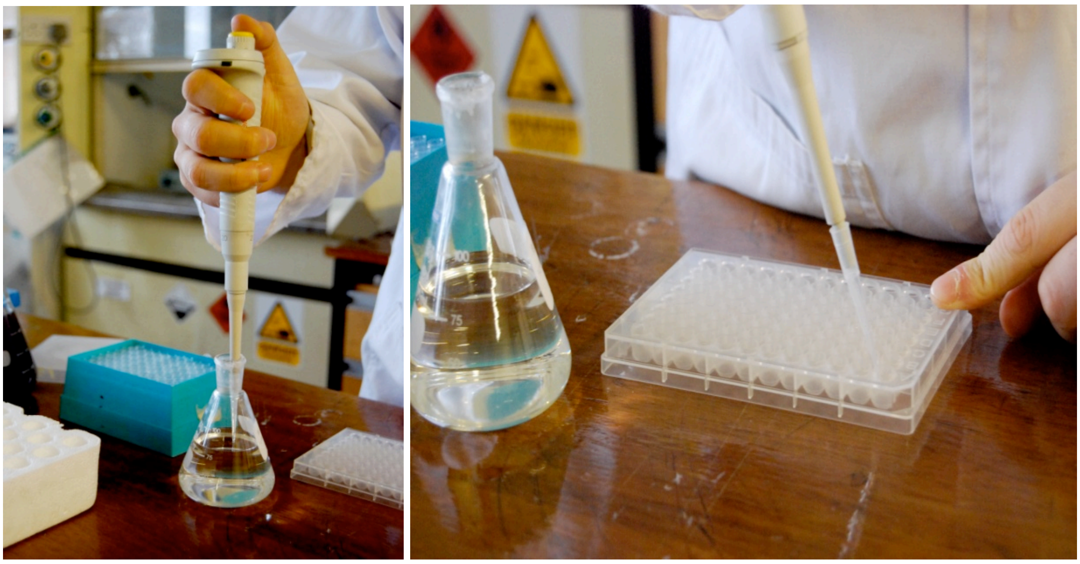
(a) (b)

Figure 2.2 Polymer sample preparatory technique; (a) polymer solution was dissolved and poured into the volumetric flask and (b) subsequently pipetted into the 96-well plate.

2.3.1.1 Binary blends based on poly(α-ester) homologues of PLLA

The following families of binary blends based on poly(α-ester) homologues of PLLA were studied to determine their miscibilities.

- Blends of poly(α-ester)homologues/poly(α-ester) homologues
- PLLA/poly(α-ester) homologous blends
- Blends of PLLA or PDLLA with poly(ε-caprolactone) (PCL), cellulose acetate butyrate (CAB) or α4(cyclohexyl)
- PLLA/other biodegradable polymer blends; poly(ethylene glycol) (PEG), poly(ethylene succinate) (PES), poly(butylene succinate) (PBS), poly (hydroxy butyrate-hydroxyvalerate) (P(HB-HV)), PCL, and CAB

All polymers were dissolved in solvent with a concentration of 7 % (w/v). All poly(α-esters) were dissolved in chloroform, excluding α2 (diethyl), which was dissolved in hexafluoroisopropanol. The 100 μl sample solutions were pipetted into the 96-well plates with various binary blend compositions of 0, 25, 50, 75 and 100 wt% and then 100 μl extra solvent was also added to allow more time for interpenetration of each polymer molecule. The solvent in the polymer solutions was allowed to evaporate completely at room temperature and placed on to the Molecular Devices Spectra Max M2 to observe the clarity and miscibility with using a wavelength of 450 nm.

2.3.1.2 Ternary blends based on PLLA

Three-component blends based on PLLA were prepared using the technique described in Section 2.3.1.1. The clarity and miscibility of these blended films were observed using 96-well plates and a UV-visible multi-wavelength plate reader. The different families of three-component blends based on PLLA are shown below:

- PLA/PCL/CAB: effect of stereochemistry using PLLA and PDLLA
- PLLA/PCL/CAB: effect of molecular weight of PLLA and PCL
- PLLA/PCL/CAB and PDLLA/PCL/CAB: effect of solvents
- PLLA/PCL/cellulose esters using CAP and CP
- Blends of PLLA modified with polyester adipate (G40) and P(HB-HV)
- PLLA/PCL/LLA-co-PCL
- PLLA/PCL/TPU
- PLLA/PCL/bionolle 1020 and 3010
- PLLA/PCL/PPS
- PLLA/PCL/PES

The range of ternary blends is shown in Table 2.3 using the symbol X, Y, Z to represent the three component polymers.

Table 2.3 The composition ranges of polymer X/Y/Z blends. For X = PLLA,Y = PCL, Z = CAB the whole range was investigated. For other combination selection from this range were used.

Composition of Polymers (wt%)					
X	**Y**	**Z**	**X**	**Y**	**Z**
5	5	90	15	35	50
5	10	85	15	40	45
5	15	80	15	45	40
5	20	75	15	50	35
5	25	70	15	55	30
5	30	65	15	60	25
5	35	60	15	65	20
5	40	55	15	70	15
5	45	50	15	75	10
5	50	45	15	80	5
5	55	40	20	5	75
5	60	35	20	10	70
5	65	30	20	15	65
5	70	25	20	20	60
5	75	20	20	25	55
5	80	15	20	30	50
5	85	10	20	35	45
5	90	5	20	40	40
10	5	85	20	45	35
10	10	80	20	50	30
10	15	75	20	55	25
10	20	70	20	60	20
10	25	65	20	65	15
10	30	60	20	70	10
10	35	55	20	75	5
10	40	50	25	5	70
10	45	45	25	10	65
10	50	40	25	15	60
10	55	35	25	20	55
10	60	30	25	25	50
10	65	25	25	30	45
10	70	20	25	35	40
10	75	15	25	40	35
10	80	10	25	45	30
10	85	5	25	50	25
15	5	80	25	55	20
15	10	75	25	60	15
15	15	70	25	65	10
15	20	65	25	70	5
15	25	60	30	5	65
15	30	55	30	10	60

Table 2.3 The composition ranges of polymer X/Y/Z blends. For X = PLLA,Y = PCL, Z = CAB the whole range was investigated. For other combination selection from this range were used. (Continued)

Composition of Polymers (wt%)					
X	**Y**	**Z**	**X**	**Y**	**Z**
30	15	55	45	40	15
30	20	50	45	45	10
30	25	45	45	50	5
30	30	40	50	5	45
30	35	35	50	10	40
30	40	30	50	15	35
30	45	25	50	20	30
30	50	20	50	25	25
30	55	15	50	30	20
30	60	10	50	35	15
30	65	5	50	40	10
35	5	60	50	45	5
35	10	55	55	5	40
35	15	50	55	10	35
35	20	45	55	15	30
35	25	40	55	20	25
35	30	35	55	25	20
35	35	30	55	30	15
35	40	25	55	35	10
35	45	20	55	40	5
35	50	15	60	5	35
35	55	10	60	10	30
35	60	5	60	15	25
40	5	55	60	20	20
40	10	50	60	25	15
40	15	45	60	30	10
40	20	40	60	35	5
40	25	35	65	5	30
40	30	30	65	10	25
40	35	25	65	15	20
40	40	20	65	20	15
40	45	15	65	25	10
40	50	10	65	30	5
40	55	5	70	5	25
45	5	50	70	10	20
45	10	45	70	15	15
45	15	40	70	20	10
45	20	35	70	25	5
45	25	30	75	5	20
45	30	25	75	10	15
45	35	20	75	15	10

Table 2.3 The composition ranges of polymer X/Y/Z blends. For X = PLLA, Y = PCL, Z = CAB the whole range was investigated. For other combination selection from this range were used. (Continued)

Composition (wt%)					
X	**Y**	**Z**	**X**	**Y**	**Z**
75	20	5	85	5	10
80	5	15	85	10	5
80	10	10	90	5	5
80	15	5	95	2.5	2.5

The advantage of the rapid screening method is that it generates a large quantity of data which needs to be processed in a visual form. The ternary phase diagrams of a range of three-component blend films were prepared, illustrating ranges in behaviour varying from miscible blends giving rise to clear films and to immiscible blends which give opaque films. To understand how to read the triangle diagram of ternary blends, Figure 2.3 shows the phase miscibility diagram of polymer X, Y and Z with composition along three axes of triangle.

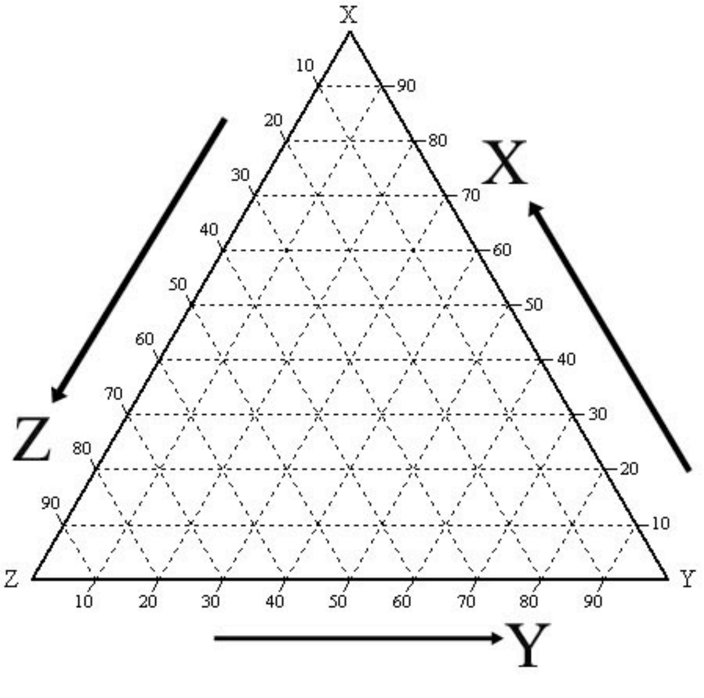

Figure 2.3 Triangle diagram of polymer X/Y/Z.

2.3.2 Melt blending process

Melt blending and reactive blending were used to study the miscibility of ternary blends based on poly(lactic acid). Their compositions were selected from preliminary miscibility observation using the solvent blending technique. The polymer mixtures were melted and blended using a two-roll mill, as shown in Figure 2.4. The polymer samples were pre-heated at 170 ^{o}C for 5 minutes and then mixed together by the two counter-rotating rolls. The ternary blends were normally cut diagonally periodically and folded over several times during mixing for 10 minutes before being removed from the mills. The observed properties of the melt blending composites were analysed by DSC for thermal properties, hot-stage microscopy for morphology, and FT-IR for functional groups.

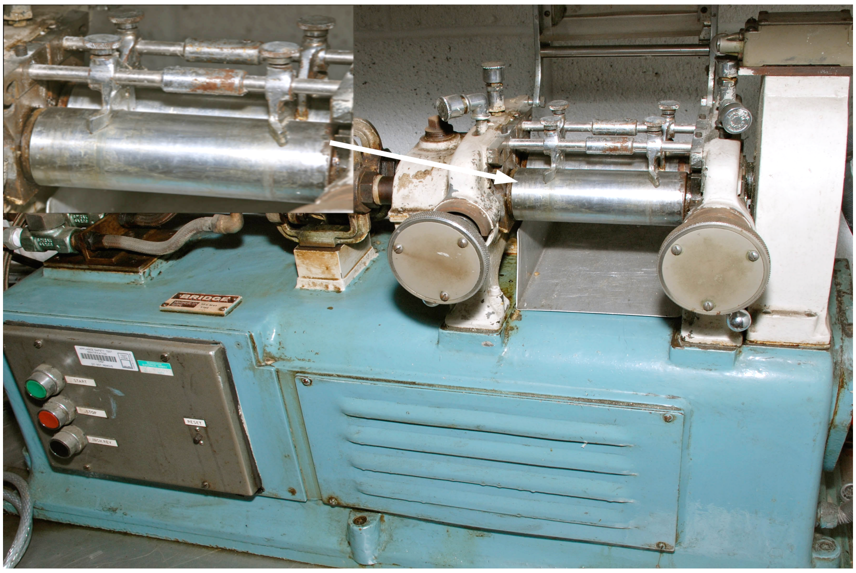

Figure 2.4 Bridge two-roll mill.

2.4 General experimental techniques

The polymer samples were analysed using a variety of different techniques to determine specific properties. Each one of the following techniques is described in more detail in the following sections.

- Microplate reader for % transmittance
- Gel Permeation Chromatography (GPC) for measuring the relative molecular weight distributions
- ^{13}C and ^{1}H Nuclear Magnetic Resonance Spectroscopy (NMR) for observing the molecular structures
- Fourier Transform Infrared Spectroscopy (FT-IR) for observing the functional groups and the C-H environment along the back-bone
- Differential Scanning Calorimetry (DSC) for observing the thermal properties
- Scanning Electron Microscopy (SEM) for observing morphologies
- Hot Stage Microscopy (HSM) for observing thermal properties and morphologies
- Wide-Angle X-ray Scattering (WAXS) for observing the distance between polymer segments and the extent of crystallinity in the polymer samples

2.4.1 UV/Visible Plate Reader

The Molecular Devices Spectra Max M2, which is a UV/Visible plate reader, was used to observe the percent transmittance (%T) of solvent blends. The Molecular Devices Spectra Max M2 is a multi-detection microplate reader with dual-mono chromators, dual-mode cuvette ports and top-reading capability. Detection modalities include absorbance (UV-Visible absorbance) and fluorescence intensity (FI). The system has optical performance comparable to a top-of-the-range dedicated spectrophotometer or spectro-fluorometer and can read 6- to 384-well microplates. The optical system has an integrated dual-mode cuvette port and microplate reading. A schematic diagram is shown in Figure 2.5 [68].

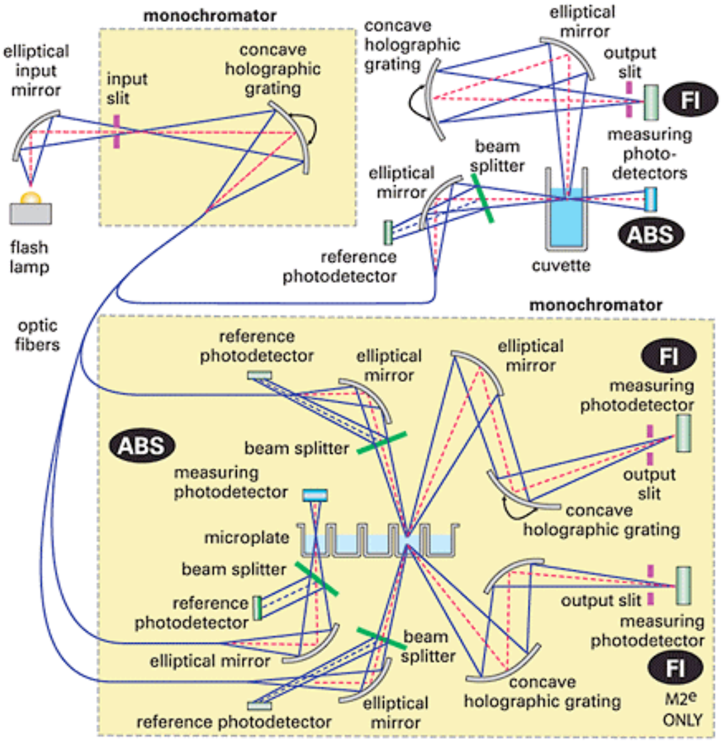

FI = fluorescence intensity; ABS = absorbance (UV-Vis Abs)

Figure 2.5 The operating systematic diagram of UV/Visible plate reader.

2.4.2 Gel Permeation Chromatography (GPC)

The relative molecular weight distribution of the organic-soluble polymers was analysed using a Knauer gel chromatograph fitted with two PLgel 5μm mixed-C columns which is shown in Figure 2.6. A personal computer running in built PL Calibre software was used to calculate the relative molecular weight by using polystyrene as a calibrating standard. The organic solvent, usually tetrahydrofuran, was used as a mobile phase.

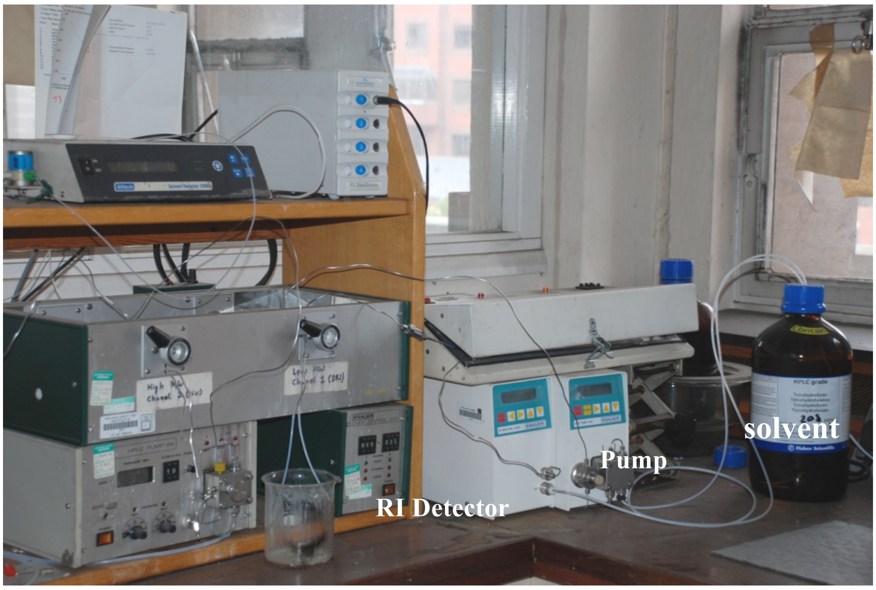

Figure 2.6 Gel Permeation Chromatography (GPC) equipment.

0.1 mg/ml polymer solutions were prepared using THF as a solvent and a few drops of toluene as a marker and injected into the column with a flow rate 1.0 ml/min. Low molecular weight polymers take longer to elute from the columns due to the greater permeable volume of solvent within the pores, which contain cross-linked PS gel. A plot of retention time versus detector response (mV) and log MW was recorded. The molecular weights of PLLA and PCL samples were analysed by GPC, which separates polymer chains according to size, due to distribution of pores.

2.4.3 ^{13}C and ^{1}H Nuclear Magnetic Resonance Spectroscopy (NMR)

^{13}C and ^{1}H NMR were used to study the molecular structures. When a sample is placed in a magnetic field and perturbed with a pulse of radio frequency energy, the nuclei in the molecule generate a bulk macroscopic magnetisation. The response of the system as it relaxes back towards equilibrium is observed in terms of chemical shift (δ) in parts per million (ppm) from the resonance associated with tetramethylsilane (TMS), an internal standard [69].

The molecular structures of the pre-synthesised α-ester homologues of poly(lactic acid) were determined with both ^{13}C NMR and ^{1}H NMR. α1(dimethyl), α4(cyclohexyl),

α5(cycloheptyl), α6(chloromethyl-methyl), ArS1(pentafluorophenyl-methyl), ArS3(phenyl), copolymer of ArS1 and ArS3, copolymer of ArS1 and PGA(synthesised), were dissolved in deuterated chloroform ($CDCl_3$), while α2(diethyl) was firstly dissolved in hexafluoro-isopropanol and then in $CDCl_3$. α3(cyclopentyl) was prepared in deuterium chloride (DCl) containing 25% deuterium oxide (D_2O). ArS2(phenyl-methyl) was prepared in $CDCl_3$ and deuterated dimethyl sulfoxide (d_6-DMSO). PGA (synthesised) was prepared in DMSO. The samples were studied with a Bruker 300 MHz NMR instrument using the polarisation enhancement during analysis nuclei technique (PENDANT) [70, 71]. Both ^{13}C NMR and ^{1}H NMR spectra were integrated and edited on a personal computer using Win NMR software from Bruker.

The PENDANT technique allows the detection of any insensitive nuclei, principally ^{13}C coupled to ^{1}H. In particular, it enables the simultaneous detection of C, CH, CH_2 and CH_3 carbon resonances. Carbon as CH_3 and CH appear as positive peaks whereas the ones of CH_2 and C as negative peaks in the ^{13}C PENDANT spectra.

2.4.4 Fourier Transform Infrared Spectroscopy (FT-IR)

In this work, FT-IR (Thermo Nicolet 380 model) was used to identify the miscibility of ternary blends. The first step, a background spectrum was measured to be a relative scale for the absorption intensity. This can be compared to the measurement with the sample in the beam to determine the percent transmittance (%T). In the second step, a solid sample was placed onto the sample compartment and pressed with a diamond plate. The beam emitted from a glowing black-body source passes through an aperture which controls the amount of energy presented to the sample, enters the interferometer resulting the interferogram signal, and then enters the sample compartment. The beam finally passes to the detector, which is specially designed to measure the special interferogram signal and sent to the computer where the Fourier transformation takes place. The final infrared spectrum is then presented. These processes are simple as described in Figure 2.7 [72].

Figure 2.7 The operating systematic diagram of Fourier Transform Infrared Spectroscopy (FT-IR) equipment [72].

2.4.5 Differential Scanning Calorimetry (DSC)

DSC is widely used to characterise the thermal properties of polymers. It can measure thermoplastic properties including melting temperature (T_m), glass transition temperature (T_g), percent crystallinity, and heat of melting. In this work, however, T_g and T_m are the most important properties to be observed. A Perkin Elmer DSC7 Differential Scanning Calorimeter, with and without an intercooler for subambient operation, was used. Perkin Elmer DSC7 runs the Pyris software and is equipped with the hardware and software to conduct Dynamic DSC (DDSC). In DDSC, a modulated temperature profile is directly applied to the sample and the response of the sample analysed by Fourier transformation [73] .

Indium was used to calibrate the equipment and a baseline was then performed by running a reference pan (an empty alumimum pan). A polymer sample, approximately 6.0-10.0 mg, is placed in the aluminum pan, covered with an aluminum plate cover, and pressed by using a press plate. A reference and sample pan were placed into the reference and sample holders, respectively, and operated with a scanning rate 20 ^{o}C/min, heating from 20 to 190 ^{o}C under a nitrogen atmosphere. However, these operating conditions depend on the thermoplastic properties of polymer samples. The difference in the amount of heat required to increase the temperature of a sample and reference were measured as a function of temperature. When the temperature increases, an amorphous phase in polymer molecule will become viscous that means T_g may occur. As the sample is heated eventually reaches its T_m, the melting process results in an endothermic peak in the DSC curve which plots the heat flow (mV) versus temperature (^oC).

2.4.6 Scanning Electron Microscopy (SEM)

The morphology of polymer solution blended films was examined by SEM, using a Cambridge Stereoscan S90B model. Polymer films were mounted on metal stubs and placed in a small sputter coater vacuum chamber. Argon gas and electric field cause an electron to be removed from argon, making the atoms positively charged, and attracted to a negatively charged gold foil. Argon ions knock gold atoms from the gold foil surface and these gold atoms then fall and settle onto the film surfaces giving higher electron density cover. This sample preparation technique is necessary because SEM is an instrument that produces a large magnification by using electrons to form an image.

The gold covered sample films were placed onto the stage of the SEM machine. An electron beam is produced at the top of microscope by an electron gun. The electron beam passes through the microscope in a vertical direction and moves through electromagnetic fields and lenses, which focus the electron beam down toward the sample films. As the electron beam hits the sample films, electron and X-rays are ejected from the films (Figure 2.8). These X-rays, backscattered electrons, and secondary electrons are collected and converted by detectors into a signal that is sent to a screen producing an SEM image. The schematic diagram of SEM is shown in Figure 2.9 [74].

Figure 2.8 Ejected beams of SEM samples [74].

Figure 2.9 The operating systematic diagram of SEM equipment [74].

2.4.7 Hot Stage Microscopy (HSM)

Hot stage microscope (HSM) (model Mettler FP 82 Hot Stage with central processor- Mettler Toledo FP90 and lens-Leica DME 10X) was used to observe thermal properties and morphology of polymers, as shown in Figure 2.10. A small amount of polymer sample was put onto the microscope slide, pre-melted at its melting temperature, covered with the cover-slid, and then cooled to room temperature before testing. This sample was placed into the hot stage box and then placed on the microscope stage. The sample was heated rapidly to its melting temperature, held for 5 minutes, and then cooled down to room temperature at the constant rate of 10 °C/min. The intensity of light, image, and video were recorded.

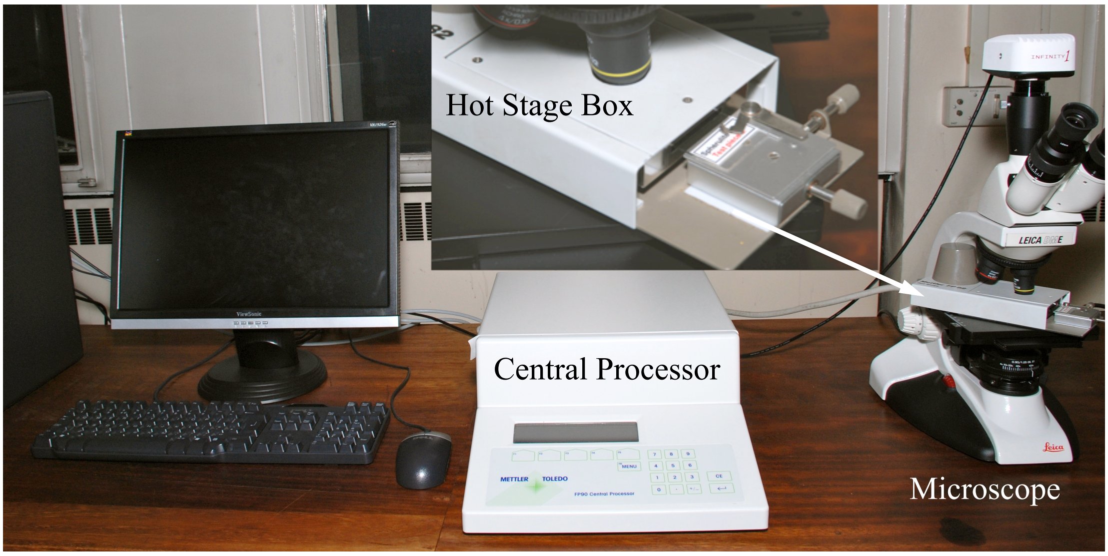

Figure 2.10 Hot stage microscope with computer processor.

2.4.8 Wide-Angle X-ray Scattering (WAXS) Analysis

Wide-angle X-ray scattering (WAXS) was used to analyse the distance between polymer segments and the extent of crystallinity in the samples. Two samples; (i) powders of pre-synthesised α-ester homologues of poly(lactic acid) reproducing from a previous worker in these laboratories [5], and (ii) solution blended films, were studied.

(i) Pre-synthesised α-ester homologues of poly(lactic acid) powders

X-ray powder photographs were taken using a Phillips 11.46 cm diameter powder camera fitted with a 0.5 mm collimator. The samples were mounted in lithium beryllium borate tubes and the X-rays generated from a copper target at 40 kV using a nickel fitter enabling only copper K_α radiation to be used. The film was processed after one and a half hours of exposure. For some (later) samples, the film was replaced by a defractometer/ plotter system. The powder photographs, reproduced from Blackbourn [5] are shown in Figure 2.11.

Figure 2.11 The X-ray powder photographs of pre-synthesised poly(α-esters) [5].

(ii) Solution-blended films

The solution-blended films were prepared for WAXS analysis. WAXS experiments were performed using Beamline I22 at the Diamond Light Source, Rutherford, UK. Scans of intensity versus scattered angle (2θ) were recorded at room temperature with identical settings of the instrument by using an In-vacuum U25 undulator source (1.241 Å) and an operating voltage of 10 keV. The sample intensities were normalised (to remove the effect of the film thickness and fluctuations in beam intensity) and then subtracted with the background intensities. To calculate the distance between polymer segments (d spacing), Bragg's law [75] was applied, as shown below.

$$n\lambda = 2d \sin(\theta) \qquad \text{Eq. 2.1}$$

where; n is an integer, λ is the wavelength of the x-rays (Å), d is the distance between polymer segments referred to as d spacing, and θ is scattering angle. The WAXS traces of samples were plotted to show intensity versus d spacing value.

CHAPTER 3

CHARACTERISATION OF POLY(α-ESTER) HOMOLOGUES

Chapter 3

Characterisation of poly(α-ester) homologues

The materials characterised in this chapter are all homologues of poly(lactic acid). They share the poly(α-ester) repeat unit:

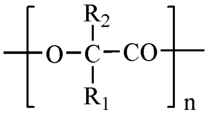

$$\left[-O-\overset{R_2}{\underset{R_1}{C}}-CO- \right]_n$$

in which R_1 = H and R_2 = CH_3 for PLA itself. These materials were all synthesised in these laboratories, as described in Chapter 2. The synthetic routes are summarised briefly in Figure 3.1.

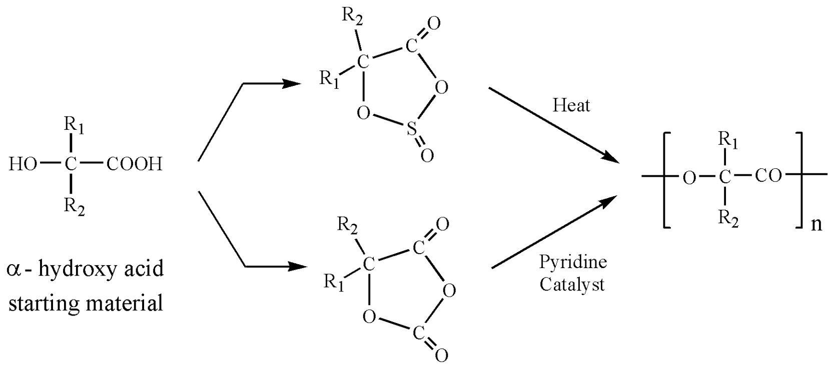

Figure 3.1 The synthetic routes for poly(α-ester) homologues.

Poly(lactic acid) and its homologues are poly(α-esters), which contain the ester functional group and substituent, aliphatic and aromatic groups, on the position of the α-carbon in their main chains. These poly(α-esters) possess different characteristic chain structures consisting of the different multiple repeat units that are related to a particular trend of miscibility in polymer blends based on PLLA. Therefore, ^{13}C and ^{1}H nuclear magnetic resonance spectroscopy (NMR), differential scanning calorimetry (DSC) and hot-stage microscope are used to characterise novel polyesters, particularly poly(α-esters) to notify the effect of substituent groups on the compatibility of polymers. All poly(α-ester) homologues used in this work are shown in Table 3.1.

Table 3.1 Pre-synthesised poly(α-esters).

Symbols	Poly(α-esters)	Pendent groups	Molecular Structures
Aliphatic α-polyesters			
PGA (synthesised)	Poly(2-hydroxy ethanoic acid) or Poly(glycolic acid)	-H, -H	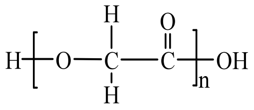 $H\!\left[O-\underset{H}{\overset{H}{C}}-\overset{O}{\overset{\|}{C}}\right]_n\!OH$
α1(dimethyl)	Poly(2-hydroxy-2-methyl-propanoic acid)	$-CH_3$, $-CH_3$	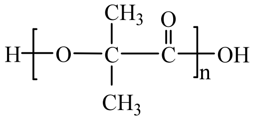 $H\!\left[O-\underset{CH_3}{\overset{CH_3}{C}}-\overset{O}{\overset{\|}{C}}\right]_n\!OH$
α2(diethyl)	Poly(2-hydroxy-2-ethyl-butanoic acid)	$-C_2H_5$, $-C_2H_5$	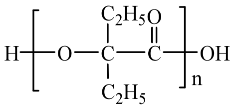 $H\!\left[O-\underset{C_2H_5}{\overset{C_2H_5}{C}}-\overset{O}{\overset{\|}{C}}\right]_n\!OH$
α3(cyclopentyl)	Poly(2-hydroxy-2-cyclopentyl-ethanoic acid)	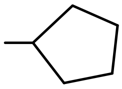	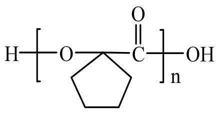
α4(cyclohexyl)	Poly(2-hydroxy-2-cyclohexyl-ethanoic acid)	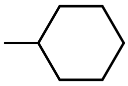	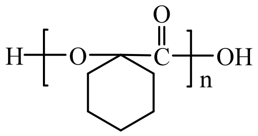
α5(cycloheptyl)	Poly(2-hydroxy-2-cycloheptyl-ethanoic acid)	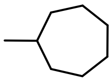	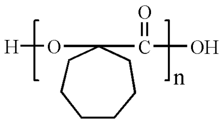
α6(chlorometyl -methyl)	Poly(2-hydroxy-2-chloromethyl-propanoic acid)	$-CH_3$, $-CH_2Cl$	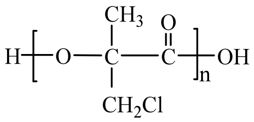 $H\!\left[O-\underset{CH_2Cl}{\overset{CH_3}{C}}-\overset{O}{\overset{\|}{C}}\right]_n\!OH$

Table 3.1 Pre-synthesised poly(α-esters). (Continued)

Symbols	**Poly(α-esters)**	**Pendent groups**	**Molecular Structures**
Aromatic α-polyesters			
ArS1 (pentafluoro phenyl-methyl)	Poly PFAAC: Poly(2-hydroxy-2-pentafluorophenyl propanoic acid)	$-CH_3$, 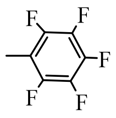	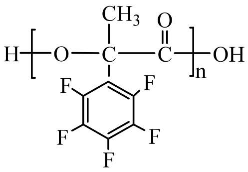
ArS2 (phenyl-methyl)	Poly AAAC: Poly(2-hydroxy-2-phenyl propanoic acid	$-CH_3$, 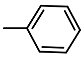	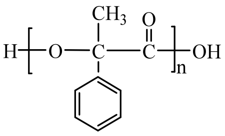
ArS3 (phenyl)	Poly MAAC: Poly(2-hydroxy-2-phenyl ethanoic acid	-H, 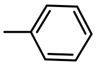	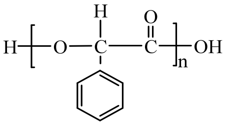
Copolymer of ArS1 and ArS3	Copolymer of poly(2-hydroxy-2-pentafluoro phenyl propanoic acid) and poly(2-hydroxy-2-phenyl ethanoic acid)	Pendent of ArS1 and ArS3	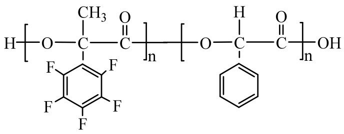
Copolymer of ArS1 and PGA (synthesised)	Copolymer of poly(2-hydroxy-2-pentafluoro phenyl propanoic acid) and poly(glycolic acid)	Pendent of ArS1 and PGA (synthesised)	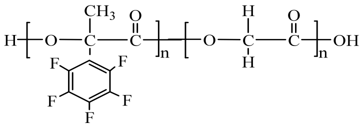

Pre-synthesised poly(α-esters) were analysed to determine their number average molecular weights (M_n) and approximate average degree of polymerisation (DP) by gel permeation chromatography (GPC) [5, 6] The M_n and some general properties of these poly(α-esters) are given in Table 3.2.

Table 3.2 Number average molecular weight (M_n), degree of polymerisation (DP), crystallinity, and solubility in chloroform of pre-synthesised poly(α-esters).

Pre-synthesised poly(α-esters)	**M_n**	**DP**	**Crystallinity**	**Solubility (in chloroform)**
Aliphatic α-polyesters:				
α1(dimethyl)	6000	70	Crystalline	Yes
α2(diethyl)	19000	165	Crystalline	No[*1]
α3(cyclopentyl)	9260	83	Amorphous	Yes
α4(cyclohexyl)	12240	97	Amorphous	Yes
α5(cycloheptyl)	1760	12	Amorphous	Yes
α6(chlorometyl-methyl)	12000	149	Amorphous	Yes
Aromatic α-polyesters:				
ArS1 (pentafluorophenyl-methyl)	2900	-	Amorphous	Yes
ArS2(phenyl-methyl)	1774	-	Amorphous	Yes[*2]
ArS3(phenyl)	2972	-	Amorphous	Yes
Copolymer of ArS1 and ArS3	801	-	Amorphous	Yes
Copolymer of ArS1 and PGA(synthesised)	696	-	Amorphous	Yes

Note: [*1] α2(diethyl) required addition of hexafluoroisopropanol to aid dissolution. [*2] difficult to dissolve.

3.1 NMR analysis of the molecular structures of poly(α-esters)

^{1}H NMR and ^{13}C NMR were carried out to study the molecular structures of these polymers. The assignment of the chemical shifts, as shown by letters (a, b, c etc.), are shown along with the corresponding polymer structures.

3.1.1 α1(dimethyl):

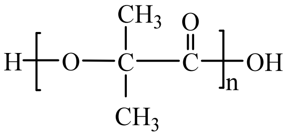

$$H\left[O-\overset{CH_3}{\underset{CH_3}{C}}-\overset{O}{\overset{\|}{C}}\right]_n OH$$

α1(dimethyl) is effectively the first systematic homologue of PLA, having two symmetrical methyl pendent groups at the α-carbon in the backbone. It was dissolved in deuterated chloroform ($CDCl_3$) for the NMR analysis. Figures 3.2(A) and (B), respectively, display the ^{1}H NMR and ^{13}C NMR spectra of α1(dimethyl).

It is clear from the proton spectrum, Figure 3.2(A), that peak *a* at a chemical shift of 1.6 ppm corresponds to the constituent protons of the two-methyl groups. The methyl protons in α1(dimethyl) are shown as a single peak because they do not cause splitting among themselves.

From the carbon spectrum, Figure 3.2(B), peaks at positions *a, b* and *c* at chemical shifts of 23.9, 78.8 and 170.7 ppm are assigned to $-CH_3$, -C-, and C=0, respectively. Both of the proton and carbon spectra show aromatic hydrocarbon contaminant peaks (probably from nitrobenzene used as a solvent in polymerisations) at a chemical shift of 7.6-8.4 and 123-135 ppm, respectively. ^{1}H and ^{13}C NMR peaks of $CDCl_3$ are also shown in the figure.

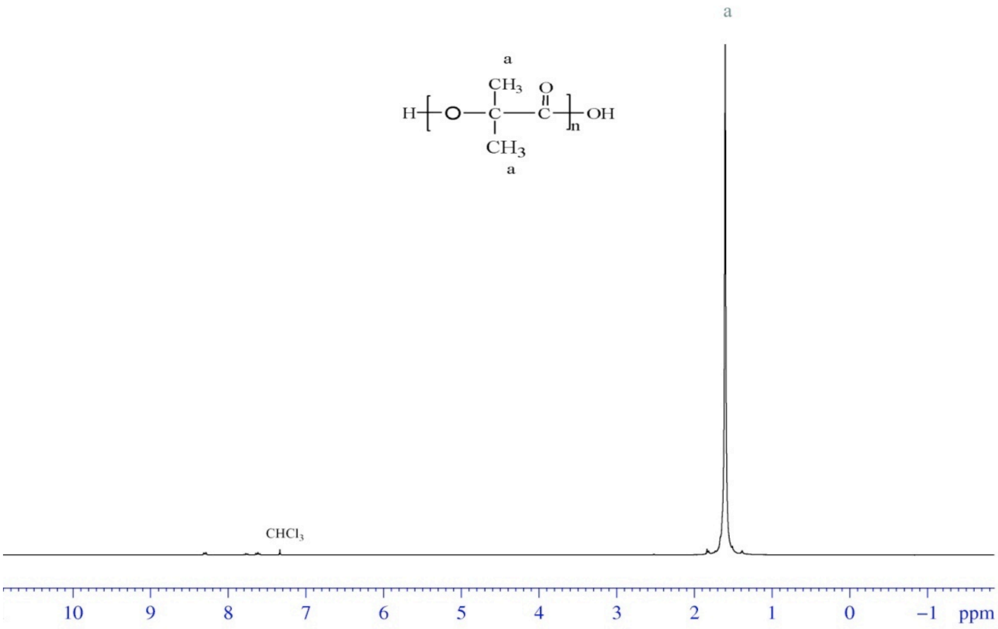

(A)

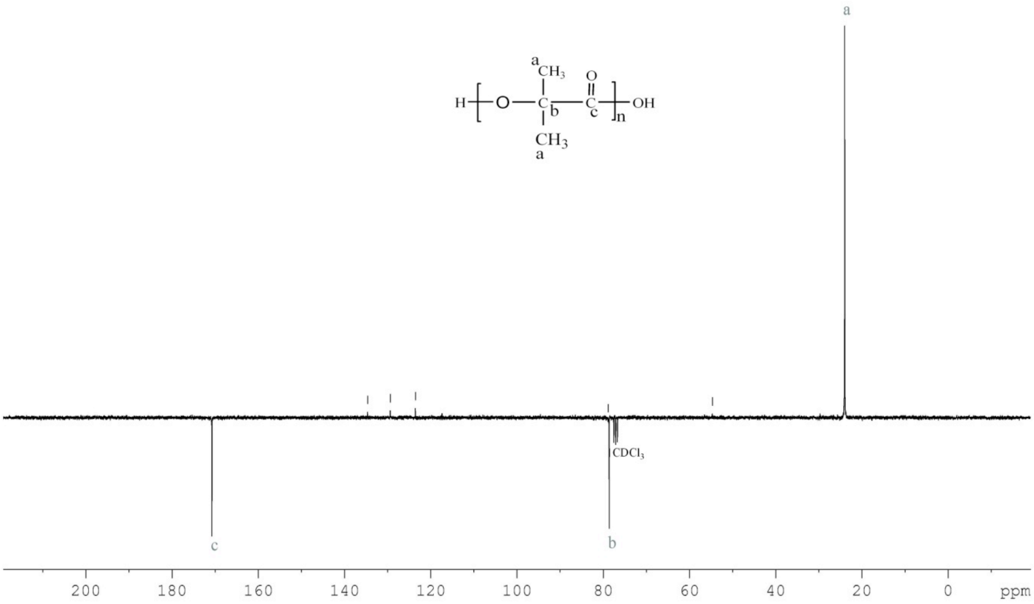

(B)

Figure 3.2 ^{1}H NMR (A) and ^{13}C NMR (B) spectra of α1(dimethyl) recorded in $CDCl_3$.

3.1.2 α2(diethyl):

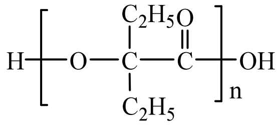

$H\left[O-\overset{C_2H_5}{\underset{C_2H_5}{C}}-\overset{O}{\overset{\|}{C}}\right]_n OH$

α2(diethyl) is effectively the second poly(α-ester) homologue after α1(dimethyl) studied in this research. It contains two ethyl groups at the α-carbon in the backbone, which gives α2(diethyl) a symmetrical structure. The chemical structure of α2(diethyl) was also studied by NMR. α2(diethyl) was dissolved in $CDCl_3$ and a few drops of hexafluoroisopropanol (HFIP) were added to aid dissolution. Figures 3.3(A) and (B), respectively, display the ^1H NMR and ^{13}C NMR spectra of α2(diethyl).

It can be seen from the proton spectrum, Figure 3.3(A), that peak *a* represents protons from $–CH_3$ groups at a chemical shift of 0.9 ppm and peak *b* protons from $–CH_2$ which appear at a chemical shift of 2.0 ppm. Proton peaks from $CDCl_3$ occur at a chemical shift of 7.3 ppm and HFIP at a chemical shift of 4.4 ppm. The peak at a chemical shift of 3.2 ppm is that of hydroxyl protons (-OH). These hydroxyl protons are expected because protons from water or residual hydroxy acid starting material may be presented.

From the carbon spectrum, Figure 3.3(B): peak *a* at a chemical shift of 7.0 ppm represents carbon atoms from $–CH_3$ groups; peak *b* at a chemical shift of 27.0 ppm corresponds to carbon atoms from $–CH_2$ groups; peak *c* at a chemical shift of 86.0 ppm corresponds to α-carbons in the backbone; peak *d* at a chemical shift of 170.0 ppm corresponds to carbonyl carbons from –C=O groups. Two peaks of the carbon atoms from –CH and –CF in HFIP and one peak of the carbon atom from $CDCl_3$ are also shown in this figure.

It can be observed that the methyl groups of α1(dimethyl) resonate at lower field strengths increasing the chemical shift values compared to that of α2(diethyl). The NMR spectra of α2(diethyl) shows a number of changes when compared with α1(dimethyl).

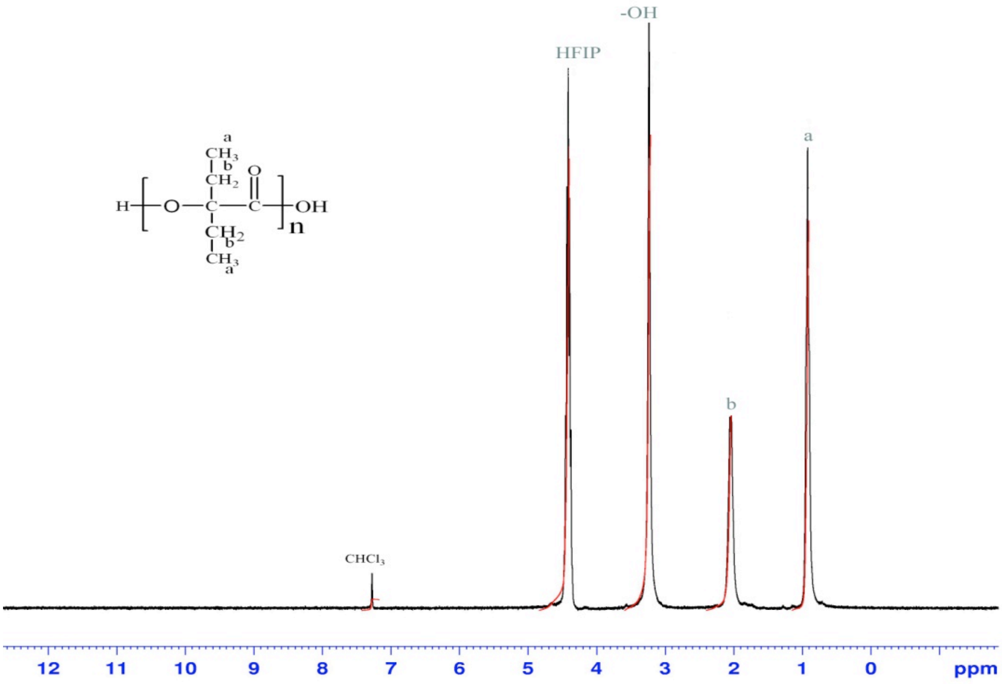

(A)

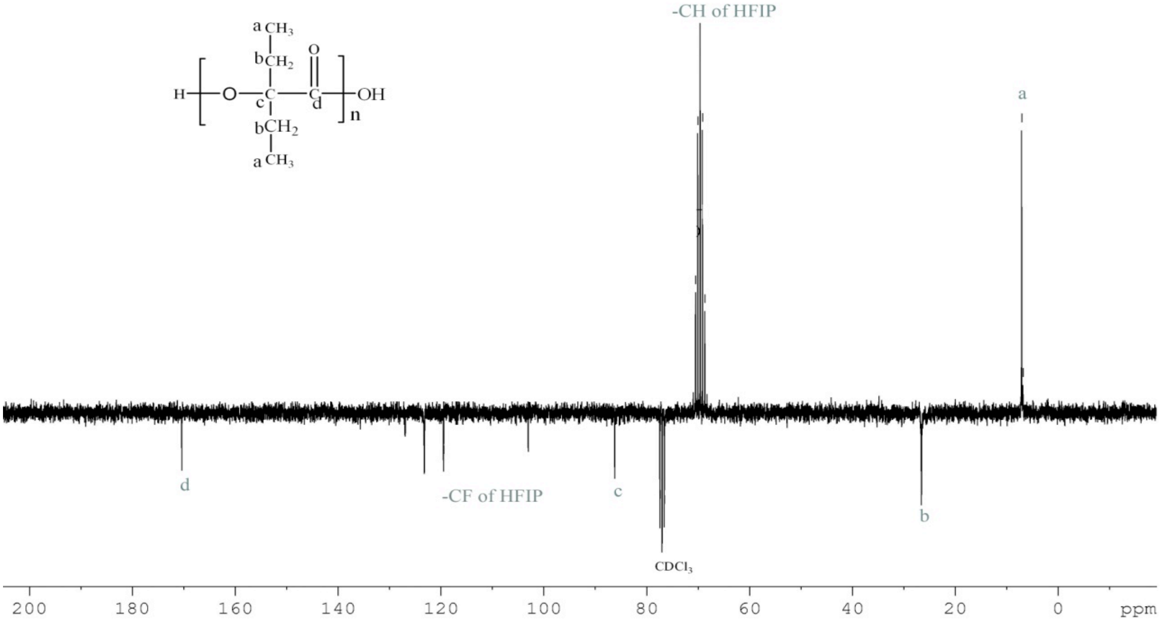

(B)

Figure 3.3 ^{1}H NMR (A) and ^{13}C NMR (B) spectra of α2(diethyl) recorded in HFIP and $CDCl_3$.

3.1.3 α3(cyclopentyl):

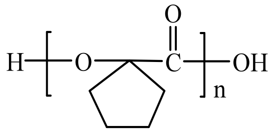

α3(cyclopentyl) is one of the poly(α-ester) homologues having cycloalkyl groups, in this case cyclopentyl linked to the backbone with a carbon atom shared between the backbone and cyclic substituent. It is dissolved in deuterated water (D_2O) and deuterium chloride (DCl) for NMR analysis. The ^1H NMR and ^{13}C NMR spectra of α3(cyclopentyl) with the detailed assignment of the different peaks are shown in Figures 3.4(A) and (B), respectively.

A typical proton spectrum, Figure 3.4(A), shows three different proton peaks corresponding to three different positions of methylene hydrogens in cyclopentyl rings, in addition to peak *a* at a chemical shift of 1.6 ppm, *b* at 1.7 ppm and *c* at 2.0 ppm. Proton peaks of water and hydrochloric acid show at a chemical shift of 8.6 ppm.

From the carbon spectrum, Figure 3.4(B), two carbon peaks located at the positions *a* and *b* are methylene protons at the symbol a and b in cyclopentyl ring, which appear at chemical shifts of 21.5 ppm and 38.0 ppm, respectively. Peak *c* at a chemical shift of 79.6 ppm represents quaternary carbons in cyclopentyl ring at the position c in the structure. The ^{13}C NMR peak of carbonyl carbons (C=O) shows a very weak signal at a chemical shift of around 170 ppm.

However, both NMR spectra confirm the particular structure of α3(cyclopentyl) and show no other contaminating substances in this sample.

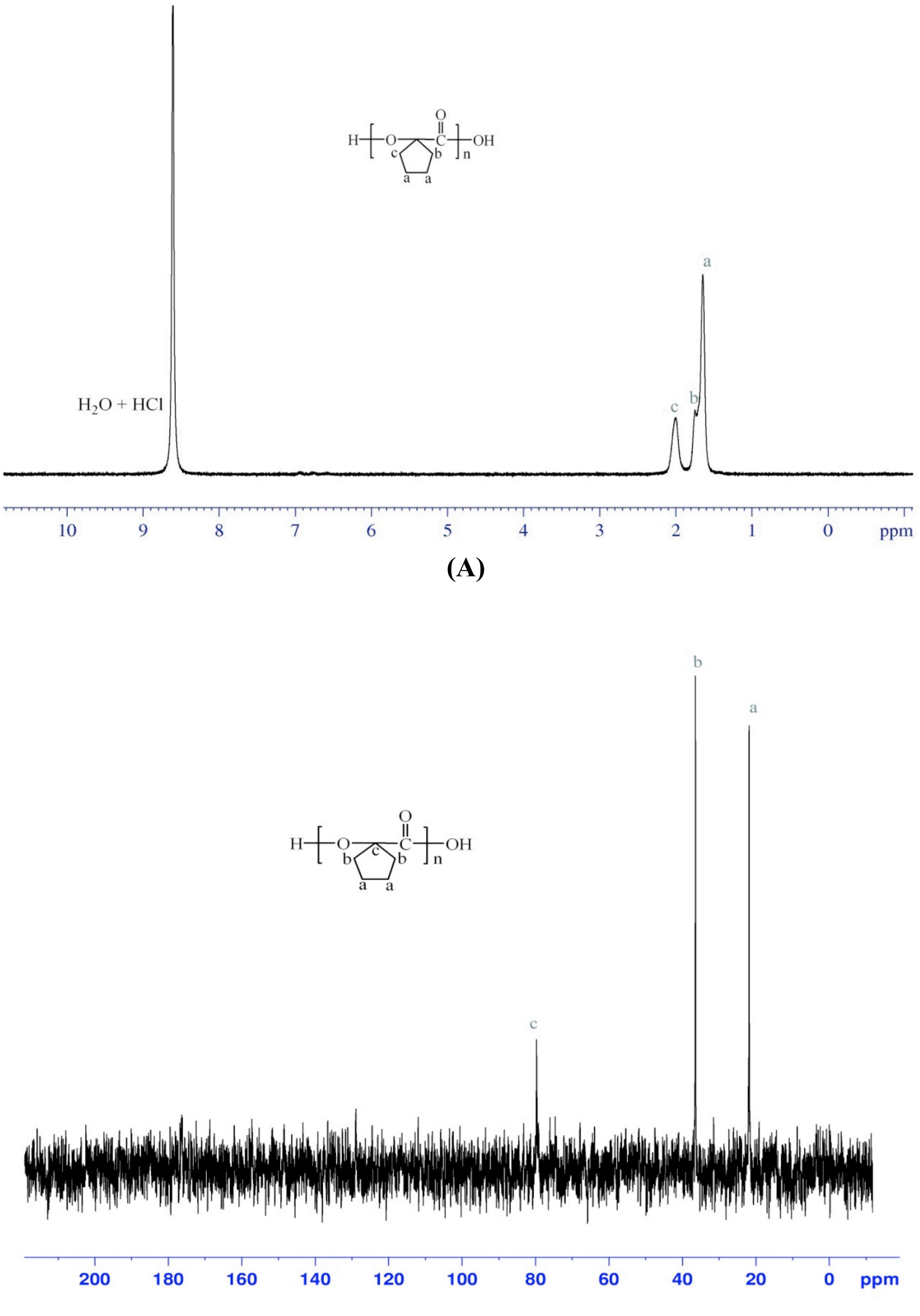

(A)

(B)

Figure 3.4 ^{1}H NMR (A) and ^{13}C NMR (B) spectra of α3(cyclopentyl) recorded in D_2O and DCl.

3.1.4 α4(cyclohexyl):

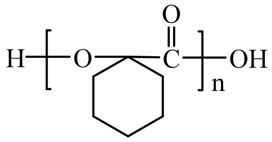

^{1}H and ^{13}C NMR spectroscopy was used to characterise the molecular structure of α4(cyclohexyl) by dissolving α4(cyclohexyl) in deuterated chloroform. α4(cyclohexyl) has a six-membered ring of cyclohexyl at the α-position of the backbone instead of a five-member ring of cyclopentyl as seen in α3(cyclopentyl). The cyclohexyl ring in α4(cyclohexyl) contains four different methylene protons, which have dissimilar neighbours and would be expected to show four different proton peaks in NMR spectra.

Figure 3.5(A), shows the ^{1}H NMR spectrum of α4(cyclohexyl) with annotated assignments. The four different methylene proton peaks of α4(cyclohexyl) at the positions *a*, *b*, *c* and *d* appear at chemical shifts of 1.4 ppm, 1.7 ppm, 1.9 ppm and 2.2 ppm, respectively. The peak at the chemical shift of 7.3 ppm is of chloroform protons, which is seen at the same position in the spectrum of α1(dimethyl) and α2(diethyl). The protons from contaminating aromatic hydrocarbon (likely to be from nitrobenzene used as a solvent in the polymerisation) are also shown at chemical shifts between 7.6 and 8.4 ppm, corresponding to those seen in the spectrum of α1(dimethyl).

The ^{13}C NMR spectrum of α4(cyclohexyl) is shown in Figure 3.5(B) with the detailed structure assignments. Peaks at the positions *a*, *b* and *c*, at chemical shifts of 21.2 ppm, 25.1 ppm and 32.1 ppm, are assigned to methylene carbons contained in the cyclohexyl ring at the symbols a, b and c as shown in the chemical structure. Peak *d* is assigned to the quaternary carbon, appearing at a chemical shift of 80.8 ppm. Peak *e* corresponds to carbonyl carbons α4(cyclohexyl), and can be observed at a chemical shift of 170.6 ppm. The carbon peak from $CDCl_3$ is seen at the chemical shift of 78.0 ppm.

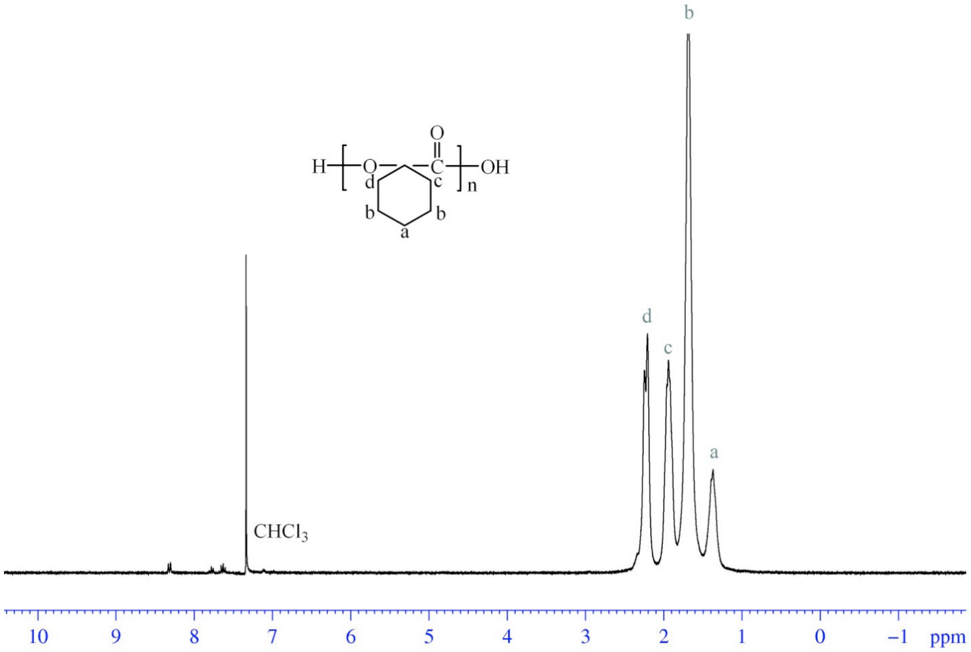

(A)

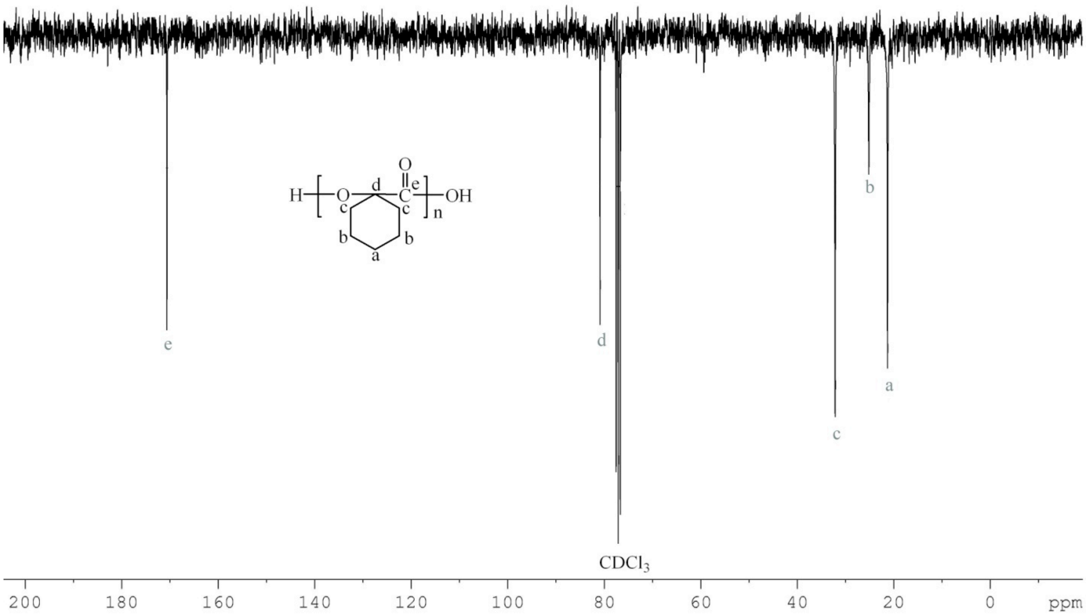

(B)

Figure 3.5 ^{1}H NMR (A) and ^{13}C NMR (B) spectra of α4(cyclohexyl) recorded in $CDCl_3$.

3.1.5 α5(cycloheptyl):

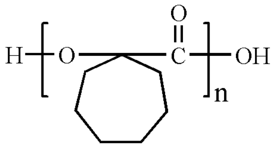

α5(cycloheptyl) is a poly(α-ester) containing the cycloheptyl group in the backbone. Its molecular structure was studied by NMR after first dissolving in $CDCl_3$. Figures 3.6(A) and (B), respectively, display the ^1H NMR and ^{13}C NMR of α5(cycloheptyl) with molecular assignment.

Peaks at the positions *a*, *b* and *c*, at chemical shifts of 1.6, 2.1 and 2.3 ppm in the proton spectrum (Figure 3.6(A)), are assigned to the three different regions of the methylene protons shown with the symbols a, b and c in the chemical structure. The peak at the chemical shift of 7.3 ppm corresponds to chloroform protons, which is seen at the same position in the spectrum of α1(dimethyl), α2(diethyl), and α4(cyclohexyl).

The carbon spectrum, Figure 3.6(B), shows three single peaks of *a*, *b* and *c*, approximately the same height of the equal amount of methylene carbons at the symbols a, b, and c in the chemical structure. Peak *d*, at a chemical shift of 85.0 ppm, is that of the quaternary carbon in cycloheptyl. Peak *e* corresponds to carbonyl carbons certainly observed at the chemical shift of 170.0 ppm. The carbon peak from $CDCl_3$ is seen at the chemical shift of 78.0 ppm.

The relative assignment of all peaks in compounds confirmed that the α5(cycloheptyl) sample contains a comparatively small quantity of contaminants.

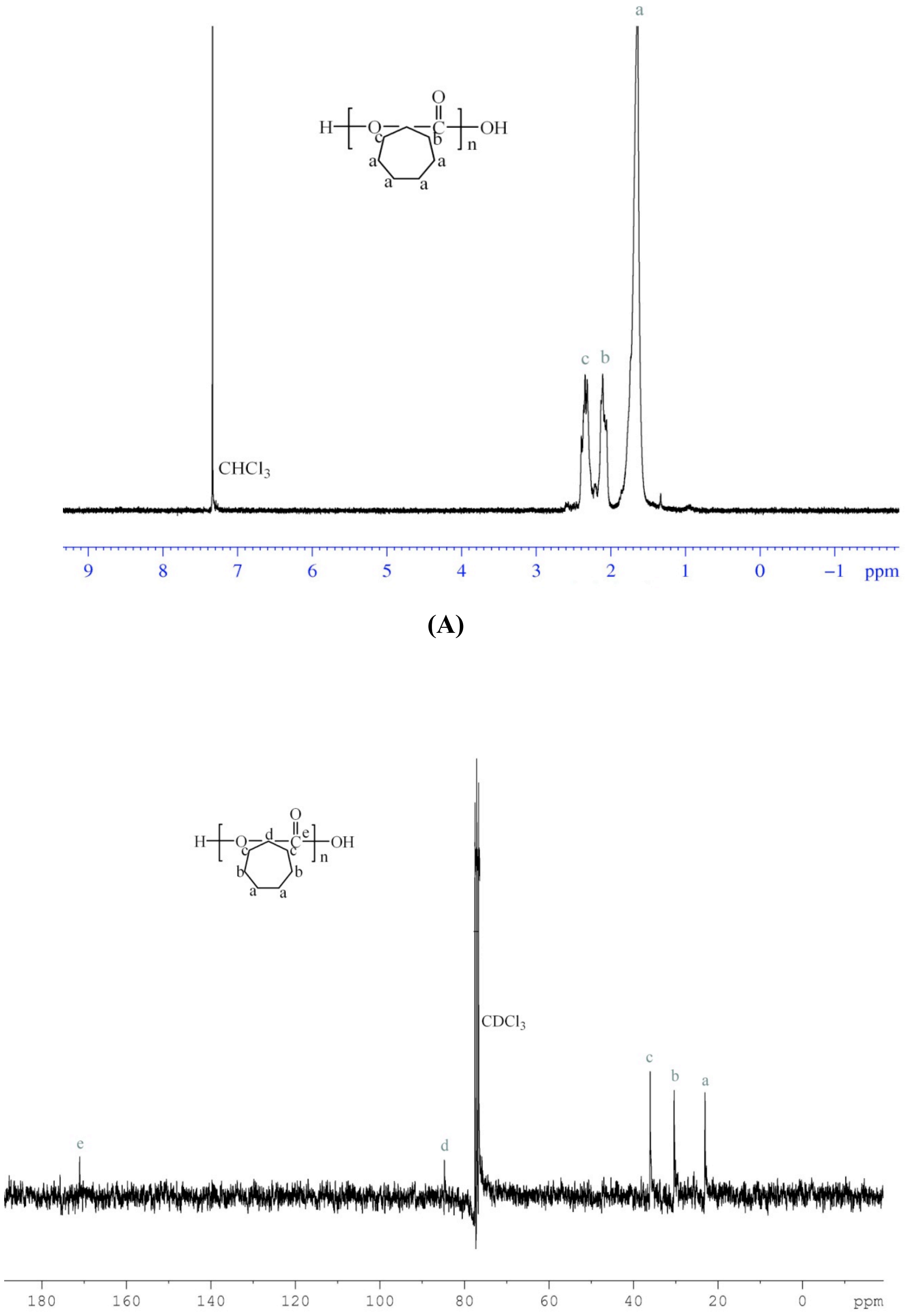

(A)

(B)

Figure 3.6 ^{1}H NMR (A) and ^{13}C NMR (B) spectra of α5(cycloheptyl) recorded in $CDCl_3$.

3.1.6 α6(chloromethyl-methyl):

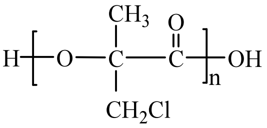

$$H-\left[O-\overset{CH_3}{\underset{CH_2Cl}{C}}-\overset{O}{\overset{\|}{C}}\right]_n-OH$$

α6(chloromethyl-methyl) is an unsymmetrically substituted poly(α-ester) containing a methyl group and chloromethyl group at the α-carbon in the backbone. Its molecular structure was studied by NMR after first dissolving in $CDCl_3$. Figures 3.7(A) and (B), respectively, display the ^1H NMR and ^{13}C NMR of α6(chloromethyl-methyl) with molecular assignment.

From the proton spectrum, Figure 3.7(A), peak *a* corresponds to the methyl protons shown at a chemical shift of 1.6 ppm. Peaks *b1* and *b2* at chemical shifts of 3.8 and 4.1 ppm are slightly different. This poly(α-ester) has an asymmetric carbon atom (like PLA). It will thus have effectively D and L sequences in the backbone. Such a chemical shift is consultant with the difference between DD or LL and D-L. It is the strong polarisation of the CH_2Cl that causes the shift. The peak at a chemical shift of 7.3 ppm corresponds to chloroform protons

From the carbon spectrum, Figure 3.7(B); peaks *a1* and *a2* at chemical shifts of 18.0 and 19.0 ppm correspond to the methyl carbons: peaks *b1 and b2* at chemical shifts of 46.0 and 47.0 correspond to the methylene carbons: peaks *c1* and *c2* at chemical shifts of 82.0 and 83.0 correspond to the quaternary carbons: peaks *d1* and *d2* at chemical shifts of 168.0 and 168.5 correspond to the hydroxyl carbons. It can be seen the slightly difference of carbon peaks between a1 and a2 for instant, which is caused by the difference between DD or LL and D-L sequences in the α6(chlorometyl-methyl) backbone. It is the strong polarisation of the CH_2Cl that causes the shift. The carbon peak from $CDCl_3$ is seen at the chemical shift of 78.0 ppm.

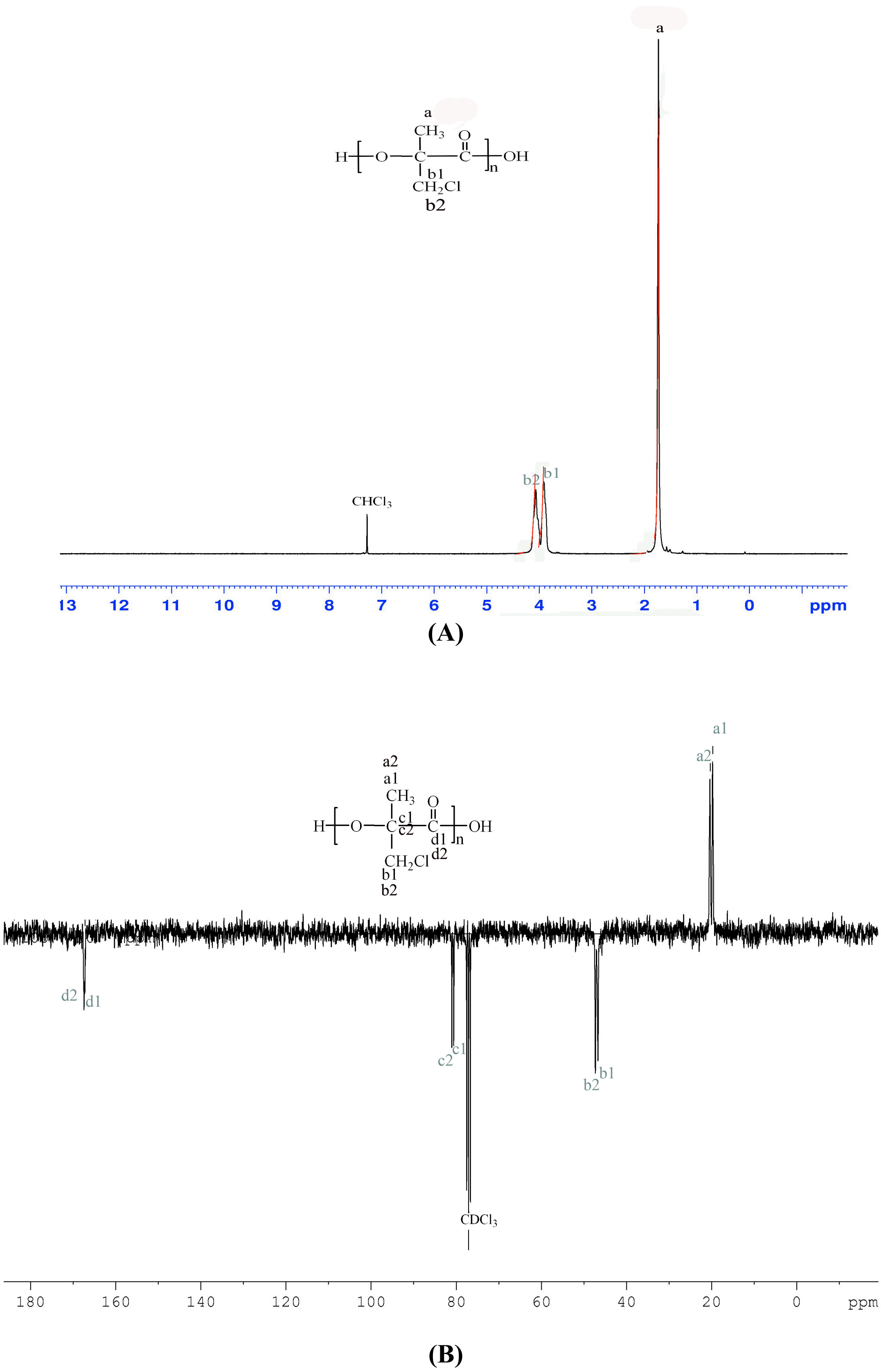

Figure 3.7 ^{1}H NMR (A) and ^{13}C NMR (B) spectra of α6(chloromethyl-methyl) recorded in $CDCl_3$.

3.1.7 ArS1(pentafluorophenyl-methyl):

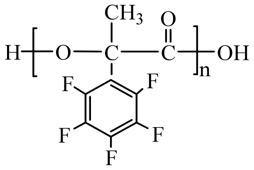

ArS1(pentafluorophenyl-methyl) or poly(2-hydroxy-2-pentafluorophenyl propanoic acid) is a novel poly(α-ester) substituted with pentafluorophenyl and methyl groups at the α-carbon in the backbone. ^1H and ^{13}C NMR were used to monitor the chemical structure of ArS1(pentafluorophenyl-methyl), shown in Figure 3.8(A) and (B), respectively. It was dissolved in deuterated chloroform ($CDCl_3$) for the NMR analysis.

In the proton spectrum, Figure 3.8(A), peak *a*, at a chemical shift approximately at 2.1 ppm, corresponds to the methyl protons. The peak at the chemical shift of 7.3 ppm corresponds to protons from the solvent. Peaks at approximately 8, 8.5 and 8.9 ppm correspond to the protons from pyridine, which was used as an initiator for polymerisation. The upfield peaks from peak *a* are expected to correspond to the proton peaks of pentafluoro atrolactic, acid which has pentaflurophenyl and methyl groups as substituted groups. The broad peak at approximately 3 ppm corresponds to the hydroxyl protons.

In the carbon spectrum, Figure 3.8(B), two peaks of *a* in the region of 22 ppm and 26 ppm correspond to the methyl carbons of ArS1(pentafluorophenyl-methyl). One is of the methyl carbon, the coupling peak of carbon coupled long range to ^{19}F. Four peaks of *b* around 136 ppm, 139 ppm, 143 ppm and 147 ppm correspond to pentafluorophenyl carbons. The upfield peaks around peak a are expected to be the carbon peaks of methyl from the parent acid and that of peak b the carbon peaks of pyridine. However, the peak of the alpha-carbon cannot be observed. Because of the electron-withdrawing power of the –Cl group and C_6F_5 groups it seems that the α-carbon lies under the $CDCl_3$ solvent. The peak at a chemical shift of 78 ppm corresponds to the carbon from solvent.

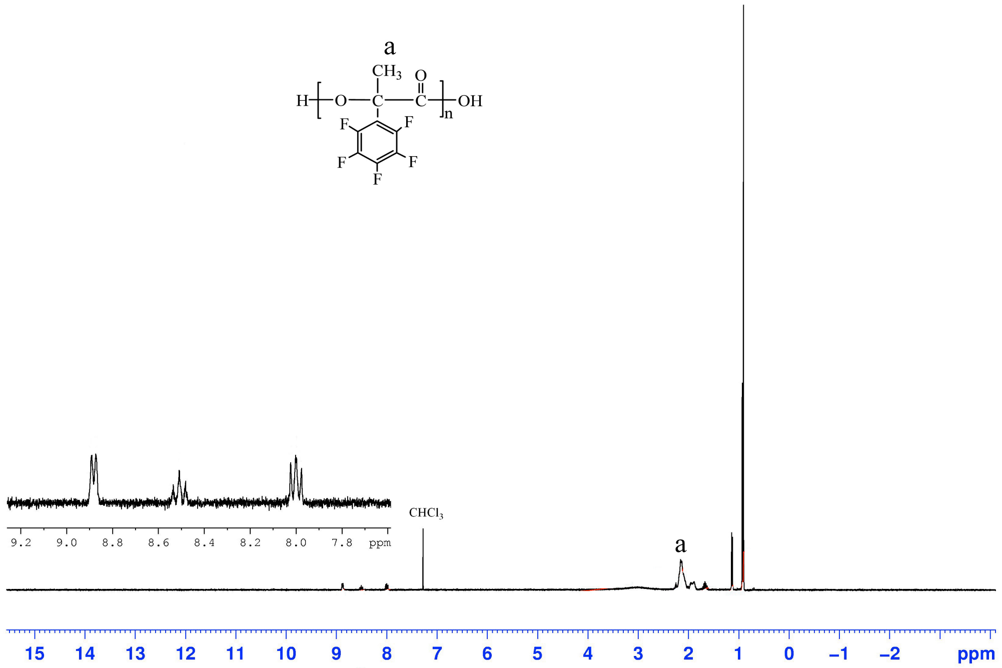

(A)

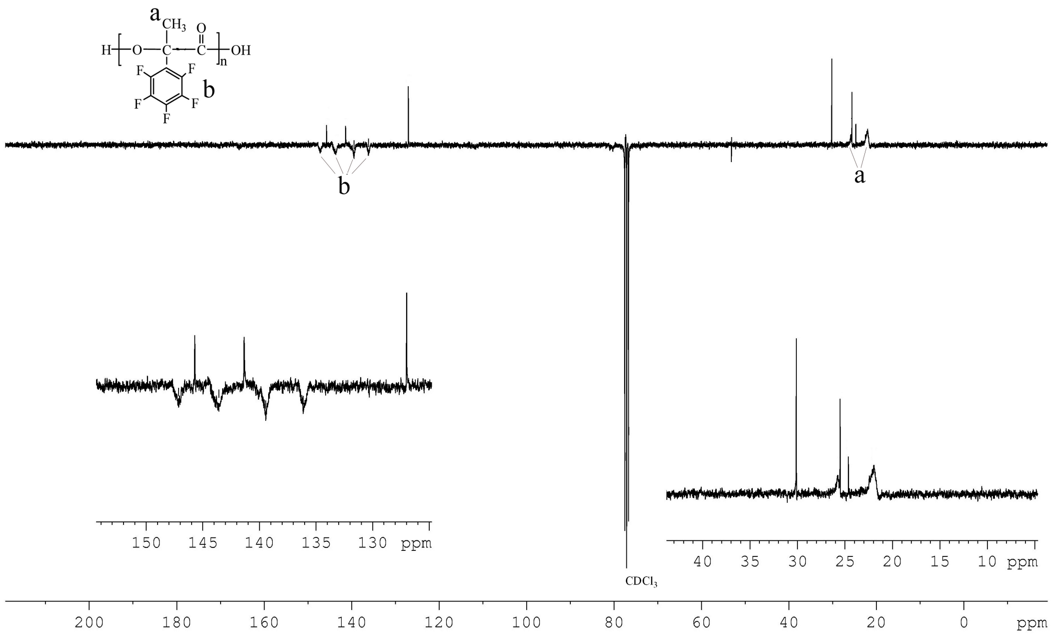

(B)

Figure 3.8 ^{1}H NMR (A) and ^{13}C NMR (B) spectra of ArS1(pentafluorophenyl-methyl) recorded in $CDCl_3$.

3.1.8 ArS2(phenyl-methyl):

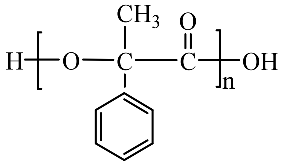

ArS2(phenyl-methyl) or poly(2-hydroxy-2-phenyl propanoic acid) is a novel poly(α-ester) substituted with phenyl and methyl groups at the α-carbon in the backbone. It was dissolved in deuterated chloroform ($CDCl_3$) and deuterated dimethyl sulfoxide (d_6-DMSO) for NMR analysis. ^{1}H NMR and ^{13}C NMR spectra of ArS2(phenyl-methyl) are shown in Figure 3.9 (A) and (B), respectively.

In the proton spectrum, Figure 3.9 (A), two peaks of *a* at approximately 2.0 and 2.5 ppm correspond to the methyl protons and *b* to the phenyl protons. The peak at a chemical shift of around 1.1 ppm and broad peak at approximately 6.5 ppm are, respectively, expected to be the methyl protons and the hydroxyl protons from the parent acid. Three peaks at chemical shifts of 7.4, 7.6 and 8.0 ppm correspond to the phenyl protons from pyridine, the initiator for polymerisation. The proton peaks of d_6-DMSO and $CHCl_3$ are shown at chemical shifts approximately at 3.6 and 7.3 ppm, respectively.

In the carbon spectrum, Figure 3.9 (B), peaks *a* at chemical shifts approximately at 130 ppm correspond to phenyl carbons. Peaks of methyl, quaternary, and carbonyl carbons could not be observed. The carbon peaks of d_6-DMSO and $CDCl_3$ are shown at chemical shifts of 40 and 78 ppm, respectively. The rest of the peaks are expected to be the carbon peaks of pyridine and the parent acid.

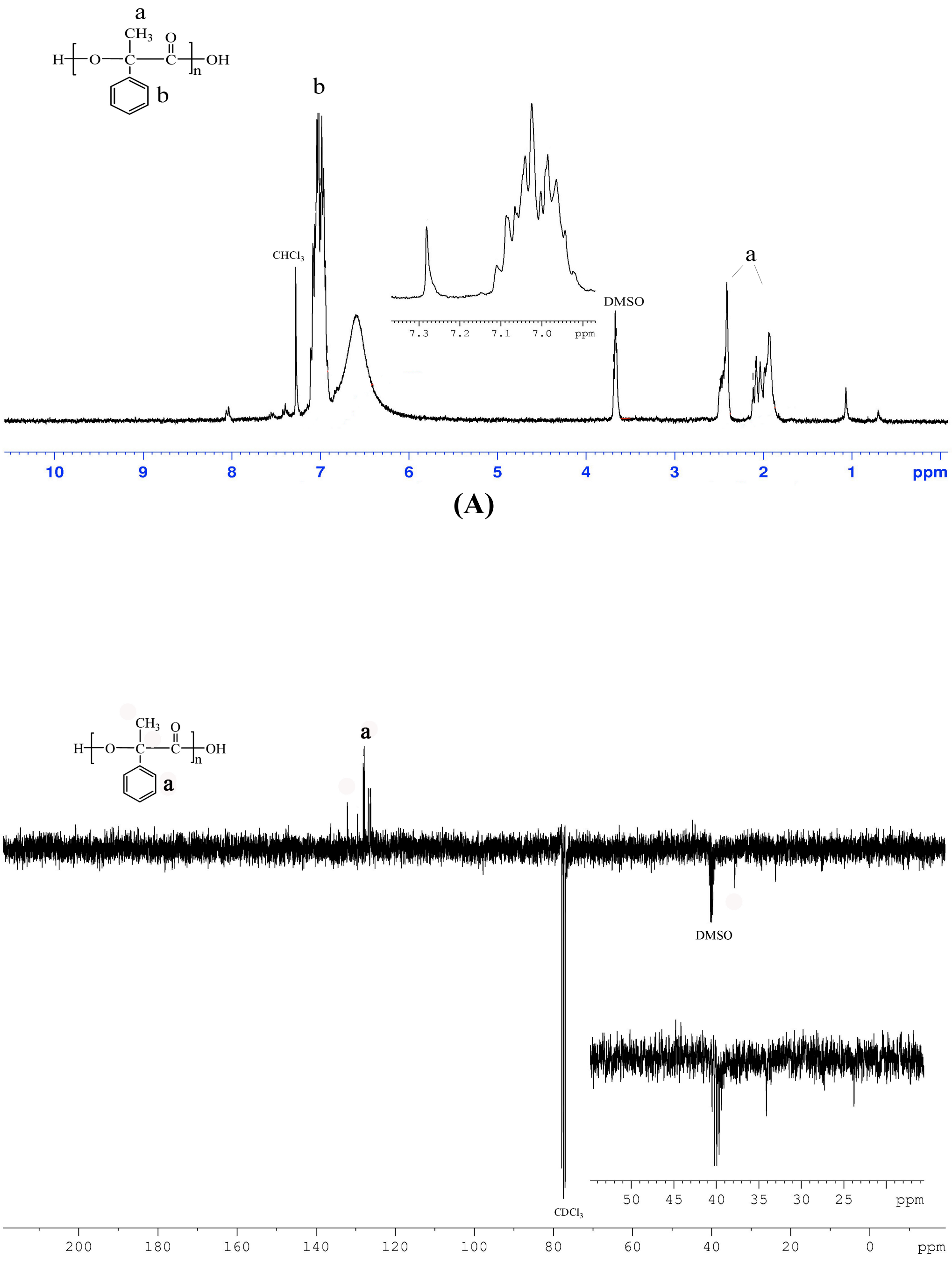

(A)

(B)

Figure 3.9 ^{1}H NMR (A) and ^{13}C NMR (B) spectra of ArS2(phenyl-methyl) recorded in $CDCl_3$ and d_6-DMSO.

3.1.9 ArS3(phenyl) :

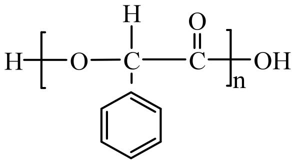

ArS3(phenyl) or poly (2-hydroxy-2-phenyl ethanoic acid) is a novel poly(α-ester) substituted with hydrogen and phenyl groups at the α-carbon in the backbone. It was dissolved in deuterated chloroform ($CDCl_3$) for NMR analysis. ^{1}H NMR and ^{13}C NMR spectra of ArS3(phenyl) are shown in Figures 3.10(A) and (B), respectively.

In the proton spectrum, Figure 3.10(A), peak *a* at a chemical shift of approximately 4.3 ppm corresponds to the protons at alpha-carbon and peak *b* at a chemical shift of approximately 7.2 ppm to the phenyl protons. At the phenyl proton region, the proton peak of chloroform is observed at a chemical shift of 7.3 ppm. The rest of the peaks are expected to be the proton peaks of the parent acid and pyridine.

In the carbon spectrum, Figure 3.10(B), peak *a* at a chemical shift of 75 ppm corresponds to alpha-carbon. Peak *b* at a chemical shift of 126 ppm corresponds to the five carbons of the phenyl ring (at the position b in the chemical structure). Peak *c* at a chemical shift of 132 ppm corresponds to the quaternary carbon in the phenyl ring. Peak *d* at a chemical shift of 166.5 ppm corresponds to the carbonyl carbon. The carbon peak of $CDCl_3$ is shown at a chemical shift of 78 ppm. The rest of the peaks are expected to be the carbon peaks of the parent acid and pyridine.

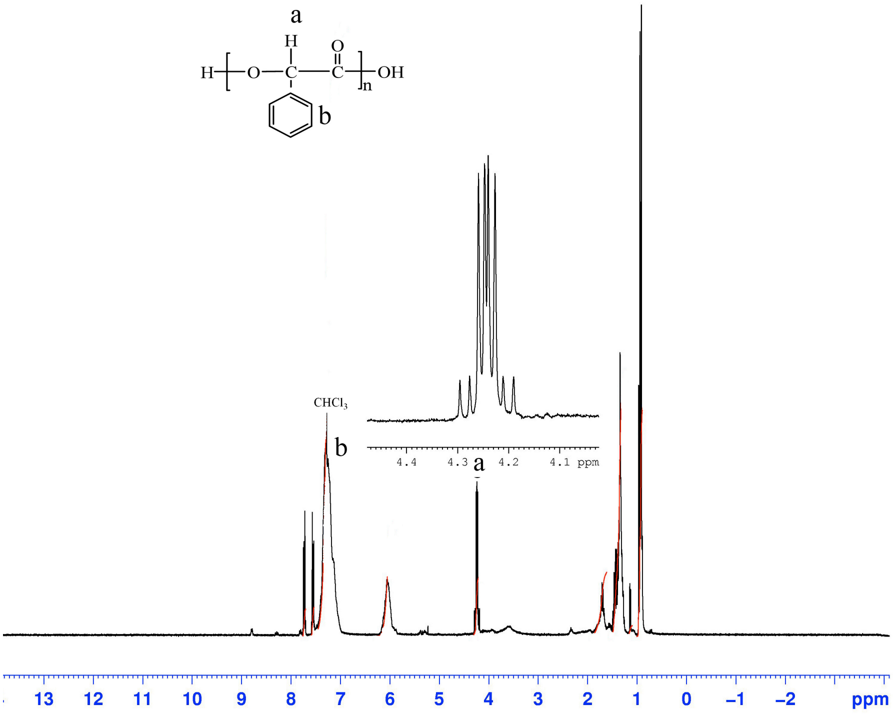

(A)

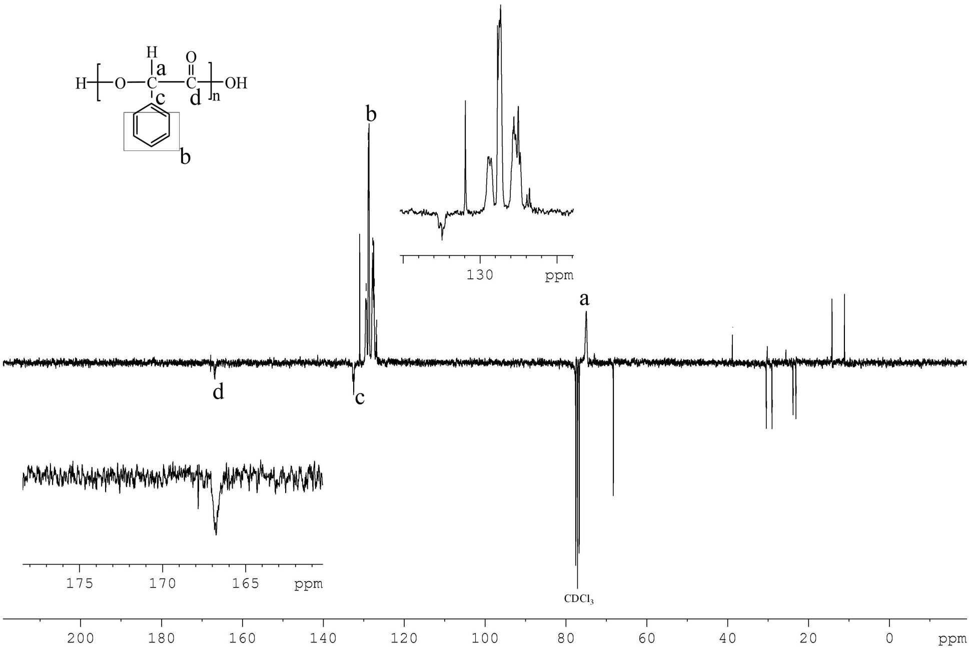

(B)

Figure 3.10 ^{1}H NMR (a) and ^{13}C NMR (b) spectra of ArS3(phenyl) recorded in $CDCl_3$.

3.1.10 PGA(synthesised) :

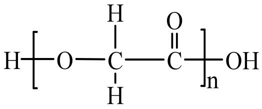

$$H-\left[O-\overset{H}{\underset{H}{\overset{|}{\underset{|}{C}}}}-\overset{O}{\overset{\|}{C}}\right]_n-OH$$

This sample of PGA was synthesised via the anhydrosulphite route. Poly(glycolic acid) or poly(2-hydroxy ethanoic acid) is the simplest structure of the poly(α-esters), which is substituted with two hydrogen atoms at the α-carbon in the backbone. It was dissolved in deuterated dimethyl sulfoxide (d_6-DMSO) for NMR analysis. ^1H and ^{13}C NMR spectra of PGA(synthesised) are shown in Figure 3.11(A) and (B), respectively.

In the proton spectrum, Figure 3.11(A), peak *a* at a chemical shift of 4.9 ppm corresponds to the two protons at the α-carbon. The proton peak of DMSO is observed at a chemical shift of 2.5 ppm. The broad peak observed at a chemical shift of approximately 3.4 ppm corresponds to the hydroxyl proton, which is expected to be from water. This is because poly(glycolic acid) is very susceptible to moisture. The proton peak of d_6-DMSO is observed at a chemical shift of 2.5 ppm. The rest of the peaks are expected to be the proton peaks of the parent acid and pyridine.

In the carbon spectrum, Figure 3.11 (B), peak *a* at a chemical shift of 61 ppm corresponds to the methylene carbons. Peak *b* at a chemical shift of 167 ppm corresponds to the carbonyl carbons. It can be observed that the carbonyl carbon peak of PGA (synthesised) is a remarkable peak compared with other poly α-esters. The carbon peak of d_6-DMSO is shown at a chemical shift of 40 ppm. The rest of the peaks are expected to be the carbon peaks of the parent acid and pyridine.

This is unlikely to be high molecular weight polymer since glycolic anhydrosulfide is one of the most difficult anhydrosulfide to purify and polymerise. The reasons are because; poly(glycolic acid) is very susceptible to moisture and the parent acid is very hydroscopic.

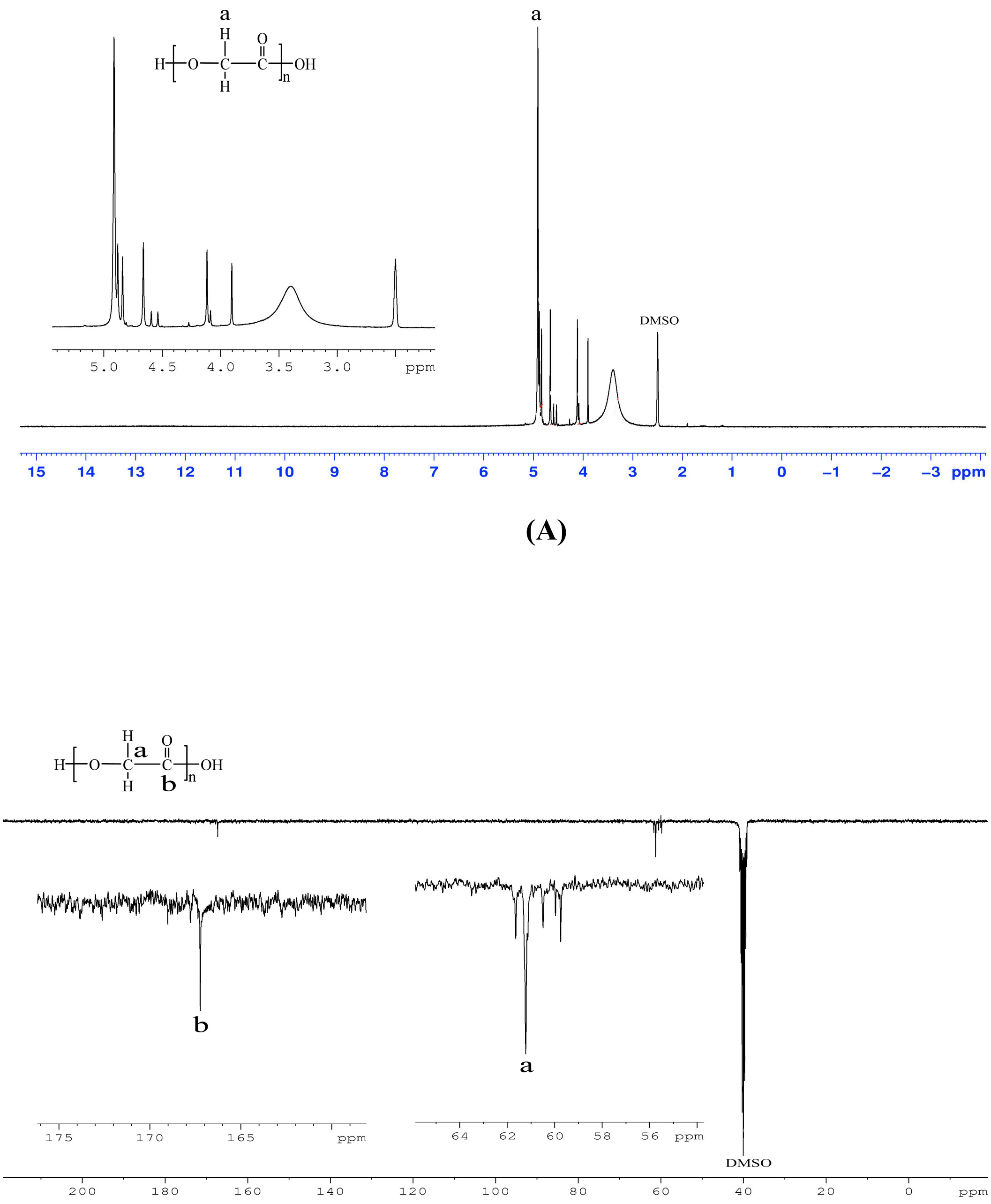

(A)

(B)

Figure 3.11 ^{1}H NMR (A) and ^{13}C NMR (B) spectra of PGA(synthesised) recorded in d_6-DMSO.

3.1.11 Copolymer of ArS1(pentafluorophenyl-methyl) and ArS3(phenyl):

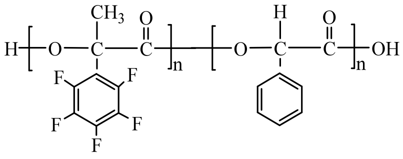

The copolymer of ArS1(pentafluorophenyl-methyl) and ArS3(phenyl) is expected to be a copolymer of poly(2-hydroxy-2-pentafluorophenyl propanoic acid and poly(2-hydroxy-2-phenyl ethanoic acid). It was dissolved in deuterated chloroform ($CDCl_3$) for NMR analysis. ^1H and ^{13}C NMR spectra of the copolymer are shown in Figure 3.12(A) and (B), respectively.

In the proton spectrum, Figure 3.12(A), peak *a* corresponds to the methyl protons in ArS1(pentafluorophenyl-methyl). It is shown at a chemical shift of 2.1 ppm similar to ArS1(pentafluorophenyl-methyl) itself. Peak *b* at a chemical shift of 6.0 ppm corresponds to the proton peaks at the alpha-carbon of ArS3(phenyl), which shifts from ArS3(pentafluorophenyl-methyl) itself (shown at 4.28-4.30 ppm). Peak *c* at a chemical shift of approximately 7.3 ppm corresponds to the phenyl protons of ArS3(pentafluorophenyl-methyl). The proton of chloroform is observed at a chemical shift of 7.3 ppm. Peaks at approximately 1.2 and 1.3 ppm are expected to be the methyl proton peaks of parent acid. The broad peak at 3.5 ppm corresponds to the hydroxyl protons. Peaks at approximately 7.9, 8.5, and 8.9 ppm correspond to the pyridine protons.

In the carbon spectrum, Figure 3.12(B), peak *a* at chemical shifts of 22 and 26 ppm corresponds to the methyl carbons of ArS1(pentafluorophenyl-methyl). Peak *b* at a chemical shift of 78 ppm corresponds to the proton at the alpha-carbon of ArS3(phenyl). Peak *c* at a chemical shifts of approximately 130 ppm corresponds to the phenyl carbons of ArS3(phenyl). Peak *d* at 136, 140, 144 and 147 ppm corresponds to the pentafluorophenyl carbons of ArS3(phenyl). Peak *e* at 170 ppm corresponds to the carbonyl carbon of both ArS1(pentafluorophenyl-methyl) and ArS3(phenyl). The carbon of chloroform is observed at 78 ppm. The rest of the peaks are expected to be the carbon peak of parent acid and pyridine.

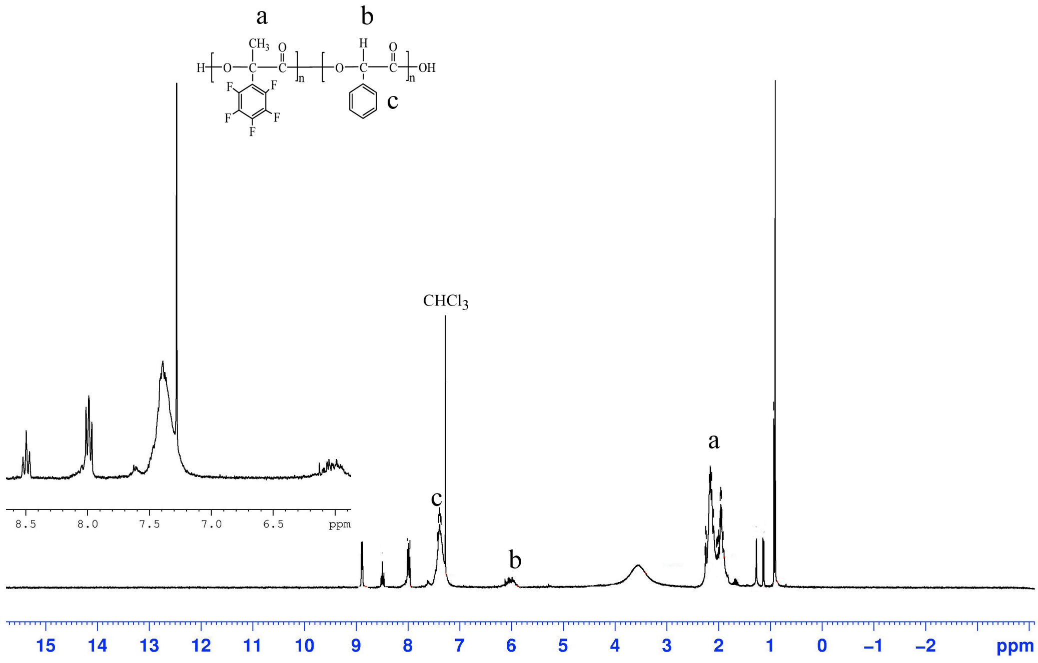

(A)

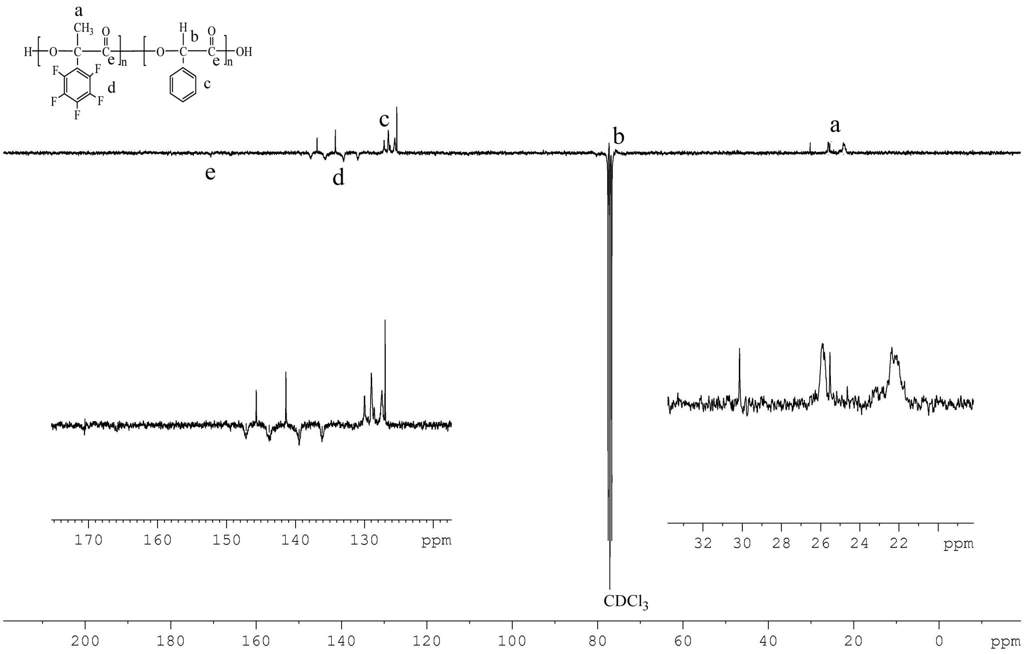

(B)

Figure 3.12 ^{1}H NMR (A) and ^{13}C NMR (B) spectra of copolymer of ArS1(pentafluoro phenyl-methyl) and ArS3(phenyl) recorded in $CDCl_3$.

3.1.12 Copolymer of ArS1(pentafluorophenyl-methyl) and PGA(synthesised):

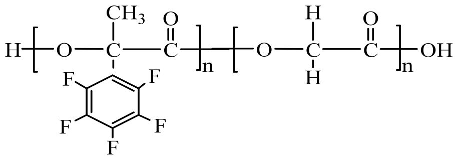

This copolymer is expected to be a copolymer of poly(2-hydroxy-2-pentafluoro phenyl propanoic acid) and poly(glycolic acid). It was dissolved in deuterated chloroform ($CDCl_3$) for NMR analysis. ^1H and ^{13}C NMR spectra of the copolymer are shown in Figure 3.13(A) and (B), respectively.

In proton spectrum, Figure 3.13(A), peak *a* at a chemical shift of approximately 22 ppm corresponds to the methyl protons of ArS1(pentafluorophenyl-methyl). Peak *b* at a chemical shift of approximately 4.8 ppm corresponds to the protons at the α-carbon of PGA(synthesised). The proton of chloroform is observed at a chemical shift of 7.3 ppm. The proton peaks at very low chemical shifts (less than 1.0 ppm) are expected to be the proton peaks of grease and silicone used in the process. The rest of the peaks are expected to be the proton peaks of parent acid and pyridine.

In carbon spectrum, Figure 3.13(B), peak *a* at chemical shifts of 22 and 26 ppm corresponds to the mehyl carbons of ArS1(pentafluorophenyl-methyl). Peak *b* at a chemical shift of 29.5 ppm corresponds to the α-carbon of PGA(synthesised). Peak *c* at 136, 139, 144 and 147 ppm corresponds to the pentafluorophenyl carbons of ArS1(pentafluorophenyl-methyl). The carbon of chloroform is observed at 78 ppm. The rest of the peaks are expected to be the carbon peak of parent acid and pyridine.

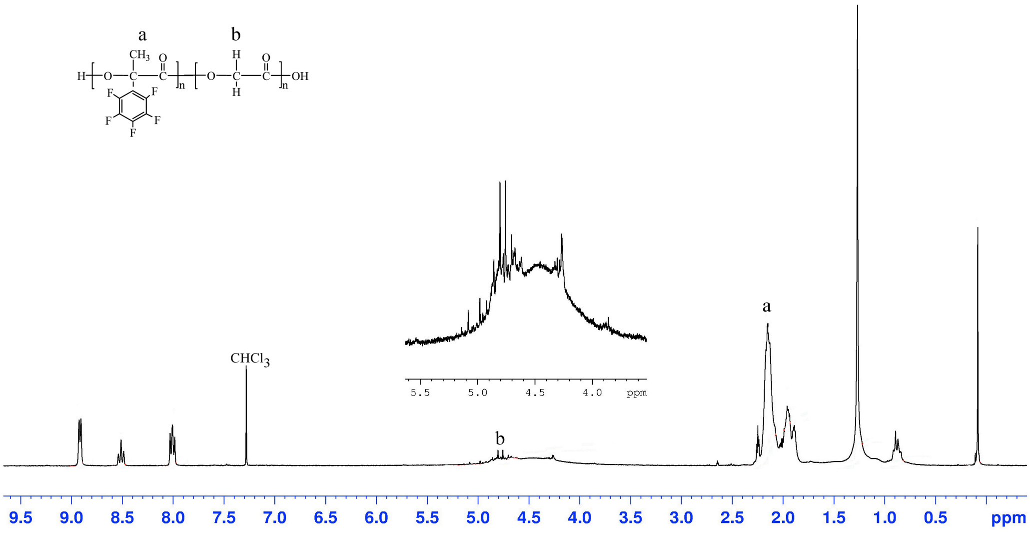

(A)

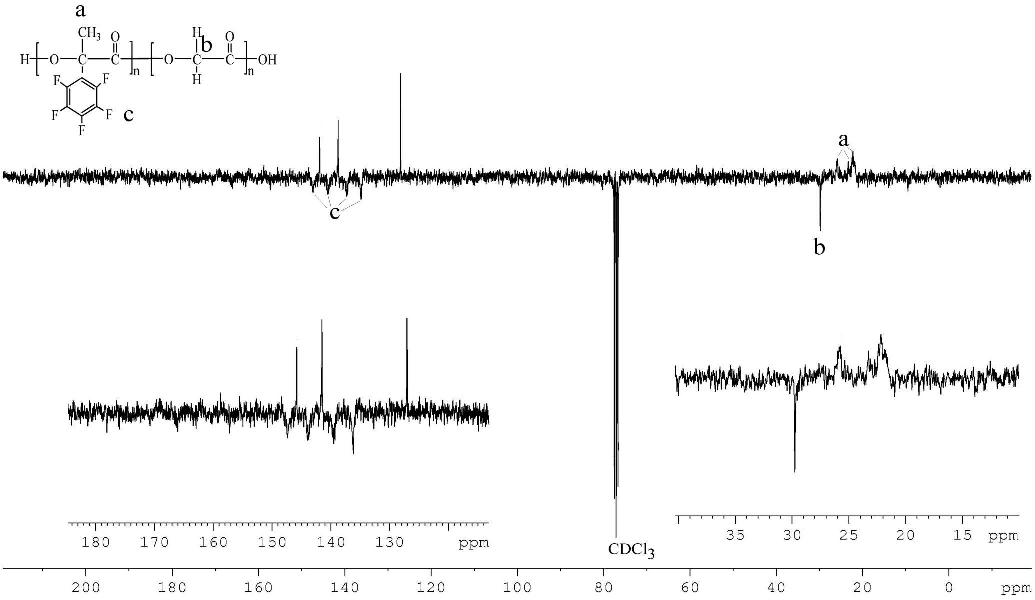

(B)

Figure 3.13 ^{1}H NMR (a) and ^{13}C NMR (b) spectra of copolymer of ArS1(pentafluoro phenyl-methyl) and PGA(synthesised) recorded in $CDCl_3$.

3.2 Thermal analysis by differential scanning calorimetry (DSC)

The considerable thermal properties, such as the glass transition temperature (T_g), the melting temperature (T_m), and the melting enthalpy (ΔH_m), of the pre-synthesised poly(α-ester) homologues including poly(lactic acid) (PLA), poly(ε-caprolactone) (PCL), and cellulose acetate butyrate (CAB), were observed by DSC analysis. The DSC traces - plotted between heat flow endothermic up and temperature (°C) - of PLLA1 ($M_w = 28000$) and PLLA2 ($M_w = 94800$) for instance are shown in Figure 3.14.

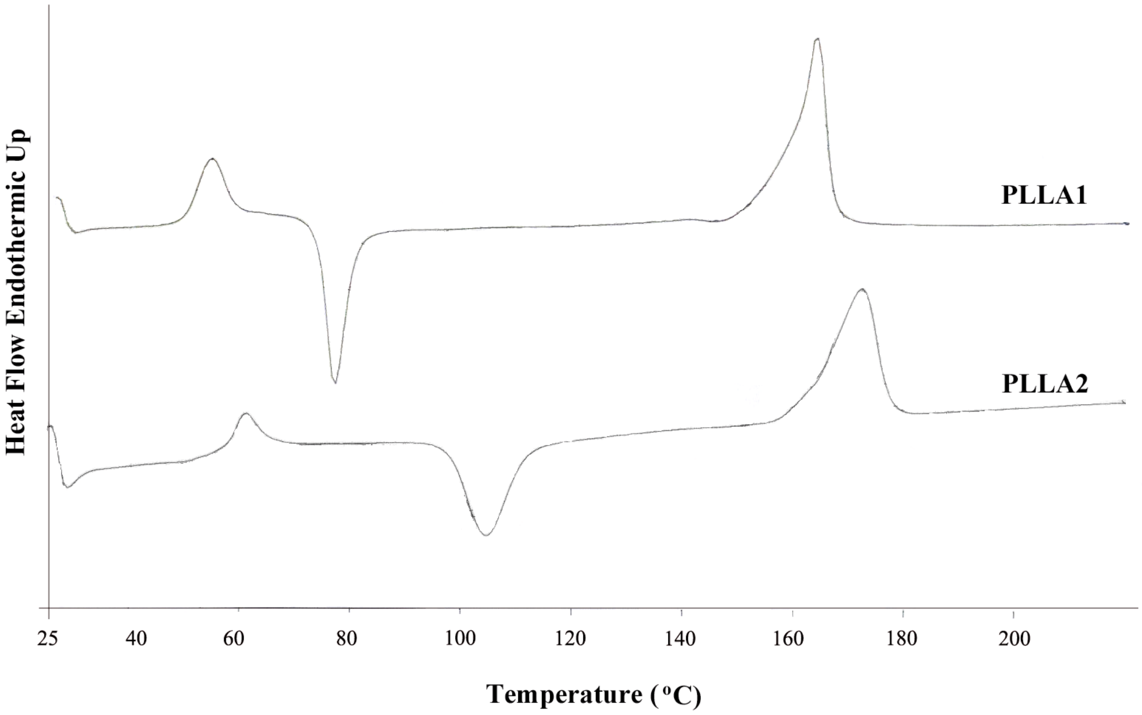

Figure 3.14 DSC traces of PLLA1 and PLLA2: heated from 25°C to 220 °C at 20°C/min.

The T_g, T_m, and ΔH_m of PLA, the pre-synthesised poly(α-ester) homologues, and other polymers used for blending are shown in Table 3.3.

Table 3.3 The T_g, T_m, and ΔH_m of the pre-synthesised poly(α-ester) homologues.

Poly α-esters	**T_g (°C)**	**ΔH_m (J/g)**	**T_m(°C)**
PLLA1 (M_n = 18,700)	53	52.02	162
PLLA2 (M_n = 63,500)	61	42.06	172
PDLLA	59	-	-
Aliphatic Substitutions:			
PGA(synthesised)	-	62.11	120
α1(dimethyl)	-	51.60	175
α2(diethyl)	-	52.02	185
α4(cyclohexyl)	-	24.90	82
α5(cycloheptyl)	-	42.34	148
α6(chlorometyl-methyl)	60	8.33	134
α2(diethyl)-high MW	74	3.14^{*2}	192
Aromatic Substitutions:			
ArS1(pentafluorophenyl-methyl)	72	0.01	103
ArS3(phenyl)	71	0.20	115
Copolymer of ArS1 and ArS3	80	1.94	158-195^{*1}
Copolymer of ArS1 and PGA(synthesised)	77	17.6	115-185^{*1}
PCL1 (M_n = 7,500)	-	69.23	53
PCL2 (M_n = 57,800)	-	53.47	58
CAB	114	14.32^{*2}	151
PGA	38	55.4	218
TPU	63	-	-

Note: $*^1$ the T_m peaks were very broad. ^{*2} some of these values are unusual, however, the ΔH_m value depends on the sample and applied experimental conditions, i.e. sample size, sample's thermal history, molecular weight, heating and cooling rates which were similar in each case.

From Table 3.3, it can be seen that the T_m of high molecular weight polymer (e.g. PLLA2, PCL2) is higher than low molecular weight (e.g. PLLA1, PCL1) whereas the ΔH_m in contrast is slightly lower. In the case of amorphous polymers-PDLLA-which cannot crystallise, there can be no T_m. The T_g of the aliphatic poly(α-ester) homologues are not generally observed, excluding α6(chloromethyl-methyl) and α2(diethyl)-high MW, whereas the T_g of aromatic poly(α-ester) homologues can be observed. PLLA, α1(dimethyl), and α2(diethyl) show higher T_m and ΔH_m than other aliphatic poly(α-ester) homologues. The T_m of the copolymer of aromatic poly(α-ester) homologues are very broad, which might be caused by the molar mass dispersity of the samples.

The percent crystallinity of PLLA1, PLLA2, PCL1, and PCL2 is calculated using the following equation: [51]

$$\%Crystallinity = \frac{\Delta H_m}{\Delta H_m^{ideal}} \times 100\% \qquad \text{Eq.3.1}$$

where ΔH_m is the measured melting enthalpy and ΔH_m^{ideal} is the melting enthalpy of a 100% crystalline polymer. Table 3.4 shows ΔH_m, ΔH_m^{ideal}, and percent crystallinity (after crystallisation has already taken place) of PLLA and PCL.

Table 3.4 ΔH_m, ΔH_m^{ideal}, and percent crystallinity of PLLA and PCL.

Polymer	**ΔH_m (J/g)**	**ΔH_m^{ideal} (J/g) [76]**	**% Crystallinity**
PLLA1	52.02	135.7	38
PLLA2	42.06		31
PCL1	69.23	93.7	74
PCL2	53.47		57

3.3 Crystallite imaging by hot-stage microscopy (HMS)

Hot-stage microscopy analysis can be used to observe the crystal form, however, the usefulness of the technique depends on the temperature and the heating and/or cooling rate used during the process. It was used to be a guide-line to observe the crystallinity of all poly(α-ester) homologues and polymers used in this work, e.g. PCL, CAB. The light intensity obtained from HSM images is an alternative value to describe the changes occurring at the surface of the polymer. It diminishes the crystallinity of polymers. The HSM images were observed at the same magnification. A few HSM images were shown in this section to demonstrate whether the polymers were crystalline or amorphous.

Figure 3.15 shows HSM images of PLLA1 (M_n = 18,700) and PLLA2 (M_n = 63,500) films. The crystalline spherulites of both PLLA1 and PLLA2, which are semi-crystalline polymers can be clearly seen. The HSM images of PCL1 (M_n = 7,500) and PCL2 (M_n = 57,800) films also show crystalline spherulites. However, PLLA1 and PCL1 cast films are opaque whereas PLLA2 and PCL2 cast films are clear although the reason for this marked difference is not entirely obvious. The HSM image of cellulose acetate butyrate (CAB) does not show crystalline spherulites because CAB is an amorphous polymer.

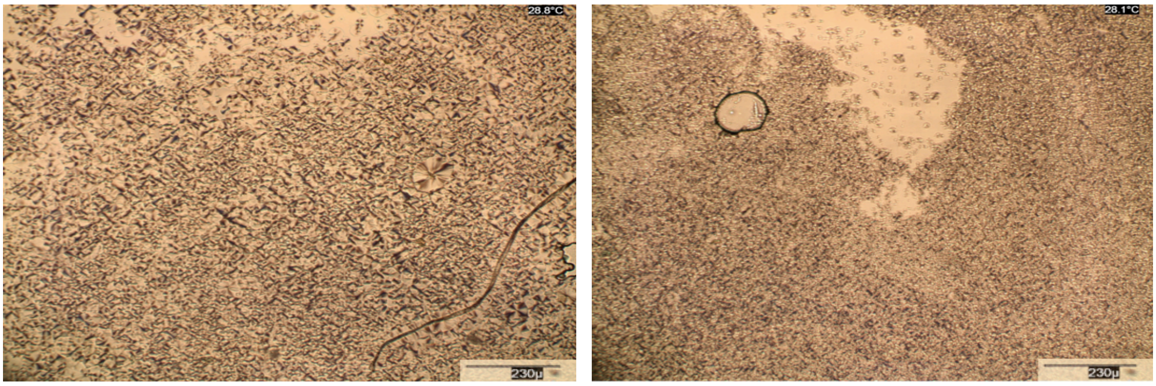

PLLA1 **PLLA2**

Figure 3.15 The HSM images of PLLA1 (M_n = 18,700) and PLLA2 (M_n = 63,500) films.

Figure 3.16 shows the HSM image of PGA(synthesised) at the initial stage of crystallisation (left) and during continuing growth (right). It shows good crystalline spherulites even though this PGA(synthesised) is not of high molecular weight. PGA from commercial sources has a very high degree of crystallinity and small spherulites sizes compared to PGA(synthesised).

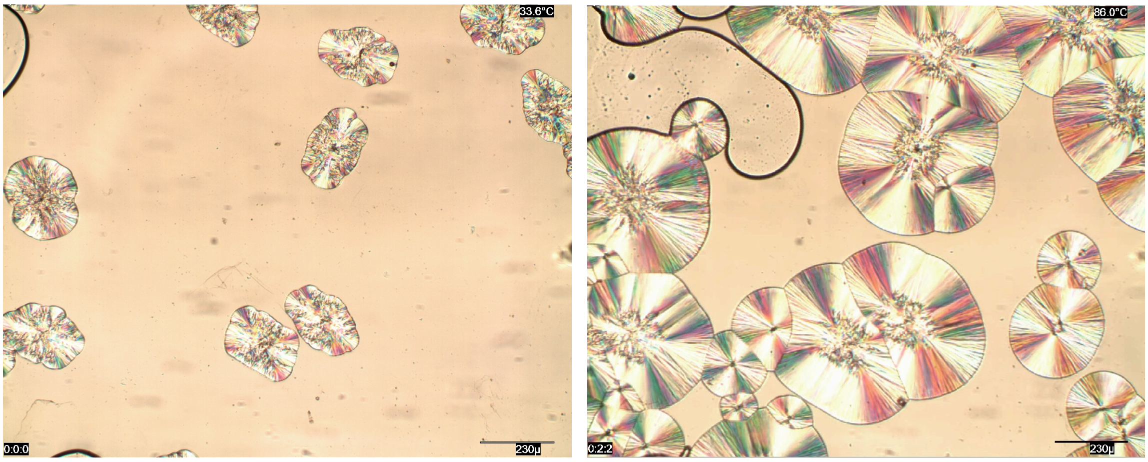

Figure 3.16 The HSM images of PGA(synthesised).

Figure 3.17 shows the HSM images of α2(diethyl) and α6(chloromethyl-methyl). The crystalline spherulite can be observed in α2(diethyl) which is a crystalline polymer, whereas it can not be observed in α6(chloromethyl-methyl) which is an amorphous polymer. The HSM image of α1(dimethyl), a semi-crystalline polymer also shows crystalline spherulites similar to α2(diethyl). However, the degree of crystallinity of both α1(diethyl) and α2(diethyl) are less than PLLA1 and PLLA2 as observed from their HSM images. The HSM images of other aliphatic poly(α-esters), all aromatic poly(α-esters), and the copolymer of ArS1 and ArS3 are similar to the HSM image of α6(chloromethyl-methyl). However, the HSM image of the copolymer of ArS1 and PGA(synthesised) shows some crystalline spherulites.

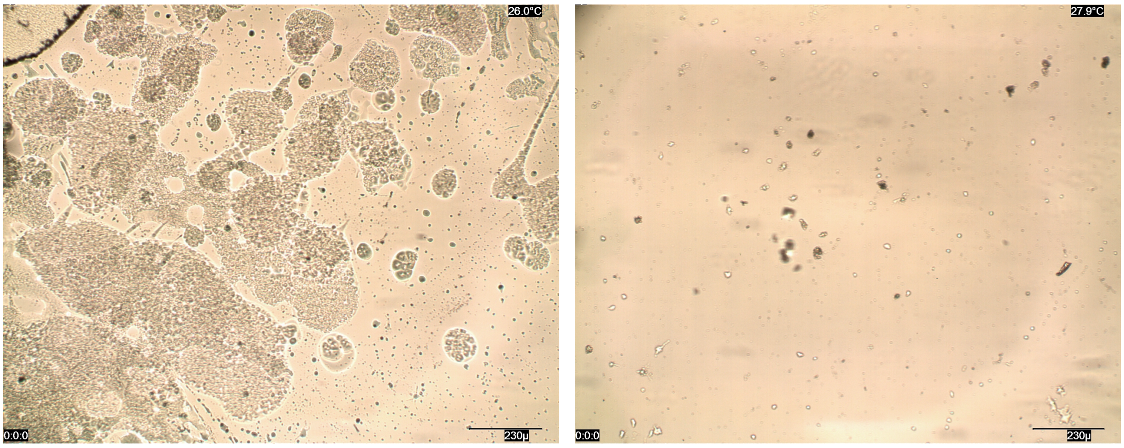

α2(diethyl) **α6(chloromethyl-methyl)**

Figure 3.17 The HSM images of α2(diethyl) and α6(chloromethyl-methyl).

3.4 SUMMARY OF THE CHAPTER

Hot-stage microscopy analysis showed that α1(dimethyl) and α2(diethyl) are crystalline polymers, while other pre-synthesised poly(α-ester) homologues are amorphous polymers. In addition, the DSC analysis showed that α1(dimethyl) and α2(diethyl) have high T_m compared to the others. This is because of the small and the symmetrical substituted side groups (less than ca. 5 Å). The solubility of α2(diethyl) is effected by the high degree of crystallinity, for example, α2(diethyl) will not dissolve in chloroform. It can be seen at the different thermal analysis that T_g, T_m, and crystallinity of poly(α-ester) homologues are different.

In summary, the characterisation worked here confirmed these are polymers. They have appropriate structure NMR. They are novel poly(α-esters) which could not find in the commercial sources. These characterisation results will help to understand the miscibility of the blends in the next chapter.

CHAPTER 4

SOLVENT BLENDING:
BINARY BLENDS

Chapter 4

Solvent Blending: Binary Blends

In this work, the solvent blends were utilised as a preliminary technique to study the miscibility of polymer pairs and thus identify the composition ranges for ternary polymer blends, which will be discussed in Chapter 5. Solutions of individual polymers were mixed and the solvent allowed to evaporate slowly. The polymer chains either remain intermingled (i.e. they show miscibility) or separate as the bridging solvent is removed as each polymer "decides" whether to mix or to separate. If they separate into phases whose dimensions are greater than, or equal to the wavelength of light (i.e. 450-500 nm) they scatter light. In this case the films will be opaque and the strength or toughness of the blend will be reduced, because the interfacial forces between the immiscible phases will be lower than the forces required to separate the intermolecular entanglements within a uniform phase. If there are no particles or separated phases greater than the wavelength of light, light will pass through the polymer without significant scattering. These films will therefore be translucent or clear.

On the basis of visual examinations the boundaries in percentage transmission would translate into four phases: opaque, semi-translucent, translucent, and clear. From those observations, the transmission boundaries were opaque when %T is 0-30%, semi-translucent when %T is 31-45%, translucent when %T is 46-75%, and clear when %T is 76-100%, and represented with the linear gradient colours from black (opaque), semi-translucent (grey), translucent (light grey), and white (clear) as shown in Figure 4.1.

Figure 4.1 The visual shading miscibility boundaries in percentage transmittance.

4.1 Development of the technique

The first objective of this research was to find a novel technique that would enable a small amount (mg range) of the test polymers to be used and would provide a rapid method to observe the clarity and miscibility of the polymer solution blends. This was particularly important for blends based on the novel poly(α-ester) homologues of poly(lactic acid) which were only available in small quantity. With this purpose in mind, an ultraviolet/visible (UV) multi-wavelength plate reader, Molecular Devices Spectra Max M2, together with 96-well plates (shown in Figure 4.2), were chosen to explore a rapid screening procedure to observe the clarity and miscibility of the solution-blended polymer films. This method, using a combination of the UV-visible spectroscopy and the 96-well plates, was named "a combinatorial screening method" or "a rapid screening method" in this work. This description arose because of the way in which it permitted rapid sequential combination of small (microlitre level) volumes of the polymer solutions under examination.

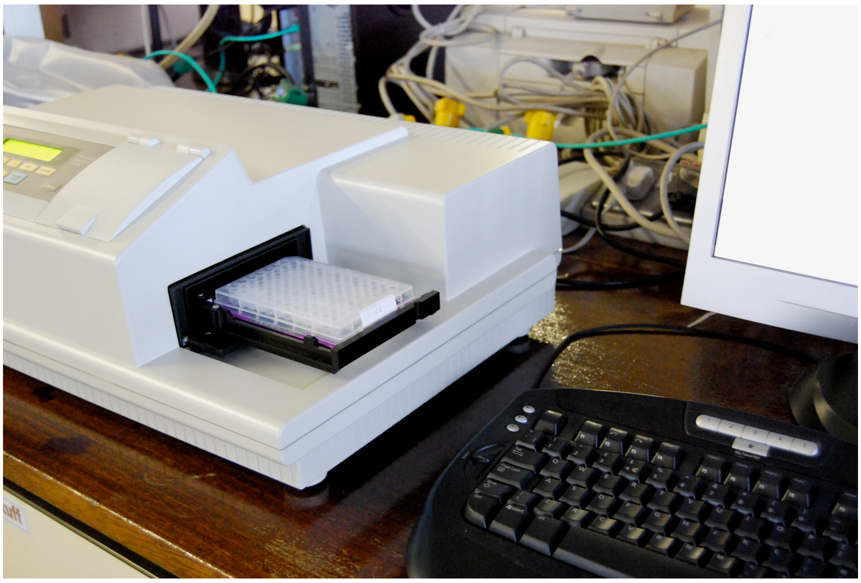

Figure 4.2 The UV/Visible plate reader: Molecular Devices Spectra Max M2 together with 96-well plates.

The clarity and miscibility of the resultant polymer solution blends was measured by the plate reader in the UV-visible region and expressed as either an absorbance or percent transmittance (%T). The important experimental variables for this combinatorial screening method are the concentration (wt.%) and quantity of polymer solutions (μl), and wavelength (nm) of UV-light. Details of the technique are described in the following sections.

4.1.1 Types of well-plate

There are two types of the 96-well-plates, a 96-well sterile polystyrene plate with round bottom wells (P5366 from Sigma-Aldrich, Figure 4.3a) and a 96-well non-sterile polypropylene plate with round bottom (CL S3365 from Sigma-Aldrich, Figure 4.3b). From Figure 4.3, the different physical features between PS and PP well plates can be seen: PS is a transparent plate, while PP is a translucent plate. These two plates were examined to find which did not react with the solvents used in this work: methylene chloride or dichloromethane (CH_2Cl_2), chloroform or trichloromethane ($CHCl_3$), and hexafluoroisopropanol (HFIP). A simple test was used - 200 μl of each solvent was pipetted into both well-plates and allowed to evaporate. The percent transmittance and physical condition of well-plates was then observed. The results are shown in Table 4.1.

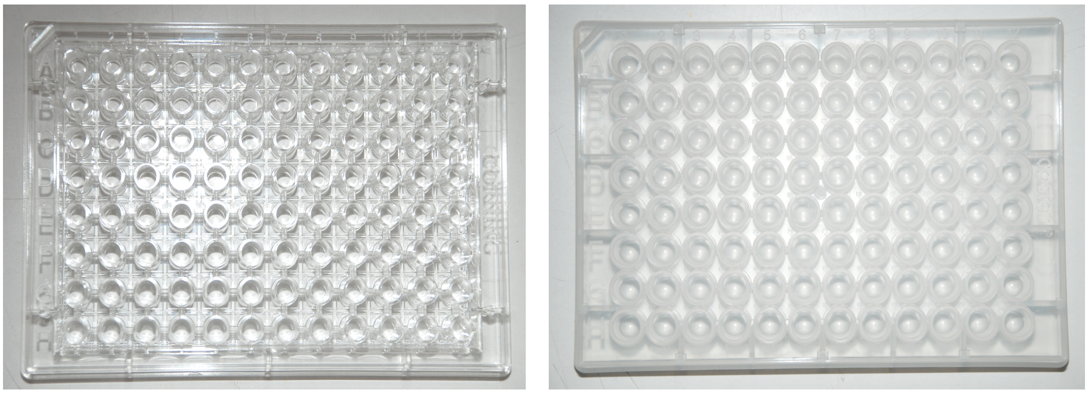

(a) (b)

Figure 4.3 The 96 well-plates made from: (a) polystyrene and (b) polypropylene.

Table 4.1 The results from pipetting various solvents into PS and PP well-plates.

Solvent	PS well-plate		PP well-plate	
	%T	Physical condition after test	%T	Physical condition after test
CH_2Cl_2	33	Plate lost clarity	100	No change
$CHCl_3$	88	Plate lost clarity	100	No change
HFIP	95	Sticky sample at the bottom	100	No change

From Table 4.1, PP well-plates containing all solvents show absolutely 100% of transmittance and their physical appearances did not change but not in PS well-plates. It can be supposed that CH_2Cl_2, $CHCl_3$ and HFIP dissolved PS well-plates and caused changes in their physical conditions. Therefore, PP well-plates were suitable for studying the polymer solvated blends in this work.

4.1.2 Concentration and volume of polymer solutions

Different concentrations of polymer solutions have been used for blending studies in recent work. For example, 10 wt% solutions of P(HB-HV) copolymers, CAB and plasticiser in chloroform were used by Yasin and coworkers [77]. Jin-San Yoon and coworkers blended PLLA and PHB in chloroform at 3 wt% [78]. In the present work, 7 wt% polymer solutions were used for blending studies using the rapid screening method. In parallel experiments 1 wt% solutions of PLLA, PCL and CAB were used to prepare ternary blends at various compositions, however, the percent transmittances of all these blends could not be observed because the concentration of polymer was too low.

The volume of polymer solutions used in the solution blending experiments was 100 μl of the mixed composition, which was pipetted into PP well-plates. Thus, for example, 20 μl of PLLA and 80 μl of PCL were used in a blend experiment. 100 μl of additional solvent was also pipetted into the polymer blend samples as they evaporated, providing the constituent polymer chains with an opportunity to become mixed and intermingled for a longer time during the room temperature solvent evaporation process.

4.1.3 Wavelengths

Polymer samples were dissolved, the solutions placed into the 96-well plates, and then tested in the UV-Visible spectrometry mode of the plate reader. A reference sample was prepared by pipetting pure solvent into a well-plate. Samples were scanned with various wavelengths, from 200 to 700 nm to determine the absorbance (A) of the blends at various compositions. The absorbance of the PLLA/PCL blends prepared in methylene chloride is shown in Figure 4.4.

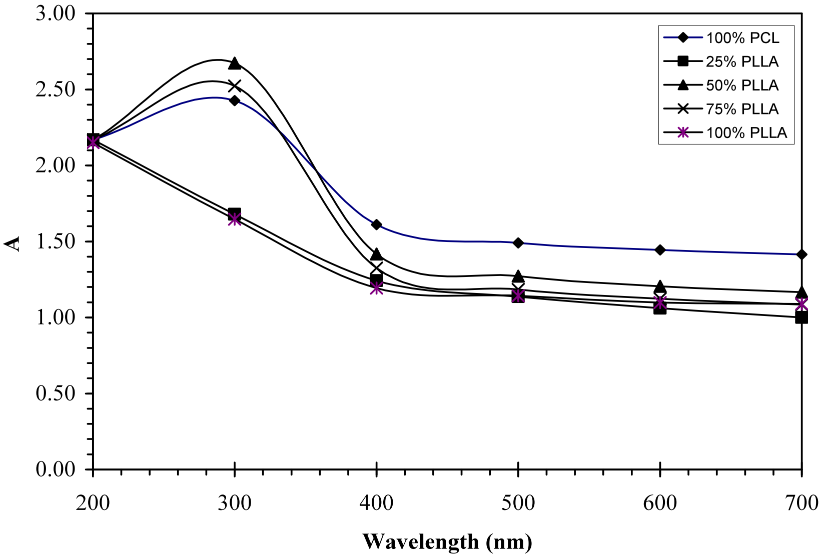

Figure 4.4 Absorbance of the PLLA/PCL blends with various compositions as a function of wavelength (nm).

From Figure 4.4, it can be seen that all absorbance lines dropped dramatically at the wavelength of 400 nm and then slightly decrease until 700 nm. The absorbance of all samples is approximately 1.0-1.5 at the wavelength 400-500 nm. The light at 450 nm, the intermediate wavelength of 400-500 nm, is therefore chosen for studying the clarity and miscibility of polymer blends. However, the lack of absorbance of the solvent at this wavelength enabled it to be used as a blank in UV-Visible spectroscopy analysis.

4.2 Binary blends

Blending two homopolymers is one of the most inexpensive and widely used techniques in polymer composites to improve mechanical properties of polymers for suitable applications. To understand systematically the effect of structure on miscibility of binary blends of poly(lactic acid) (PLA) is the first aspect of this study.

The poly(α-ester) homologues are a useful class of polymer to investigate principles that effect miscibility. Their binary blends were initially studied by using the combinatorial method described in Section 4.1. Polymer samples were dissolved in either chloroform or hexafluoroisopropanol with a concentration of 7 % (w/v), pipetted into the 96-well plate, and the percent transmittance observed by UV-Visible spectrometry at 450 nm. The different types of polyesters, homologous series of α-polyesters, β-polyesters, and diacid-diol polyester, PCL, and CAB, were preliminarily interested to assess the binary blends prior to study the potentially interesting ternary blends.

To easily represent and compare the miscibility of binary blends, therefore, the "visual shading miscibility diagram of binary blend" is used in Sections 4.2.2-4.2.5. The shading colours represent the clarity of films observed from %T: black-opaque (0-30%), grey-semi-translucent (31-45%), light grey-translucent (46-75%), and white-clear (76-100%). The visual shading miscibility diagram of binary blends is plotted from 100 wt.% (left) to 0 wt.% (right) of one polymer used in the binary blend.

4.2.1 Pre-synthesised poly(α-ester) homologous blends

Pre-synthesised poly(α-ester) homologues have differences in the substituent groups (R_1 and R_2) in each polymer structure, which are shown in Table 3.1. Table 4.2 shows the percent transmittances (%T) of binary blends together with their structures and associated crystallinity. From the table, the values of the %T are shown together with shading block colours to represent the miscibility: opaque (black), semi-translucent (grey), translucent (light grey), and clear (white).

Table 4.2 Percent transmittances (%T) of binary blends of pre-synthesised poly(α-ester) homologues:

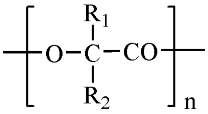

$$\left[O-\overset{R_1}{\underset{R_2}{C}}-CO \right]_n$$

Poly α-esters	α1 (dimethyl)	α2 (diethyl)	α3 (cyclopentyl)	α4 (cyclohexyl)	α5 (cycloheptyl)	α6 (chlorometyl-methyl)
	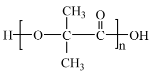	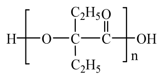	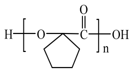	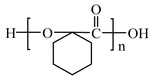	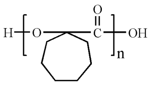	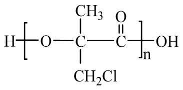
%T	2	1	89	86	80	100
	Crystalline*	Crystalline*	Amorphous*	Amorphous*	Amorphous	Amorphous

Blends of αX / αY (For X, Y = Poly α-esters	%T at different composition of αX / αY					Miscibility
	100/0	**75/25**	**50/50**	**25/75**	**0/100**	
α1/ α2	2	19	28	10	1	Poor
α1/ α3	2	95	100	85	89	Good
α1/ α4	2	32	63	91	86	Moderate
α1/ α5	2	95	77	82	80	Good
α1/ α6	2	22	19	28	100	Poor
α2/ α4	1	21	26	19	86	Poor
α2/ α5	1	1	1	1	80	Poor
α2/ α6	1	52	60	94	100	Moderate
α3/ α4	89	98	100	100	86	Good
α3/ α5	89	100	100	100	80	Good
α4/ α5	86	87	72	84	80	Good
α4/ α6	86	25	67	78	100	Moderate
α5/ α6	80	19	32	69	100	Moderate

Note: * The X-ray powder photographs shown in Figure 2.11.

From Table 4.2, it can be observed that the %T of neat α1(dimethyl) and α2(diethyl) are less than 30% (opaque) and that of other pre-synthesised poly(α-ester) homologues are more than 75% (clear). This is because of their molecular chain structures. α1(dimethyl) and α2(diethyl) show a symmetrical arrangement of their pendent groups, methyl and ethyl, respectively. This enables their polymer chains to form well-packed structures and thus to form crystalline regions. α3(cyclopentyl), α4(cyclohexyl), α5(cycloheptyl), and α6(chloromethyl-methyl) are asymmetrical structures and have bigger pendent groups of cyclopentyl, cyclohexyl, cycloheptyl, and chloromethyl, respectively, which restrict the close packing of their molecular chains.

α1(dimethyl)/α2(diethyl) blends are poorly miscible. This is because of their high ability to form crystalline regions. However, α1(dimethyl) shows more miscibility; with other pre-synthesised poly(α-ester) homologues (except with α6(chloromethyl-methyl)) than does α2(diethyl). This is probably because α1(dimethyl) has a less perfect crystalline structure than α2(diethyl) - as seen in the X-ray powder photographs (Figure 2.11) - that lead the chains to be more mobile and to interact with other amorphous poly(α-esters) more easily than α2(diethyl). One possible (and logical) explanation is that α1(dimethyl) can pack as a planar zig-zag but α2(diethyl) is driven to form a helical structure.

α2(diethyl) shows partial miscibility with α6(chloromethyl-methyl), whereas α1(dimethyl) shows immiscibility. This may be because the dipole-dipole interaction between the chains produced from the polar group of $-CH_2Cl$ in α6(chloromethyl-methyl) is more effective with the diethyl polymer and its tendency to form helical structures than with the dimethyl polymer.

The amorphous poly(α-esters) are mutually miscible, i.e. α3(cyclopentyl)/α4 (cyclohexyl), α4(cyclohexyl)/α5(cycloheptyl). However, α6(chloromethyl-methyl) seems only to show partial miscibility with amorphous poly(α-esters), i.e. α4(cyclohexyl), α5(cycloheptyl). This may be because the cycloalkyl group (the bulky group) in α4(cyclohexyl) and α5(cycloheptyl) cannot easily disrupt the polar interaction of chains with α6(chloromethyl-methyl) substituents.

4.2.2 PLLA/pre-synthesised poly(α-ester) homologous blends

To understand the effect of structure on miscibility, the crystalline pre-synthesised poly(α-ester) homologues (α1(dimethyl) and α2(diethyl)) and the amorphous (α4(cyclohexyl) and α6(chloromethyl-methyl)) were chosen to blend with PLLA. Two different molecular weights of PLLA; PLLA1 and PLLA2 (as shown in Table 4.3) were used to study the effect of molecular weight on miscibility.

Table 4.3 Molecular weights and percent transmittances of PLLA.

PLLA:	MW Average			%T
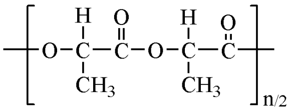 $\left[-O-\overset{H}{\underset{CH_3}{C}}-\overset{O}{\overset{\Vert}{C}}-O-\overset{H}{\underset{CH_3}{C}}-\overset{O}{\overset{\Vert}{C}}-\right]_{n/2}$	M_n	M_w	M_w/M_n	
PLLA1	18,700	28,000	1.497	18
PLLA2	63,500	94,800	1.493	98

As can be seen in Table 4.3, PLLA has –H and $–CH_3$ as substituent groups but it cannot form a planar zig-zag because of its asymmetrical structure, therefore, it forces gently into a helical structure and also shows polar interactions between backbones. PLLA1 itself is opaque (%T less than 30) while PLLA2 itself is clear (%T more than 75). This is because lower molecular weight PLLA1 allows a more rapid and complete crystallisation from solution, due to increased chain mobility, whereas higher molecular weight PLLA2 allows less crystallisation, due to decreased chain mobility and increased chain entanglement [79]. Thus, it can be said that PLLA1 crystallises more rapidly than PLLA2 does.

This will help in the understanding of the effect of molecular weights of PLLA on miscibility in the next two sections; PLLA1/pre-synthesised poly(α-ester) homologous blends (Section 4.2.2.1), PLLA2/pre-synthesised poly(α-ester) homologous blends (Section 4.2.2.2).

4.2.2.1 PLLA1/pre-synthesised poly(α-ester) homologous blends

Table 4.4 shows the percent transmittance and miscibility of the PLLA1/pre-synthesised poly(α-ester) homologous blends at different compositions. Figure 4.5 shows the visual shading miscibility diagram of these blends.

Table 4.4 Percent transmittance (%T) and miscibility of the PLLA1/pre-synthesised poly(α-esters) homologous blends.

Poly(α-esters)	PLLA1 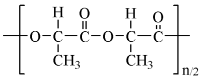 $-[O-CH(CH_3)-C(=O)-O-CH(CH_3)-C(=O)]_{n/2}-$	α1 (dimethyl) 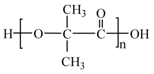 $H-[O-C(CH_3)_2-C(=O)]_n-OH$	α2 (diethyl) 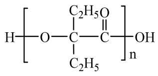 $H-[O-C(C_2H_5)_2-C(=O)]_n-OH$	α4 (cyclohexyl) 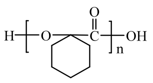	α6 (chloromethyl -methyl) 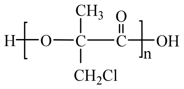 $H-[O-C(CH_3)(CH_2Cl)-C(=O)]_n-OH$
%T	18	2	1	86	100
Crystallinity	Semi-Crystalline	Crystalline	Crystalline	Amorphous	Amorphous

PLLA1 (wt.%)	**100**	**90**	**70**	**50**	**30**	**10**	**0**	**Miscibility**
αX (wt.%) (For X = Poly α-esters	**0**	**10**	**30**	**50**	**70**	**90**	**100**	
Blends	**%T at different compositions**							
PLLA1/α1	18	8	4	6	10	17	2	Poor
PLLA1/α2	18	10	10	22	7	3	1	Poor
PLLA1/α4	18	30	46	72	89	71	86	Moderate
PLLA1/α6	18	18	6	15	19	65	100	Poor

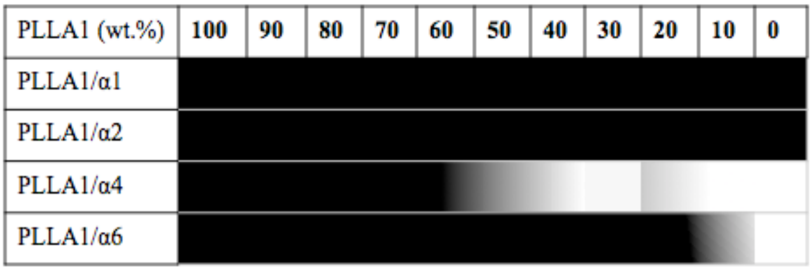

Figure 4.5 The visual shading miscibility diagram of the PLLA1/pre-synthesised poly(α-ester) homologous blends.

From the visual shading miscibility diagram shown in Figure 4.5, it can be seen that PLLA1/poly(α-ester) series blends are almost all immiscible even though they have similar structures. However, the amorphous polymers; α4(cyclohexyl) is partially miscible or fully miscible depending on blend composition, whereas α6(chloromethyl-methyl), which is also amorphous, seems to be unusual and is immiscible with PLLA1. It could be that the chloromethyl chains have strong mutual affinity and the dimethyl and diethyl have structural affinity (rapidly crystallisable), whereas cyclohexyl is the only one of the set that is neither crystalline nor has strong polar-polar interactions between its chains.

4.2.2.2 PLLA2/pre-synthesised poly(α-ester) homologous blends

Table 4.5 shows the percent transmittance and miscibility of PLLA2/pre-synthesised poly(α-ester) homologous blends at different compositions. The chemical structures of all polymers used in this section can also be seen in Table 4.4. Figure 4.6 shows the visual shading miscibility diagram of the PLLA2/poly(α-ester) series blends.

Table 4.5 Percent transmittance (%T) and miscibility of the PLLA2/pre-synthesised poly(α-ester) homologous blends.

PLLA2 (wt.%)	**100**	**90**	**70**	**50**	**30**	**10**	**0**	**Miscibility**
αX (For X = Poly α-esters	**0**	**10**	**30**	**50**	**70**	**90**	**100**	
Blends	**%T at different compositions**							
PLLA2/α1(dimethyl)	97	100	80	73	61	28	2	Moderate
PLLA2/α2(diethyl)	97	32	8	8	1	8	1	Poor
PLLA2/α4(cyclohexyl)	97	78	36	65	82	96	86	Moderate
PLLA2/α6(chloromethyl-methyl)	97	94	54	53	78	64	100	Moderate

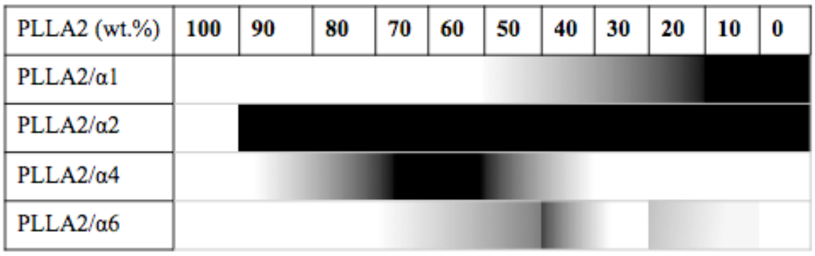

Figure 4.6 The visual shading miscibility diagram of the PLLA2/pre-synthesised poly (α-ester) homologous blends.

From the visual shading miscibility diagram shown in Figure 4.6, it can be seen that PLLA2/poly(α-ester) series blends show partially miscible behaviour, except, the well-packed α2(diethyl) which crystallises rapidly and thus restricts the interaction between their chains and PLLA2 chains. It is instructive to compare Figure 4.6 with Figure 4.5. Slower crystallisation from solution seems the logical reason for the enhanced miscibility of PLLA2 relative to PLLA1.

4.2.3 PLLA/PCL blends: Molecular weight effect

The effect of different molecular weights of PLLA to the miscibility was further studied by blending PLLA1 and PLLA2 with PCL, a well-known toughening agent for PLA [20, 23]. Two different molecular weight PCLs (PCL1 and PCL2) were used to study the blend miscibility. Details of molecular weights of PLLA and PCL are shown in Table 4.6.

Table 4.6 Molecular weights of PLLA and PCL.

Sample ID	MW Average		
	M_n	M_w	M_w/M_n
PLLA1	18,700	28,000	1.497
PLLA2	63,500	94,800	1.493
PCL1	7,500	13,300	1.773
PCL2	57,800	81,700	1.413

Therefore, four different blends: PLLA1/PCL1, PLLA2/PCL1, PLLA1/PCL2, and PLLA2/PCL2, were studied. Table 4.7 shows the percent transmittances and Figure 4.7 shows percent transmittance (%T) versus composition of PLLA. Figure 4.8 shows the visual shading miscibility diagram of these blends.

Table 4.7 Percent transmittance (%T) and miscibility of PLLA/PCL blends of different compositions and molecular weights of PLLA and PCL.

Polyesters	PLLA1	PLLA2	PCL1	PCL2
	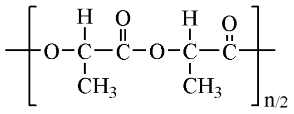 $\left[-O-\underset{CH_3}{\overset{H}{C}}-\overset{O}{\overset{\|}{C}}-O-\underset{CH_3}{\overset{H}{C}}-\overset{O}{\overset{\|}{C}}-\right]_{n/2}$		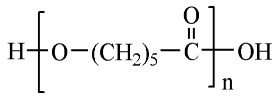 $H\left[-O-(CH_2)_5-\overset{O}{\overset{\|}{C}}-\right]_n OH$	
%T	18	98	10	84
% Crystallinity	38	31	74	54

	Composition of PLLA/PCL									**Miscibility**
PCL (wt.%)	**10**	**20**	**30**	**40**	**50**	**60**	**70**	**80**	**90**	
PLLA (wt.%)	**90**	**80**	**70**	**60**	**50**	**40**	**30**	**20**	**10**	
Blends	**%T**									
PLLA1/PCL1	9	10	13	10	14	13	8	9	8	Poor
PLLA1/PCL2	20	10	13	10	8	8	10	7	7	Poor
PLLA2/PCL1	97	91	30	23	28	12	11	12	14	Poor
PLLA2/PCL2	94	94	85	82	80	77	81	82	50	Good

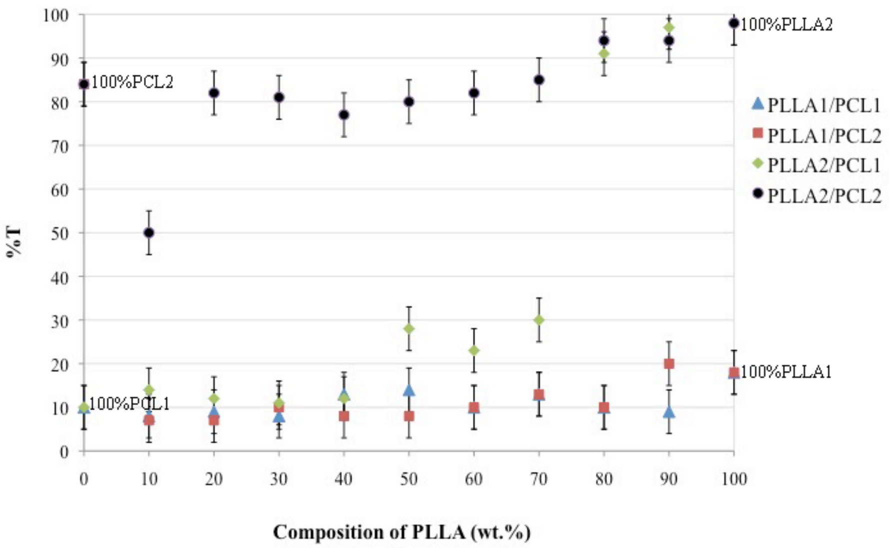

Figure 4.7 Percent transmittance (%T) of the PLLA/PCL blends of different molecular weights and compositions of PLLA and PCL.

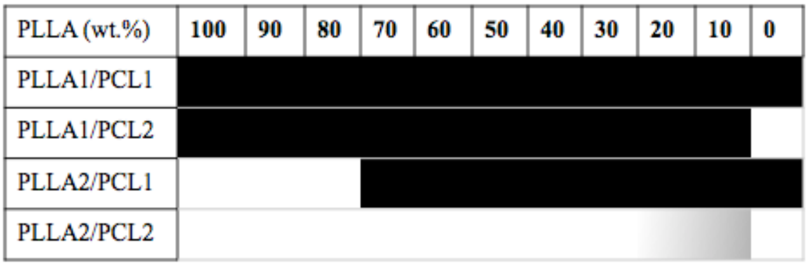

PLLA (wt.%)	**100**	**90**	**80**	**70**	**60**	**50**	**40**	**30**	**20**	**10**	**0**
PLLA1/PCL1	■	■	■	■	■	■	■	■	■	■	■
PLLA1/PCL2	■	■	■	■	■	■	■	■	■	■	
PLLA2/PCL1				■	■	■	■	■	■	■	■
PLLA2/PCL2									▨	▨	

Figure 4.8 The visual shading miscibility diagram of the PLLA/PCL blends of different molecular weights and compositions of PLLA and PCL.

From the miscibility diagram shown in Figure 4.8, there is another example of the effect of crystallisation rate on miscibility. It seems to confirm that polymers that crystallise more rapidly (PLLA1 > PLLA2 and PCL1 > PCL2) are less miscible. For example, it can be seen that the PLLA1/PCL1 blends are immiscible (PLLA1 and PCL1 both show fast crystallisation), whereas the PLLA2/PCL2 blends are miscible (PLLA2 and PCL2 both slow slower crystallisation).

4.2.4 PLLA/CAB and PCL/CAB blends: Molecular weight effect

The different molecular weights PLLA and PCL (Table 4.6) were further studied in relation to miscibility behaviour by blending with cellulose acetate butyrate (CAB), a hydrogen-bonding polymer and a well-known polymer for blending [77].

Four different blends: PLLA1/CAB, PLLA2/CAB, PCL1/CAB, and PCL2/CAB were used to blend with different compositions. Table 4.8 shows percent transmittance and miscibility of these blends. Figure 4.9 shows percent transmittance (%T) versus composition of CAB and Figure 4.10 shows the visual shading miscibility diagram of these blends.

Table 4.8 Percent transmittance (%T) and miscibility of PLLA/CAB and PCL/CAB blends of different compositions and molecular weights of PLLA and PCL.

Polyesters	PLLA1	PLLA2	PCL1	PCL2	CAB
	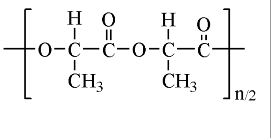 $\left[-O-\underset{CH_3}{\overset{H}{C}}-\overset{O}{\overset{\|}{C}}-O-\underset{CH_3}{\overset{H}{C}}-\overset{O}{\overset{\|}{C}}-\right]_{n/2}$		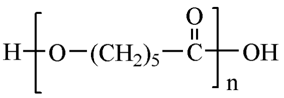 $H\left[O-(CH_2)_5-\overset{O}{\overset{\|}{C}}\right]_n OH$		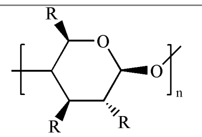 R= $(OH)_x$, $(O\overset{O}{\overset{\|}{C}}CH_3)_y$, $(O\overset{O}{\overset{\|}{C}}CH_2CH_2CH_3)_z$ where: $x + y + z = 3$, x, y > 0
%T	18	98	10	84	100
% Crystllinity	38	31	74	54	-

	Composition of PLLA/PCL									**Good miscibility* when using CAB**
CAB (wt.%)	**10**	**20**	**30**	**40**	**50**	**60**	**70**	**80**	**90**	
PLLA or PCL (wt.%)	**90**	**80**	**70**	**60**	**50**	**40**	**30**	**20**	**10**	
Blends	**%T**									
PLLA1/CAB	8	9	10	7	31	71	79	85	95	≥ 70 wt.%
PLLA2/CAB	43	51	41	78	81	95	96	95	98	≥ 40 wt.%
PCL1/CAB	12	14	32	39	44	64	69	97	98	≥ 80 wt.%
PCL2/CAB	35	15	39	33	86	98	100	100	99	≥ 50 wt.%

Note: * Good miscibility is denoted when the percent transmittance of the blend is more than 75%

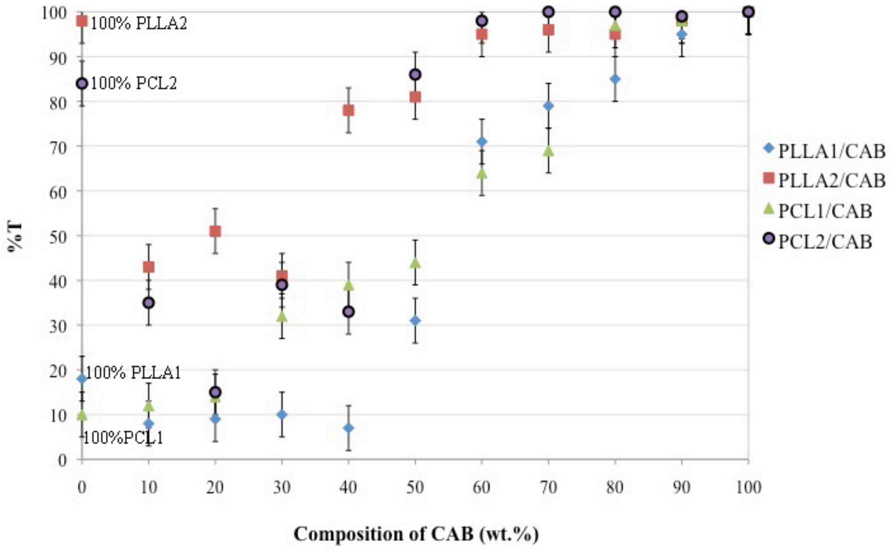

Figure 4.9 Percent transmittance (%T) of the PLLA/CAB and PCL/CAB blends of different molecular weights and compositions of PLLA and PCL.

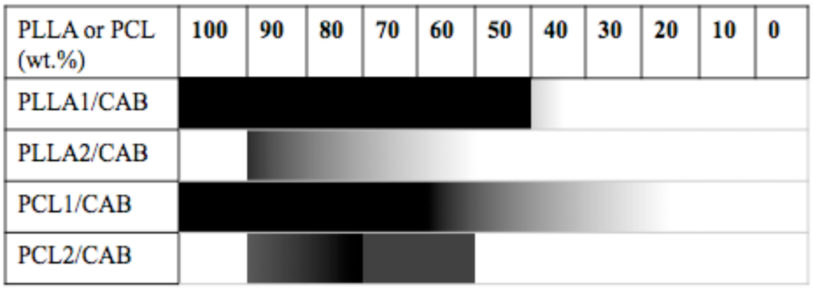

Figure 4.10 The visual shading miscibility diagram of the PLLA/CAB and PCL/CAB blends of different molecular weights and compositions of PLLA and PCL.

The miscibility diagram shown in Figure 4.10 appears to confirm that polymers that crystallise more rapidly (PLLA1 > PLLA2 and PCL1 > PCL2) are less miscible with CAB. However, CAB, which is amorphous, seems to be able to slow down the crystallisation of PLLA1 and PCL1 by intermingling and forming hydrogen bonding and/or dipole-dipole interactions with PLLA1 and PCL1. The order of miscibility of PLLA/CAB and PCL/CAB blends can be shown below:

PLLA2/CAB ≥ PCL2/CAB > PLLA1/CAB ≥ PCL1/CAB

4.2.5 Blends of PLLA or PDLLA with PCL1, CAB, or α4(cyclohexyl): Effect of stereochemistry/crystallinity

PLLA1, PLLA2, and PDLLA were particularly interesting in observing miscibility in binary blends. PLLA has a semi-crystalline structure which has a crystallinity of approximately 30-40%, whereas, PDLLA is not crystalline, but amorphous [80].

To observe the effect of polymer structure on the miscibility of blends, three different structure polymers; α4(cyclohexyl), poly(ε-caprolactone) (PCL) and cellulose acetate butyrate (CAB) were used to blend with PLLA1, PLLA2, and PDLLA. The miscibility of these polymers blended with either PLLA1, PLLA2, or PDLLA are described in the following sections.

4.2.5.1 PLLA1, PLLA2, and PDLLA blended with PCL1

Table 4.9 shows percent transmittance and miscibility of these blends at various compositions. Figure 4.11 shows percent transmittance (%T) versus composition of PCL1. Figure 4.12 shows the visual shading miscibility diagram of these blends.

Table 4.9 Percent transmittance (%T) and miscibility of PLLA1, PLLA2, and PDLLA blended with PCL1 at different compositions.

Polyesters	PLLA1	PLLA2	PDLLA	PCL1
	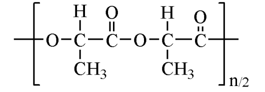 $\left[-O-\overset{H}{\underset{CH_3}{C}}-\overset{O}{\overset{\Vert}{C}}-O-\overset{H}{\underset{CH_3}{C}}-\overset{O}{\overset{\Vert}{C}}- \right]_{n/2}$		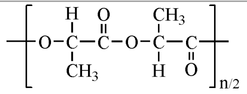 $\left[-O-\overset{H}{\underset{CH_3}{C}}-\overset{O}{\overset{\Vert}{C}}-O-\overset{CH_3}{\underset{H}{C}}-\underset{O}{\underset{\Vert}{C}}- \right]_{n/2}$	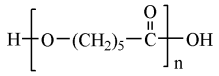 $H\left[O-(CH_2)_5-\overset{O}{\overset{\Vert}{C}} \right]_n OH$
%T	18	98	100	10
% Crystallinity	38	31	-	74

PCL1 (wt.%)	**10**	**20**	**30**	**40**	**50**	**60**	**70**	**80**	**90**	**Miscibility**
PLA (wt.%)	**90**	**80**	**70**	**60**	**50**	**40**	**30**	**20**	**10**	
Blends	**%T**									
PLLA1/PCL1	9	10	13	10	14	13	8	9	8	Poor
PLLA2/PCL1	97	91	30	23	28	12	11	12	14	Poor
PDLLA/PCL1	93	52	64	83	73	75	59	69	21	Moderate

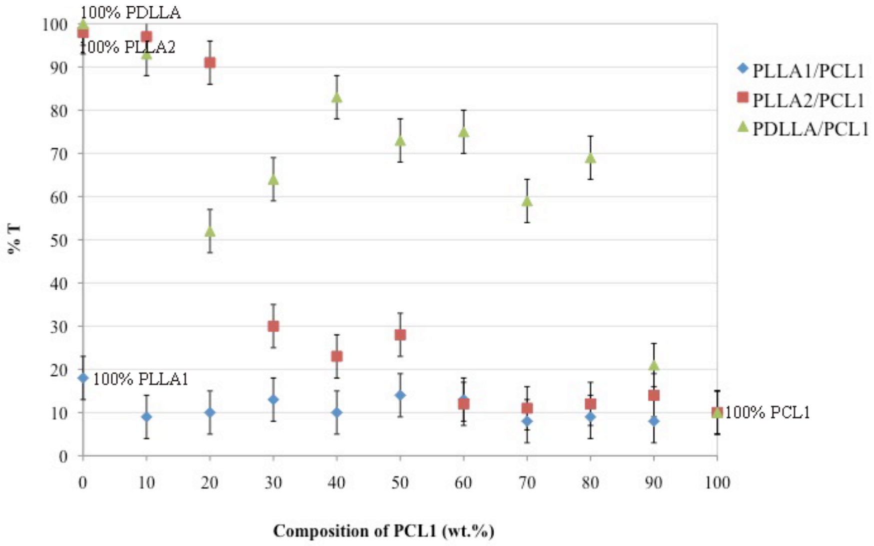

Figure 4.11 Percent transmittance (%T) of PLLA1, PLLA2, and PDLLA blended with PCL1 at different compositions.

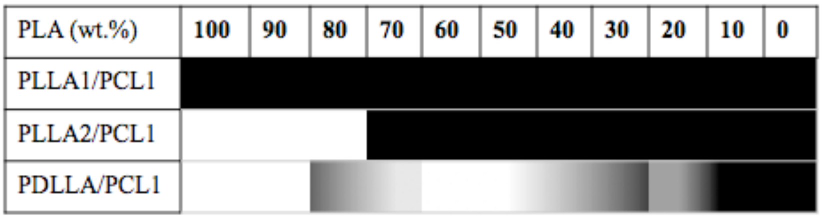

Figure 4.12 The visual shading miscibility diagram of PLLA1/PCL1 and PDLLA/PCL1 blends at different compositions.

From the miscibility diagram shown in Figure 4.12, it seems to show that polymers that crystallise more rapidly (PLLA1 > PLLA2) are less miscible with PCL1 which is a crystalline polymer. For example, it can be seen that the PLLA1 and PCL1 blend is immiscible because both show rapid crystallisation, while PLLA2 seems to slow down the crystallisation rate of the blend. Finally, the amorphous PDLLA, which shows no crystallisation, shows greater miscibility than the crystalline PLLA1 and PLLA2 polymers.

4.2.5.2 PLLA1, PLLA2, and PDLLA blended with CAB

The effect of stereochemistry and crystallinity on miscibility of PLLA1/CAB, PLLA2/CAB, and PDLLA/CAB blends was further studied. Table 4.10 shows the percent transmittance and miscibility of these blends at different compositions. Figure 4.13 shows the percent transmittance (%T) versus composition of CAB and Figure 4.14 shows the visual shading miscibility diagram.

Table 4.10 Percent transmittance (%T) and miscibility of PLLA1, PLLA2, and PDLLA blended with CAB at different compositions.

Polyesters	PLLA1	PLLA2	PDLLA	CAB
	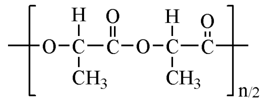		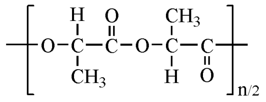	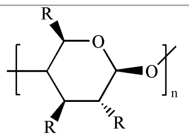 $R = (OH)_x, (O\text{-}\overset{O}{\overset{\|}{C}}\text{-}CH_3)_y, (O\text{-}\overset{O}{\overset{\|}{C}}\text{-}CH_2CH_2CH_3)_z$ where: $x + y + z = 3, x, y > 0$
%T	18	98	100	100
% Crystallinity	38	31	-	-

CAB (wt.%)	**10**	**20**	**30**	**40**	**50**	**60**	**70**	**80**	**90**	**Miscibility**
PLA (wt.%)	**90**	**80**	**70**	**60**	**50**	**40**	**30**	**20**	**10**	
Blends	**%T**									
PLLA1/CAB	8	9	10	7	31	71	79	85	95	Moderate
PLLA2/CAB	43	51	41	78	81	95	96	95	98	Good
PDLLA/CAB	61	57	81	74	78	83	94	97	100	Very Good

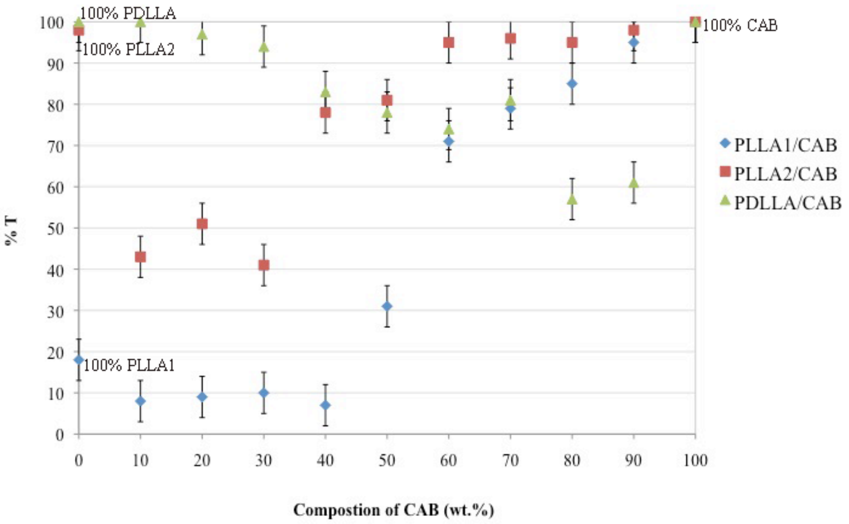

Figure 4.13 Percent transmittances (%T) of PLLA1, PLLA2, and PDLLA blended with CAB at different compositions.

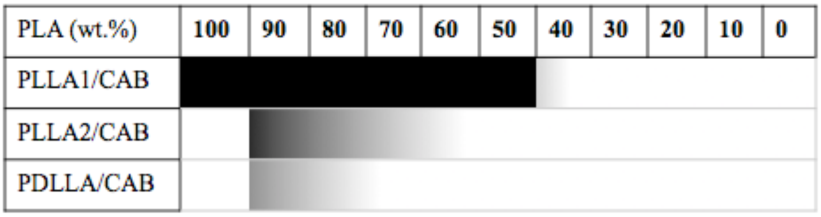

PLA (wt.%)	100	90	80	70	60	50	40	30	20	10	0
PLLA1/CAB											
PLLA2/CAB											
PDLLA/CAB											

Figure 4.14 The visual shading miscibility diagram of the PLLA1/CAB and PDLLA/CAB blends at different compositions.

From the miscibility diagram shown in Figure 4.14, it can be seen that polymers that crystallise more rapidly (PLLA1 > PLLA2) are less miscible with CAB which is an amorphous and hydrogen bonding polymer. For example, the slow crystallisation rate of PLLA2 (helical and crystalline polymer) allows CAB to disrupt its organisation, and there is more intermingling and miscibility with CAB than with PLLA1. In addition, the helical and crystalline PLLA2 shows less miscibility than the amorphous PDLLA, which is not able to crystallise.

4.2.5.3 PLLA1, PLLA2, and PDLLA blended with α4(cyclohexyl)

The effect of stereochemistry and crystallinity on miscibility of PLLA1, PLLA2, and PDLLA blended with α4(cyclohexyl) was studied. Table 4.11 shows the percent transmittance and miscibility of the blends at different compositions. Figure 4.15 shows the visual shading miscibility diagram.

Table 4.11 Percent transmittance (%T) and miscibility of PLLA1, PLLA2, and PDLLA blended with α4(cyclohexyl) at different compositions.

Polyesters	PLLA1	PLLA2	PDLLA	α4(cyclohexyl)
	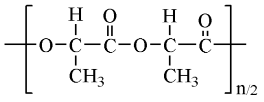		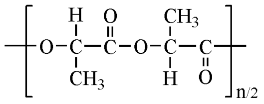	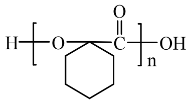
%T	18	98	100	86
% Crystallinity	38	31	-	-

α4(cyclohexyl) (wt.%)	**0**	**25**	**50**	**75**	**100**	**Miscibility**
PLLA1, PLLA2, or PDLLA (wt.%)	**100**	**75**	**50**	**25**	**0**	
Blends	**%T**					
PLLA1/α4(cyclohexyl)	18	35	72	71	86	Moderate
PLLA2/ α4(cyclohexyl)	98	40	65	85	86	Moderate-Good
PDLLA/α4(cyclohexyl)	100	30	72	92	86	Moderate-Good

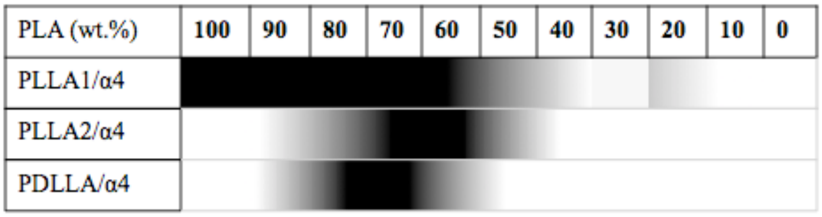

Figure 4.15 The visual shading miscibility diagram of PLLA1, PLLA2, and PDLLA blended with α4(cyclohexyl) at different compositions.

The miscibility diagram shown in Figure 4.15 confirms the hypothesis that polymers that crystallise more rapidly (PLLA1 > PLLA2) are less miscible with α4(cyclohexyl) which is an amorphous polymer. However, PLLA1 is miscible with α4(cyclohexyl) in regions which depend on the blend compositions.

4.2.5.4 Overview: Effect of stereochemistry/crystallinity

The miscibility of poly(lactic acid) (PLA) blended with different polymer structures of PCL1 (a flexible and crystalline polymer), CAB (a H-bonding polymer), or α4(cyclohexyl) (an amorphous polymer) were compared and discussed in this section. Their chemical structures are shown below. Figure 4.16 shows the visual shading miscibility diagram of the blends.

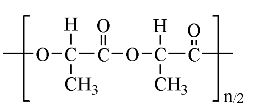 PLLA1, PLLA2	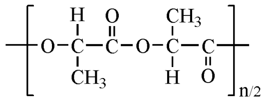 PDLLA	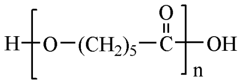 PCL1
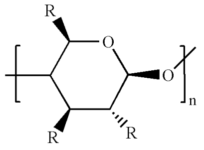 CAB	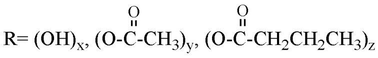 $R = (OH)_x, (O\text{-}\overset{O}{\overset{\|\|}{C}}\text{-}CH_3)_y, (O\text{-}\overset{O}{\overset{\|\|}{C}}\text{-}CH_2CH_2CH_3)_z$ where: $x + y + z = 3$, $x, y > 0$	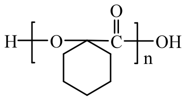 α4(cyclohexyl)

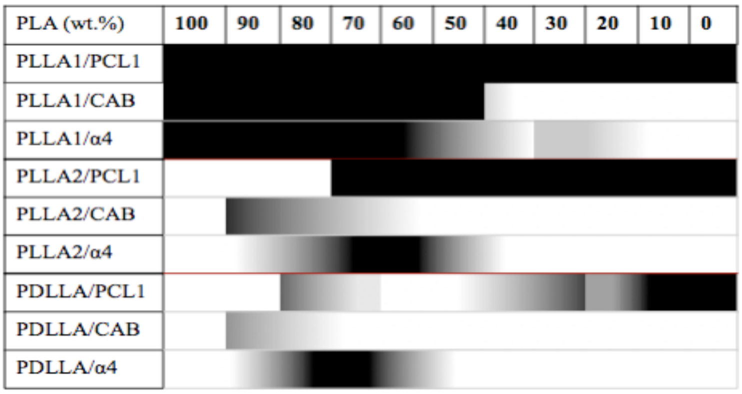

Figure 4.16 The visual shading miscibility diagram of PLLA1, PLLA2, and PDLLA blended with PCL1, CAB, or α4(cyclohexyl) at various compositions.

From the miscibility diagram shown in Figure 4.16, it appears that polymers that crystallise more rapidly (PLLA1, PCL1 > PLLA2 > α4(cyclohexyl), CAB, PDLLA) are less miscible, whereas none-crystalline polymers are more miscible. For example, the PLLA1/PCL1 blend - both show fast crystallisation - is totally immiscible, while PDLLA/CAB blend – both are non-crystalline- is totally miscible. In addition, CAB - the non-crystalline and hydrogen bonding polymer - seems to show miscibility with PLLA1, PLLA2, and PDLLA, more than α4(cyclohexyl) (a polymer that shows a very low level of crystallinity) and PCL1 (a fast crystallisation polymer) do.

One interesting complementary observation is that PCL1 shows enhanced PDLLA miscibility in the 30-50% composition ranges relative to the near-isomeric α4(cyclohexyl). The flexible repeat unit in PCL1 enables more effective dipole-dipole interactions than α4(cyclohexyl), as shown in Figure 4.17 (a). Although poly(α-esters) have similar distances between points of polarity, the dipole-dipole interactions are impeded by steric consideration of α4(cyclohexyl), as shown in Figure 4.17 (b). This suggests that mobility of the polar ester groups is more beneficial than matching their spatial disposition along the polymer backbone.

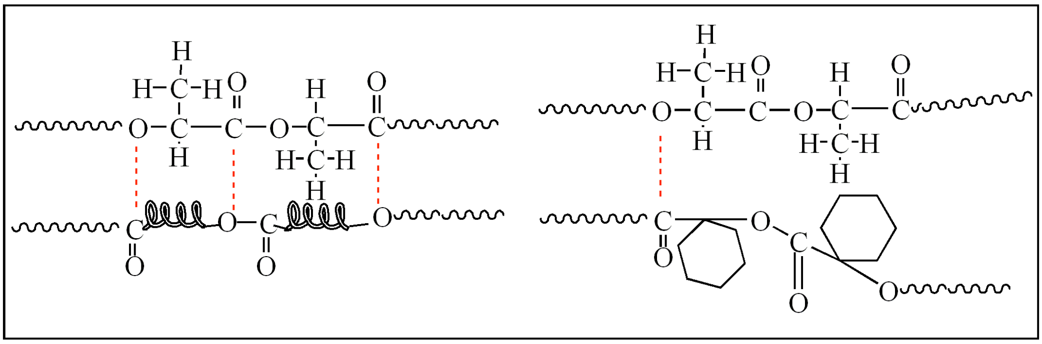

(a) **(b)**

Figure 4.17 The presumed micro-phase structure of the PDLLA/PCL1 and PDLLA/α4(cyclohexyl) chains interaction.

4.2.6 PLLA1/other biodegradable polymers blends

PLLA1 has historically been blended with a number of different polymers to modify its properties for particular applications [21, 36, 81-84]. In this section, poly(ethylene glycol) (PEG), poly(ethylene succinate) (PES) and poly(butylene succinate) (PBS) were chosen to blend with PLLA1. PEG is a hydrophilic polymer which has been used as a compatible plasticiser to improve mechanical properties of PLA [36, 85]. PES and PBS are diacid-diol aliphatic polyesters, which have high flexibility and excellent mechanical properties.

Table 4.12 shows the percent transmittance and miscibility of PLLA1 blended with PEG, PES, and PBS at different compositions and Figure 4.18 shows the visual shading miscibility diagram.

Table 4.12 Percent transmittance (%T) and miscibility of PLLA1 blended with either of PEG, PES, or PBS at different compositions.

<table>
<tr><td colspan="2">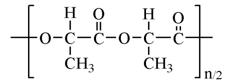 $\left[O-\underset{CH_3}{\overset{H}{C}}-\overset{O}{\overset{\|}{C}}-O-\underset{CH_3}{\overset{H}{C}}-\overset{O}{\overset{\|}{C}} \right]_{n/2}$</td><td>$\left[O-CH_2-CH_2-O \right]_n$</td><td>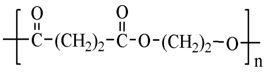 $\left[\overset{O}{\overset{\|}{C}}-(CH_2)_2-\overset{O}{\overset{\|}{C}}-O-(CH_2)_2-O \right]_n$</td><td>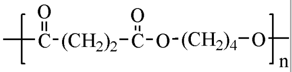 $\left[\overset{O}{\overset{\|}{C}}-(CH_2)_2-\overset{O}{\overset{\|}{C}}-O-(CH_2)_4-O \right]_n$</td></tr>
<tr><td colspan="2">PLLA1</td><td>PEG</td><td>PES</td><td>PBS</td></tr>
<tr><td>%T</td><td>18</td><td>19</td><td>10</td><td>20</td></tr>
</table>

PEG, PES, or PBS (wt.%)	**0**	**25**	**50**	**75**	**100**	**Miscibility**
PLLA1 (wt.%)	**100**	**75**	**50**	**25**	**0**	
Blends	**%T**					
PLLA1/PEG	18	10	13	10	19	Poor
PLLA1/ PES	18	7	14	5	10	Poor
PLLA1/PBS	18	59	58	6	20	Poor

PLLA1 (wt.%)	100	90	80	70	60	50	40	30	20	10	0
PLLA1/PEG											
PLLA1/PES											
PLLA1/PBS											

Figure 4.18 The visual shading miscibility diagram of PLLA1 blended with either PEG, PES, or PBS at various compositions.

One interpretation of the low percent transmittances maybe that immiscibility is caused by the rapid crystallisation of the polymers (PLLA1, PEG, PES, and PBS). PEG, PES, and PBS seem to precipitate rapidly because their polarities are greater than that of $CHCl_3$. However, the flexible chains of PBS (from butylene groups) may help to improve the miscibility of PLLA1/PBS blends.

4.3 SUMMARY OF THE CHAPTER

The discovery of the rapid screening method helps to do fast laboratory experimental screening work. The technique allows the use of very small (mg-ranges) of samples in microlitres of solvents, which is useful for studying solvent blending not only of binary blends in this chapter but also of ternary blends in the next chapter.

As observed from the binary blend results, this is the pattern that is emerging.

1. The structures of pre-synthesised poly(α-esters) homologues

- α1(dimethyl) and α2(diethyl) are the polymers that cannot easily form clear films because they are crystalline with different forms of structures. α2(diethyl) tends to form a helical structure (coiled structure) because it cannot easily pack -C_2H_5- groups into a planar zig-zag whereas α1(dimethyl) will not be driven into coil but a planar zig-zag from -CH_3 groups [5].

- Poly(α-esters): α3(cycloheptyl), α4(cyclohexyl), and α5(cycloheptyl) are amorphous having large side-groups. The chains can entangle and align through their polar backbone but are very asymmetric and hydrophobic, as the solvent evaporates the polymer chains remain enlarged and do not pack well.

- Chloromethyl-methyl poly(α-ester) (α6) is an unusual poly(α-ester) because it is the only one of those polymers that has polarity in its side-chain (-CH_2Cl). The -CH_2Cl group is a dipolar group, which can bind with itself. This polarity enhances the ability of polymer to interact with itself and also to disrupt the polarity and the structure of other poly(α-esters). The α6(chloromethyl-methyl) chains cannot pack as a planar zig-zag because of the larger size of the -CH_2Cl relative to CH_3 and also because the substituent cannot easily organise itself in space in a crystal, but it is still going to coil to form a polymer chain with helical segments. Therefore, α2(diethyl) and α6(chloromethyl-methyl) are the only two polymers driven into a coil.

2. The miscibility of the binary solvent blends

- α1(dimethyl)/α2(diethyl) form immiscible blends because of their crystalline structure, but α2(diethyl) shows less miscibility with other pre-synthesised poly(α-esters) homologues (except α6(chloromethyl-methyl)) than α1(dimethyl) because of its tendency to force helical structures. α3(cyclopentyl), α4 (cyclohexyl), and α5(cycloheptyl) are mutually miscible but they cannot easily disrupt the polar interactions between α6(chloromethyl-methyl) chains (from –CH_2Cl), so they tends to separate.

- α6(chloromethyl-methyl) interferes with the crystallinity of diethyl poly(α-ester) (α2) more than it does the crystallinity of dimethyl poly(α-ester) (α1). This is because the –CH_2Cl (from α6 – tends to form a helical structure) enabling it to entangle more effectively with the helical structure of α2(diethyl) than with the more linear α1(dimethyl). Not only because of these coils, but also the dipolar –CH_2Cl can interact strongly with the α2(diethyl) polymer and combine to inhibit the crystallisation of α2(diethyl). However, PLLA (a helical polymer) would interact with α6(chloromethyl-methyl) but it is less sterically hindered than α2(diethyl) which means that the crystalline structure of PLLA is more difficult to disrupt. Therefore, there is only one polymer in which crystallisation is interrupted strongly by α6(chloromethyl-methyl), this is α2(diethyl) - although both poly(α-esters) form helical structures.

- The stereochemistry, the molecular weight, and the crystallinity of poly(lactic acid) (PLA) affects the crystallisation rate – an important factor to explain why PLLA1 behaves in solvent blending differently from PLLA2 and PDLLA. This aspect of behaviour is largely responsible for the miscibility behaviour of PLLA1, PLLA2, and PDLLA blended with other polymers. PLLA1 (semi-crystalline structure) crystallises rapidly which means their chains have less opportunity to intermingle and to interact with other polymers such as PCL, CAB, and pre-synthesised poly(α-ester) homologues. On the other hand PLLA2 (semi-crystalline structure) crystallises more slowly, therefore, the balance between mutual entanglement and crystallisation favours entanglement. PDLLA is unable to crystallise, therefore, it is able to show the most mutual intermingling and miscibility.

- PLLA1 can only mix its entangled amorphous region with amorphous polymer structures, i.e. α4(cylohexyl), which have more apparent mutual solubility in PLLA1 than crystalline polymer structures, such as α1(dimethyl) and α2(diethyl). Moreover, PLLA1 cannot mix its very tight and polar helical crystalline region with the helical amorphous regions of α6(chloromethyl-methyl), whereas it appears that the less polar helical α2(diethyl) chains can intermingle with α6(chloromethyl-methyl).

- An important effect on miscibility of PLLA blended with either PCL or CAB is not only the crystallisation rates of PLLA and PCL but also the presence of CAB and the solvent. The ability to form molecular interactions between the polymer chains of the hydrogen bonding polymer (CAB) together with polymer morphology (the helical polymer (PLLA), and the planar zig-zag polymer (PCL) are important.

CHAPTER 5

SOLVENT BLENDING: TERNARY BLENDS

Chapter 5

Solvent Blending: Ternary Blends

5.1 Preliminary discussion

Studies of binary blends provide a useful indication of potentially interesting ternary blends based on PLLA. In moving from binary blends to ternary blends, another method of presentation that deals with clarity was used – ternary phase miscibility diagrams, as shown in Figure 2.3 and for convenience is included in Figure 5.1.

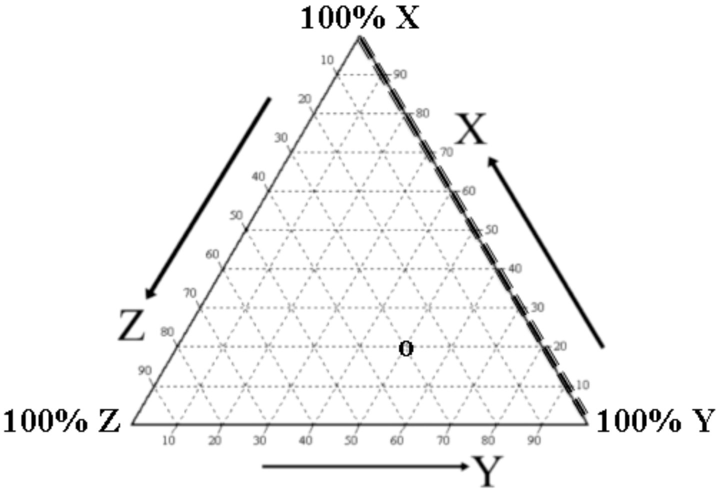

Figure 5.1 The demonstration of the ternary phase miscibility diagram for X/Y/Z blend.

To understand how the ternary phase miscibility diagram works, there are two approaches:

1. The lines along the axes "**the binary lines**" correspond to two-component blends, this is when the third component is set to zero, for example; X/Y binary line (dashed line) represents the miscibility of the polymer X and Y blend at different compositions when Z is 0 wt%.
2. The area inside the triangle represents the three-component blends, for example; the circle marked in Figure 5.1 represents the three-component blend of X/Y/Z at 20/50/30.

The visual shading miscibility diagrams of polymer pairs studied in the previous chapter, which were used in the three-component blends (such as PLLA/PCL/CAB blends), were collected and are shown in Figure 5.2. They are the miscibilities shown at the binary lines of a ternary phase miscibility diagram. However, the miscibility of the ternary blends may or may not correspond to the results obtained from a binary blend as a third component adds extra complexity.

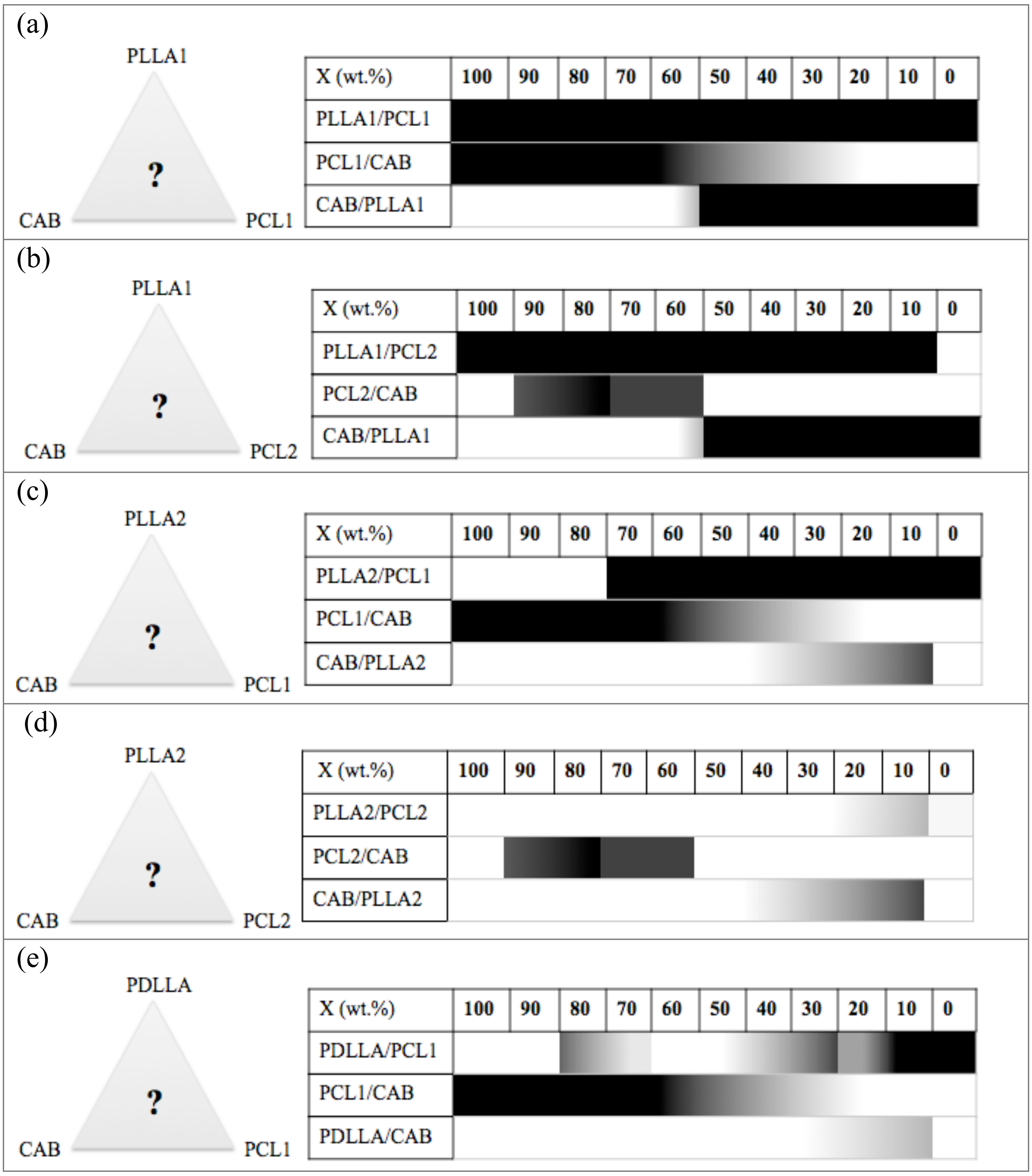

Note: X = the polymer in the blends of X/Y, i.e. PLLA1/PCL1, X = PLLA1.

Figure 5.2 The visual shading miscibility diagrams of binary blends for ternary blends.

Ternary phase miscibility diagrams illustrate a range of films of given clarity (opaque to clear), which are determined by percent transmittances (%T) the same as the binary phase diagram. The sample films are designated: opaque when %T is in range of 0-30; semi-translucent - in range of 31-45; translucent - in range of 46-75; and clear – in range of 76-100.

The PLLA/PCL/CAB blends are principal polymers used for miscibility studies in this chapter. The effect of stereochemistry and molecular weights of poly(lactic acid) (PLA: PLLA, PDLLA) on miscibility of ternary blends was observed. Other candidate polymers, such as plasticisers, cellulose polymers, thermoplastic polyurethane, and diacid-diol polyesters**,** were also used to blend with PLLA.

5.2 PLLA1/PCL1/CAB blends

PLLA1, PCL1, and CAB (chemical structures shown below) were blended using the rapid screening method. The percent transmittances are observed and presented in the ternary phase miscibility diagram in Figure 5.3.

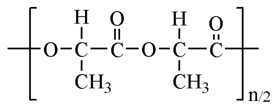

$$\left[-O-\overset{H}{\underset{CH_3}{C}}-\overset{O}{\overset{\|}{C}}-O-\overset{H}{\underset{CH_3}{C}}-\overset{O}{\overset{\|}{C}}-\right]_{n/2}$$

PLLA1

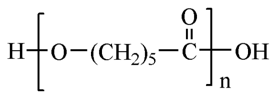

$$H-\left[O-(CH_2)_5-\overset{O}{\overset{\|}{C}}\right]_n-OH$$

PCL1

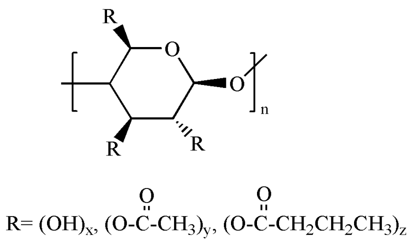

$R = (OH)_x, (O-\overset{O}{\overset{\|}{C}}-CH_3)_y, (O-\overset{O}{\overset{\|}{C}}-CH_2CH_2CH_3)_z$

where: $x + y + z = 3$, $x, y > 0$

CAB

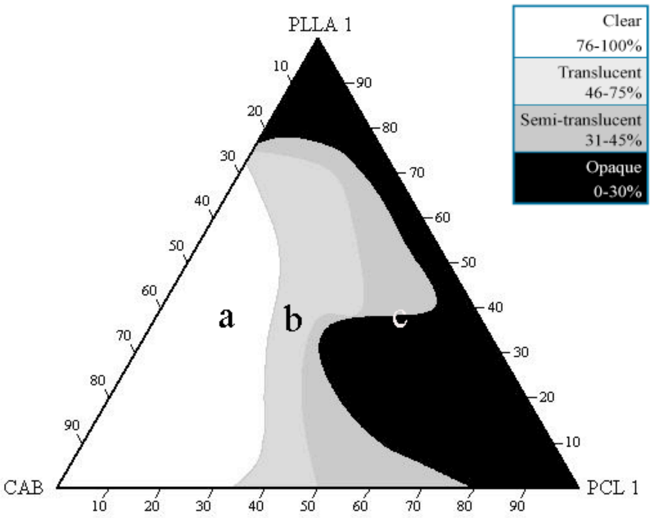

Figure 5.3 The ternary phase miscibility diagram of the PLLA1/PCL1/CAB blends.

From the ternary phase miscibility diagram (Figure 5.3), it can be seen that the opaque region moves from the PLLA1 and PCL1 binary line (PCL1-PLLA1 axis), therefore, it can be said that PLLA1 and PCL1 influences the PLLA1/PCL1/CAB blends to be more immiscible. This can be confirmed by the results from the binary blends of PLLA1/PCL1 being immiscible in all composition ranges, while PLLA1 and PCL1 blended with CAB are miscible at certain compositions (as shown by binary diagram in Figure 5.2 a.).

By following the composition line corresponding to 40 wt% PLLA1 through various compositions of CAB and PCL1 in Figure 5.3, the boundaries of phase behaviour can be illustrated with the different clarity of the films: clear (at position a), translucent (at position b), and opaque (at position c); and Figure 5.4a, b and c shows their films (the bright light observed in each film is from the light reflecting from the camera flash).

a. clear film **b.** translucent film **c.** opaque film

Figure 5.4 Photographs of the film samples of the PLLA/PCL/CAB blends from well-plates at different compositions: (a) 40/15/45 (clear), (b) 40/35/25 (translucent), and (c) 40/50/10 (opaque).

The phase separations of these three component blend films were also observed by using SEM, which is shown in Figure 5.5.

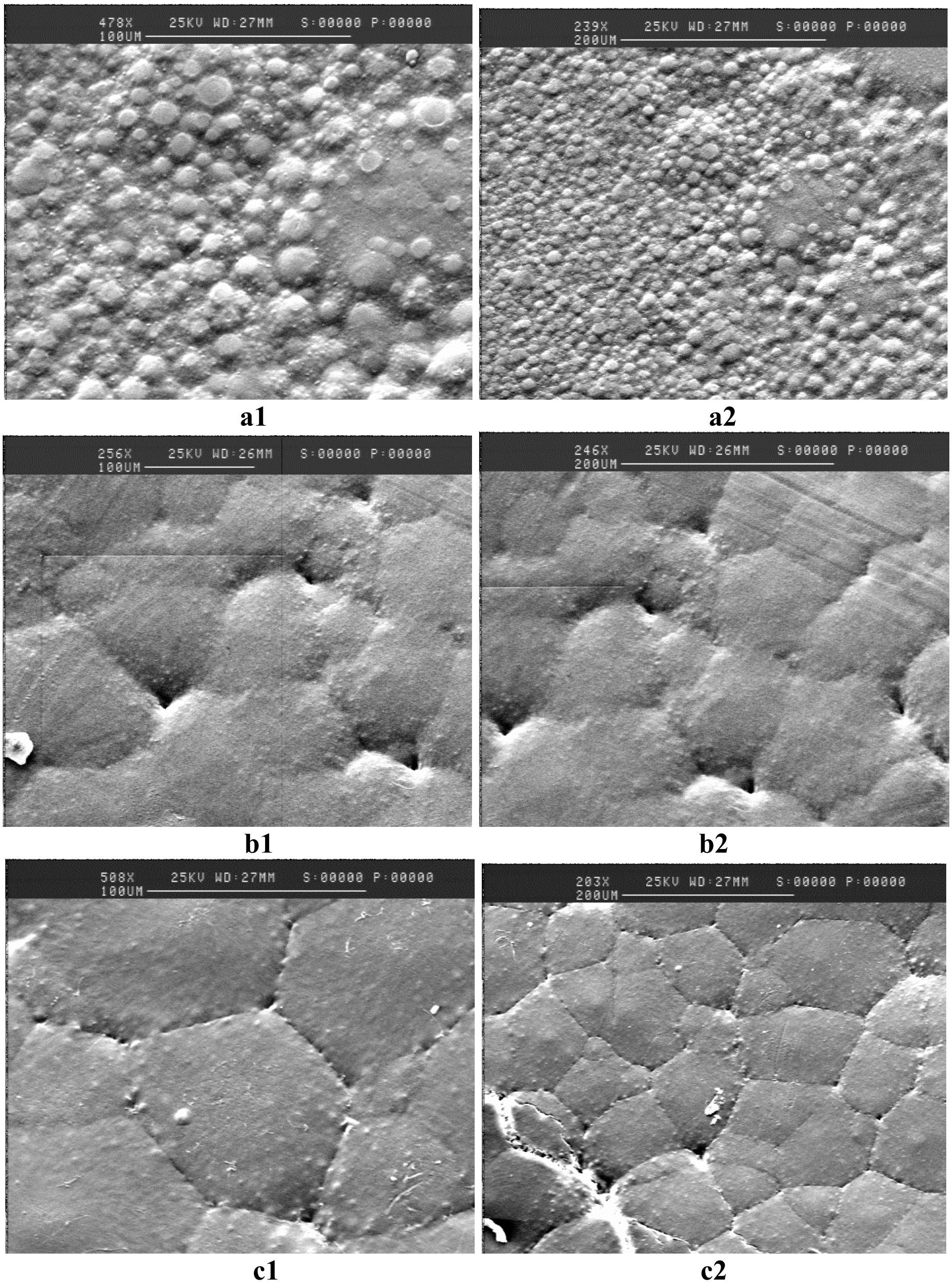

a1 **a2**

b1 **b2**

c1 **c2**

Figure 5.5 SEM images of the PLLA1/PCL1/CAB blend films at various
compositions; 40/15/45 - clear film (a1 x100, a2 x 200),
40/35/ 25 - translucent film (b1 x100, b2 x 200), and
40/50/10 - opaque film (c1 x100, c2 x 200).

From Figure 5.5a, it can be seen that the dispersed phase was finely dispersed in the matrix for the clear film (40/15/45 PLLA1/PCL1/CAB) with approximate diameters of 0.3-10 µm. In addition, the consistent distribution and homogeneous dispersion are observed in this clear blend film, in agreement with miscibility. The phase separation appears more apparent in the opaque film (40/50/10 PLLA1/PCL1/CAB, Figure 5.5c) but there is no clear separation of phases in the translucent film (40/25/35 PLLA1/PCL1/CAB, Figure 5.4b).

All of these results indicate that the miscibility of the PLLA1/PCL1/CAB blends are depend on composition. The reason for miscibility of this blend is influenced by the crystallinity of either of PLLA1, PCL1 or both PLLA1 and PCL1. Therefore, PLLA1/PCL1/CAB was an interesting blend to be further studied by wide angle X-ray scattering (WAXS) analysis (see Chapter 6).

5.3 PDLLA/PCL1/CAB blends

PDLLA, PCL1 and CAB (chemical structures shown below) were blended using the rapid-screening method to observe the miscibility. The miscibility of the PDLLA/PCL/CAB blends is represented by a ternary phase miscibility diagram, as shown in Figure 5.6.

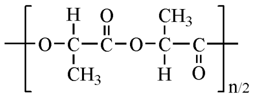 $\left[-O-\underset{CH_3}{\overset{H}{C}}-\overset{O}{\overset{\Vert}{C}}-O-\underset{H}{\overset{CH_3}{C}}-\underset{O}{\underset{\Vert}{C}}- \right]_{n/2}$ PDLLA	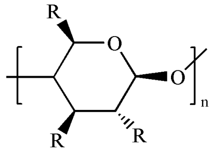
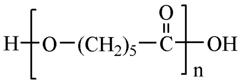 $H-\left[O-(CH_2)_5-\overset{O}{\overset{\Vert}{C}} \right]_n-OH$ PCL1	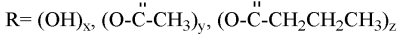 R= $(OH)_x$, $(O-\overset{O}{\overset{\Vert}{C}}-CH_3)_y$, $(O-\overset{O}{\overset{\Vert}{C}}-CH_2CH_2CH_3)_z$ where: $x + y + z = 3$, $x, y > 0$ CAB

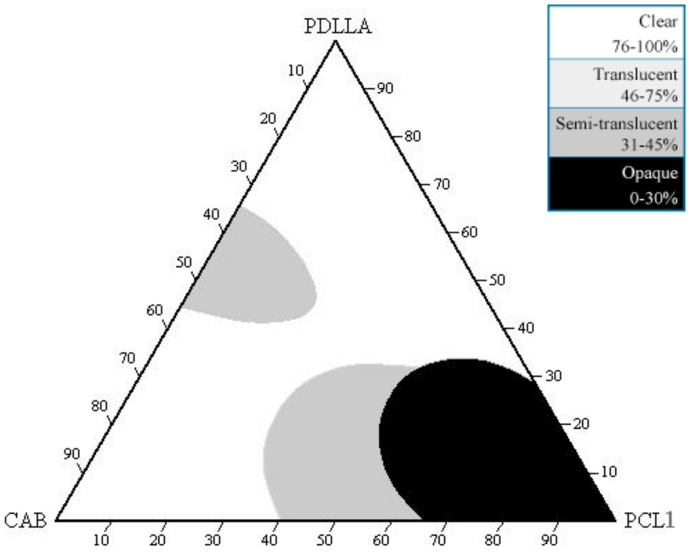

Figure 5.6 The ternary phase miscibility diagram of the PDLLA/PCL1/CAB blends.

The opaque region of the PDLLA/PCL1/CAB blends appears at the PCL1 corner in the ternary phase diagram (Figure 5.6). This means that a high loading of PCL1 (> 65 wt%) leads to the PDLLA/PCL1/CAB blends becoming immiscible. In addition, the results from binary blends (Figure 5.2e) show that PCL1 (a semi-crystalline and faster crystallising polymer) is less miscible with CAB (an amorphous and hydrogen bonding polymer) than PDLLA (an amorphous and slower crystallising polymer) is. Therefore, the strong hydrogen bonding interaction between PDLLA and CAB is expected to occur and to improve the blend miscibility. The miscibility of all PDLLA, PCL1, and CAB may occur as long as PCL1 does not crystallise rapidly from solution.

5.4 PLA/PCL1/CAB blends: The effect of stereochemistry and crystallinity

The stereochemistry, the molecular weight, and the crystallinity, which affect crystallisation rates of PLA (PLLA1, PLLA2, and PDLLA), have been studied in the previous chapter and show that they have an important effect on miscibility of binary blends. Therefore, it was interesting to study this further in the ternary blends; PLLA1/PCL1/CAB, PLLA2/PCL1/CAB, and PDLLA/PCL1/CAB. The phase miscibility diagrams are shown in Figure 5.7.

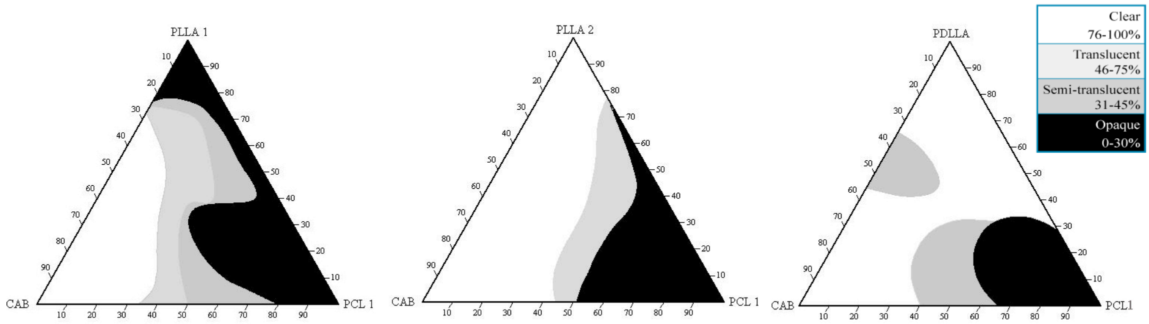

a
PLLA1/PCL1/CAB

b
PLLA2/PCL1/CAB

c
PDLLA/PCL1/CAB

Figure 5.7 The ternary phase miscibility diagrams of: **a.** PLLA1/PCL1/CAB, **b.** PLLA2/PCL1/CAB, and **c.** PDLLA/PCL1/CAB blends.

The phase miscibility diagrams shown in Figure 5.7 seem to show that faster crystallisation and higher degree of crystallinity (PLLA1, PCL1 > PLLA2 > PDLLA) causes the blend to be less miscible. More specifically, the PLLA1/PCL1/CAB blend is less miscible than the PLLA2/PCL1/CAB and PDLLA/PCL1/CAB blends. This result corresponds to the results from binary blends (Figure 5.2a, c, and e). Therefore, it can be said that PDLLA (an amorphous polymer) leads the blend more miscible than does PLLA (a semi-crystalline polymer). As discussed in the summary of Chapter 4, this is because PDLLA is unable to crystallise, therefore, it is able to show the most mutual intermingling and miscibility. Whereas, PLLA crystallises more rapidly which means their chains have less opportunity to intermingle and to interact with other polymers.

5.5 PLLA/PCL/CAB blends : The effect of molecular weight (MW)

Molecular weight (MW) is one of characteristics affecting the miscibility of polymer blends. Many researchers have studied the effect of molecular weight on the miscibility of binary blends [23, 86], including this study as discussed in Section 4.2.4, but not on ternary blends. Therefore, the effect of molecular weight of both PLLA and PCL was systematically further investigated with cellulose acetate butyrate (CAB) in ternary blends.

Two different molecular weights of PLLA and PCL (as used in binary blends and shown in Table 4.6) were solvent blended using the combinatorial screening method. Therefore, four different blends; PLLA1/PCL1/CAB, PLLA1/PCL2/CAB, PLLA2/PCL1/CAB, and PLLA2/PCL2/CAB, were studied and their miscibility compared in ternary phase miscibility diagrams.

Figure 5.8 shows the ternary phase miscibility diagrams of (a) PLLA1/PCL1/CAB, (b) PLLA1/PCL2/CAB, (c) PLLA2/PCL1/CAB, and (d) PLLA2/PCL2/CAB, with various compositions. The visual shading miscibility diagrams of the two component blends of these blends are shown in Figure 5.2a, b, c, and d, respectively.

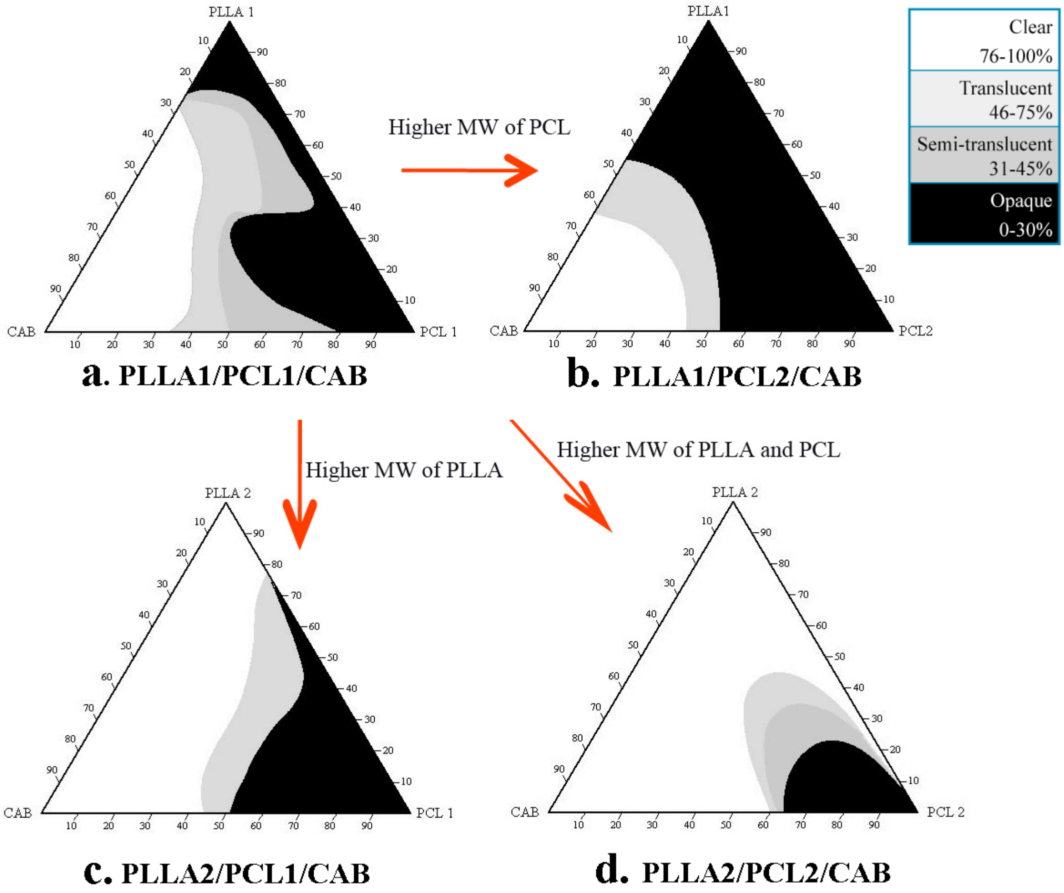

Figure 5.8 The ternary phase miscibility diagrams of the PLLA/PCL/CAB blends (the effect of molecular weights of PLLA and PCL): **a.** PLLA1/PCL1/CAB, **b.** PLLA1/PCL2/CAB, **c.** PLLA2/PCL1/CAB, and **d.** PLLA2/PCL2/CAB.

Figure 5.8 shows that the slower crystallising PLLA2 and PCL2 lead the PLLA2/PCL2/CAB blend (Figure 5.8d) to be the most miscible blend. It is more miscible than the PLLA2/PCL1/CAB (Figure 5.8c), PLLA1/PCL1/CAB (Figure 5.8a), and PLLA1/PCL2/CAB blends (Figure 5.8b), respectively.

However, the effect of molecular weights of PLLA and PCL is discussed in more details following the arrows shown in Figure 5.8.

1. Using higher molecular weight PCL: if considering the relative rate of crystallisation (PCL2 < PCL1), the miscibility of the PLLA1/PCL2/CAB blend (Figure 5.8b) is expected to show a larger miscible region than the PLLA1/PCL1/CAB blend (Figure 5.8a) (since both PLLA1 and PCL1 are more rapid crystallising polymers), but it does not. It can be seen from the ternary phase diagram of the PLLA1/PCL2/CAB blend that the reason for the immiscibility is the crystallinity of either of PLLA1 or PCL2, or both PLLA1 and PCL2.

2. Using higher molecular weight PLLA: it can be seen that using slower crystalline PLLA2 improves the blend miscibility (Figure 5.8c). PCL1 seems to cause the blend to be less miscible (as seen the opaque region at the PCL1 corner). However, the reason for immiscibility may come from either PLLA2 or PCL1.

3. Using higher molecular weight PLLA and PCL: it can be seen that the slower crystallisations (PLLA2 < PLLA1 and PCL2 < PCL1) lead the PLLA2/PCL2/CAB blend (Figure 5.8d) to show a much greater miscible region than the PLLA1/PCL1/CAB blend (Figure 5.8a). However, it is clear that the crystallinity at high PCL2 loading leads to an immiscible blend.

From these results, it can be concluded that the higher molecular weight (slower crystallisation) and the lower molecular weight (faster crystallisation) of PLLA and PCL affect the miscible regions of PLLA/PCL/CAB blends. The reason for changes in miscibility comes from the crystallinity of either of PLLA, PCL or both PLLA and PCL. Therefore, the crystallinity of these blends at chosen compositions of clear, translucent, and opaque were further studied by WAXS analysis in Chapter 6.

5.6 PLA/PCL1/CAB blends: The effect of solvents

The three different polarities of solvents; low, moderate, and polar, were used to form the PLA/PCL1/CAB blends. Chloroform or trichloromethane ($CHCl_3$) is a solvent with low polarity and is miscible with most organic liquids. Tetrahydrofuran (THF) is a moderately polar solvent and water-miscible organic liquid, which can dissolve a variety of non-polar and polar compounds. Hexafluoroisopropanol (HFIP), which used to dissolve some polar polymers, is a polar solvent and can exhibit strong H-bonding from its hydroxyl group.

The effect of these solvents on the clarity of individual polymers (PLLA1, PCL1, CAB, and PDLLA) is discussed in Section 5.6.1. Two types of PLA/PCL1/CAB blends; PLLA1/PCL1/CAB and PDLLA/PCL1/CAB were studied in Section 5.6.2 and 5.6.3, respectively.

5.6.1 The effect of solvents on the clarity of individual polymers

The effects of solvents: chloroform ($CHCl_3$), tetrahydrofuran (THF), hexafluoroisopropanol (HFIP), and the mixture of $CHCl_3$ and HFIP, on the clarity of individual polymers are shown in Table 5.1. From the table, the values of the %T are shown together with the shading block colours to represent the miscibility: opaque (black), semi-translucent (grey), and clear (white).

Table 5.1 The percent transmittance (%T) and clarity of individual polymers.

Polymers	% T			
	$CHCl_3$	HFIP	THF	80:20 % (v/v) $CHCl_3$:HFIP
PLLA1	15	99	2	8
PCL1	12	48	12	14
CAB	100	100	100	87
PDLLA	92	100	100	-

In general, the polymers crystallise during evaporation because solvents assist crystallisation and then precipitate when the solvents cannot dissolve. As observed from Table 5.1, it can be said that PLLA1 and PCL1 show more rapid crystallisation in $CHCl_3$, THF, and a mixture of $CHCl_3$ and HFIP (as shown opaque film).

However, the PLLA1 film is clear in HFIP (the strong hydrogen bonding solvent). This may because HFIP can break up the crystallinity of PLLA1, as HFIP is known as a solvent that breaks up polymer crystallinity. While it is too polar for the flexible hydrocarbon component (-$(CH_2)_5$-) of PCL1. CAB and PDLLA, which both are amorphous polymers, show no crystallisation in any solvents (as seen clear films). This helps to understand the miscibility of these blends and to know which polymer caused the blend to be immiscible.

5.6.2 PLLA1/PCL1/CAB blends: The effect of solvents

The PLLA1/PCL1/CAB blends dissolved in the different solvents: $CHCl_3$, HFIP, a mixture of $CHCl_3$ and HFIP, and THF, were prepared using the rapid screening method. The miscibility of the blends were observed and shown by the ternary phase miscibility diagrams in Figure 5.9.

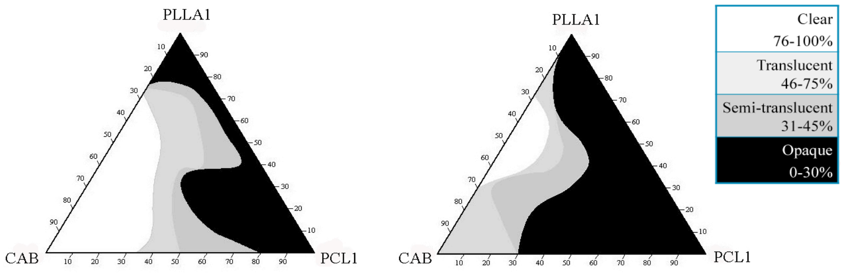

a. in $CHCl_3$ b. in HFIP

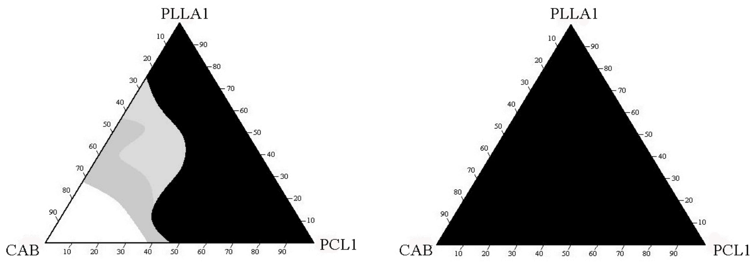

c. in 80/20 $CHCl_3$ / HFIP d. in THF

Figure 5.9 The ternary phase miscibility diagrams of the PLLA1/PCL1/CAB blends in the different solvents; (a) $CHCl_3$, (b) HFIP, (c) 80/20 $CHCl_3$/HFIP, and (d) THF.

From the ternary phase miscibility diagram shown in Figure 5.9, it seems to show that $CHCl_3$ is the most suitable solvent for PLLA1/PCL1/CAB blends, even if PLLA1 and PCL1 show more rapid crystallisation in $CHCl_3$. HFIP and the mixture of $CHCl_3$ and HFIP seem to cause PLLA1 and PCL2 to crystallise faster (in blend solution) than does $CHCl_3$. THF is not a suitable solvent for the PLLA1/PCL1/CAB blend even though it is a moderate polar solvent, which can dissolve a variety of non-polar and polar compounds including polyesters.

5.6.3 PDLLA/PCL1/CAB blends: The effect of solvents

The PDLLA/PCL1/CAB blends dissolved in three different solvents, $CHCl_3$, HFIP and THF - as with PLLA1/PCL1/CAB- were prepared using the rapid screening method. The miscibility of the blends were observed and shown by the ternary phase miscibility diagrams in Figure 5.10.

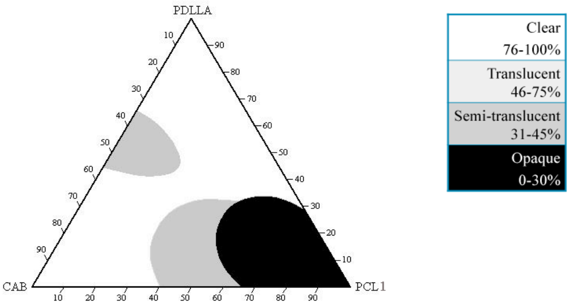

a. in $CHCl_3$

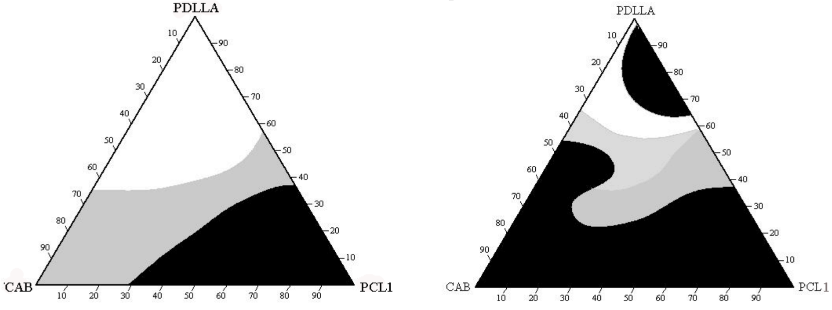

b. in HFIP

c. in THF

Figure 5.10 The ternary phase miscibility diagrams of the PDLLA/PCL1/CAB blends in the different solvents; (a) $CHCl_3$, (b) HFIP, and (c) THF.

From the ternary phase miscibility diagram shown in Figure 5.10, it can be deduced that crystallisation of PCL1 strongly influences the miscibility of PDLLA/PCL1/CAB blends. The immiscibility "spreads" from the higher concentration region of PCL (bottom right-hand corner). PCL1 seems to crystallise faster in HFIP and more especially in THF than in $CHCl_3$, which leads the blends to be more immiscible.

5.7 PLLA1/PCL1 and PLLA2/PCL2 blended with cellulose polymers

Cellulose, the general material of plant cell walls, is a long chain polymer containing a repeating unit of glucose. CAB, which has acetate and butyrate as substituent groups, is the first derivative of cellulose used to blend with PLLA and PCL in this study (as discussed in Section 5.2). In this section, two other different types of cellulose polymers with different substituent groups; cellulose acetate propionate (CAP) and cellulose propionate (CP), were further studied to investigate their effect on the miscibility of PLLA and PCL. In addition, the different molecular weights of PLLA and PCL were used to blend with these cellulose polymers.

5.7.1 PLLA1/PCL1/CAP and PLLA2/PCL2/CAP blends

Cellulose acetate propionate (CAP) is one of the cellulose derivatives substituted with hydroxy or acetate and propionate groups (chemical structure shown below). CAP was blended with PLLA1/PCL1 and PLLA2/PCL2 using the rapid screening method. The percent transmittances of their blends were recorded and the ternary phase miscibility diagrams are shown in Figure 5.11.

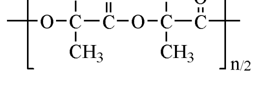

$$\left[-O-\underset{CH_3}{\overset{H}{C}}-\overset{O}{\overset{\|}{C}}-O-\underset{CH_3}{\overset{H}{C}}-\overset{O}{\overset{\|}{C}}-\right]_{n/2}$$

PLLA1, PLLA2

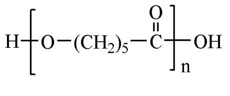

$$H\left[O-(CH_2)_5-\overset{O}{\overset{\|}{C}}\right]_n OH$$

PCL1, PCL2

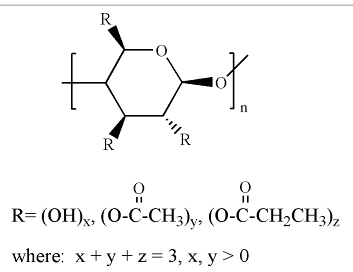

$$R = (OH)_x,\ (O-\overset{O}{\overset{\|}{C}}-CH_3)_y,\ (O-\overset{O}{\overset{\|}{C}}-CH_2CH_3)_z$$

where: $x + y + z = 3$, $x, y > 0$

CAP

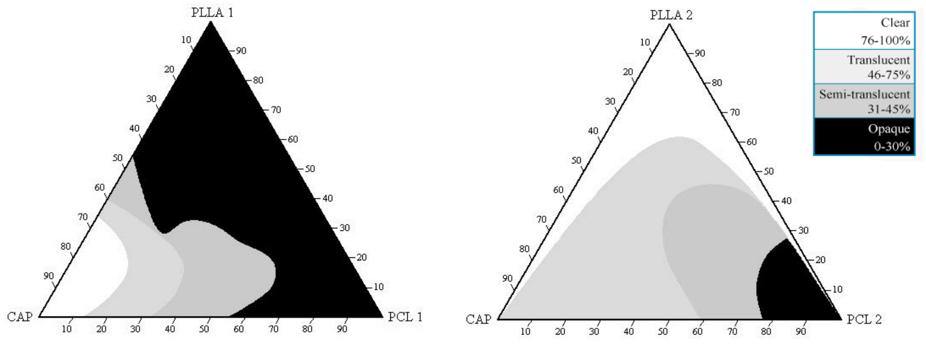

a
PLLA1/PCL1/CAP

b
PLLA2/PCL2/CAP

Figure 5.11 The ternary phase miscibility diagrams of : (a) PLLA1/PCL1/CAP and (b) PLLA2/PCL2/CAP blends.

From the ternary phase miscibility diagrams shown in Figure 5.11, it can be seen that the PLLA2/PCL2/CAP blend shows more miscible regions than the PLLA1/PCL1/CAP blend. For the PLLA1/PCL1/CAP blend, the opaque region starts from PLLA1-PCL1 binary line. For the PLLA2/PCL2/CAP blend, a small opaque region shows at the PCL2 corner (PCL2 > 80 wt%). In addition, a clear region is observed at the PLLA2 corner, but not the PLLA1 corner.

Therefore, this seems to show that more rapidly crystallising polymers (PLLA1 > PLLA2 and PCL1 > PCL2) cause the PLLA1/PCL1/CAP blend to be less miscible. In addition, the miscible blends of PLLA/PCL/CAP are expected to be influenced by the hydrogen bonding interactions between substituent groups of CAP and carbonyl groups of the polyester (PLLA and PCL).

5.7.2 PLLA1/PCL1/CP and PLLA2/PCL2/CP blends

Cellulose propionate (CP) is another cellulose derivative, substituted with hydroxy and propionate (chemical structure shown below). CP was blended with PLLA1/PCL1 and PLLA2/PCL2 using the rapid screening method. The percent transmittance of their blends was recorded and the ternary phase miscibility diagrams are shown in Figure 5.12.

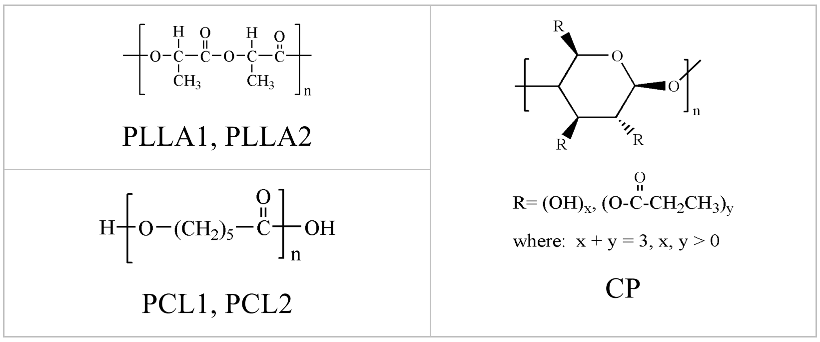

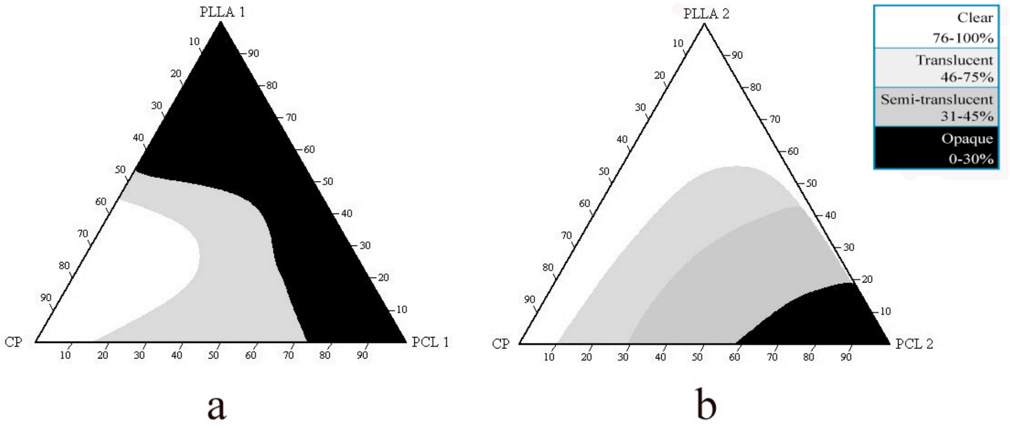

PLLA1/PCL1/CP **PLLA2/PCL2/CP**

Figure 5.12 The ternary phase miscibility diagrams of: (a) PLLA1/PCL1/CP and (b) PLLA2/PCL2/CP blends.

From the ternary phase miscibility diagrams (Figure 5.12), it can be seen that the PLLA2/PCL2/CP blend shows a larger miscible region than the PLLA1/PCL1/CP blend. The opaque region moves from PLLA1-PCL1 binary line for PLLA1/PCL1/CP blend, whereas it shows a small opaque area at the PCL2 corner (PCL2 > 60 wt%) for the PLLA2/PCL2/CP blend. In addition, the clear region is observed at the PLLA2 corner but not at the PLLA1 corner, as was the case with CAP.

Therefore, it can be said that the argument previously raised (relative crystallisation rate) is further supported by the data in this section. This is more evidence that shows crystallisation influences the miscibility. In addition, the miscible blends of PLLA/PCL/CP are expected to be enhanced by the hydrogen bonding interactions between substituent groups of CP and carbonyl groups of the polyesters (PLLA and PCL).

5.7.3 PLLA/PCL/cellulose polymers: The summary

The ternary phase miscibility diagram of the PLLA/PCL/CAB (Figure 5.8a and d), PLLA/PCL/CAP (Figure 5.11), and PLLA/PCL/CP (Figure 5.12) blends with different molecular weights of PLLA and PCL are shown together in Figure 5.13.

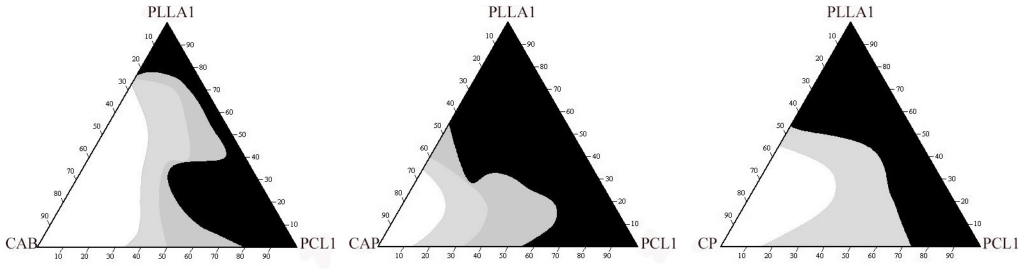

a. **PLLA1/PCL1/CAB** **b.** **PLLA1/PCL1/CAP** **c.** **PLLA1/PCL1/CP**

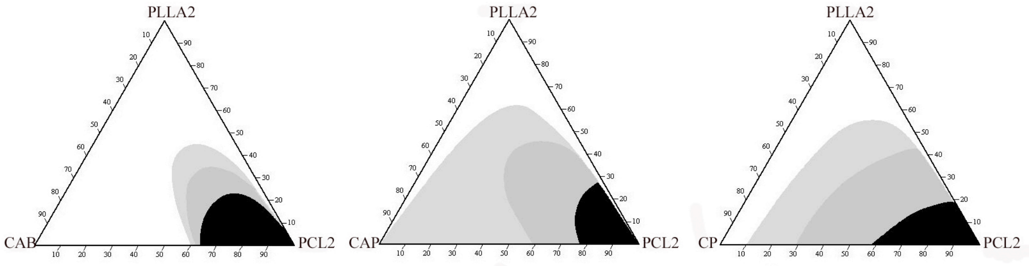

d. **PLLA2/PCL2/CAB** **e.** **PLLA2/PCL2/CAP** **f.** **PLLA2/PCL2/CP**

Figure 5.13 The ternary phase miscibility diagram of : (a) PLLA1/PCL1/CAB, (b) PLLA1/PCL1/CAP, (c) PLLA1/PCL1/CP, (d) PLLA2/PCL2/CAB, (e) PLLA2/PCL2/CAP, and (f) PLLA2/PCL2/CP blends.

From the ternary phase miscibility diagram shown in Figure 5.13, it can be seen that the boundary miscibility lines show the same trend in each case. PLLA1/PCL1 blended with cellulose polymers illustrate less miscible regions than PLLA2/PCL2. The miscibility of the cellulose polymers with PLLA and PCL: CAB > CP > CAP, can be observed.

In summary, it can be observed that an effect associated with crystallisation reduces the tendency for polymers to form miscible blends. If the crystallisation is more rapid (PLLA1 > PLLA2, PCL1 > PCL2) – the tendency for the polymers to exclude a second or third component is enhanced. The tendency to crystallise is a tendency for self-interaction (it makes both PLLA and PCL want to interact with itself to form crystalline regions), which reduces the ability of the polymer to interact with others.

5.8 Ternary blends of PLLA1 modifying with polyester adipate (G40)

There are many ways to improve the mechanical properties of PLLA, either by blending with other biodegradable polymers or non-degradable polymers [8, 51, 82, 84, 87-90], by using compatibilisers of PLA and other polyesters [78, 81], or by chain orientation [91, 92], for suitable applications and to reduce the price in the market. Using plasticisers is one of the useful ways to improve the mechanical properties of PLLA [4, 93].

Polyester adipate (G40), a flexible and non-crystallisable polyester, was used as a plasticiser for the blend of PLLA with the possible candidate polymers; PCL, CAB, and polyhydroxybutyrate (PHB) and its copolymers with hydroxyvalerate (HV) [94]. Figure 5.14 shows the ternary phase miscibility diagrams of G40 blended with PLLA and a series of additional components.

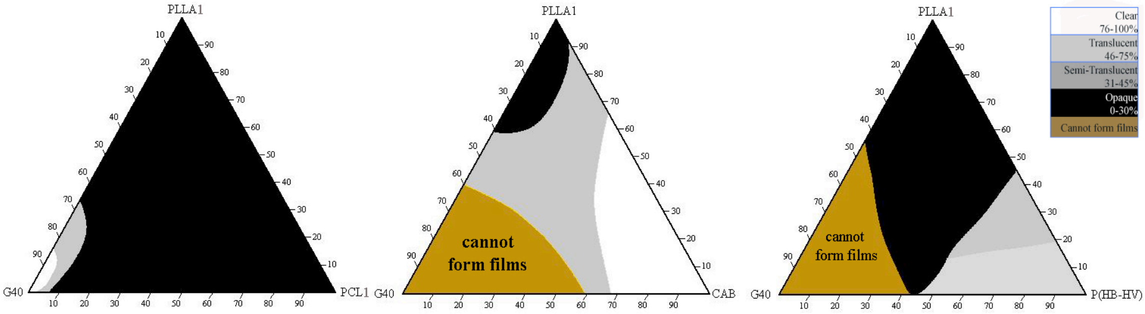

a. **PLLA1/PCL1/G40** **b.** **PLLA1/CAB/G40** **c.** **PLLA1/P(HB-HV)/G40**

Figure 5.14 The ternary phase miscibility diagrams of: a. PLLA1/PCL1/G40, b. PLLA1/CAB/G40, and c. PLLA1/P(HB-HV)/G40 blends.

From the ternary phase miscibility diagrams (Figure 5.14a), PLLA1/PCL1/G40 blend is immiscible at almost all composition ranges. Therefore, it can be said that G40 cannot improve the miscibility of the PLLA1/PCL1 blend (as observed in Chapter 4 - PLLA1/PCL1 is an immiscible blend).

The PLLA1/CAB/G40 blend (Figure 5.14b) shows more miscible regions than the PLLA1/P(HB-HV)/G40 blend (Figure 5.14c). It is logical to assume that CAB (a hydrogen bonding and amorphous polymer) leads the blends to be more miscible than P(HB-HV) which is a non-hydrogen bonding and semi-crystalline polymer.

5.9 PLLA1/PCL1/LLA-co-PCL blends

LLA-co-PCL is a copolymer of L-lactide and poly(ε-caprolactone) (chemical structure shown below). It was used as a compatibiliser in an attempt to improve the miscibility of PLLA1/PCL1 blends in this study. Two different molecular weights of LLA-co-PCL were used; LY127 (M_n 10,600, PD 1.56) and LY128 (M_n 3,100, PD 1.99), to blend with PLLA1/PCL1 using the rapid screening method. Figures 5.15a and b show the ternary phase miscibility diagrams of PLLA1/PCL1/LY127 and PLLA1/PCL1/LY128, respectively.

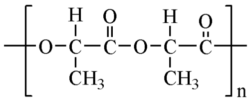 $-[O-CH(CH_3)-C(=O)-O-CH(CH_3)-C(=O)]_n-$ PLLA1	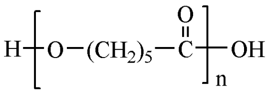 $H-[O-(CH_2)_5-C(=O)]_n-OH$ PCL1	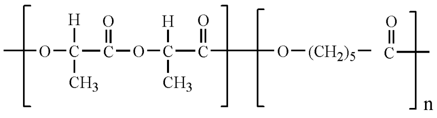 $-[O-CH(CH_3)-C(=O)-O-CH(CH_3)-C(=O)]-[O-(CH_2)_5-C(=O)]_n-$ LLA-co-PCL

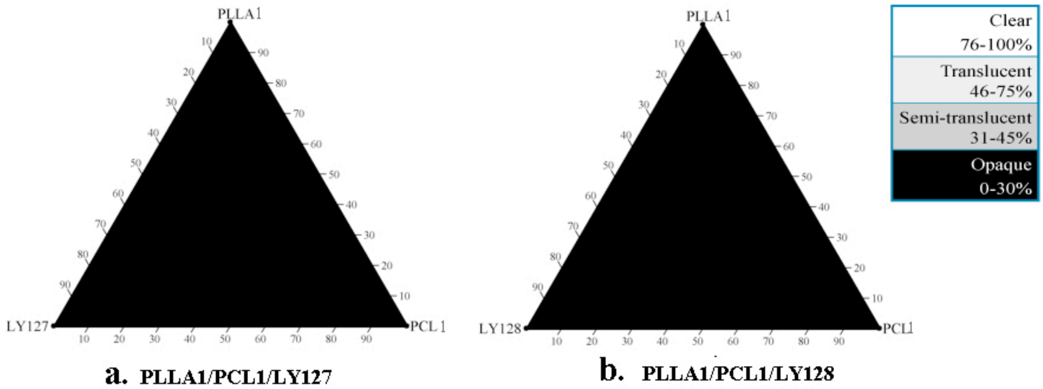

a. PLLA1/PCL1/LY127 b. PLLA1/PCL1/LY128

Figure 5.15 The ternary phase miscibility diagrams of PLLA1/PCL1 blended with different molecular weights of LLA-co-PCL; (a) LY127 and (b) LY128.

From the ternary phase miscibility diagrams (Figure 5.15), the blends show opaque regions in all compositions. Therefore, it can be said that the copolymers of LLA-co-PCL cannot interact with PLLA1 and PCL1 (PLLA1 and PCL1 are immiscible as observed in Chapter 4) and do not form phase miscibility using solvent blending techniques in this study. The different molecular weights of LY127 and LY128 have no effect on miscibility in these ternary blends.

5.10 PLLA/PCL/TPU blends

PLLA and PCL were used to blend with a third component following on from the work with CAB, G40, with the aim to improve the miscibility of the blends. In this section, thermoplastic polyurethane (TPU), with the commercial name of Estane 5706P from B.F. Goodrich Company, was chosen to blend as a third component by the rapid screening method. Several other Estane TPUs were examined but found to show less ready solubility in chloroform.

Estane thermoplastic polyurethanes (TPU) are elastomeric materials, which are not yet fully understood. They have very good adhesion properties, good resistance to abrasion, corrosion, and oils, hydrolysis and temperature degradation [95]. TPU chains used in this study are composed of 4,4'-methylenediphenyl 1,1'-diisocyanate (MDI) as hard segments, 1,4-cyclohexanedimethanol as a chain extender, and poly(butylene adipate), a low molecular weight polyester as soft segments (chemical structure shown in Figure 5.16). They are considered to be linear block copolymers, which show alternating hard and soft segments. The number average molecular weight (M_n) of this TPU is 38,000 and glass transition temperature (T_g) is approximately at 48 ^oC [96].

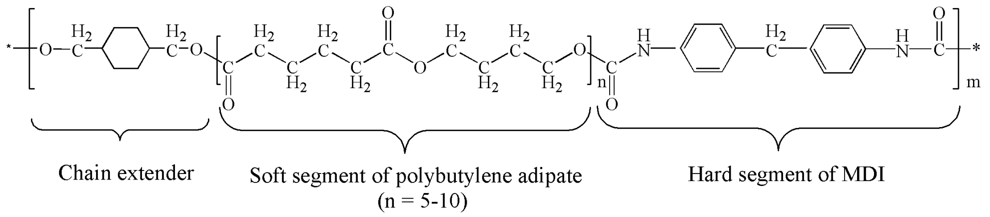

Figure 5.16 The chemical structure of Estane thermoplastic polyurethanes (TPU).

The different molecular weights of PLLA and PCL were also used to blend with TPU, the details are shown in Table 4.6 and in Section 5.5. The PLLA1/PCL1/TPU blend is discussed in Section 5.10.1, and the PLLA1/PCL2/TPU and PLLA2/PCL2/TPU blends are discussed and compared to the PLLA1/PCL1/TPU blend in Section 5.10.2.

5.10.1 PLLA1/PCL1/TPU blends

The PLLA1/PCL1/TPU blend at various compositions was solvent blended using the rapid screening method. The percent transmittance was recorded and shown in terms of miscibility by the ternary phase miscibility diagram in Figure 5.17.

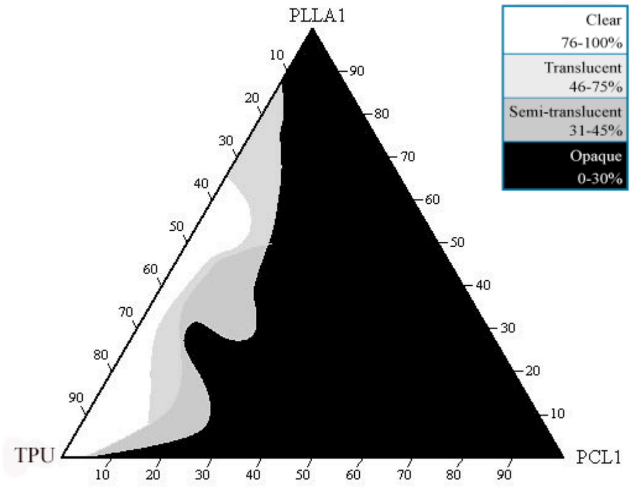

Figure 5.17 The ternary phase miscibility diagram of the PLLA1/PCL1/TPU blends.

From the ternary phase miscibility diagram (Figure 5.17), it can be seen that the opaque regions spread from the PLLA1/PCL1 and TPU/PCL1 binary lines. This means that PLLA1 and PCL1 influence the miscibility of PLL1/PCL1/TPU blend to be less miscible.

From the binary lines of the ternary phase diagram, it can be seen that PLLA1/PCL1 and PCL1/TPU are immiscible blends, while PLLA1/TPU is a miscible blend (highlighted by the binary miscibility diagram in Figure 5.18).

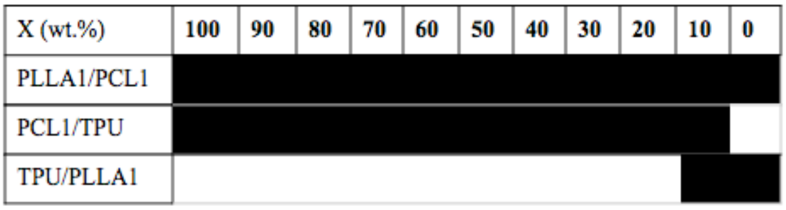

X (wt.%)	100	90	80	70	60	50	40	30	20	10	0
PLLA1/PCL1	■	■	■	■	■	■	■	■	■	■	■
PCL1/TPU	■	■	■	■	■	■	■	■	■	■	□
TPU/PLLA1	□	□	□	□	□	□	□	□	□	■	■

X = the polymer in the blends of X / Y, i.e PLLA1/PCL1, X = PLLA1

Figure 5.18 The visual shading miscibility diagram of the binary blends; PLLA1/PCL1, PCL1/TPU, and TPU/PLLA1.

One interesting complementary observation is that PLLA1 (a semi-crystalline polymer with a helical structure) can be miscible with TPU (the flexible and strong polar interaction polymer, as seen in Figure 5.16) in almost all composition ranges. In contrast, PCL1 (a semi-crystalline polymer with a planar zig-zag structure) is not miscible with TPU at any composition. One possible route in trying to understand the miscibility of the PLLA1/PCL1/TPU blend is to study the miscibility of the PLLA1/TPU and PCL1/TPU blends from their chemical structures. The presumed structure was used to explain the miscibility and is shown in Figure 5.19.

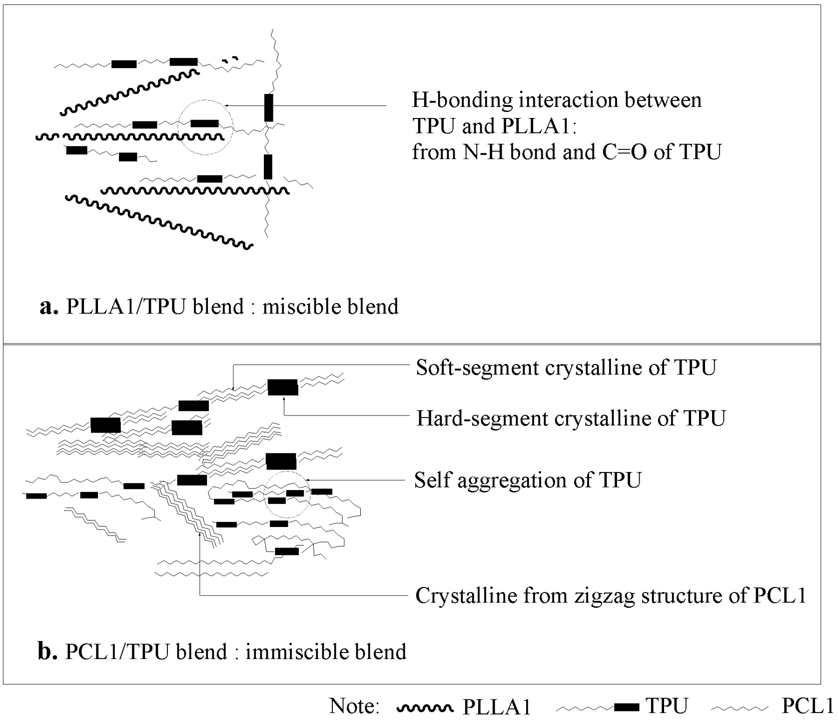

Figure 5.19 The presumed structure of (a) miscible blend of PLLA1/TPU and (b) immiscible blend of PCL1/TPU.

From the presumed structure of the PLLA1/TPU miscible blend (Figure 5.19a), one can presume that PLLA1 chains are able to interpenetrate TPU and then produce TPU-PLLA1 semi-interpenetrating networks. In addition, the TPU soft segment (poly(butylene adipate)) has its C=O double bond in the flexible chains (Figure 5.16). This causes the hydrogen donor group (NH) with the electron donor group (C=O) to be close together, which means that the H-bonding interactions between TPU and PLLA can be relatively easily produced. This generates more miscibility between PLLA and TPU.

The difference in molecular polarities of PCL1 (a non-polar polymer) and TPU (a H-bonding polymer) [97] is one possible influence on the immiscibility of the PCL1/TPU blend. The even number of carbon atoms in the polyester soft segment of TPU together with the difference in polarities between PCL1 and TPU assist: 1. the crystallisation of hard- and soft-segments and 2. the mobility of hard segments inside the soft segment generating self-aggregation (Figure 5.19b). In addition, PCL1 chains are able to crystallise because of the geometric fit of its zig-zag conformation which interrupts the possible hydrogen-bonding interaction between PLLA1 and TPU.

5.10.2 PLLA/PCL/TPU blends: Effect of molecular weight of PLLA and PCL

The PLLA/PCL/TPU blends with different molecular weights of PLLA and PCL were studied and are discussed in this section. Figure 5.20 shows the phase miscibility diagrams.

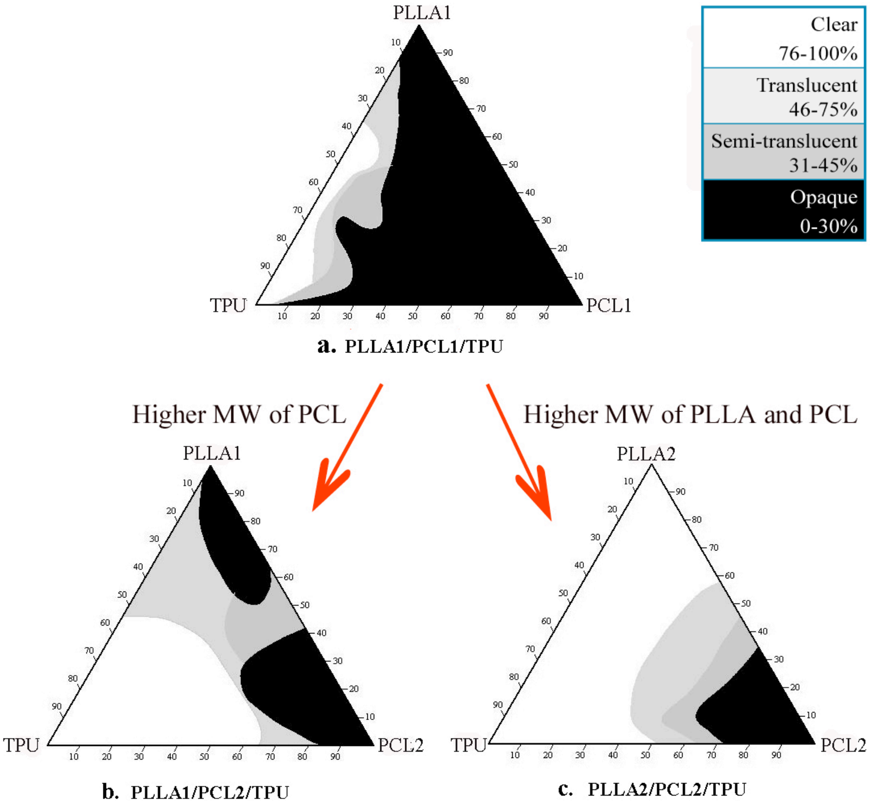

a. PLLA1/PCL1/TPU

b. PLLA1/PCL2/TPU

c. PLLA2/PCL2/TPU

Figure 5.20 The ternary phase miscibility diagrams of (a) PLLA1/PCL1/TPU blend comparing with (b) PLLA1/PCL2/TPU and (c) PLLA2/PCL2/TPU blends.

From the ternary phase miscibility diagrams (Figure 5.20), the crystalline regions of PLLA1/PCL1/TPU > PLLA1/PCL2/TPU > PLLA2/PCL2/TPU can be observed. Therefore, it can be said that using lower molecular weights PLLA1 and PCL1 reduces the blend miscibility. This result complements the result from the PLLA/PCL/CAB blends; therefore, it is possible to deduce that the more rapidly crystallising polymers (PLLA1 > PLLA2 and PCL1 > PCL2) lead the blend to be less miscible.

If considering in terms of molecular structure, it can be said that the increase in C=O bonds in PLLA2 and PCL2 leads to the increase in H-bonding interactions between their blend chains. This avoids:

1. the crystalline formation of the zigzag structure of PCL2
2. some crystalline formation from the helical structure of PLLA2
3. the self-aggregation of TPU from the moving of the hard-segment inside the soft-segment
4. the soft- and hard-segment crystallisation of TPU.

Figure 5.21 shows the presumed structures of an immiscible PLLA1/PCL1/TPU blend, which shows the four effects (above), and that of a miscible PLLA2/PCL2/TPU blend. However, this is a suggestion to help to understand the miscibility of the PLLA/PCL/TPU blends associated with the chemical structures.

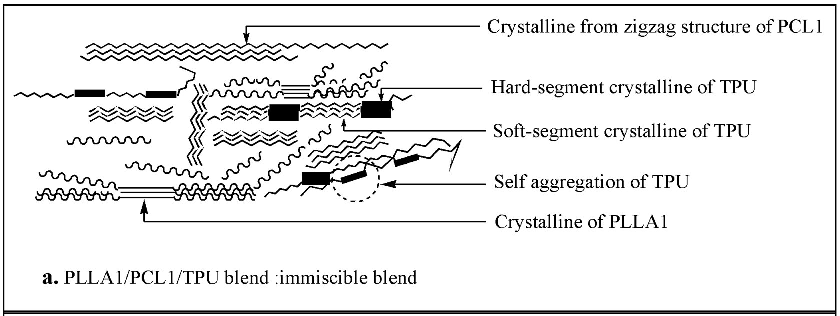

a. PLLA1/PCL1/TPU blend :immiscible blend

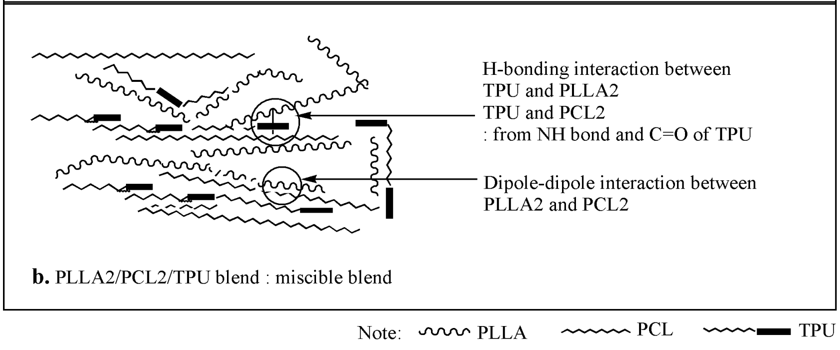

b. PLLA2/PCL2/TPU blend : miscible blend

Figure 5.21 The presumed structures of the immiscible blend of PLLA1/PCL1/TPU and the miscible blend of PLLA2/PCL2/TPU.

However, the reason for changes in miscibility comes from the crystallinity of either of PLLA, PCL, or both PLLA and PCL. Therefore, the crystallinity of these blends at chosen compositions of clear, translucent, and opaque has been further studied by WAXS analysis, as discussed in Chapter 6.

5.11 PLLA1/PCL1/diacid-diol polyesters blends

PLLA1 and PCL1 were used to blend with various polymers with the aim of improving the miscibility in the earlier sections. Diacid-diol polyester, e.g. poly(butylene succinate) (PBS-Bionolle 1020), poly(butylene succinate adipate) (PBSA-Bionolle 3010), poly(propylene succinate) (PPS) and poly(ethylene succinate) (PES) were the other biodegradable polyesters used to blend with PLLA1 and PCL1 in this section. Their chemical structures are shown below.

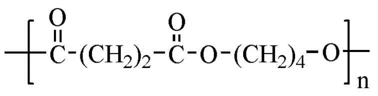

$$\left[\overset{O}{\overset{\|}{C}}-(CH_2)_2-\overset{O}{\overset{\|}{C}}-O-(CH_2)_4-O \right]_n$$

PBS

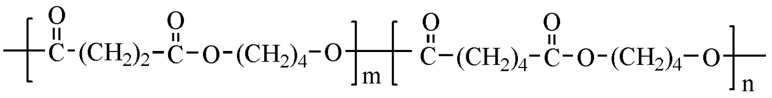

$$\left[\overset{O}{\overset{\|}{C}}-(CH_2)_2-\overset{O}{\overset{\|}{C}}-O-(CH_2)_4-O \right]_m \left[\overset{O}{\overset{\|}{C}}-(CH_2)_4-\overset{O}{\overset{\|}{C}}-O-(CH_2)_4-O \right]_n$$

PBSA

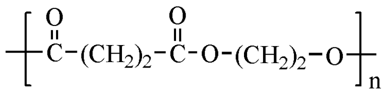

$$\left[\overset{O}{\overset{\|}{C}}-(CH_2)_2-\overset{O}{\overset{\|}{C}}-O-(CH_2)_2-O \right]_n$$

PES

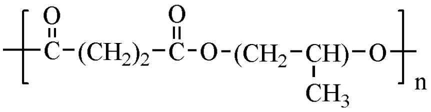

$$\left[\overset{O}{\overset{\|}{C}}-(CH_2)_2-\overset{O}{\overset{\|}{C}}-O-(CH_2-\underset{CH_3}{\underset{|}{CH}})-O \right]_n$$

PPS

The blends were prepared using the rapid screening method and the percent transmittance was recorded and shown by the ternary phase miscibility diagrams in Figure 5.22.

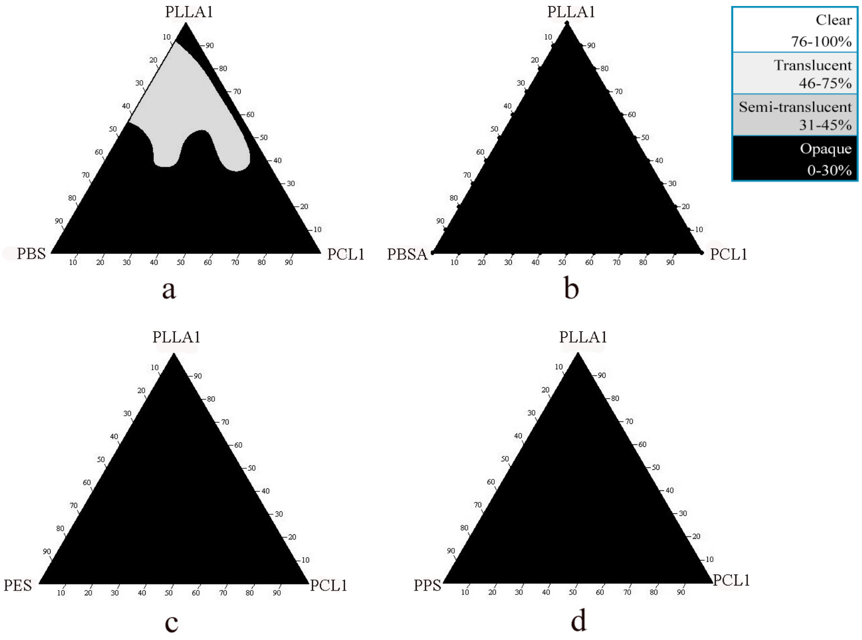

Figure 5.22 The ternary phase miscibility diagrams of PLLA1/PCL1 blended with (a) PBS, (b) PBSA, (c) PES and (d) PPS.

From the ternary phase miscibility diagram shown in Figure 5.22, it can be seen that all PLLA1/PCL1 blended with diacid-diol polyesters are immiscible, except the PLLA1/PCL1/PBS blend shows partial miscibility at high loading of PLLA1 and low loading of PBS. This may be because of the different polarity between diacid-diol polyester and PLLA1 and PCL1, which cannot produce the interaction between their chains.

5.12 SUMMARY OF THE CHAPTER

- The factors observed to affect the miscibility of ternary blends (especially PLA/PCL blended with cellulose polymers and TPU) in this study are: the blend compositions, the nature of solvents ($CHCl_3$, HFIP, THF), the stereo-chemistry of PLA (PLLA, PDLLA), the crystallinity, and the molecular weights of PLA and PCL. They are the effects associated with crystallisation that reduces the tendency for polymers to form miscible blends. If the crystallisation is more rapid – the tendency for the polymers to exclude a second or third component is enhanced.

- The crystallisation of PLLA1 > PLLA2 > PDLLA shows that the underlying miscibility is shown by the behaviour of PDLLA - the tendency to crystallise is a tendency for self-interaction (PLLA chains interact with themselves to form crystalline regions), which reduces the ability of the polymer to interact with others. Also the more polar PLLA is driven to a tight helix with little steric hindrence and high polar interaction. For example, the miscibility of PLA/PCL/CAB blends shows:

PDLLA/PCL1/CAB > PLLA2/PCL1/CAB > PLLA1/PCL1/CAB

Therefore, the crystallinity of PLLA/PCL/CAB was studied by WAXS analysis in and is discussed in Chapter 6.

- The effect of solvent is very important for the miscibility of the solvent blending - PLA/PCL1/CAB blends. It solvates the polymer and influences the rate of crystallisation from solution. The different solvents will also influence the rate of crystallisation not only by an evaporation but because the solvents interact differently with the polymer chains. This is because some solvents disrupt the evaporating polymer surface more than other solvents. The matching polarity of the solvent and polymer (depending on the molecular structure of polymer) is also disrupting the crystal structure. It was observed that chlorform ($CHCl_3$) is a more suitable solvent to use in this study than hexafluoroisopropanol (HFIP) and tetrahydrofuran (THF), respectively.

- The miscible blends of PLLA and PCL blended with cellulose polymers: cellulose acetate butyrate (CAB), cellulose acetate propionate (CAP), and cellulose propionate (CP), are expected to be influenced by the hydrogen bonding interactions between the substituent groups of cellulose polymers and the carbonyl groups of polyesters. CAB is observed to lead PLLA and PCL to be more miscible than CP and CAP, respectively.

- The miscibility of the PLLA/PCL/TPU blends with different molecular weights of PLLA and PCL shows: PLLA2/PCL2/TPU > PLLA1/PCL2/TPU > PLLA1/PCL1/TPU. This is another ternary blend that the miscibility was observed to be influenced by the crystallisation of PLLA and PCL. Therefore, the crystallinity of PLLA/PCL/TPU was again studied by WAXS analysis in Chapter 6.

However, the reason for the miscibility of the PLLA/PCL/TPU blend was discussed in terms of molecular structure dealing with the molecular interactions between the polymer pairs (PLLA/TPU-miscible blend, PCL/TPU-immiscible blend). The formation of crystalline regions by the PCL zig-zag conformation and low polarity (compared with TPU) interrupts the interaction between their chains, therefore, self-aggregation of TPU (the mobility of hard segment insides the soft segment) and the soft- and hard-segment crystallisation of TPU can occur. Whereas, PLLA chains (a helical and semi-crystalline polymer) can intermingle and form hydrogen bonded interaction with TPU chains (an amorphous and hydrogen bonding polymer).

CHAPTER 6

CRYSTALLINITY OBSERVATIONS

Chapter 6

Crystallinity Observations

In the earlier chapters, it was observed that the extent and rate of crystallisation of polymer blends is an important parameter affecting polymer miscibility. However, it could not be observed visually which of the blends exhibited crystallinity as a factor in their miscible or immiscible behaviour. In this chapter, therefore, wide-angle X-ray scattering (WAXS) was used to investigate this by measurement of the d-spacing values relating to distances between the polymer chains and by the intensity values of the electrons diffracted in the crystal cell. High electron density differences in an ordered state reflect strongly and give rise to intense peaks.

As discussed in Section 5.2 (PLLA1/PCL1/CAB blend), Section 5.5 (PLLA/PCL/CAB blends: effect of molecular weight), and Section 5.10 (PLLA/PCL/TPU), the reason for changes in miscibility of these blends appears to come from the crystallinity of either of PLLA, PCL or both PLLA and PCL. Therefore WAXS studies were carried out to determine which component has crystallised and which has not crystallised – or crystallised less effectively - in the different compositions: clear, translucent, and opaque.

Therefore, the first task was to identify the characteristic d spacings of PLLA1, PLLA2, PCL1 and PCL2 (their respective molecular weights are shown in Table 4.6), and the second task was to interpret the different WAXS traces of PLLA/PCL/CAB blends and PLLA/PCL/TPU blends. The samples were selected at the same compositions of PLLA (40 wt% for PLLA/PCL/CAB blend, 20 wt% for PLLA/PCL/TPU blend), which give clear, translucent, and opaque films. To facilitate presentation and understanding of the WAXS results, the samples with sample codes used to study the crystallinity are shown in Table 6.1.

Table 6.1 Film samples (from solvent casting in 96-well plates) studied by WAXS.

Sample Codes	Three component blends	Composition (wt%)	Clarity of films
A1 A2 A3	PLLA1/PCL1/CAB	40/10/50 40/25/35 40/45/15	Clear Translucent Opaque
B1 B2 B3	PLLA1/PCL2/CAB	40/10/50 40/25/35 40/45/15	Translucent Translucent Opaque
C1 C2 C3	PLLA2/PCL1/CAB	40/10/50 40/25/35 40/45/15	Clear Clear Translucent
D1 D2 D3	PLLA2/PCL2/CAB	40/10/50 40/25/35 40/45/15	Clear Clear Clear
E1 E2 E3	PLLA1/PCL1/TPU	20/30/50 20/50/30 20/70/10	Opaque Opaque Opaque
F1 F2 F3	PLLA1/PCL2/TPU	20/30/50 20/50/30 20/70/10	Clear Translucent Opaque
G1 G2 G3	PLLA2/PCL2/TPU	20/30/50 20/50/30 20/70/10	Clear Translucent Opaque

6.1 Identification of d-spacing values of individual components

To identify the d-spacing values of individual polymers (PLLA1, PLLA2, PCL1, and PCL2), two types of two different traces at the same composition of 40/45/15 PLLA/PCL/CAB were used. These were: (i) A3 (PLLA1/PCL1/CAB) compared with B3 (PLLA1/PCL2/CAB) (Figure 6.1), and A3 (PLLA1/PCL1/CAB) compared with C3 (PLLA2/PCL1/CAB) (Figure 6.2). The rationale behind the choice of use this composition was that it contained the highest loading of PLLA and PCL, and is expected to show the highest level of crystalline material for each.

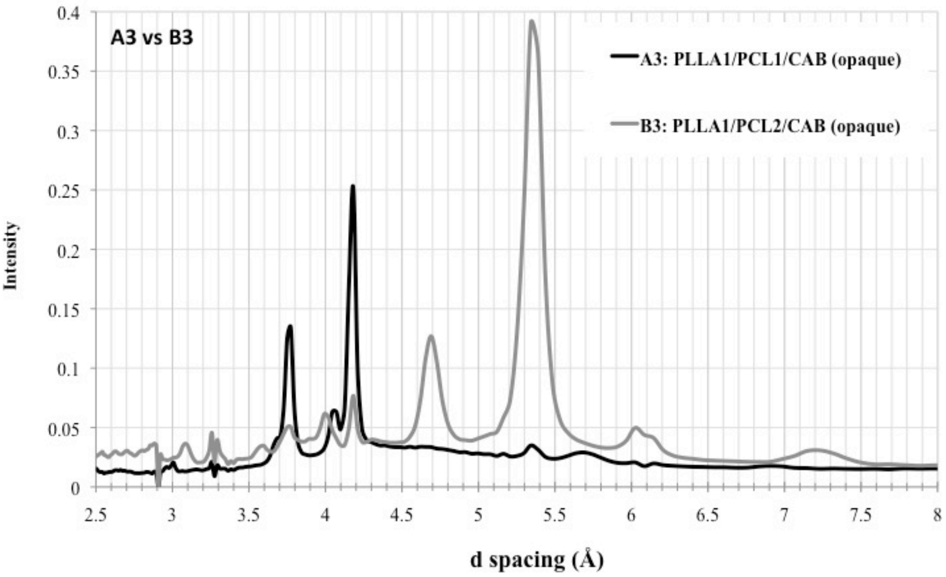

Figure 6.1 WAXS traces of A3 : PLLA1/PCL1/CAB blends and B3: PLLA1/PCL2/CAB blends, at 40/45/15.

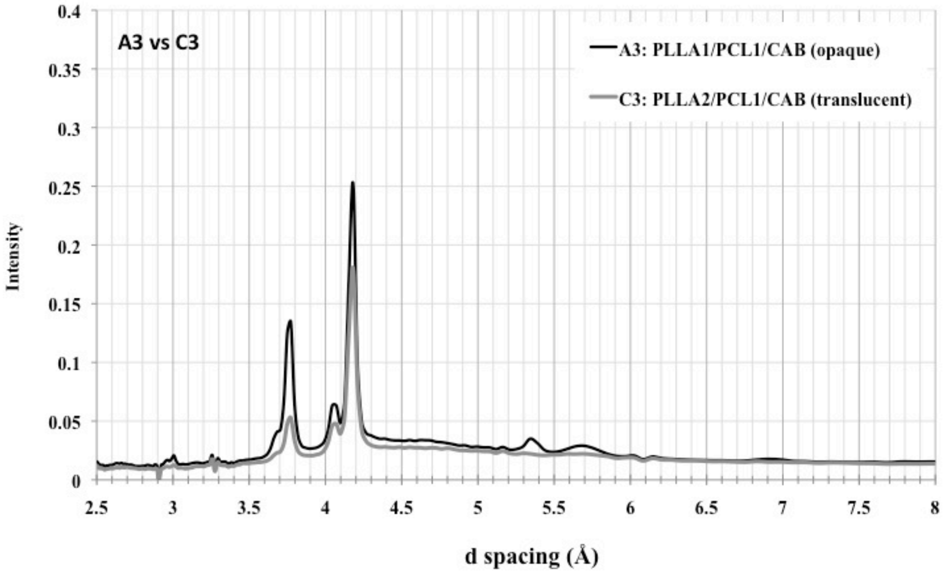

Figure 6.2. WAXS traces of A3: PLLA1/PCL1/CAB blends and C3: PLLA2/PCL1/CAB blends, at 40/45/15.

In order to identify the peaks in Figure 6.1 and 6.2, the d-spacing values of PLLA [47, 98-100] and PCL [101-103] from literature sources were used as references, and then the d-spacing values of both PLLA and PCL from this study were calculated and are shown in Table 6.2.

Table 6.2 The crystallinity and d-spacing values of PLLA and PCL.

Polymers	% Crystallinity (from DSC)	d-spacing (Å)	
		From literature references	From this study*
PLLA1	38	4.67, 5.34	3.10, 3.57, 4.00, **4.67**, **5.35**, 6.17
PLLA2	31		
PCL1	74	2.95, 3.67, 3.95, 4.09, 5.49, 6.61	2.86, **3.75**, 4.05, **4.15**, 5.16, 5.70
PCL2	54		

Note: * The d-spacing values of PLLA at 4.67 and 5.35 Å and PCL at 3.75 and 4.15 Å are the two strongest peaks.

From Table 6.2, it can be seen that the d-spacing values of PCL and PLLA are not dependent on molecular weights. However, the lower molecular weights (PLLA1 and PCL1) show higher intensity (higher crystallinity) than the higher molecular weight (PLLA2 and PCL2). In addition, it can be observed that PCL has a narrower distribution of the mean distance between polymer segments (d spacing) as compared to PLLA (comparing at those two strongest peaks).

The strong peaks of PCL (3.75 Å and 4.15 Å) and PLLA (4.67 Å and 5.35 Å) underpin the discussion of the WAXS results in the following sections.

6.2 PLLA/PCL/CAB blends

As mentioned previously, the crystallinity of either PLLA, PCL, or PLLA and PCL can affect to the miscibility of PLLA/PCL/CAB blends. In addition, the different molecular weights of PLLA and PCL used in the blends showed different phase miscibility diagrams, as discussed in Section 5.5. The ternary phase miscibility diagram was shown in Figure 5.5 and for convenience is included here, following Figure 6.3.

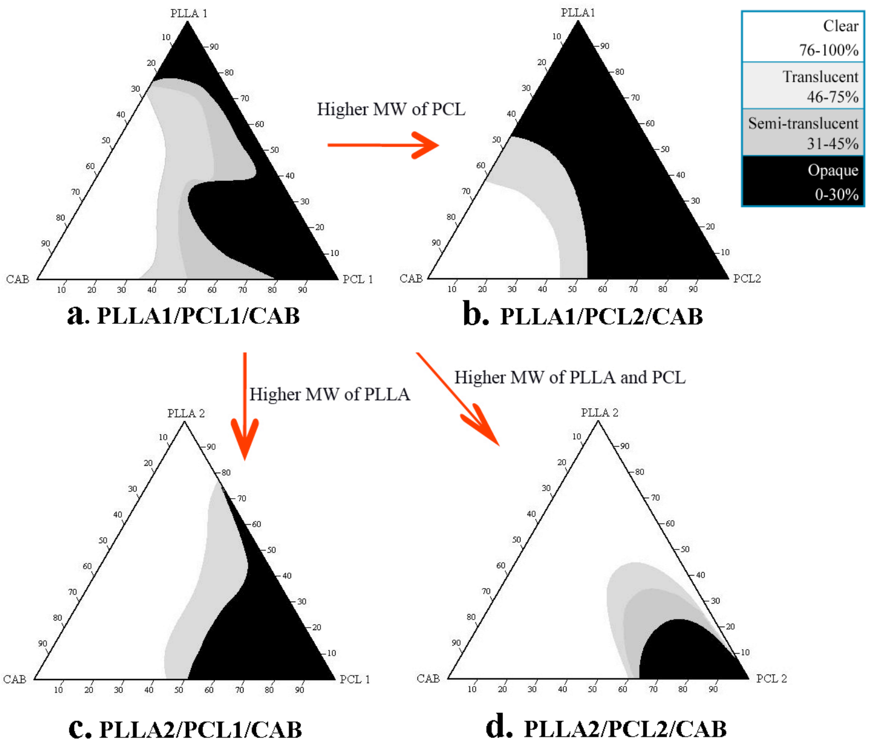

a. **PLLA1/PCL1/CAB** **b.** **PLLA1/PCL2/CAB**

c. **PLLA2/PCL1/CAB** **d.** **PLLA2/PCL2/CAB**

Figure 6.3 The ternary phase miscibility diagrams of different molecular weights of PLLA and PCL blended with CAB: **a.** PLLA1/PCL1/CAB, **b.** PLLA1/PCL2/CAB, **c.** PLLA2/PCL1/CAB, and **d.** PLLA2/PCL2/CAB.

The crystallinity observations are discussed for the individual blends in the following sections. A more detailed collective interpretation of the results from these blends is then presented.

6.2.1 PLLA1/PCL1/CAB blends

Three different clarities of films; clear (A1: 40/10/50), translucent (A2: 40/25/35) and opaque (A3: 40/45/15), were submitted for WAXS analysis. Figure 6.4 shows WAXS traces of these blends together with the visual shading miscibility of binary blends and the ternary phase miscibility diagram.

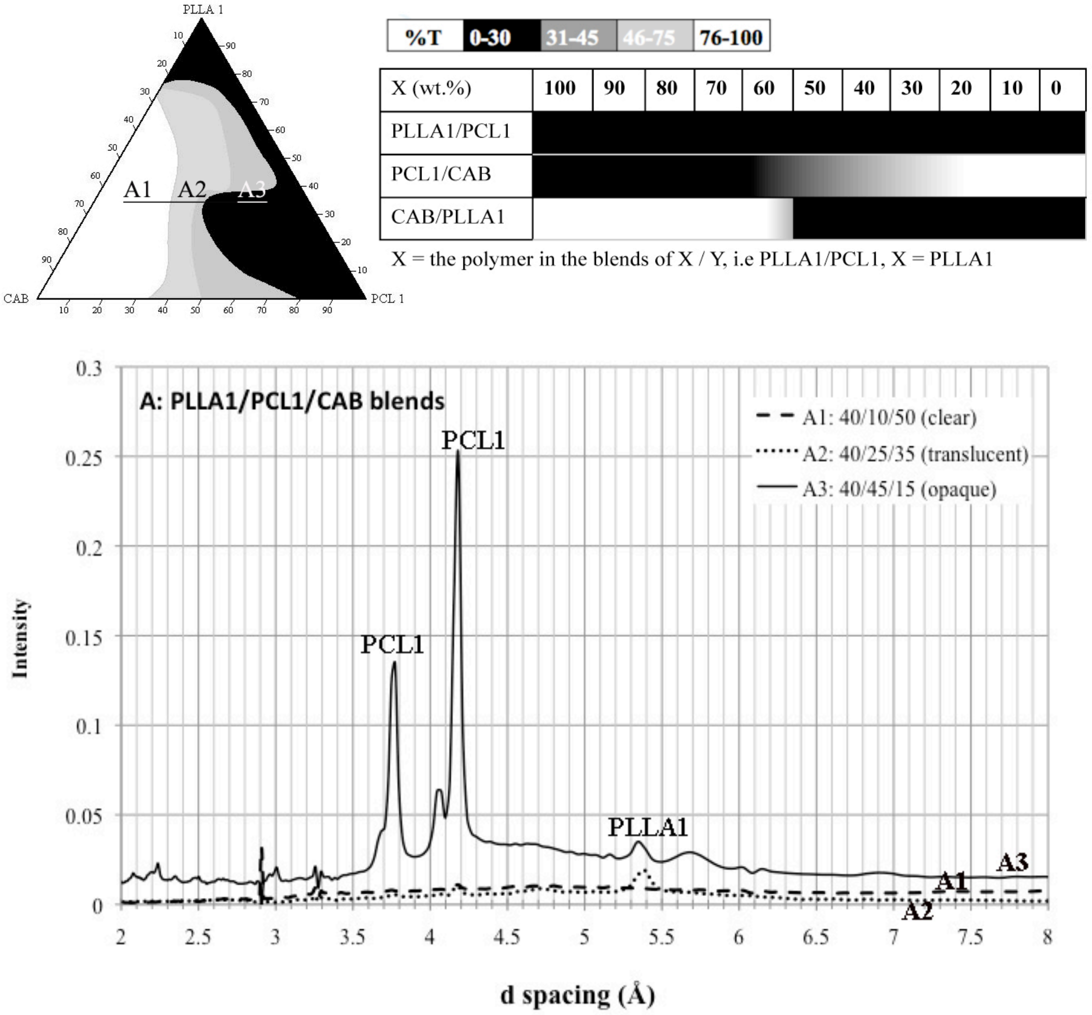

Figure 6.4 WAXS traces of the PLLA1/PCL1/CAB blends at different compositions; A1: 40/10/50-clear, A2: 40/25/35-translucent, and A3: 40/45/15-opaque; together with the visual shading miscibility diagram of binary blends and the ternary phase miscibility diagram.

From the WAXS traces shown in Figure 6.4, it can be seen that the crystallinity of PCL1 correlates with the 40/45/15 (A3) blend being opaque. The ratio of PCL1 peak height of an opaque film (A3) compared with that of a translucent film (A2) at a d spacing of 4.15 Å, is 25:1, while the comparable ratio of PLLA at a d spacing of 5.35 Å is 1.75:1. This indicates the significant effect of more rapid crystallisation – PCL1 is much more influential in causing PLLA1/PCL1/CAB to be immiscible blend than PLLA1.

One interesting point observed from the WAXS trace of the clear film (A1) is that the film, although optically clear, has some crystalline regions of PCL1, as shown in Figure 6.5. It appears that the crystalline regions are smaller than the wavelength of light used to determine clarity of films, and therefore cannot be seen. Thus it can be said that the three-component blends of PLLA1/PCL1/CAB can be miscible and clear, even if one polymer forms some crystalline regions. It is important to note that this degree of crystallinity is extremely low.

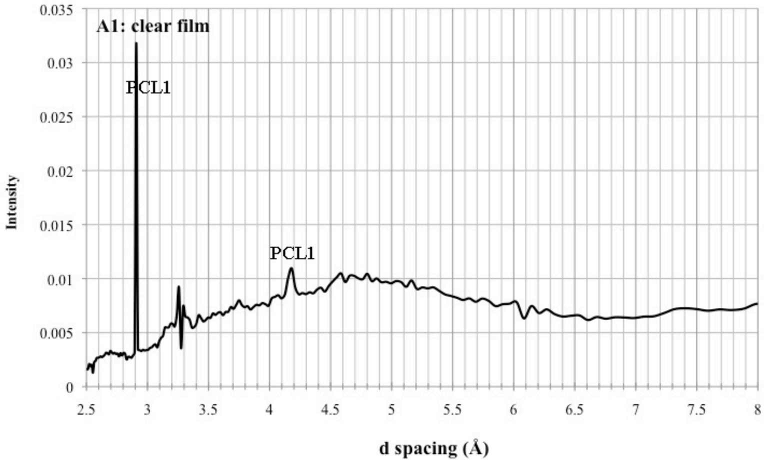

Figure 6.5 WAXS trace of the clear film (A1: PLLA1/PCL1/CAB blend at 40/10/50)

The point discussed above, that the crystallinity of PCL1 seems to cause PLLA1/PCL1/CAB to be less miscible than does that of PLLA1, can be confirmed by the images observed by hot-stage microscopy, as shown in Figure 6.6. This illustrates that the number of crystalline spherulites of PCL1 in the PLLA1/PCL1/CAB is greater than the comparable number of PLLA1 spherulites at their final crystallisation temperatures (~70 °C for PLLA1, 28 °C for PCL1).

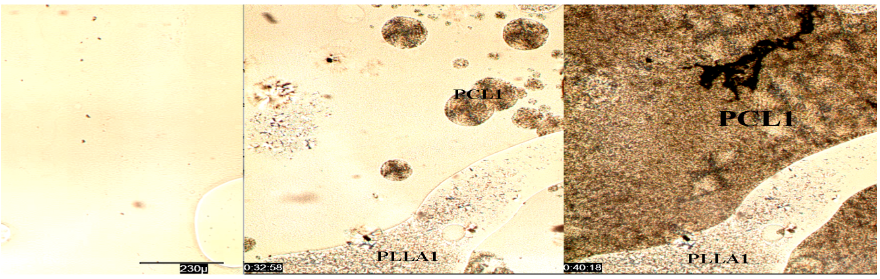

a. 170 °C **b**. 29.1 °C **c**. 27.5 °C

Figure 6.6 An image of crystallinity of PCL1 and PLLA1 in an opaque film of 40/45/15 PLLA1/PCL1/CAB blend at different temperatures:
a. 170 °C – melting temperature
b. 29.1 °C – approximately temperature that PCL1 started to crystallise
c. 27.5 °C – temperature that PCL1 finished to crystallise.

6.2.2 PLLA1/PCL2/CAB blends

Three films of two different clarities (at 40 wt% PLLA1): translucent (B1: 40/10/50 and B2: 40/25/35) and opaque (B3: 40/45/15), were used to study the crystallinity by WAXS analysis. Figure 6.7 shows WAXS traces of these blends together with the visual shading miscibility of binary blends and the ternary phase miscibility diagram.

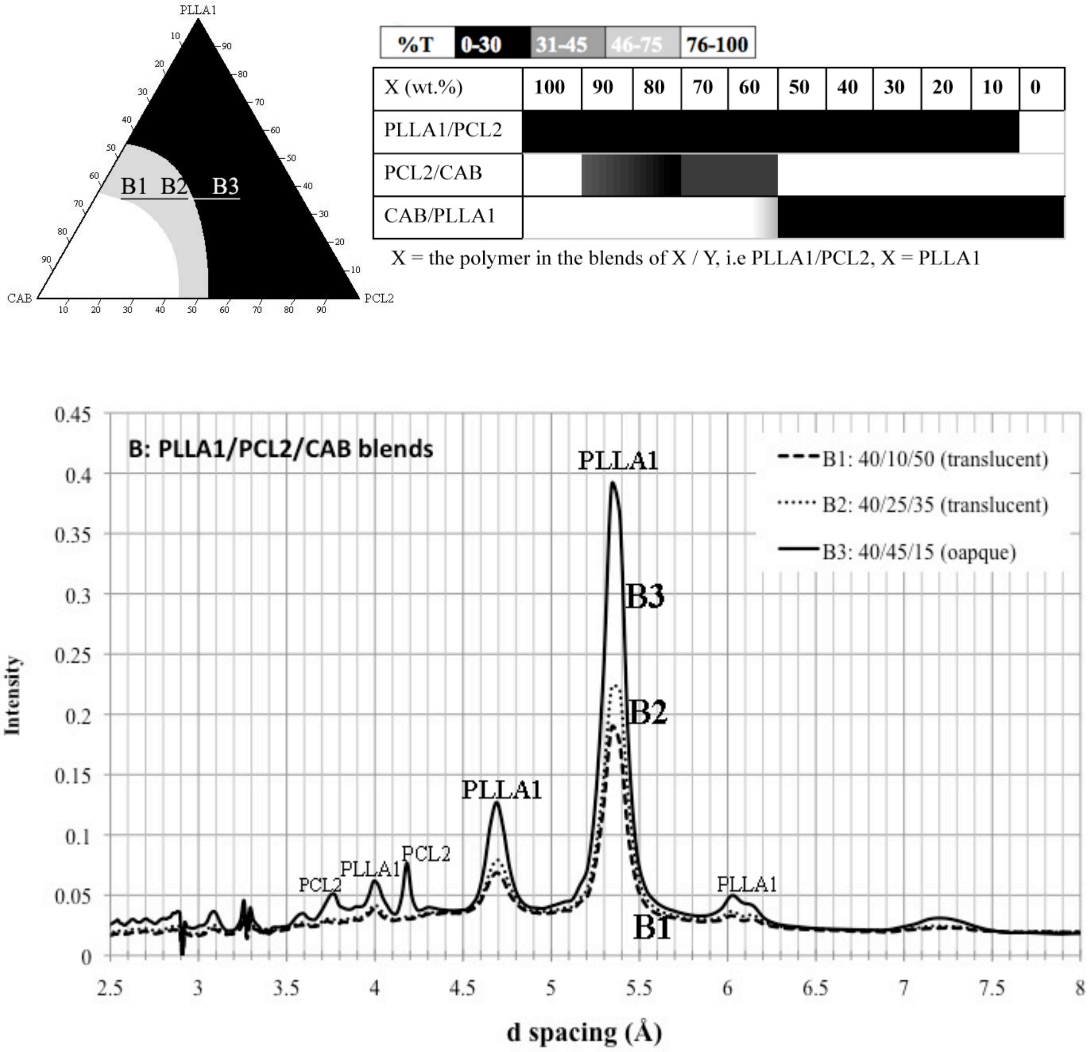

Figure 6.7 WAXS traces of the PLLA1/PCL2/CAB blends at different compositions; B1: 40/10/50-translucent, B2: 40/25/35-translucent, and B3: 40/45/15-opaque, together with the visual shading miscibility diagram of binary blends and the ternary phase miscibility diagram.

From the WAXS traces of the PLLA1/PCL2/CAB blends (Figure 6.7), the identical crystalline peaks of PLLA1 can all be observed and they are greater than that of PCL2. Therefore, it can be inferred that PLLA1 has the greatest effect on the reduction in blend miscibility. As discussed in Chapters 4 and 5, this is because PLLA1 shows more rapid crystallisation than the higher molecular weight grade of PCL (PCL2).

Considering the visual shading miscibility diagram of the binary blends together with the WAXS data, it seems to show that the miscibility of PLLA1/PCL2/CAB blends is enhanced by the miscibility of the polymer pairs: PLLA1/CAB and PCL2/CAB, and impeded by the combination of PLLA1/PCL2 which are immiscible at all compositions.

6.2.3 PLLA2/PCL1/CAB blends

Three films of two different clarities (at 40 wt% PLLA2); clear (C1: 40/10/50 and C2: 40/25/35) and translucent (C3: 40/45/15), were studied by WAXS. Figure 6.8 shows WAXS traces of these blends together with the visual shading miscibility of binary blends and the ternary phase miscibility diagram.

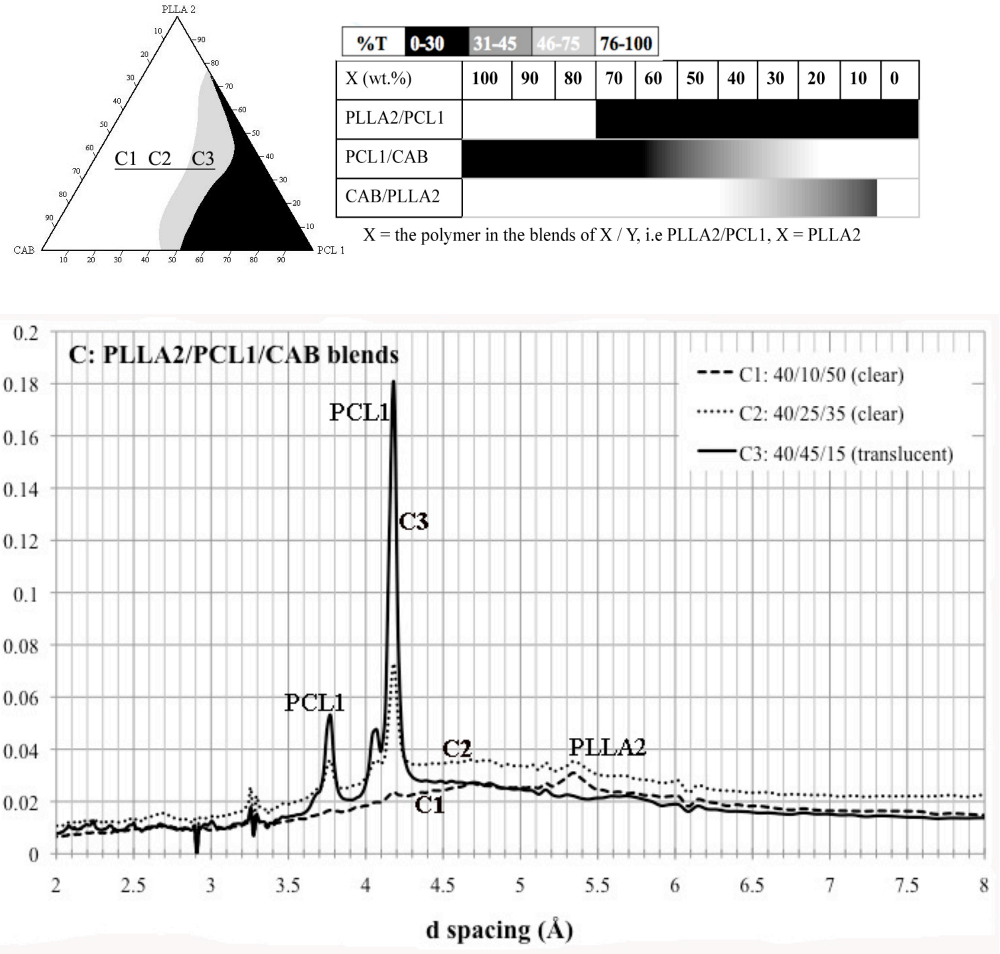

Figure 6.8 WAXS traces of the PLLA2/PCL1/CAB blends at different compositions; C1: 40/10/50-clear, C2: 40/25/35-clear, and C3: 40/45/15-translucent; together with the visual shading miscibility diagram of binary blends and the ternary phase miscibility diagram.

From Figure 6.8, it can be seen that the presence of PCL1 has the major influence in causing the blend to be more opaque. Considering the blend at 40/45/15 (C3: translucent film), it shows no crystalline peak of PLLA2 although a large crystalline peak of PCL1 can be observed, even though their composition differs by only 5 wt%. This indicated that PLLA2 is more miscible with CAB than PCL1 is with CAB, which is also confirmed by the binary diagrams. This follows the pattern previously observed that more rapid crystallisation reduces miscibility. In this case PCL1 shows more rapid crystallisation than PLLA2. Considering the WAXS analysis of the opaque blend, the crystallinity of PCL1 is seen to be greater than that of PLLA2 which provides supporting evidence explanation.

It can be seen from the WAXS traces of the clear films (C1 and C2) that they have shown some crystallinity for both PLLA2 and PCL1. As discussed earlier in Section 6.2.1, this implies that the crystalline regions are smaller than the wavelength of light, therefore cannot be seen.

6.2.4 PLLA2/PCL2/CAB blends

The three compositions of PLLA2/PCL2/CAB chosen for crystallinity study by WAXS analysis; D1: 40/10/50, D2: 40/25/35 and C3: 40/45/15, were all clear. Figure 6.9 shows the WAXS traces of these blends together with the visual shading miscibility of binary blends and the ternary phase miscibility diagram.

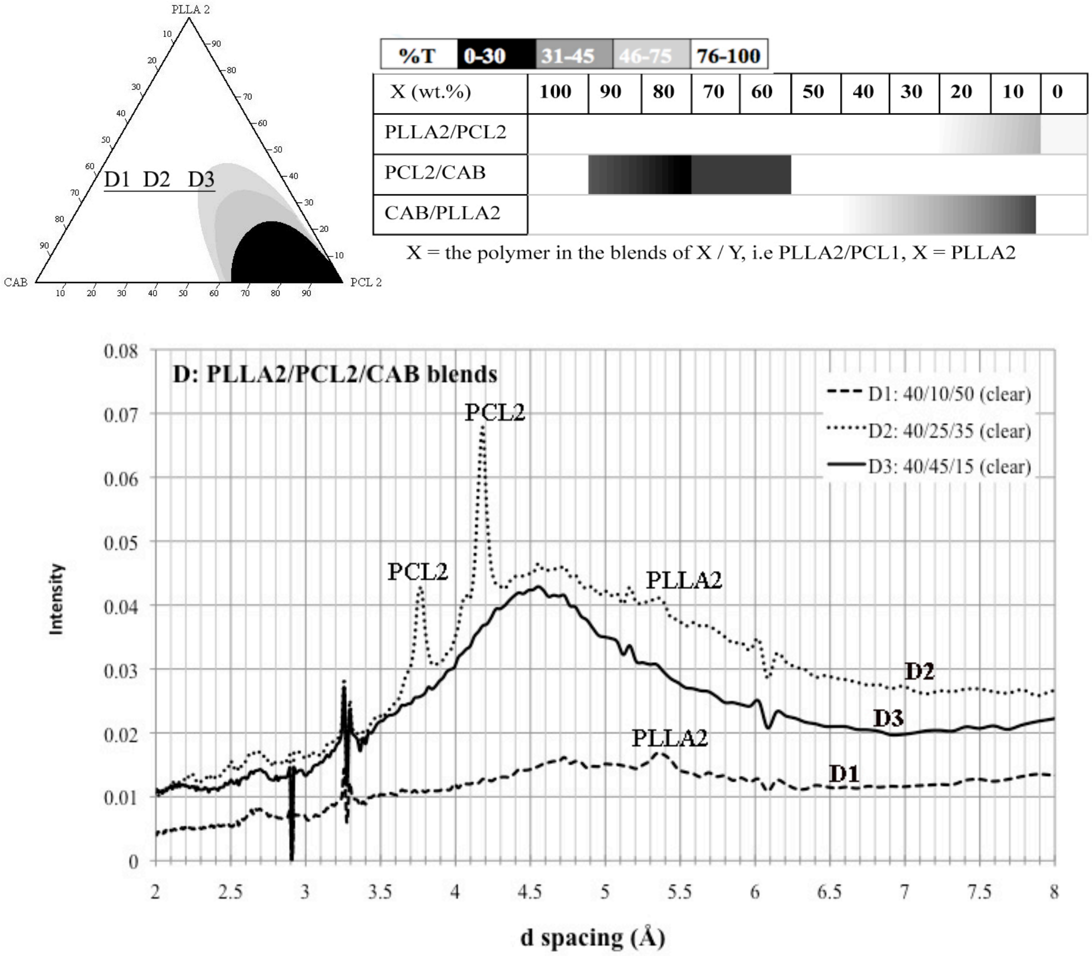

Figure 6.9 WAXS traces of the clear PLLA2/PCL2/CAB blend films at different compositions; D1: 40/10/50, D2: 40/25/35, and D3: 40/45/15; together with the visual shading miscibility diagram of binary blends and the ternary phase miscibility diagram.

From Figure 6.9, it can be seen that the clear films of PLLA2/PCL2/CAB blends have some crystalline regions of both PLLA2 and PCL2, however, their intensities are very weak. As observed from the binary and ternary phase diagrams together with the WAXS data, it can be inferred that the much greater miscibility of PLLA2/PCL2/CAB blends is influenced by the wide miscibility ranges of the three polymer pairs (PLLA2/CAB, PCL2/CAB and PLLA2/PCL2). This means that PLLA2/PCL2/CAB blends show good miscibility because PLLA2 and PCL2 show more miscibility in wider composition ranges than those incorporating the lower molecular weight polymers. However, it appears that it is the crystallinity of PCL2, more than that of PLLA2, which leads to the opaque blends, which are found at high loadings of PCL2.

6.2.5 PLLA/PCL/CAB blends: Interpretation of the results

It can be seen that the components, which cause the PLLA/PCL/CAB blends to be more opaque, can be identified from the WAXS traces. The technique shows clearly the influence of the different molecular weights of PLLA and PCL.

Table 6.3 shows a summary of the results from the crystallinity observations from WAXS studies of the blends at 40/45/15 PLLA/PCL/CAB. The WAXS traces are shown at the same scale of d-spacing values (X-axis), but different intensity scales (Y-axis). The table also shows the ternary phase miscibility diagrams and the sample code refers to the clarity of the films; (O) is opaque, (T) is translucent, and (C) is clear. The conclusions for each set of blend components are included in the table.

Table 6.3. Summary of the crystallinity observation by WAXS analysis.

Ternary Blends	Sample Code	WAXS Traces of 40/45/15 PLLA/PCL/CAB	Conclusions
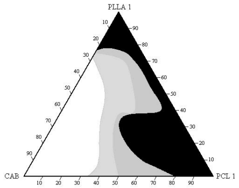 **PLLA1/PCL1/CAB**	**A3** **(O)**	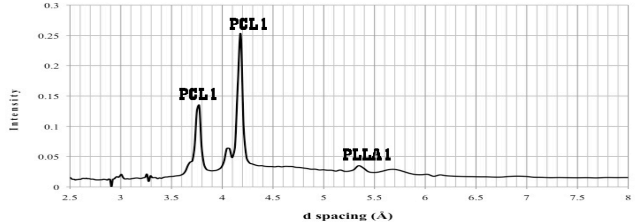	PCL1 has the key effect on the miscibility of the blend more than PLLA1, although both show rapid crystallisation. This may be a consequence of the fact that the planar zig-zag (PCL1) allows more complete crystallisation than the helical structure of PLLA1. PLLA1 chains thus have more opportunity to intermingle with CAB before crystallisation.
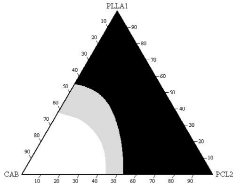 **PLLA1/PCL2/CAB**	**B3** **(O)**	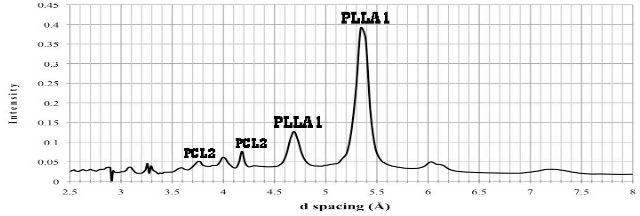	PLLA1 has the key effect on miscibility of the blend and shows a greater tendency to form crystalline regions than PCL2. The relative crystallinity of PLLA1 changes dramatically when the PCL1 (A3) blend component is changed to PCL2 (B3). Crystallisation is competitive and affected by the state of the co-blend components.
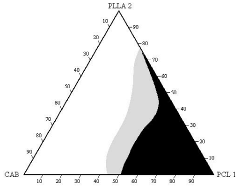 **PLLA2/PCL1/CAB**	**C3** **(T)**	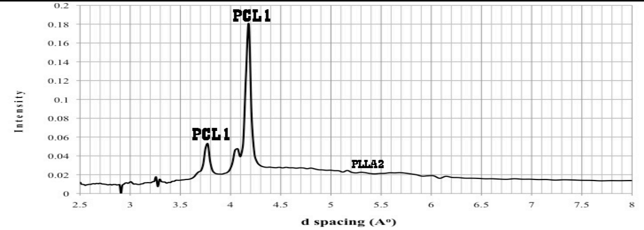	PCL1 appears to crystallise rapidly and dominate the miscibility behaviour. However, both PLLA2 and CAB seem to slow down the crystallisation rate of PCL1 as the blends show partial miscibility. The slower crystallisation of PLLA2 vs PLLA1 results in greater miscibility in the ternary diagram of C3 compared to that of A3.
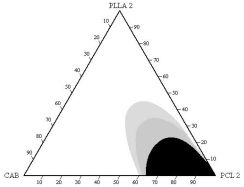 **PLLA2/PCL2/CAB**	**D3** **(C)**	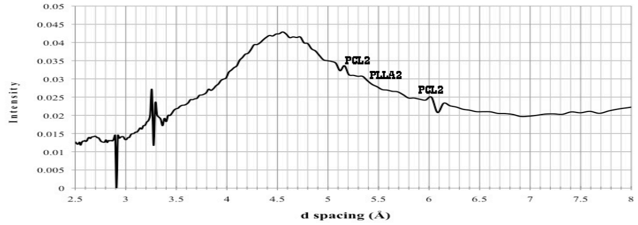	The higher molecular weight PLLA2 and PCL2 crystallise more slowly than PLLA1 and PCL1 resulting in a reduced region of opacity. PCL2 has the greatest influence in generating opacity. The low level of crystalline regions of PLLA2 and PCL2 in the clear films does not cause appreciable translucency, probably because the spherulitic structures are smaller than the wavelength of visible light.

6.3 PLLA/PCL/TPU blends

It was suggested in Section 5.10 that the crystallinity of PCL is an important factor in causing the PLLA/PCL/TPU blends to be less miscible. To investigate this proposition, WAXS was used to investigate the crystallinity of the PLLA/PCL/TPU blends. Three different types of the PLLA/PCL/TPU blends: PLLA1/PCL1/TPU, PLLA1/PCL2/TPU, and PLLA2/PCL2/TPU, show different phase miscibility diagrams, as illustrated in Figure 5.19 and again here in Figure 6.10.

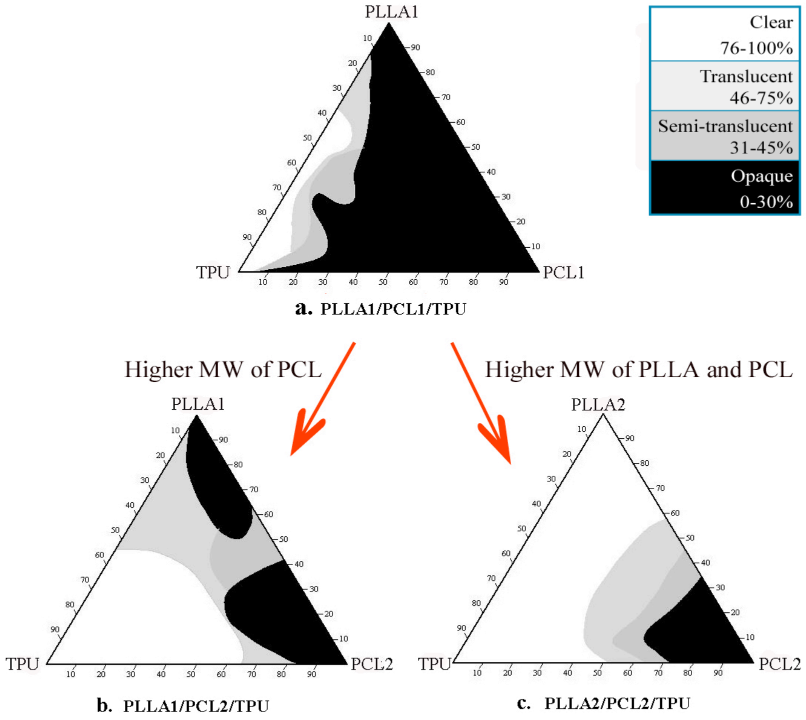

a. PLLA1/PCL1/TPU

b. PLLA1/PCL2/TPU

c. PLLA2/PCL2/TPU

Figure 6.10 The ternary phase miscibility diagrams of: **a.** PLLA1/PCL1/TPU blend, **b.** PLLA1/PCL2/TPU blend, and **c.** PLLA2/PCL2/TPU blend.

The crystallinity observations of the individual blends at different compositions; 20/30/50, 20/50/30 and 20/70/10, is presented in the following sections.

6.3.1 PLLA1/PCL1/TPU blends

PLLA1/PCL1/TPU forms opaque blends at each of the compositions studied; E1: 20/30/50, E2: 20/50/30 and E3: 20/70/10. Figure 6.11 shows WAXS traces of these blends together with the visual shading miscibility of binary blends and the ternary phase miscibility diagram.

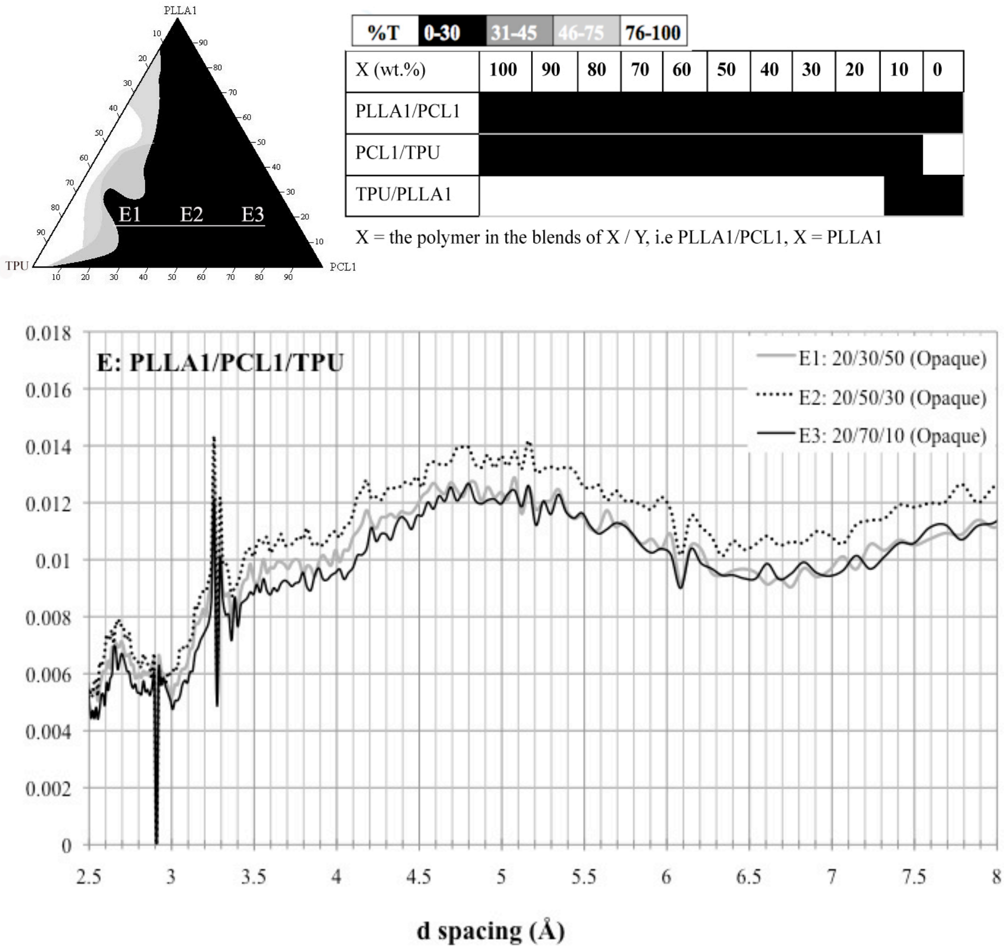

%T	■ 0-30	▨ 31-45	░ 46-75	□ 76-100

X (wt.%)	100	90	80	70	60	50	40	30	20	10	0
PLLA1/PCL1	■	■	■	■	■	■	■	■	■	■	■
PCL1/TPU	■	■	■	■	■	■	■	■	■	■	□
TPU/PLLA1	□	□	□	□	□	□	□	□	□	■	■

X = the polymer in the blends of X / Y, i.e PLLA1/PCL1, X = PLLA1

Figure 6.11 WAXS traces of the opaque PLLA1/PCL1/TPU blend films at different compositions; E1: 20/30/50, E2: 20/50/30, and E3: 20/70/10; together with the visual shading miscibility diagram of binary blends and the ternary phase miscibility diagram.

From the WAXS traces shown in Figure 6.11, the traces show identical peaks with no real crystalline regions. They indicate that all of the blends are completely amorphous despite the fact that (unlike the PLA/PCL/CAB systems) the blends are opaque. Information on other TPU-containing blends may help to understand this behaviour (see Section 6.4).

6.3.2 PLLA1/PCL2/TPU blends

Replacement of PCL1 by PCL2 produced blends of different clatity at the three chosen compositions. These blends; clear (F1: 20/30/50), translucent (F2: 20/50/30) and opaque (F3: 20/70/10), were studied for their crystallinity by WAXS. Figure 6.12 shows WAXS traces of these blends together with the visual shading miscibility of binary blends and the ternary phase miscibility diagram.

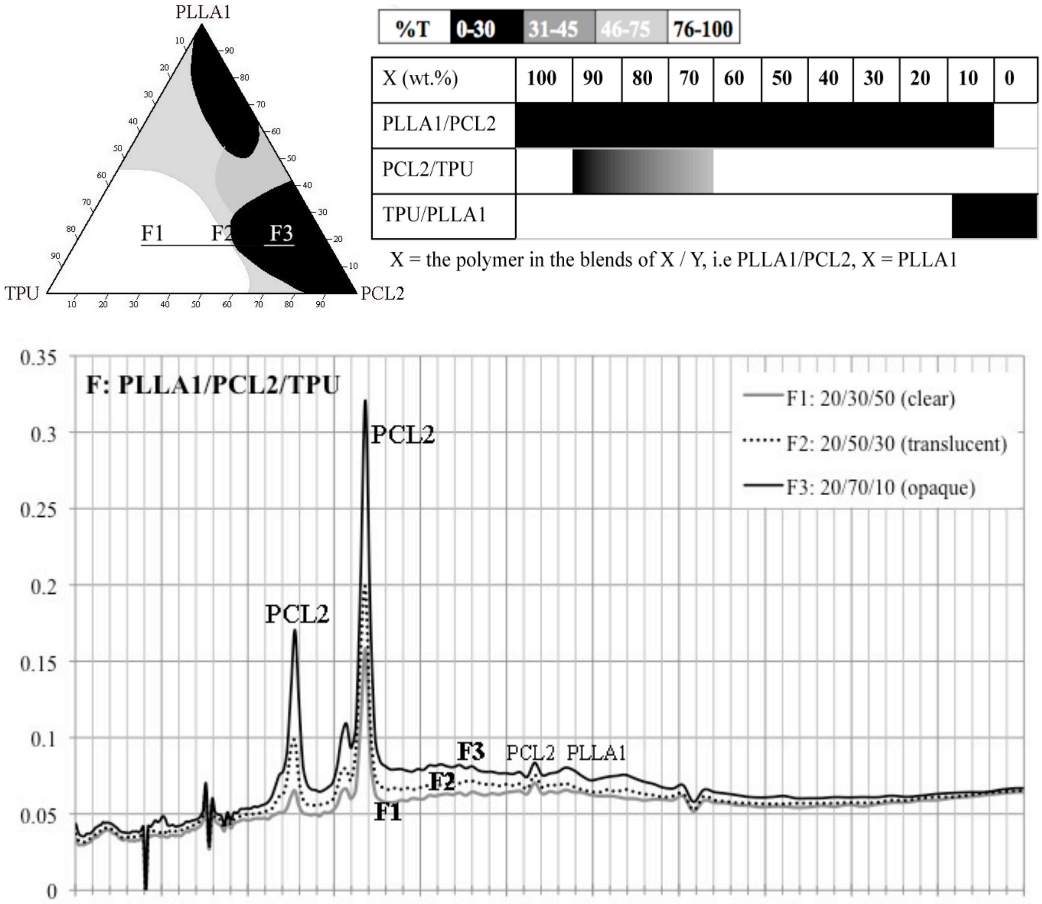

Figure 6.12 WAXS traces of the PLLA1/PCL2/TPU blends at different compositions; F1: 20/30/50-clear, F2: 20/50/30-translucent, and F3: 20/70/10-opaque; together with the visual shading miscibility diagram of binary blends and the ternary phase miscibility diagram.

From Figure 6.12, the peaks of PCL2 can all be observed in all the WAXS traces: clear, translucent, and opaque. The peak intensities are, however, different (opaque (F3) > translucent (F2) > clear (F1)). This suggests that the crystallinity of PCL2 is the key effect to the miscibility of the PLLA1/PCL2/TPU blend.

It seems to show that the more rapidly crystallising PLLA1 behaves in a PLLA1/PCL2/TPU blend differently from in the blend of PLLA1/PCL2/CAB. This can be seen in Figure 6.6 – which shows a strong crystalline peak of PLLA1.

6.3.3 PLLA2/PCL2/TPU blends

These blends produced films of three different clarity; clear (G1: 20/30/50), translucent (G2: 20/50/30) and opaque (G3: 20/70/10). These were used studied for their crystallinity by WAXS. Figure 6.13 shows WAXS traces of these blends together with the visual shading miscibility of binary blends and the ternary phase miscibility diagram.

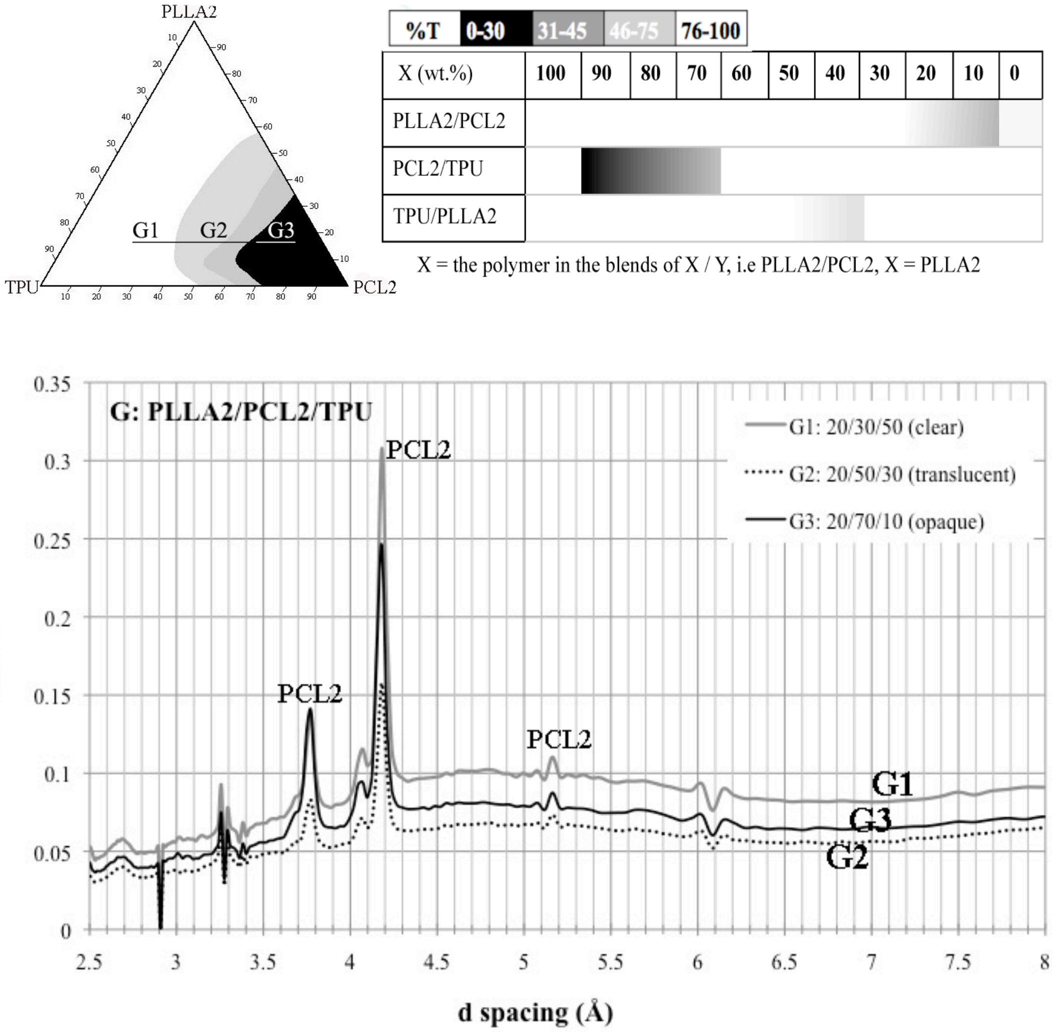

Figure 6.13 WAXS traces of the PLLA2/PCL2/TPU blends at different compositions; G1: 20/30/50-clear, G2: 20/50/30-translucent, and G3: 20/70/10-opaque; together with the visual shading miscibility diagram of binary blends and the ternary phase miscibility diagram.

From the WAXS traces shown in Figure 6.13, the peaks of PCL2 can all be observed in the samples of different clarity: clear, translucent, and opaque, but they are different in intensities. These WAXS traces are very similar to that of PLLA1/PCL2/TPU (Figure 6.12), and suggest those the crystallinity of PCL2 is the key effect to the miscibility of PLLA2/PCL2/TPU. In addition, it was observed that PLLA2 is more miscible with TPU than PCL2 is, which can be seen from the binary blends. This is possibly because the molecular interactions of PLLA2/TPU are greater than that of PCL2/TPU.

6.4 SUMMARY OF THE CHAPTER

This chapter has brought together observation on the crystallinity of a series of polymer blends. The compositions were chosen to show the range of miscibility behaviour (clear, translucent, opaque) that was obtained with these component blends of (a) PLLA, PCL, and CAB, and (b) PLLA, PCL, and TPU. A further variation was introduced by the use of two molecular weights of PLLA and PCL.

From the summary shown in Table 6.3, two broad observations can be made:

- The more crystalline polymers (PLLA1 > PLLA2, and PCL1 > PCL2) cause the blends to be more opaque, as seen the large crystalline peaks of PLLA1 and PCL1 in the blends: PLLA1/PCL2/CAB (B3) and PLLA2/PCL1/CAB (C3). This result confirmed the conclusions from the chapters dealing with solvent blending (Chapters 4 and 5).
- Poly L-lactic acid (PLLA) seems to be more miscible with CAB than does poly ε-caprolactone (PCL), as shown by the larger crystallinity peaks of PCL compared to PLLA in the PLLA1/PCL1/CAB (A3) blend and the opaque region shown at the PCL2 corner (high loading of PCL2) of the ternary phase diagram of PLLA2/PCL2/CAB (D3).

The enhanced miscibility of PLLA may be influenced by the difference in conformation of crystalline PLLA (a helical structure) and PCL (a planar zig-zag structure). The zig-zag structure of PCL, from a $(CH_2)_5$ backbone, helps the PCL chains to align via hydrophobic-hydrophobic interactions more easily than the helical structure of PLLA, which presents the polar ester groups around the helices. This allows PLLA chains to intermingle and to interact with CAB (the hydrogen bonding polymer) and enhance the miscibility between them. On the other hand the more rapid crystalling PCL structure excludes polar polymer during the course of crystallisation. Polyurethanes also contain hydrogen bondable repeat units, which in a similar way to CAB, can interact with the polar groups of PLLA. Thus, PLLA is able to interact with TPU more than PCL does (a very small WAXS peak of crystalline of PLLA is observed compared with PCL).

There is a common factor that overlays the miscibility of both PLLA/PCL/CAB and PLLA/PCL/TPU blends and that is the effect of molecular weight. With the exception of one apparently anomalous family (the WAXS traces in Figure 6.11), amorphous blends of PLLA/PCL blends with either CAB or TPU correlate with high crystallinity. There may be an explanation for this that is separate from the rationale governing all other combinations, which will now be dealt with, beginning with the CAB blends.

The information relating to the molecular weight of PLLA (PLLA1 < PLLA2) and PCL (PCL1 < PCL2) is clearly summarised in Table 6.3. From the information, it can be concluded that PLLA1 and PCL1 (more rapidly crystallising polymers) cause the blends to be less miscible in all combinations between them, as can be seen by comparing with PLLA1/PCL2/CAB and PLLA2/PCL1/CAB blends. However, PLLA seems to show less crystallinity than PCL: as observed by comparing PLLA1/PCL1/CAB and PLLA2/PCL2/CAB blends. The slower crystallisation allows PLLA2 and PCL2 chains to interact more freely with other chains producing blends that are more miscible in contrast with situations in which more rapid and thus complete crystallisation excludes the co-blend components.

The WAXS traces of PLLA1/PCL2/TPU and PLLA2/PCL2/TPU blends tell a similar story which can be summarised into the following points.

- The crystallisation rates of PLLA and PCL are observed to affect the blend miscibility as compared to all blend types. The more rapid crystallisations (PLLA1 > PLLA2, PCL1 > PCL2) cause the blends to be less miscible, as seen:

  PLLA1/PCL1/TPU < PLLA1/PCL2/TPU < PLLA2/PCL2/TPU

- It appears that the miscibility of PLLA/PCL/TPU blends is affected not only by the crystallisation rates of PLLA and PCL but also by the molecular interactions between PLLA, PCL, and TPU (TPU/PLLA > TPU/PCL > PLLA/PCL). It appears that this is associated with the structural conformations of PLLA (a helical structure) and PCL (a planar zig-zag structure).

In summary, this chapter has demonstrated the correlation between molecular weight and crystallinity and between crystallinity and opacity. This pattern corresponds very well for PLLA, PCL, and CAB blends and for PLLA, PCL, and TPU blends. There are some similarities between TPU and CAB which both contain polar groups with different backbone structures. The one anomalous feature of this work is the WAXS traces in Figure 6.11. The DSC trace confirms the expected transitions in authentic samples of the three blends. Subsequent re-examination confirms that it is simply a background spectrum for those three samples (for some reason the WAXS spectrum of these samples was not recorded). These WAXS samples of PLLA1/PCL1/TPU blends were repeated (Figure 6.14) and the results confirmed the initial hypothesis that the traces in Figure 6.11 are that of the background as polymer peaks were now visible. In addition, PCL1 was observed to cause these blends immiscibility as shown by the large peaks of PCL1 (at d spacing of 3.75 Å and 4.15 Å), compared to PLLA1 (at d spacing of 4.60 Å and 5.40 Å).

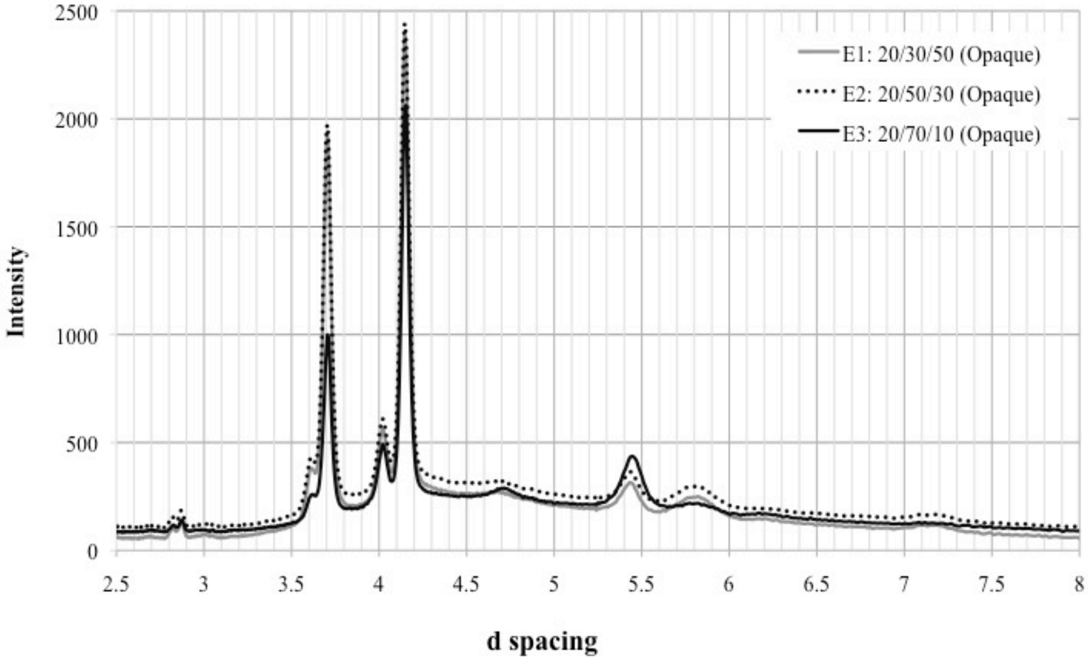

Figure 6.14 WAXS traces of the opaque PLLA1/PCL1/TPU blend films at different compositions; E1: 20/30/50, E2: 20/50/30, and E3: 20/70/10; together with the visual shading miscibility diagram of binary blends and the ternary phase miscibility diagram (repeat).

CHAPTER 7

SOLVENT BLENDING: THE COLEMAN AND PAINTER APPROACH

Chapter 7

Solvent Blending: The Coleman and Painter Approach

The Coleman and Painter principle for describing the miscibility of binary blend systems is well-established [1]. One of the most important conclusions lies in the fact that Coleman-Painter indicates the differences that weak interactions, moderate interactions and strong interactions make to blend miscibility. Therefore, this approach was used to explain some pairs of polymers used for ternary blends in this study, e.g. PLLA/PCL in PLLA/PCL/CAB blends. An extension of the Coleman-Painter miscibility guide to ternary polymer blends by Espi and coworkers was also studied [104]. This was not a major part of this thesis, merely and attempts to explore quantitative explanations of observed miscibility phenomenon.

7.1 The Coleman and Painter Principle

7.1.1 Introduction of polymer solutions and blends

The binary mixtures of molecules can be expressed in the terms of Gibbs free energy of mixing (ΔG_m). There are three terms corresponding to the Gibbs free energy of mixing: free volume of molecules, non-polar force, and polar force. For mixtures of ideal miscibility, the components should have: a random mixing caused by interaction forces (non-polar or polar interactions) between like molecules and unlike molecules; the same size and shape of molecules; and no free volume of molecules.

For polymer solutions, the free energy of mixing of monodisperse polymers and solvents are described by the equation of Flory and Huggins [105, 106], which is shown in Eq 7.1.

$$\frac{\Delta G_m}{RT} = n_s \ln\Phi_s + n_p \ln\Phi_p + n_s\Phi_p\chi_s \qquad \text{Eq.7.1}$$

where; n_s and n_p are the number of moles of solvent and polymer; Φ_s and Φ_p are volume fraction of solvent and polymer, respectively; χ_s is equal to the term zw/RT, where w is the exchange energy per mole; and z is the lattice coordination number. The first two terms represent the combinatorial entropy of mixing [1, 107]. The flexible polymer segments are each equal in size to a solvent molecule which is defined by a lattice cell size. The simple lattice model is shown in Figure 7.1.

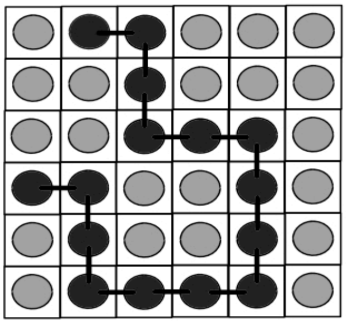

Figure 7.1 A lattice model occupying of polymer chain into solvent lattice cells.

Coleman, Painter and coworkers considered that both types of molecules in Eq.7.1 are polymers A and B and used molecule B to identify the lattice cell size. This causes a very large value of χ, which is dependent on the molar volume of the repeating unit of either polymer A or B (V_A, V_B) or defined as reference volume (V_r). They multiplied Eq. 7.1 by V_r/V, where V is the total volume of the system, given by [1]:

$$\frac{\Delta G'_m}{RT} = \frac{\Phi_A}{M_A}\ln\Phi_A + \frac{\Phi_B}{M_B}\ln\Phi_B + \Phi_A\Phi_B\chi_r \qquad \text{Eq.7.2}$$

where: Φ_A and Φ_B are the volume fractions of polymer A and B; M_A and M_B are degree of polymerisation of polymer A and B; χ_r is the interaction parameter, which is assumed to be purely energetic and for largely non-polar molecules, defined as

$$\chi_r = \frac{V_r}{RT}(\delta_A - \delta_B)^2 \qquad \text{Eq.7.3}$$

where δ is the Hildebrand's solubility parameter which is the square root of the cohesive energy density, defined in his classic work on the solubility of non-electrolytes. The solubility parameter is defined as:

$$\delta = \sqrt{c} = \left[\frac{\Delta H - RT}{V_m}\right]^{1/2} \qquad \text{Eq. 7.4}$$

where: c is the cohesive energy density; ΔH the heat of vaporisation; R the gas constant; T the temperature; and V_m the molar volume of polymer. χ is related with both entropy and enthalpy to obtain:

$$\chi = \chi_H + \chi_S \qquad \text{Eq.7.5}$$

For polymer solutions, χ_s is usually a major contributor, which is related to free volume theory. The free volume parameters are necessary to accommodate the phase behavior of non-polar polymer solutions. However, it was neglected in the system of high polymer solution blends in this work, which follows the approach of Coleman, Painter and coworkers.

Hildebrand and Scott [107] discussed the terms of non-specific and specific interaction parameters in the free energy of mixing equation in detail many years ago. There are a number of ways that specific interactions can be handled, but a particularly useful approach is the use of association models that account for both non-random contacts of strongly interacting functional groups and "self-association" of the pure components by defining equilibrium constants that can be spectroscopically measured independently. The associated species are allowed random contacts with one another, however, so that the unfavourable (to mixing), London dispersion and weak polar forces are separately accounted for by the usual Flory Huggins term $\Phi_A\Phi_B\chi$. The free energy of mixing is written in the following equation:

$$\frac{\Delta G_m}{RT} = \frac{\Phi_A}{M_A}\ln\Phi_A + \frac{\Phi_B}{M_B}\ln\Phi_B + \Phi_A\Phi_B\chi + \frac{\Delta G_H}{RT} \qquad \text{Eq.7.6}$$

where ΔG_H term is the free energy changes as a result of specific interactions, Φ_A and Φ_B, and M_A and M_B, are the volume fractions and degrees of polymerisation of A and B, respectively, while χ is the Flory-Huggins interaction parameter. $\Delta G_H/RT$ represents the strong or specific intermolecular interactions, e.g. hydrogen bonds.

The phase behavior of binary polymer solution blends can be predicted by knowing the ΔG_H and χ terms. The parameters in the ΔG_H term can be measured spectroscopically in many, but not for all systems.

7.1.2 A practical approach to polymer miscibility

The critical values of χ in Eq.7.6 and the upper limits of the non-hydrogen bonded solubility parameter difference [$(\Delta\delta)^{o}_{Crit}$] of Coleman and Painter are a practical approach to polymer miscibility used in this work [1]. A summary of the range of values of $(\Delta\delta)^{o}_{Crit}$ is shown in Table 7.1. The polymer pairs will have the greatest miscibility when the values of the two non-hydrogen bonded solubility parameters ($\Delta\delta$) are very close, and the relative strengths of any specific intermolecular interactions between the polymer pairs are high values.

Table 7.1 Summary of the upper limit of the critical values of the solubility parameter difference, $(\Delta\delta)^{o}_{Crit}$ [1].

Specific Interactions Involved	Polymer Blend Examples	$(\Delta\delta)^{o}_{Crit}$ $(cal.cm^{-3})^{0.5}$
Dispersive Forces Only	PBD-PE	≤ 0.1
Dipole-Dipole	PMMA-PEO	0.5
Weak	PVC-BAN	1.0
Weak to Moderate	PC-Polyesters	1.5
Moderate	SAN-PMMA	2.0
Moderate to Strong	Nylon-PEO	2.5
Strong	PVPh-PVAc	3.0
Very Strong	PMAA-PEO	≥ 3.0

It would be anticipated that simple poly(α-ester) interactions would most likely be weak to moderate – however by incorporation of hydrogen bonded molecules it may be possible to increase the strength of interactions.

To estimate the interaction parameters (χ), the solubility parameters (δ) can be calculated by dividing the sum of molar attraction constants (F) by the molar volume of the groups present in the repeat unit of the polymer, as shown in Eq. 7.7.

$$\delta = \sum \frac{F_i}{V} \qquad \text{Eq. 7.7}$$

The values of F and V of unassociated groups and weakly associated groups, from Coleman, Painter and coworkers, are shown in Table 7.2.

Table 7.2 The molar attraction constants (F) and molar volume (V) of unassociated groups and weakly associated groups [1].

Group	V (cm^3/mole)	F ($(cal.cm^3)^{1/2}$)		Group	V (cm^3/mole)	F ($(cal.cm^3)^{1/2}$)
Unassociated				Unassociated		
$-CH_3$	31.8	218		-OCO-	19.6	298
$-CH_2-$	16.5	132		-CO-	10.7	262
>CH-	1.9	23		-O-	5.1	95
>C<	-14.8	-97		>N-	-5.0	-3
C_6H_3	41.4	562		Weakly Associated		
C_6H_4	58.8	652				
C_6H_5	75.5	735		-Cl	23.9	264
$CH_2=$	29.7	203		-CN	23.6	426
-CH=	13.7	113		$-NH_2$	18.6	275
>C=	-2.4	18		>NH	8.5	143

This additive approach provides a potential way of understanding the different contributions of novel polymer structures such as those studied in this thesis.

The polymer miscibility observations in this work are based on the Coleman and Painter miscibility guideline but only by using it as a simple guideline to predict trends in polymer miscibility - because it cannot be directly applied to three-component blends.

7.1.3 An extension of the Coleman-Painter miscibility guide to ternary polymer blends.

Espi and coworkers have used the basic concepts of Coleman-Painter to determine the miscibility of ternary polymer blends [104]. On the basis of Eq.7.6, the free energy of mixing is reduced to Eq.7.8 for high molecular weight polymers.

$$\frac{\Delta G_M}{RT} = \Phi_1 \Phi_2 \chi + \frac{\Delta G_H}{RT} \qquad \text{Eq.7.8}$$

Eq.7.8 is divided throughout by the molar volume (V_r); the free energy of mixing then becomes:

$$\frac{\Delta G_M}{RTV_r} = \Phi_1\Phi_2\frac{\chi}{V_r} + \frac{\Delta G_H}{RTV_r} \qquad \text{Eq.7.9}$$

Equation 7.9 is then multiplied throughout by RT:

$$\frac{\Delta G_M}{V_r} = \Phi_1\Phi_2\frac{RT\chi}{V_r} + \frac{\Delta G_H}{V_r} \qquad \text{Eq.7.10}$$

Espi and coworkers have combined the terms of non-specific interactions together with specific interactions into an overall interaction energy density B and written the free energy of mixing of ternary polymer systems in a classical form, as shown in Eq.7.11 and 7.12, respectively:

$$\frac{\Delta G_M}{V_r} = \Phi_1\Phi_2 B \qquad \text{Eq.7.11}$$

$$= \Phi_1\Phi_2 B_{12} + \Phi_1\Phi_3 B_{13} + \Phi_2\Phi_3 B_{23} \qquad \text{Eq.7.12}$$

where: B_{ij} are the interaction energy densities of each polymer pair. A negative value of ΔG_M has been taken to show miscibility, without considering additional conditions for the ternary polymer system. B_{ij} can be divided in two terms, the non-specific (B_{ij}^N) and specific forces (B_{ij}^{SP}).

$$B_{ij} = B_{ij}^N + B_{ij}^{SP} \qquad \text{Eq.7.13}$$

The term B_{ij}^N can be written in terms of δ, as shown in Eq.7.14, and can be calculated using Eq.7.7, the term defining group contributions to molar volumes proposed by Coleman and Painter. The specific term B_{ij}^{sp} can be estimated in the same manner as the Coleman and Painter miscibility guide.

$$B_{ij}^N = (\delta_i - \delta_j)^2 \qquad \text{Eq.7.14}$$

The approach of Espi and coworkers was used for ternary blends in an attempt to calculate the free energy of mixing following an extension of the Coleman and Painter's miscibility guide to ternary polymer blends in this study.

7.2 PLLA/pre-synthesised poly(α-ester) homologous blends: Miscibility guide

The upper limit of the non-hydrogen bonded solubility parameter difference of Coleman and Painter, $(\Delta\delta)^o_{Crit}$, as shown in Table 7.1, was used as a miscibility guide for PLLA/pre-synthesised poly(α-ester) homologous blends in this section. The solubility parameters (δ) can be calculated using Eq.7.7 and the values of the molar attraction constants (F) and molar volume (V) following Table 7.2. The calculated results are shown in Table 7.3.

Table 7.3 Coleman-Painter's miscibility prediction of PLLA/pre-synthesised poly α-ester homologous blends using critical solubility parameter difference, $(\Delta\delta)^o_{Crit}$

Polymers	PLLA	α_1	α_2	α_3	α_4	α_5	α_6
F (cal.cm^3)$^{1/2}$	598	697	956	790	918	1,050	871
V (cm^3/mole)	49.5	64.6	97.6	67.0	83.5	100	73.2
δ (cal.cm^{-3})$^{0.5}$	12.1	10.8	9.8	11.8	11.0	10.5	11.9
$\Delta\delta$ (PLLA-α_x)	-	**1.3**	**2.3**	**0.3**	**1.1**	**1.6**	**0.2**
Miscibility Guide by type of molecular interaction:							
Non-Specific Interaction:							
Dispersive force		×	×	×	×	×	×
Polar forces		×	×	×√	×	×	×√
Specific interaction:							
Weak		×	×	√	×	×	√
Weak to Moderate		**√**	**×**	**√**	**√**	**×**	**√**
Moderate		√	√	√	√	√	√
Moderate to Strong		√	√	√	√	√	√
Strong		√	√	√	√	√	√

Note: *x, ×√ and √ is referred to; the two polymer are most likely to be immiscible (x), the two polymers may be miscible but caution errors are large for polar forces (×√), and the miscibility is predicted (√).*

As mentioned previously, the simple poly(α-ester) interactions are most likely to be weak to moderate. From Table 7.3, therefore, it can be seen that all poly(α-esters) are likely to be miscible with PLLA, except that α_2(diethyl) and α_5(cycloheptyl) could be immiscible because of either high molar interaction or high molar volume. The blends are all miscible with PLLA if moderate interaction is applied, which expectedly take place for PLLA/poly(α-esters) if the incorporation of hydrogen bonded molecule occurs.

A note of caution is necessary, however, the application of the Coleman-Painter approach as shown in Table 7.3 provides a Δδ value. The application of the general concept of polar forces indicates whether the magnitude of Δδ can be compensated for by the strength of interaction between the pair of polymers involved. The Coleman and Painter approach does not take into account specific structural aspects of the interactions such as the effects of crystallinity, chain conformation and steric interference, and the ability of polar and hydrogen bonding groups to interact.

The experimental results – as studied in Sections 4.2.2.1 and 4.2.2.2 and the visual shading miscibility diagrams have been provided again in Figure 7.2 - were compared with the results from the Coleman-Painter's miscibility prediction.

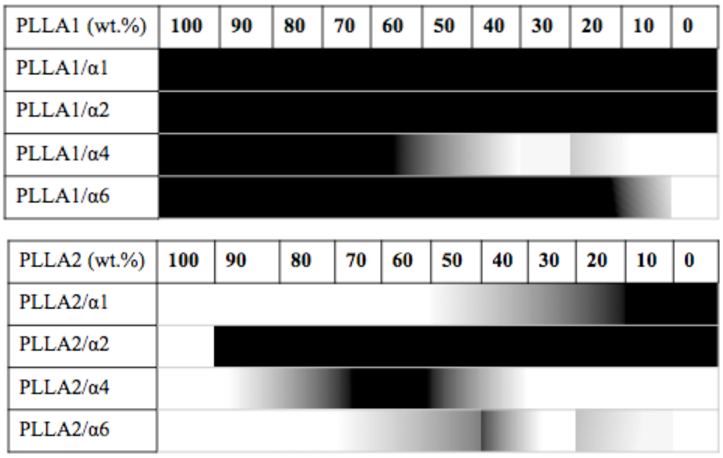

Figure 7.2 The visual shading miscibility diagram of the PLLA/pre-synthesised poly (α-ester) homologous blends.

If the weak to moderate interaction is considered, it can be seen that the miscibility prediction from Coleman and Painter (most likely to be miscible) is totally different from the experimental results (predominantly immiscible) in case of PLLA1 blending. However, in case of PLLA2 blending, the miscibility result correlates well with the Coleman-Painter miscibility prediction by critical solubility parameter difference, $(\Delta\delta)^{o}_{Crit}$.

Thus the order of miscibility found (α6(chloromethyl-methyl) > α4(cyclohexyl) > α1(dimethyl) > α2(diethyl)) corresponds well to the Δδ values (0.2, 1.1, 1.3, 2.3). Additionally the differences between PLLA1 and PLLA2 show that the crystallisation rate of the components has a major effect on the miscibility of these polymer blends. The fact that α_6(chloromethyl-methyl) shows enhanced miscibility correlates with the greatest polarity of this poly(α-ester).

7.3 PLLA blended with PCL, CAB or TPU: Miscibility guide

In this section, the Coleman-Painter approach has been used to predict the miscibility of the PLLA/PCL blends and to observe what differences are caused by changing PCL for CAB and TPU. The value of $(\Delta\delta)^{o}_{Crit}$ of their pairs is shown in Table 7.4.

Table 7.4 Coleman-Painter's miscibility prediction of the PLLA/PCL, CAB or TPU blends using critical solubility parameter difference, $(\Delta\delta)^{o}_{Crit}$

Polymers	**PLLA**	**PCL**	**CAB**	**TPU**
$F\ (cal.cm^{3})^{1/2}$	598	1,012	1,848	3,602
$V(cm^{3}/mole)$	49.5	98.3	154	290.5
$\delta\ (cal.cm^{-3})^{0.5}$	12.1	10.3	12.0	12.4
Δδ (PLLA-Polymer X)		**1.8**	**0.1**	**0.3**
Miscibility Guide by type of molecular interaction:				
Non-Specific Interaction:				
Dispersive force		×	×	×
Polar forces		×	×√	×√
Specific interaction:				
Weak		×	√	√
Weak to Moderate		×	√	√
Moderate		√	√	√
Moderate to Strong		√	√	√

Note: *x, ×√ and √ is referred to; the two polymer are most likely to be immiscible (x), the two polymers may be miscible, but caution errors are large for polar forces (×√); and the miscibility is predicted (√).*

It can be seen from Table 7.4 that Δδ of PLLA-PCL shows a greater difference than PLLA-TPU and PLLA-CAB, respectively. Therefore, PLLA should be more miscible with CAB followed by TPU and then PCL. However, the miscibility between polymer pairs depends on the molecular interactions, in which PLLA-PCL is most likely to be weak to moderate, while CAB and TPU, influenced by hydrogen bonding, is likely to be moderate or moderate to strong.

From Coleman and Painter's miscibility prediction, therefore, it appears that PCL should be immiscible with PLLA, whereas CAB and TPU are miscible with PLLA. This agrees with the experimental result shown in the binary blend diagrams in Figure 7.3. TPU seems to show more miscibility with PLLA than CAB does, because of the high molecular interaction by –NH groups. However, it is important to note that the miscibility of polymer blends depends on the composition of each polymer pairs, which cannot be predicted from $(\Delta\delta)^{o}_{Crit}$.

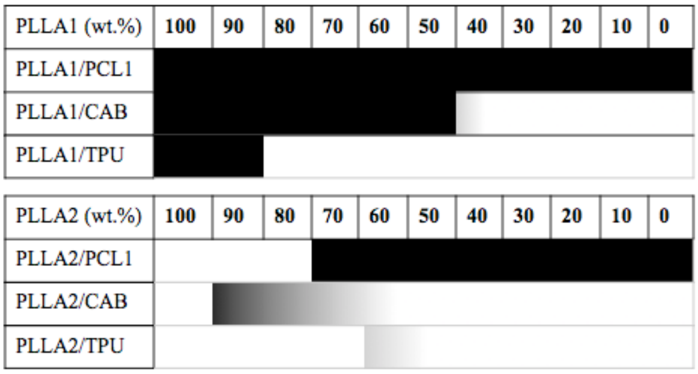

PLLA1 (wt.%)	100	90	80	70	60	50	40	30	20	10	0
PLLA1/PCL1	■	■	■	■	■	■	■	■	■	■	■
PLLA1/CAB	■	■	■	■	■	■	▨				
PLLA1/TPU	■	■									

PLLA2 (wt.%)	100	90	80	70	60	50	40	30	20	10	0
PLLA2/PCL1				■	■	■	■	■	■	■	■
PLLA2/CAB		▨	▨	▨	▨						
PLLA2/TPU					▨						

Figure 7.3. The visual shading miscibility diagram of the PLLA/PCL, PLLA/CAB, and PLLA/TPU blends of different molecular weights and compositions of PLLA.

The experimental results shown in Figure 7.3 confirm that the miscibility of the blends is affected by the crystallisation rates (as disscused in Chapter 4). For example: slower crystallisations of PLLA2 and PCL2 lead the blend to be miscibility, while more rapid crystallisations of PLLA1 and PCL1 lead the blend to be immiscible. The relative rate of crystallisation (PLLA1 > PLLA2) is related directly in all blends with PCL, CAB, and TPU. This indicates that the Coleman-Painter's miscibility prediction requires polymer structure and morphology to be taken into account.

7.4 Refining the miscibility guide: The effect of crystallinity on miscibility

PLLA1, PLLA2 and PDLLA are structural variants of PLA, which show equal values of solubility parameter. Because of this using the critical solubility parameter difference, $(\Delta\delta)^{o}_{\mathrm{Crit}}$ of Coleman-Painter to predict the miscibility may not be possible without further refinement using parameters in miscibility equation 7.6. To compare the miscibility of PLA variants with other polymers is observed and discussed in this section.

$$\frac{\Delta G_m}{RT} = \frac{\Phi_A}{M_A}\ln\Phi_A + \frac{\Phi_B}{M_B}\ln\Phi_B + \Phi_A\Phi_B\chi + \frac{\Delta G_H}{RT} \qquad \text{Eq.7.6}$$

Table 7.5 summarises the miscibility guide of the binary blends of PLA with other polymers by estimating the miscibility parameter in the free energy of mixing equation 7.6.

Table 7.5 The miscibility of PLA variants with α_4, PCL and CAB: Comparison from the miscibility estimated by miscibility parameters in the free energy of mixing equation 7.6 and from the experimental results.

Polymer Blends	**Parameters in miscibility equation**			**Miscibility From**	
	Φ	**Δδ**	**ΔG_H**	$\Delta G_m/RT$ (Eq.7.6)	**Experimental Results** (in the section 4.2.5)
PLLA1/α_4	×	similar	No	Similar	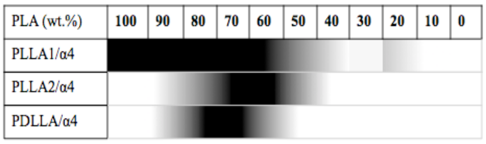PLA (wt.%) 100 90 80 70 60 50 40 30 20 10 0 PLLA1/α4 PLLA2/α4 PDLLA/α4
PLLA2/α_4	×		No		
PDLLA/α_4	x		No		
PLLA1/PCL	×	similar	No	Similar	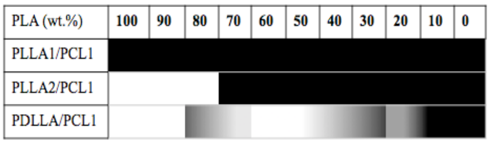PLA (wt.%) 100 90 80 70 60 50 40 30 20 10 0 PLLA1/PCL1 PLLA2/PCL1 PDLLA/PCL1
PLLA2/PCL	×		No		
PDLLA/PCL	x		No		
PLLA1/CAB	×	similar	Yes	Similar	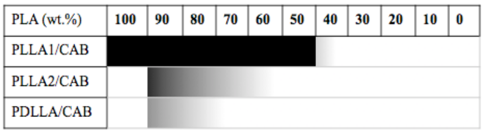PLA (wt.%) 100 90 80 70 60 50 40 30 20 10 0 PLLA1/CAB PLLA2/CAB PDLLA/CAB
PLLA2/CAB	×		Yes		
PDLLA/CAB	x		Yes		

Note: x referred to the parameter Φ can be neglected in the polymer solution blends.

From Table 7.5, it would appear that the miscibility prediction from the free energy of mixing equation cannot account for the difference in miscibility behaviour of stereochemical variants of PLA that influence crystallisation. Thus, the experimental results show that crystalline PLLA (both PLLA1 and PLLA2) is less miscible with α4(cyclohexyl), PCL, and CAB than the amorphous PDLLA.

However, this is a preliminary guide for observing miscibility in terms of using miscibility equations. The polar or weak specific interactions may occur in case of the PDLLA/PCL blends and definitely occur in the PLLA/CAB and PDLLA/CAB blends. The way to calculate ΔG_m is to add a ΔG_H term into Eq.7.6, which is obtained from group contributions and infrared spectroscopic studies [108].

7.5 Miscibility window for PLLA1/PCL1/CAB blend

In this section, an extension of the Coleman-Painter miscibility guide to ternary polymer blends by Espi and coworkers was used to predict the miscibility of the ternary blends of PLLA1/PCL1/CAB. The free energy of mixing term, $\Delta G_M/V_r$, was calculated using Eq.7.12, assuming the value of the B_{ij}^{sp} term is zero. Thus, the free energy of mixing equation is:

$$\frac{\Delta G_M}{V_r} = \Phi_1\Phi_2 B_{12}^N + \Phi_1\Phi_3 B_{13}^N + \Phi_2\Phi_3 B_{23}^N \qquad \text{Eq. 7.15}$$

Where: Φ_1, Φ_2 and Φ_3 refer to the volume fractions of PLLA1, PCL1 and CAB, respectively. B_{12}^N, B_{13}^N and B_{23}^N refer to Espi's interaction energy densities of PLLA1/PCL1, PLLA1/CAB and PCL1/CAB, respectively, which can be calculated by Eq.7.14. The δ $(\text{cal.cm}^{-3})^{0.5}$ of PLLA, PCL, and CAB are 12.1, 10.3, and 12.0, respectively.

$$B_{ij}^N = (\delta_i - \delta_j)^2 \qquad \text{Eq.7.14}$$

The free energy of mixing term was calculated based on the ternary diagram of PLLA1/PCL1/CAB shown in Figure 5.2 and shown again in Figure 7.4.

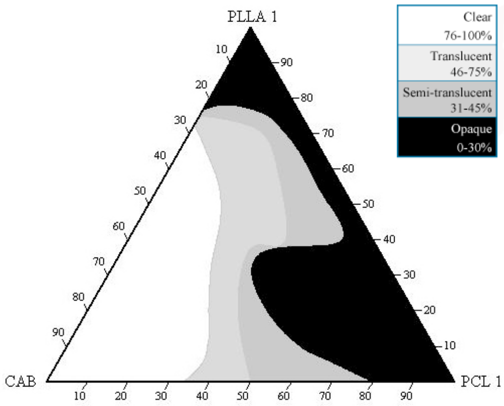

Figure 7.4 The ternary phase miscibility diagram of the PLLA1/PCL1/CAB blend.

From Figure 7.4, the composition ranges at the border between the opaque region and semi-translucent region were assumed as the compositions to change the blends from immiscible to miscible. This was then used to calculate the free energy of mixing using Eq. 7.15. The miscibility window of the PLLA1/PCL1/CAB blend is shown in Figure 7.5.

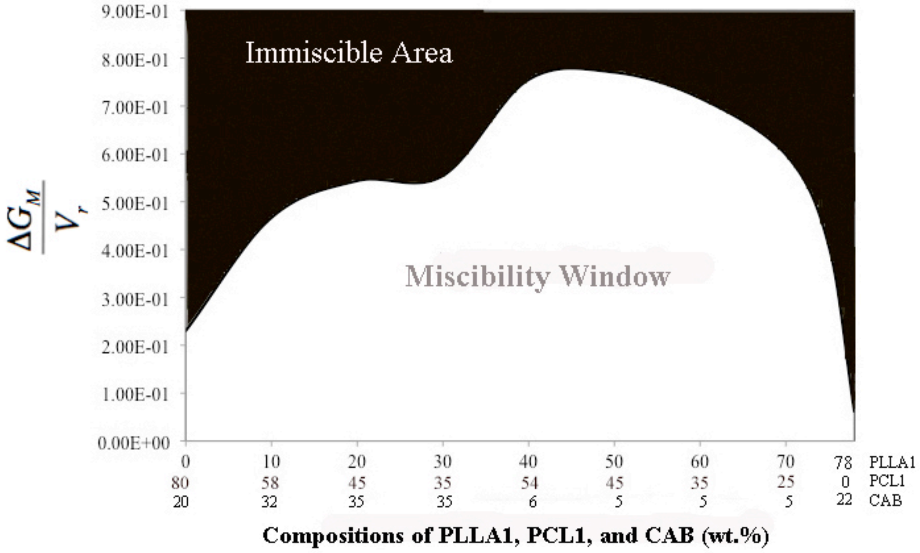

Figure 7.5. The miscibility window of the PLLA1/PCL1/CAB blend.

From the miscibility window shown in Figure 5.4, the line between the immiscible area and miscibility window is the calculated value of the free energy of mixing from Eq.7.15. It can be seen that the free energy of mixing of the miscible PLLA/PCL/CAB blend is positive, whereas it would be negative for the binary blends following the

Coleman-Painter approach. However, this calculation ignores the specific interaction (B_{ij}^{SP}) term, which is related to inter- and self-associations [104]. If the specific interaction term is taken into the calculation, the free energy of mixing value is predicted to be lower. The miscibility window would be moved to a lower level but the pattern would be the same.

7.6 SUMMARY OF THE CHAPTER

- The point of the Coleman-Painter calculation is not to find the right answer or to predict what experiments will produce, although it would be good if that happened. The point is to identify a calculation that explains in quantitative terms what effect different structural elements or features have on miscibility. It suggests ways in which the structure might be changed to enhance miscibility and helps to understand the factors that are important in controlling miscibility.

- The Coleman and Painter miscibility prediction appears to work well when effects of crystallinity, chain conformation, and steric interference are taken into account, which are related to the crystallisation rate, for example. This has a major effect on the miscibility results in this study.

- To calculate the free energy of mixing, following an extension of the Coleman and Painter miscibility guide to ternary polymer blend by Espi and coworkers in this study, is only an idea for observing miscibility in term of using miscibility equations without the specific interaction term.

CHAPTER 8

MELT BLENDING

Chapter 8

Melt Blending

Reactive blending or melt blending is a technique to mix polymer components using a temperature above the polymer melting points. There are several instruments that use this technique, such as extruders, internal mixers, and two-roll mills. To observe the miscibility, two-roll mills, the simplest machine, was used to blend some of the ternary components for comparison with solvent blending.

In order to compare the two techniques, three compositions were selected from the ternary blends of PLLA, PCL, and CAB as illustrated in the Figure 8.1: A1 (40/45/15) - clear, A2 (40/25/35) - translucent, and A3 (40/45/15) - opaque. These compositions were selected to show the three different types of behaviour observed with solvent blending and to determine if melt blending produced the same outcome.

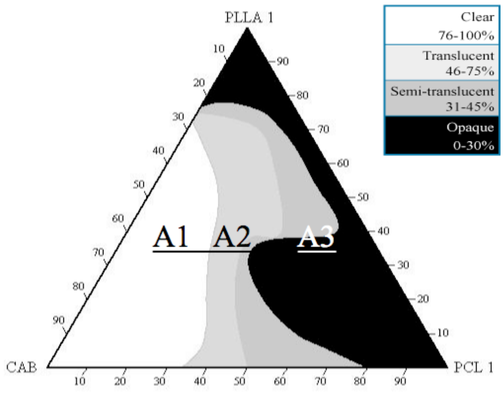

Figure 8.1 The ternary phase diagram of the PLLA1/PCL1/CAB blend from solvent blending.

These different blending compositions were blended on the two-roll mills with applied elevated temperature and shear force, and then studied for their physical properties and structural analysis. The physical properties, glass transition temperature (T_g) and melting temperature (T_m), were measured by Differential Scanning Calorimeter (DSC), the structure analysis by Fourier-Transform Infrared-Spectrophotometer (FT-IR), and morphology by hot-stage microscopy. These properties were then compared for both solvent and melt blended polymers at the same composition.

8.1 Observation: DSC

The thermal properties of the PLLA/PCL/CAB blends, using both melt and solvent blending techniques, were studied by Differential Scanning Calorimetry (DSC). Samples were heated from room temperature to 220 ^{o}C, cooled down to -60 ^{o}C and heated up to 220 ^{o}C with a heating rate of 20 ^{o}C/min under a nitrogen atmosphere. The glass transition temperature (T_g), crystalline temperature (T_c), melting temperature (T_m), cold crystallisation enthalpy (ΔH_c) and melting enthalpy (ΔH_m) were recorded and are shown in Table 8.1.

In Table 8.1, the subscripts 1 and 2 at T_g, T_m and ΔH_m refer to the first and the second peak appearing at low to high temperature, respectively. The T_g of PCL1, which should show a peak at approximately around -60 ^{o}C, could not be observed. The pre-melting percent crystallinity (χ) (or initial % crystallinity, before crystallisation) of PLLA1 in the blends is calculated using Eq.8.1.

$$\chi = \frac{(\Delta H_{m2} - \Delta H_{c2})}{\Delta H_m^{ideal}} x100\% \qquad \text{Eq. 8.1}$$

where; ΔH_{m2} is the heat of melting per gram, ΔH_{c2} is the cold crystallisation enthalpy, ΔH_m^{ideal} is the melting enthalpy of 100% crystalline PLLA, which is approximately 135.7 J/g [76]. ΔH_m^{ideal} for 100% crystalline PCL is approximately 93.7 J/g.

One suggested indication of the miscibility of polymer blends is the observation of a single T_g [11]. As mentioned previously, the glass transition region of PLLA overlaps significantly with the melting range of PCL, and the T_g of PCL could not be observed. Thus, the miscibility of the blends could not be identified from the thermogram. However, the T_g of all three-component blends showed only one peak - T_{g1} - at a slightly higher temperature than unblended PLLA, except SB3, which shows the T_g of CAB at 107 ^{o}C. Thus, it is possible to predict that all these blends except SB3 show partial-miscibility or full miscibility. It can be further said that SB3 is immiscible, which is consistent with the percentage transmission observation (%T = 20).

Table 8.1 Thermal properties and pre-melting percent crystallinity (χ) of PLLA1 in the PLLA1/PCL1/CAB blends from different techniques.

Polymer Materials	**Amorphous Regions**		**Crystalline Regions**				**Melting Regions**				**χ (%)**
	Tg_1^* (°C)	Tg_2 (CAB) (°C)	T_{c1} (PCL1) (°C)	T_{c2} (PLLA1) (°C)	ΔH_{c1} (PCL1) (J/g)	ΔH_{c2} (PLLA1) (J/g)	T_{m1} (CAB) (°C)	T_{m2} (PLLA1) (°C)	ΔH_{m1} (CAB) (J/g)	ΔH_{m2} (PLLA1) (J/g)	
PLLA1	53		91		8.75		162		52.0		32
PCL1	-		26		67.7		53		107.0		42
CAB	114		-		-		151		14.3		-
PLLA1/PCL1/CAB:											
<u>Solvent Blends</u>											
SB1: 40/10/50	61	-	-	98	-	26.5	145	165	8.2	41.2	11
SB2: 40/25/35	55	-	-	95	-	30.0	153	164	6.0	50.0	15
SB3: 40/45/15	54	107	-	82	-	42.5	148	162	20.0	60.2	13
<u>Melt Blends</u>											
MB1: 40/10/50	56	-	-	122	-	18.7	144	165	2.2	38.2	14
MB2: 40/25/35	53	-	-	97	-	29.5	148	167	5.7	47.2	13
MB3: 40/45/15	58	-	13	79	53.1	30.0	149	167	20.0	50.0	15
<u>Dissolved-Melt Blends</u>											
MS1: 40/10/50	56	-	-	93	-	8.3	144	162	14.0	22.8	11
MS2: 40/25/35	53	-	-	84	-	20.8	155	162	-	36.8	12
MS3: 40/45/15	56	-	13	82	68.0	26.7	150	162	16.0	42.5	12

Note: * Tg_1 could be the T_g of PLLA1 but it also could be the T_m of PCL1 because T_g of PLLA1 is close to the T_m of PCL1.

The pre-melting percent crystallinity (χ) of PLLA1 (before first heating from DSC) in all composition blends drops from the value of unblended PLLA1. The percentage crystallinity of PLLA1 in the three component blends is shown in Figure 8.2.

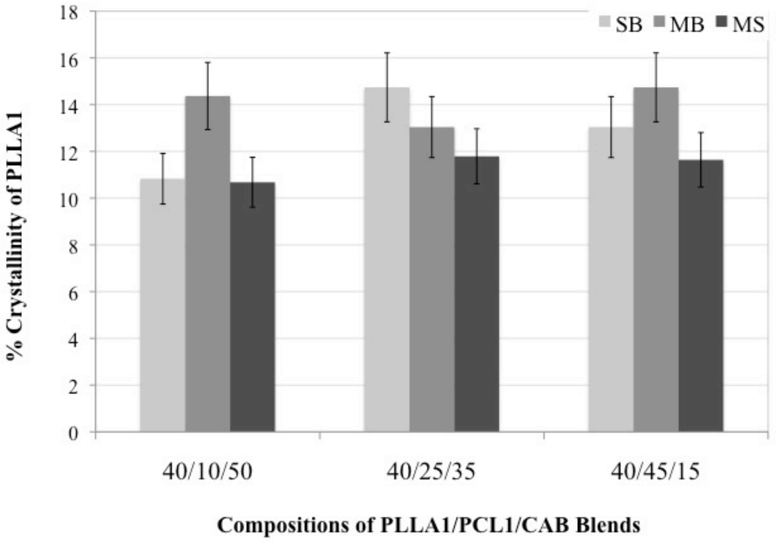

Figure 8.2 Percent Crystallinity of PLLA1 at different compositions and blending methods.

From Figure 8.2, it can be seen that the percentage crystallinity of PLLA1 shows only a small difference in all compositions and blending techniques. However, the melt blending composites seem to show on average a higher percentage crystallisation of PLLA1 than solvent blending, except for the 40/25/35 composition in which the solvent blending value is unexpectedly high. The ability to form crystalline regions depends on the thermal history of polymers and all these blends were also observed by hot-stage microscopy observation in the next section.

8.2 Observation: Hot-stage microscopy

Hot-stage microscopy was used to observe the crystallisation of the three-component blends of PLLA1/PCL1/CAB, which were blended by melt- and solvent blending techniques. The samples were melted to adhere to the glass slide and then covered with a slide-cover. The sample slides were put into the hot-stage box connected with microscope and monitor, and then heated rapidly to 220°C and cooled down to room temperature, at a cooling rate 10°C/min. Thus, the crystallisation behaviour of all polymer samples were observed from post-melt. The light intensity was recorded to show the tendency of morphology of polymers when they were cooled down from the melt stage.

The unblended CAB, PLLA1 and PCL1 samples were analysed for crystalline behaviour, and their images are shown in Figure 8.3(a), (b) and (c), respectively, with a 230 micrometre scale. The inset in Figure 8.3a is the morphology of unblended CAB at room temperature, while that of PLLA1 (Figure 8.3b) and PCL1 (Figure 8.3c) are, respectively, the morphologies of PLLA1 and PCL1 in the blends at room temperature (or when the crystals stopped growing). There are no crystalline regions observed from CAB, however, the crystalline spherulites were observed in both PLLA1, and PCL1. The different features of crystalline spherulites of PLLA1 and PCL1 can be seen in which that of PLLA1 seems to show brighter than PCL1. In addition, the crystalline image of unblended PCL1 is different from the crystalline image of PCL1 in the blend.

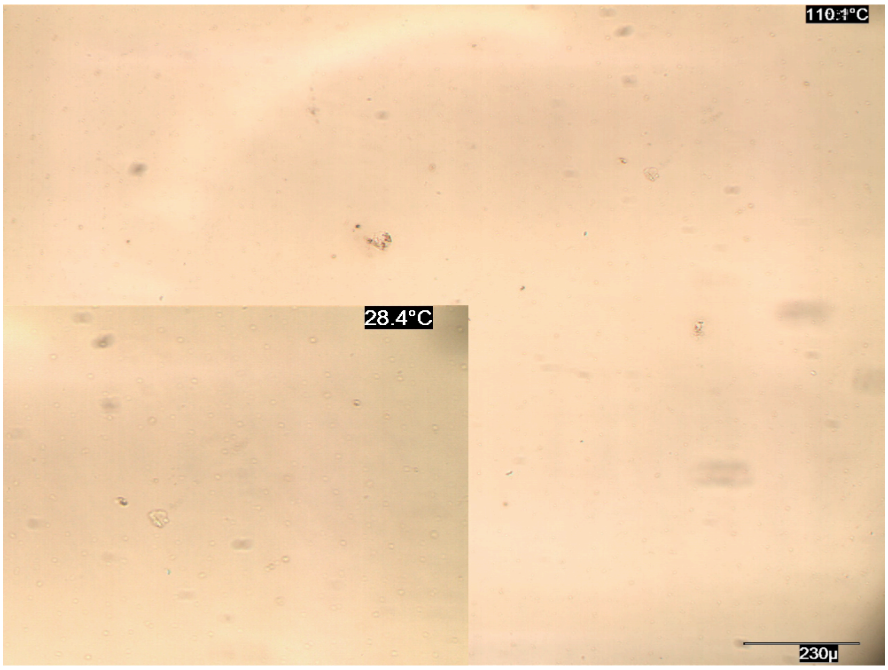

(a) CAB : melted at ~150 °C

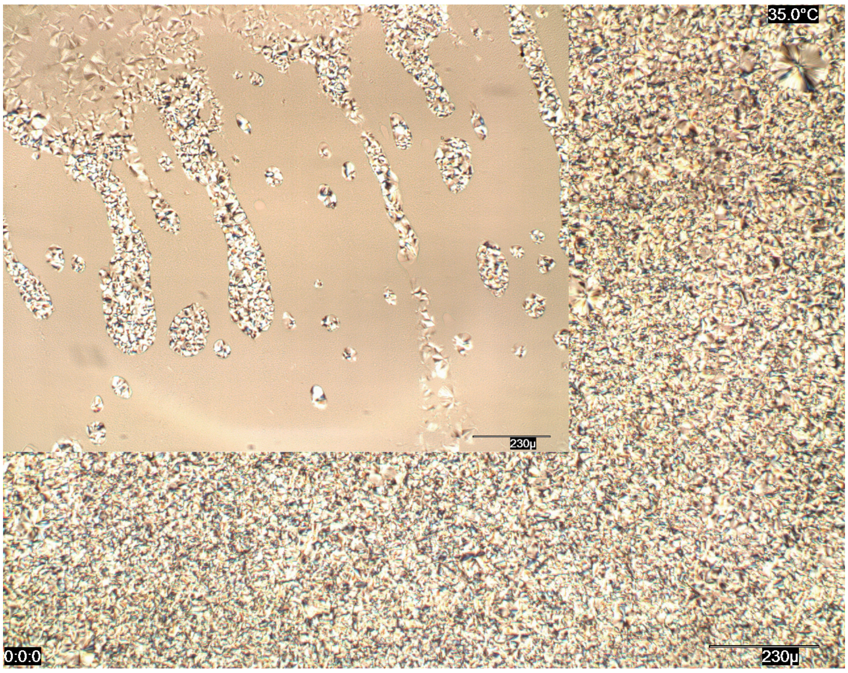

(b) PLLA1: Crystallised at ~ 75-95 °C

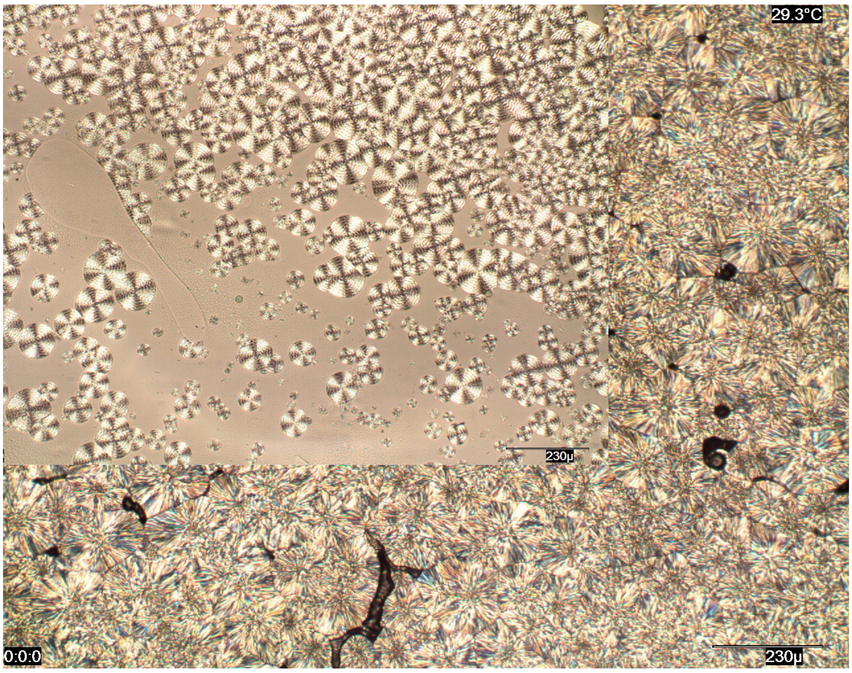

(c) PCL1: crystallised at ~25-45°C

Figure 8.3 Images of morphology behaviour of:
(a) unblended CAB at melting stage and room temperature (inset)
(b) and (c) unblended PLLA1 and PCL1: in the PLLA1/PCL1/CAB blend (inset); when cooling at 10°C/min from melt stages by HSM analysis.

The morphology images of 40/45/15 PLLA1/PCL1/CAB blends from melt blending (MB3) and solvent blending (SB3-opaque film) techniques are shown in Figure 8.4. It can be observed there is a greater amount of crystalline spherulites of PCL1 than PLLA1. This means that the crystallinity of PCL1 may also show a greater effect on the miscibility of MB3. As observed, it strongly affects SB3 (revealed by the WAXS traces in Figure 6.4).

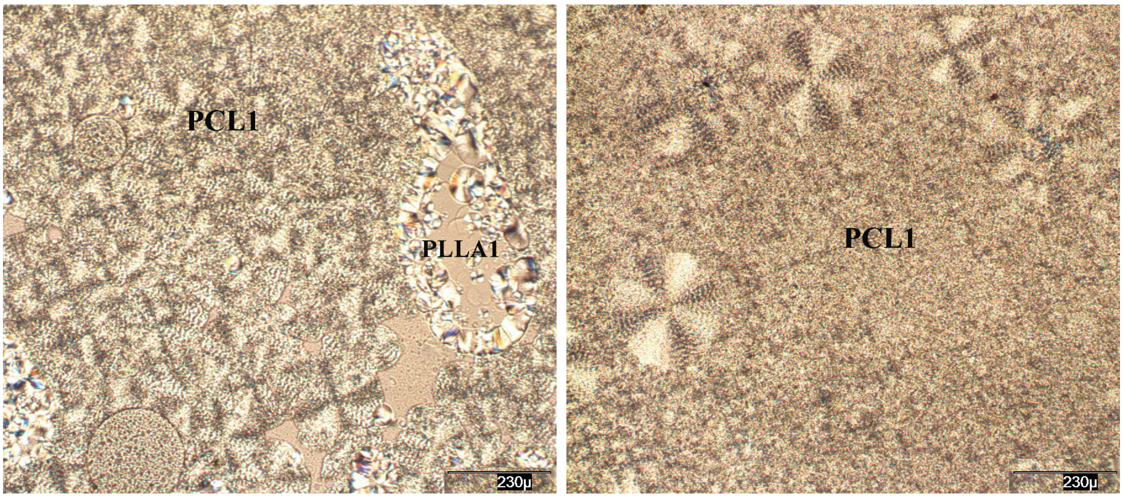

(a) MB3: 40/45/15 **(b) SB3: 40/45/15**

Figure 8.4 Images of 40/45/15 PLLA1/PCL1/CAB blends (at room temperature - after being cooled down from 220 °C) from melt blending (MB3) and solvent blending (SB3) techniques measured by hot-stage microscope.

To study further information, the light intensities of these blends together with other compositions: 40/10/50 and 40/25/35, were recorded during cooling down the samples from 220 °C to 25 °C. The results are shown in Figure 8.5 (for melt blending) and Figure 8.6 (for solvent blending). To minimise the error from the starting intensity of all samples, the intensity is shown in terms of change in intensity (Δ Intensity). Thus, the y-axis is the difference in intensity between the intensity at the measured temperature (T_x) and the intensity at the melting temperature (T_{220}). The x-axis shows the cooling temperature from 220 °C to room temperature.

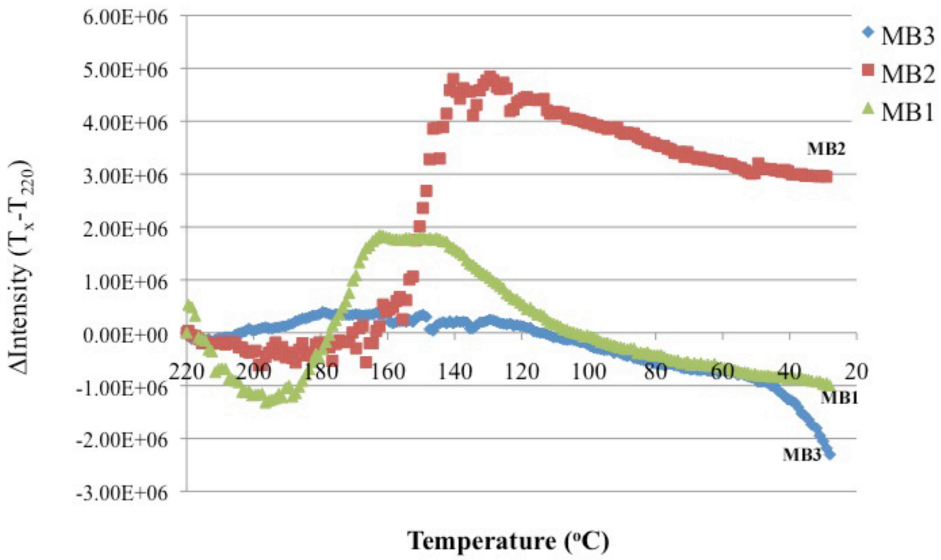

Figure 8.5 The change in light intensity of melted PLLA1/PCL1/CAB blends measured by hot-stage microscopy (cooling from 220 °C to 25 °C at 10 °C/min). Three different compositions: MB1 (40/10/50)
MB2 (40/25/35)
MB3 (40/50/10)

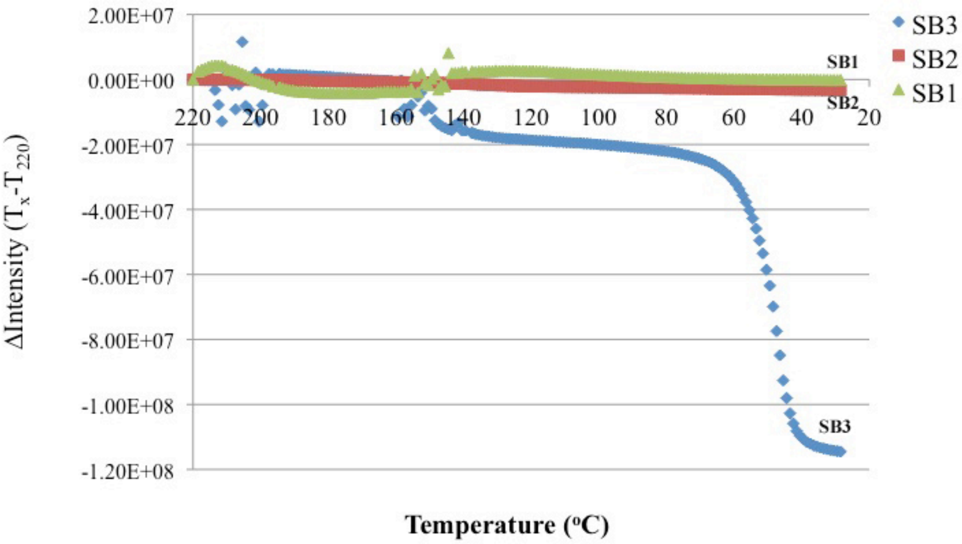

Figure 8.6 The change in light intensity of solvated PLLA1/PCL1/CAB blends measured by hot-stage microscopy (cooling from 220 °C to 25 °C at 10 °C/min). Three different compositions: SB1 (40/10/50) – clear film
SB2 (40/25/35) – translucent film
SB3 (40/50/10) – opaque film

From Figure 8.5, it can be seen that the change in light intensity of MB3 continuously decreases from melt stage and significant drops approximately at 34 ^{o}C – the crystallisation temperature of PCL1. A smaller change in light intensity (at the crystallisation temperature of PCL1 (~30-40 ^{o}C)) can be observed in MB1 and MB2 compared to MB3. This result confirms that the crystallinity of PCL significantly affects the miscibility of the PLLA1/PCL1/CAB blend, more notably at the composition of 40/45/15.

From Figure 8.6, the change in light intensity of SB1 and SB2 only slightly changes from melting temperature to room temperature. This shows a small amount of crystallinity in PLLA1 and PCL1. However, it changes significantly from melting temperature to crystallisation temperature of PLLA1 and from crystallisation temperature of PCL1 to room temperature, in SB3. This means that the crystallinity of both PLLA1 and PCL1 affects the miscibility of the blends, but PCL1 seems to have more influence, complementing the results from WAXS traces in Figure 6.4.

One emerging point seen from those two change of light intensities (Figure 8.5 and 8.6) is that the crystallinity growth rate of PCL1 in solvent blending (SB3) seems to be faster than melt blending (MB3), and shows more crystallinity, as observed by a greater change of intensity slope at the crystallisation temperature of PCL1. This may be because the chains of PCL1 in solvent blending are more mobile than in melt blending, and so PCL1 crystallises more easily.

8.3 Observation: FT-IR

In this section, Fourier-Transform Infrared-Spectrophotometry (FT-IR) was used to observe the structure and the molecular interactions of the melted- and solvated-blends of PLLA/PCL/CAB. Blends are compatible when the spectral frequency of the blends shifts. If the blends are incompatible, the spectrum of the blends is simply the spectrum of the two or three homopolymers [109, 110]. This is a potentially simple guide to analyse the miscible and immiscible blends of PLLA1/PCL1/CAB. The FTIR spectra of percent transmittances of all components; PLLA1, PCL1 and CAB, were analysed as references for that of their blends and showed in Figure 8.7.

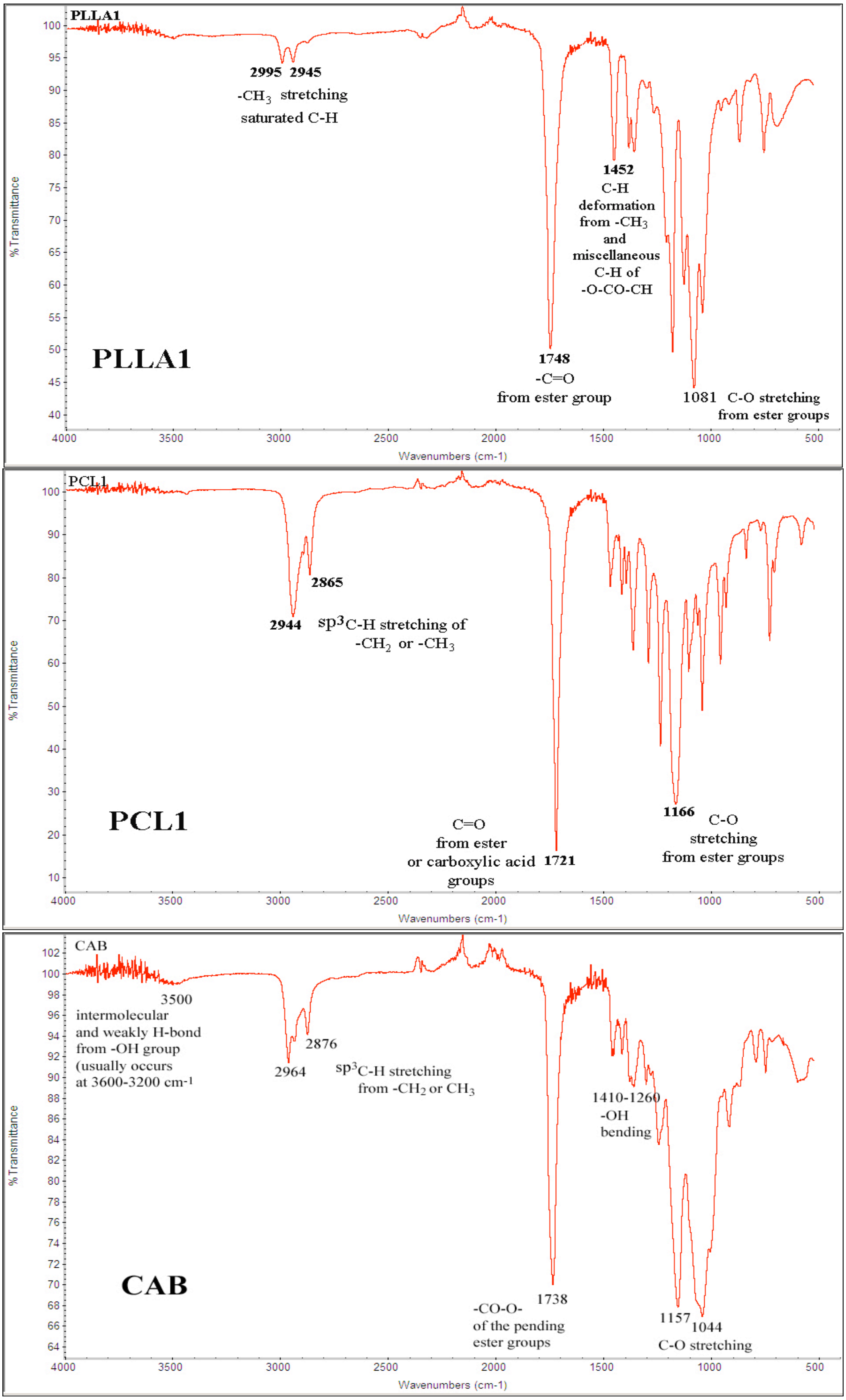

Figure 8.7 FT-IR spectra of unblended PLLA1, PCL1, and CAB.

Two different compositions of melted PLLA/PCL1/CAB blends: MB1 (40/10/50) and MB3 (40/45/15) were analysed, and their FT-IR spectra are shown in Figure 8.8.

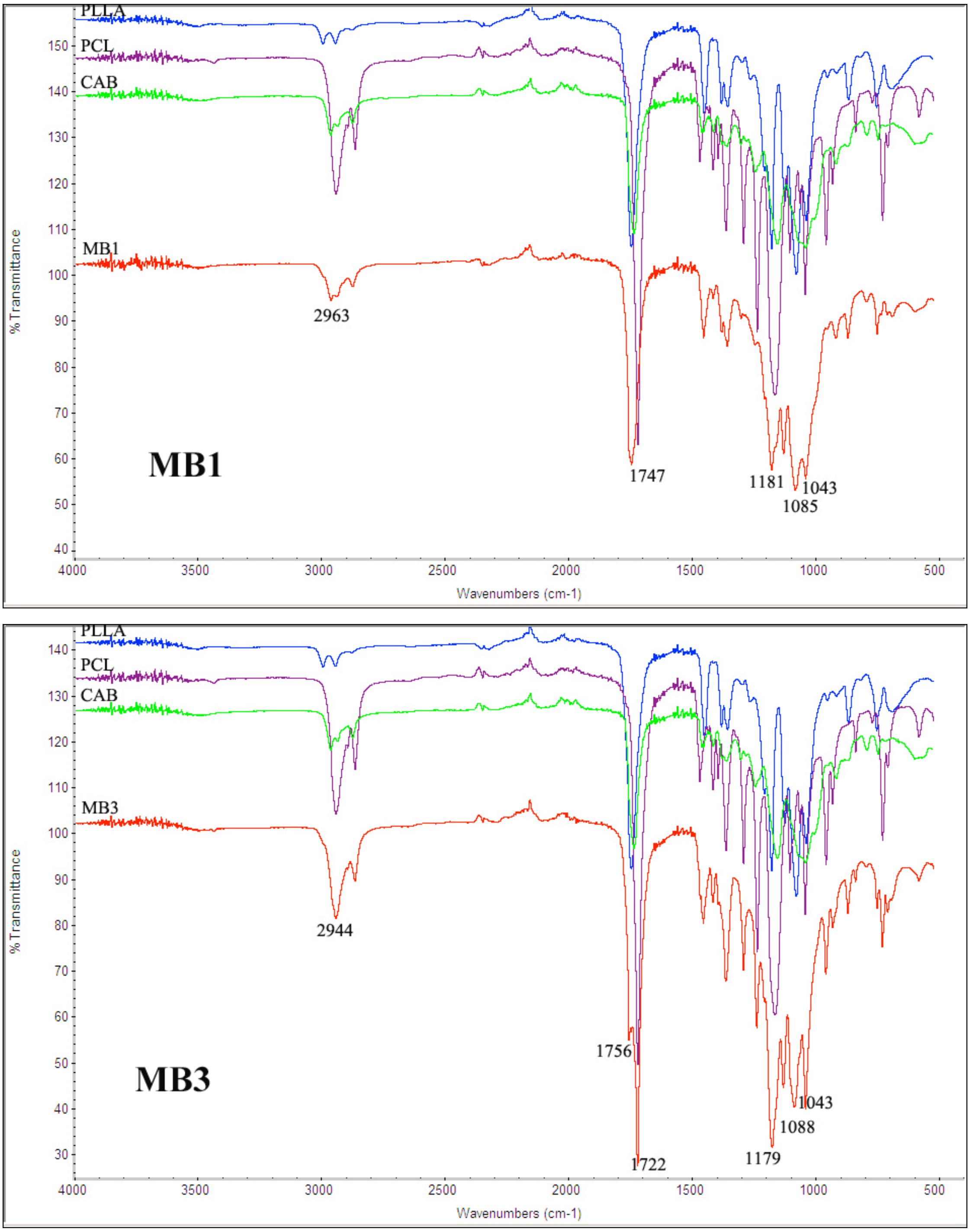

Figure 8.8 FT-IR spectra of melted PLLA1/PCL1/CAB blends of different compositions: MB1 (40/10/50) and MB3 (40/50/10), together with FT-IR spectra of unblended PLLA1, PCL1, and CAB

From the FT-IR spectra in Figure 8.8, an interaction spectrum with frequency shifts and intensity modifications, comparing with the FT-IR spectrum of unblended PLLA1, PCL1, and CAB, is observed in MB1, but not in MB3. For MB3, the frequency bands and its split at 1756 and 1722 cm^{-1} are possible to be the vibration modes of the –C=O groups from amorphous structure of materials and the –C=O groups from the crystallisation process at high temperature of PLLA [111]. This means that less interaction between PLLA1 chains with PCL1 or CAB chains may occur. In addition, the spectrum of MB3 is simply the spectral sum of PLLA1, CAB, and more especially PCL1. Therefore, it can be said that MB3 is most likely to be an immiscible blend, while MB1 is potentially a miscible blend.

Melted- and solvated-blends of PLLA1/PCL1/CAB of three different compositions: 40/10/50 (MB1, SB1), 40/25/35 (MB2, SB2) and 40/50/10 (MB3, SB3), were studied and their FT-IR spectra are shown in Figure 8.9. All melt and solvent blending compositions show similar positions of the peak frequency but different intensities (except SB3 and MB3). Both SB1 and SB2 show higher peak intensities (higher percent transmittances) than MB1 and MB2, respectively. This indicates that SB1 and SB2 show more miscibility than MB1 and MB2. In addition, the spectrum frequency shift, and the vibration region of the intermolecular and weakly hydrogen bonded –OH at 3520-3530 cm^{-1}, can be observed in MB1 (as discussed earlier), MB2, SB1, and SB2, as compared to the unblended PLLA1, PCL1, and CAB (as shown in Figure 8.7). Therefore, it can be said that these blends are most likely to be miscible.

SB3 and MB3 have a very similar peak frequency, including peak intensities. As discussed earlier, MB3 is most likely to be an immiscible blend because the spectrum of the blend is simply the spectrum of unblended PLLA1, PCL1, CAB (Figure 8.7), therefore, it can be said that SB3 is also an immiscible blend. However, the spectrum of MB3 obviously shows the vibration modes of –C=O groups of the crystallisation process at high temperature of PLLA1 at 1720-1760 cm^{-1}, but does not in SB3. This indicates that PLLA1 shows a higher degree of crystallisation in MB3 than in SB3. This result corresponds to the result from DSC (Figure 8.2), and hot-stage microscopy (Figures 8.5 and 8.6 – at the T_c of PLLA1 (140-150 ^{o}C)).

Therefore, it can be concluded that the miscibility of melted- and solvated-blends of PLLA1/PCL1/CAB can be observed by FT-IR but the difference of the miscibility between these two techniques seems difficult to compare.

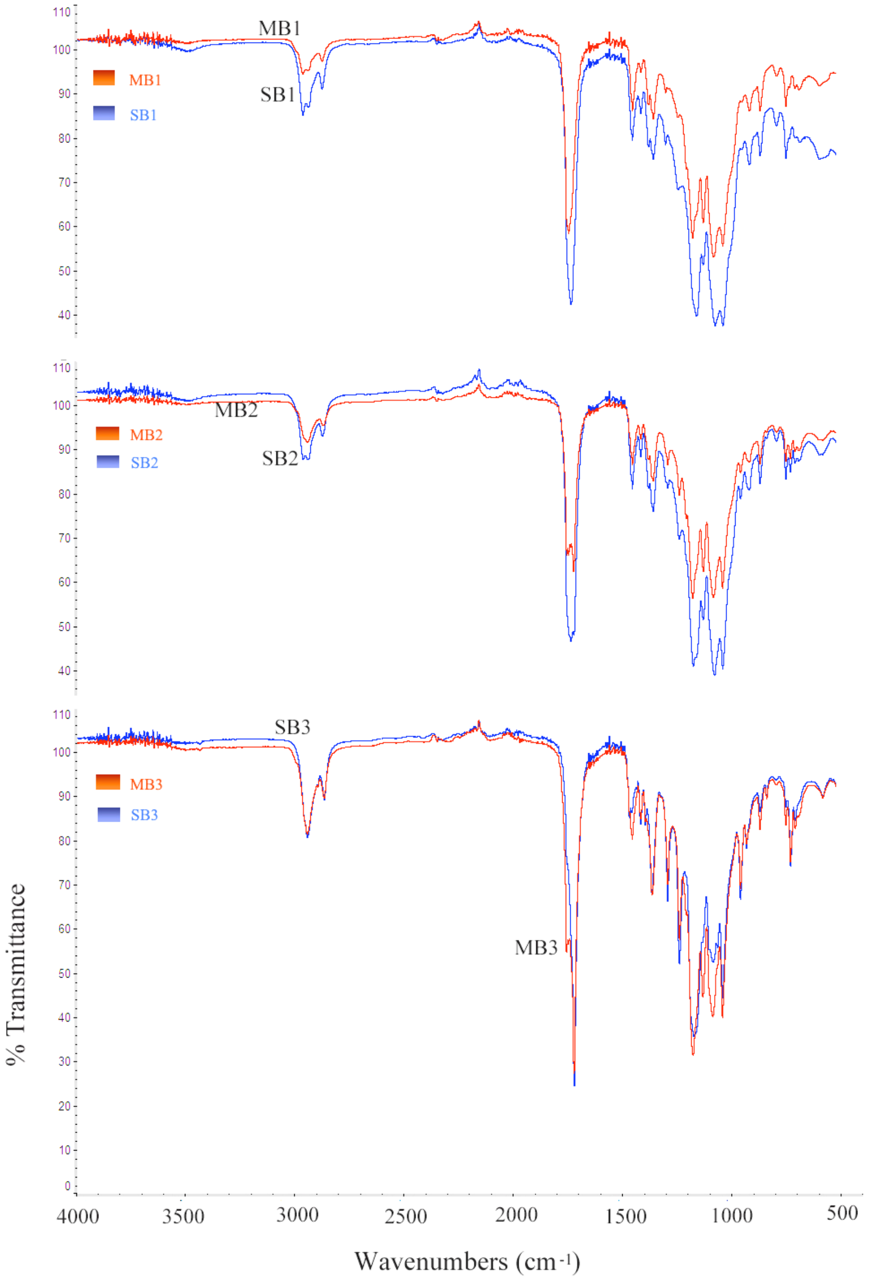

Figure 8.9 FT-IR spectra of the PLLA1/PCL1/CAB blends with melt blending (MB) and solvent blending (SB) technique of different compositions:
MB1 and SB1: 40/10/50
MB2 and SB2: 40/25/35
MB3 and SB3: 40/45/15

8.4 SUMMARY OF THE CHAPTER

Melt blending is a useful technique for preparing a larger quantity of samples. On the other hand, solvent blending is important for experimental observation. The miscibility of PLLA1/PCL1/CAB blended by both techniques were studied and compared using DSC, hot-stage microscopy, and FT-IR, with the following conclusions:

- A single glass transition temperature (T_g) – the observation to indicate the miscibility of polymer blends – could not be observed in either melted- or solvated-PLLA1/PCL1/CAB blends because the T_g of PLLA1 (~50-60 ^oC) overlaps significantly with the melting temperature (T_m) of PCL1 (~55-60 ^oC). The percent crystallinity of PLLA1 in both melted- and solvated-blends is not extensively different. The percent crystallinity of PCL1 could not be observed (because of the overlap of T_g (PLLA1) and T_m (PCL1)). Therefore, it is difficult to compare the miscibility of the blends using melt and solvent blending techniques.

- The crystallinity observed by hot-stage microscopy illustrates that the melted- and solvated-blends show different amounts of crystalline spherulites of PLLA1 and PCL1, depending on blend composition. The light intensity changes dramatically when PCL1 cystallises. For example, in the blend at 40/45/15 PLLA1/PCL1/CAB, the crystallinity growth rate of PCL1 in solvent blending seems to be faster than melt blending, and shows more crystallinity. This is possibly because PCL1 chains can more easily align themselves in the solution, and then crystallise from the solution, which cause the blend to be less miscible.

- The miscibility of melted- and solvated-PLLA1/PCL1/CAB can be observed by FT-IR analysis. The sample compositions, 40/10/50 and 40/25/35, of both blending techniques are miscible because the spectral frequency of the blends shifts from that of unblended PLLA1, PCL1, and CAB. The 40/45/15 compositions of both blending samples are immiscible because the spectra of the blends are simply the spectrum of the homopolymers (PLLA1, PCL1, and CAB). However, it seems difficult to compare and distinguish the miscibility between melt and solvent blending.

CHAPTER 9

CONCLUSIONS
AND
FUTURE WORK

Chapter 9

Conclusions and Future Work

9.1 Conclusions

This thesis is concerned with the exploration of multi-component blends of poly(lactic acid) (PLA) to determine ways of preparing a wider range of blends in order to make this valuable material more versatile. The summary and conclusions will address the following: the reason for using PLA and the blending technique; the structural aspects of other biodegradable polymers for blending with PLA; the exploration of the technique used for solvent blending; and then the miscibility study of two- and three-component blends including the use of the Coleman and Painter approach. This approach enables a quantitative interpretation of miscibility phenomena to be examined.

- **Why PLA and blends?**

Poly(lactic acid) (PLA) is synthesised by ring-opening polymerisation and its key property is that it is a hydrolytically biodegradable polymer, which makes PLA suitable for both biomedical and environmental applications. Unfortunately, PLA does not have all the properties (mechanical, surface, and transportation) required for a wide range of applications. Therefore, blending was chosen as a convenient way to change the properties of PLA while maintaining its degradable property. Blending is well-known to produce intermediate properties between the components of the blend, provided the blend can be made in a miscible and compatible way, avoiding phase separation.

- **Why three- (not two-) component blends?**

Two-component and three-component blends based on PLA were prepared and their miscibilities were studied. Although three components are more difficult to convert to miscible blends, the presence of the third component can potentially greatly enhance the blend properties. Therefore, in this work, the objective in the three-component blend work was not simply to find three components, which were completely miscible with each other, but rather to explore structural effects on complete and partial miscibility, particularly the area of miscibility. The miscibility boundary from the ternary phase diagrams can move from translucent to clear or from translucent to opaque. Sometimes with a small change in composition, the polymer blends can have the same clarity but different morphology. This does not occur within a simple two-component blend.

- **Why choose particular polymers?**

An important question to be addressed initially was the selection of polymers for study in this project. To study every biodegradable polymer in blend with other biodegradable polymers is not feasible. A more potentially useful approach is to look at the polarity of polymers, and then use the Coleman and Painter approach as a guideline to find polymers for blending. A useful illustration is poly(glycolic acid) (PGA), the first in the poly(α-ester) series, which has a chemical structure similar to PLA. This has been studied in blends with PLA and results showed that the blend is immiscible [112, 113]. This is largely because of the difference in polarity balance between PGA (δ = 15.1 $(\text{cal.cm}^{-3})^{1/2}$) and PLA ($\delta$ = 12.1 $(\text{cal.cm}^{-3})^{1/2}$). To diminish polarity, polymers with extra methylene groups in the repeat unit were used to blend with PLA. There were two approaches – lengthening the backbone by insertion of methylene groups between the ester groups in the repeat unit, or introduction of substituents on the α-carbon atom of the repeat unit. The first approach is illustrated using poly(ε-caprolactone) (PCL) which contains five methylene groups in the backbone repeat unit. Pre-synthesised poly(α-ester) homologues of PLA (as shown in Table 2.1) are a group of polymers that illustrate the second approach.

These poly(α-ester) homologues of PLA represent an important field of study but they are not commercially available and do not appear in the field of commercial blends for current practical applications. In addition to these α-substituted polyesters, other polymers used were: aliphatic β-substituent polyesters such as; poly(hydroxybutyrate-hydroxyvalerate) (P(HB-HV)), strong hydrogen bonding polymers that contain ester substituents such as cellulose acetate butyrate (CAB), and thermoplastic polyurethanes (TPU) containing -NH groups. These polymers, which combine polarity and biodegradability (to different extents), were chosen as the basis for blending studies with PLA.

- **Advantages of solvent blending studies**

Solvent blending was chosen as the main engine of the experimental work. One important reason to use this technique is because of the limitation of polymer available (in mg-range) for the important poly(α-ester) homologues. Additionally, solvent blending involving a small volume of solvent necessitated the development of a rapid-screening method, which was an advantageous way of examining a wide range of combinations.

The miscibility of polymer blends was initially monitored by observing percent transmittance (%T) and subsequently by glass transition temperature (T_g). The miscible blend was defined as %T more than 75% (clear) with a single T_g as methods of detection of miscibility under the conditions of the experiment. This is because the definition of the word “miscible” defined by International Union of Pure and Applied Chemistry (IUPAC) is based on thermodynamic theory, which is not a simple property to detect. Therefore, the optical clarity and a single T_g can be a useful guide to predict the miscibility but this is not to assume that the thermodynamic conditions for miscibility have been precisely met.

The partially miscible blend was defined as %T between 30-75% (translucent). The immiscible blend was defined as %T less than 30% (opaque) showing separate T_gs for each of the component polymers. In addition, the miscibility guide by Coleman and Painter [1] was used to interpret the miscibility behaviour of polymer blends. Optical clarity (%T), T_g, and the Coleman and Painter criteria taken together were used as a preliminarily guide to detect apparent (or temporary) miscibility of the blends, whereas they do not predict that the system obeys the criteria for thermodynamic miscibility.

- **Exploration of the rapid-screening method**

The rapid screening method is a useful method for studying the miscibility of polymer blends because; (i) it is a quick test and (ii) it uses very small amounts (mg-range) of sample. This makes the rapid screening method very suitable for these experimental observations.

A combinatorial approach using 96-well plates and ultraviolet/visible (UV) multi-wavelength plate reader was therefore explored as a rapid screening procedure enabling the percent transmittance (%T) of polymer combinations to be rapidly observed. The type of well-plate, solvent, polymer concentration, and wavelength of light were studied and optimised for this novel technique. It was observed that the polypropylene well-plates were suitable for %T study because the plates were not attacked by the solvents used and showed 100 %T. A polymer solution concentration of 7 wt% was chosen based on a review of literature studies. A wavelength of 450 nm was found to be suitable because the solvents used in this work did not absorb light at that wavelength. Finally, 7 % (w/v) polymer solutions were prepared and then pipetted into the polypropylene well-plates. The total volume of this polymer solution used for blending was 100 μL and a further 100 μL solvent was then added. Samples were then left to evaporate slowly at room temperature to allow adequate time for chains intermixing of the systems studied.

- **Physical properties of pre-synthesised α-ester homologues of PLA**

Pre-synthesised α-ester homologues of PLA (aliphatic and aromatic α-ester series) were characterised and their chemical structures determined by ^{1}H NMR and ^{13}C NMR techniques. Their results (in Section 3.1) confirmed the chemical structures of each α-ester, allowing them to be studied for miscibility. The differential scanning calorimetry (DSC) results showed that the T_g of the aliphatic α series could not be observed, while that of aromatic α-ester series showed very broad peaks at 72-80 °C. This is because the aromatic α-ester series shows more amorphous structures than the aliphatic α-ester series which all show low levels of crystallinity in X-ray studies carried out at the time of synthesis. In addition, molecular weights and the molecular weight dispersity (M_w/M_n) of the polymer were observed.

Poly(L-lactic acid) (PLLA): PLLA1 (M_n = 18,700), PLLA2 (M_n = 63,500), α1(dimethyl), and α2(diethyl) showed melting temperatures (T_m) at 162, 175, and 185 ^oC, respectively, appreciably higher than the T_m of α4(cyclohexyl) (82 ^oC), α5(cycloheptyl) (148 ^oC) and α6(chloro-methyl-methyl) (134 ^oC). It can be seen that two different pendent groups of polymer structures; (i) small alkyl symmetrical molecular structure (in PLLA, α1(dimethyl), and α2(diethyl)), and (ii) cyclic hydrocarbon pendent molecular structure (in α4(cyclohexyl), and α5(cycloheptyl)), markedly influence T_m. The greater the symmetry in the polymer molecules the more crystalline chain packing can occur which leads to polymers showing higher T_m. The bulky pendant groups affect chain packing and interfere with the degree of crystallinity of the polymer, and leads to polymers showing lower T_m.

- **Conformational structure and crystallinity of pre-synthesised α- ester homologues of PLA**

Considering the conformational structures, α2(diethyl) and PLLA chains adopt a helical conformation structure, where the methyl group of PLLA and ethyl groups of α2(diethyl) are accommodated on the outside of the helix by regular twisting of the whole chain. Because α1(dimethyl) is a symmetrical polyester containing two methyl groups at the α-carbon in the repeat unit, this enables formation of a planar zig-zag structure. The combination of steric and polar effects in the helical conformation structure of α2(diethyl) seems to be more able to affect T_m than the corresponding interactions occurring in the zig-zag structure of α1(dimethyl). This causes α2(diethyl) to show a higher T_m than α1(dimethyl). However, α1(dimethyl) structure shows a higher T_m than PLLA1 indicating the importance of the steric effect of the two-methyl substituents. α6(chloromethyl-methyl) is the only one of those polymers that has polarity in its side-chain ($-CH_2Cl$, a dipolar interaction group which can bind with itself). This polarity increases the ability of α6(chloromethyl-methyl) to interact with itself and to disrupt the polarity and the structure of other poly(α-esters). Because of the larger size of $–CH_2Cl$

relative to CH_3 and the difficulty to organise itself in space in a crystal of substituents, this leads α6(chloromethyl-methyl) chains to coil to form a polymer chain with helical segment.

The percentage crystallinity of PLLA1 and PLLA2 is approximately 38% and 31%, respectively. It can be seen that PLLA2 shows higher T_m than PLLA1 but lower crystallinity – although an increase in molecular weight influences the melting point advantageously, it is easier for shorter chains to pack more completely into crystalline regions. The understanding of crystallinity in this system was found to be critical to the understanding of blend behaviour.

- **Binary blends: The miscibility of pre-synthesised α- ester homologues of PLA**

The clarity and miscibility observed from transmittance studies of polymer solution blends was found to depend on the balance of crystallinity and amorphous regions in the polymer structure. The higher the percent crystallinity, the more difficult it became to produce miscibility with other polymers.

The amorphous poly(α-esters): α3(cyclopentyl), α4(cyclohexyl), and α5(cyloheptyl) having the bulky groups in their backbones, are mutually miscible but they have a tendency to separate from α6(chloromethyl-methyl) because they cannot easily disrupt the polar interactions between α6(chloromethyl-methyl) itself. Because of the helical structure and the dipolar –CH_2Cl, α6(chloromethyl-methyl) is able to interfere with the crystalline helical structure of α2(diethyl) more than it does in the crystalline planar zig-zag structure of α1(dimethyl). However, PLLA should interact with α6(chloromethyl-methyl) more than α2(diethyl) but it does not. This is because a tight helical structure from asymmetric pendent groups (-H, -CH_3) makes PLLA more difficult to disrupt, or it can be said that the –CH_2Cl does not improve the miscibility in a large composition blend ranges.

The potential interaction of the polymer structure is also limited by the stiffness of the chains and constrained by a short repeating unit. Nylon 6,6, for instance, is a crystalline polymer where inter-chain attraction by hydrogen bonding between the carbonyl oxygens and amide hydrogens is very much favoured to allow the chains to align in an orderly structure. Whereas, PLLA and all aliphatic α-esters have substituent groups on the α-carbon, their chains cannot approach each other to form interactions. The work discovered despite their structural similarity they do not enhance miscibility.

- **Binary blends: The molecular weight and crystallinity effect of PLA**

Different molecular weights and crystallinities of PLA: PLLA1 (M_n = 18,700), PLLA2 (M_n = 63,500) and PDLLA are observed to influence the crystallisation rate, an important factor which is responsible for the miscibility behaviour of PLA blends. The more rapidly crystallising polymers: PLLA1 > PLLA2 > PDLLA lead the blends to be less miscible. This indicates that PLLA1 chains have less time remaining in the blend solution to intermingle and to interact with other polymers, i.e. PCL, CAB, and poly(α-ester) homologues. Whereas, PLLA2 crystallises more slowly, then the balance between mutual entanglement and crystallisation favours entanglement. PDLLA (amorphous polymer) is enabling to show the most mutual intermingling and miscibility.

Not only does the crystallisation rates of PLA in the blends have an important effect on miscibility, but also the presence of: 1. hydrogen bonding polymers, i.e. CAB, TPU, 2. solvent, and 3. other crystallising polymers, i.e. PCL. The effect of molecular conformations: a helical PLLA, a planar zig-zag PCL, amorphous CAB, is also an important factor on entanglement of the polymer chains in blend solutions.

In summary, the studies of the poly(α-ester) homologues of PLA produced valuable information on miscibility requirements for PLLA blends. It also showed that matching the short repeat unit of PLA with potential blend components was not appropriate since steric interference overcomes the advantages of matched repeat unit lengths.

- **Binary blends: Use and limitations of the Coleman and Painter principle**

It is useful to introduce this discussion by summarising some of the miscibility observations – particularly the effects of crystallinity. The different structures of poly(L-lactic acid) (PLLA) and poly (D,L-lactic acid) (PDLLA), which are semi-crystalline and an amorphous, respectively, were observed to affect the miscibility of polymer blends.

PLLA and PDLLA were blended with three different polymer pairs, α4(cyclohexyl), PCL, and CAB. The miscibility of PLLA/α4(cyclohexyl) blends is similar to that of PDLLA/α4(cyclohexyl) blends, while the miscibility of the PLLA/PCL and PDLLA/PCL blends are dissimilar in that the PDLLA/PCL blends show more miscibility than PLLA/PCL blends. In contrast, blending PDLLA and PLLA with CAB produces different results from blending with α4(cyclohexyl) and PCL. It can be observed that the blend miscibility is very similar, at CAB contents above 30 % (w/v).

These results can be described using Coleman and Painter miscibility guidelines, which have three terms influencing the free energy of mixing; free volume of polymer, interaction parameter and specific interaction. The free volume term for all PLLA, PDLLA, α4(cyclohexyl), PCL and CAB can be neglected in polymer solution blends. Similarly, the interaction parameter term, which depends on solubility parameter values, is apparently not exerting a different influence on the free energy of mixing of these blends. The specific interaction term (ΔG_H), which is dominated by dipolar interactions, especially hydrogen bonding, seems to be different in these blends. It does not influence the free energy of mixing of the PLLA/α4 (cyclohexyl) and PDLLA/α4(cyclohexyl) blends. In the case of PLLA/PCL and PDLLA/PCL blends, PCL chains can penetrate more into the PDLLA phase than into PLLA phase producing more miscibility in the PDLLA/PCL blends. This suggests the specific interaction by polar ester groups in the PDLLA/PCL blends is more effective than in that of the PLLA/PCL blends. For the PLLA/CAB and PDLLA/CAB blends, the free energy of mixing is noticeably affected by the specific interaction between the polymers. This is primarily because of the ability of CAB to form hydrogen bonds with both PDLLA and PLLA.

The factor summarised in the Coleman and Painter approach drives the miscibility of amorphous polymers. An effect associated with crystallisation that reduces the tendency for polymers to form miscible blends was observed in the binary blends. If the crystallisation is more rapid – the tendency for the polymers to exclude a second or third component is enhanced. Therefore, PLLA1 > PLLA2 > PDLLA shows that the underlying miscibility is shown by the behaviour of PDLLA- the tendency to crystallise is a tendency for self-interaction. Similarly, some structural features cannot be summarised by Coleman and Painter's weak, moderate, and strong polar interactions. These are cases where the polar interaction is more specific, such as the $-CH_2Cl$ group in a poly(α-ester) side chain. This interacts preferentially with itself. Also the more polar PLLA is driven to a tight helix with little steric hindrence and high polar interactions. On the other hand, α2(diethyl) forces a helix but 2 x C_2H_5 groups reduce the polar interaction of the backbone compared to 1 x H and 1 x CH_3 (in PLA).

In summary, studies of binary blends provided a useful indication of the potentially interesting ternary blends based on PLLA and revealed the importance of crystallinity in polymers with the same repeat unit, together with the marked influence and advantage of hydrogen bonding interactions.

- **Novel PLLA/PCL/CAB blends**

PLLA blended with PCL and CAB was observed to be miscible in a wide composition range for the first time in this study; thus, it can be called as “Novel Ternary Blend”. The observed miscibility of PLLA/PCL/CAB blends shows that the crystallisation rate of the components is an important factor in causing the blends to be more or less miscible. The crystallisation rate is ralated to the molecular weights of PLLA and PCL, the crystallinity of PLLA and PDLLA, the presence of solvents, and the presence of the third components (i.e cellulose polymers: CAB, CAP, CP). A valuable method to measure the crystallinity of the blends is wide-angle X-ray scattering (WAXS), which was used to investigate which polymers were crystalline. The indication of miscibility from a single T_g cannot be used to predict the miscibility of PLLA/PCL/CAB blends because the T_g of PLLA is very close to the T_m of PCL.

The effect of molecular weight on crystallinity infers an effect of molecular weight on blend miscibility. PLLA1 (M_{wn}= 18,700), PLLA2 (M_n = 63,500), PCL1 (M_n = 7,500), and PCL2 (M_n = 57,800) were used in four different blend types; PLLA1/PCL1/CAB, PLLA1/PCL2/CAB, PLLA2/PCL1/CAB, and PLLA2/PCL2/CAB. The results show that the PLLA2/PCL2/CAB blend produces a much higher degree of miscibility (Figure 5.8) and the degree of miscibility “series” can be shown as;

PLLA2/PCL2/CAB >> PLLA2/PCL1/CAB > PLLA1/PCL1/CAB > PLLA1/PCL2/CAB

More crystalline forms of polymers (PLLA1 > PLLA2 and PCL1 > PCL2) cause the blend to be less miscible. This is confirmed by the appropriate WAXS traces (as discussed in Section 6.2), which show the stronger crystalline peaks of PCL1 (in the PLLA2/PCL1/CAB and PLLA1/PCL1/CAB blends) and PLLA1 (in the PLLA1/PCL2/CAB blend). The crystalline peaks of both PLLA and PCL can be observed in a clear blend film, therefore, the miscibility is just optical clarity and is related to size of crystalline domains and the wavelength of light (ca 500 nm.). Moreover, PLLA shows more ability to be miscible with CAB, than PCL does (PLLA/PCL blend is immiscible). This result is similar to what is predicted from the Coleman-Painter miscibility guide. Similarly, it is clear that in three component blends all three components do not have to be miscible with each other to improve the properties of the blend, if only two components are miscible this still can be beneficial.

The most logical explanation of the molecular weight effect is that higher molecular weight, and consequently higher viscosity, reduces molecular mobility and therefore reduces incorporation into the crystalline regions formed during solvent evaporation. Thus, higher molecular weight polymers (PLLA2, PCL2) show lower degrees of crystallinity (slower crystallisation rate) than lower molecular weight polymers (PLLA1, PCL1), which means they produce less extensive crystalline structures, leading the blend films to be less clear.

The miscibility of PLA/PCL/CAB was found to be affected by the different stereo structures of PLA: PLLA and PDLLA. PDLLA/PCL/CAB blends are almost completely miscible in a wide range of compositions (Figure 5.6) and show more miscible regions than PLLA1/PCL1/CAB and PLLA2/PCL1/CAB blends (Figure 5.7), respectively. It can be concluded that PDLLA forms more miscible blends than does PLLA. This appears to be because PDLLA is not driven to form crystalline regions and that the formation of crystalline regions by definition excludes other polymer chains.

The PLLA1/PCL1/CAB blends in four different solvents: chloroform ($CHCl_3$), hexafluoroisopropanol (HFIP), mixture of 80/20 $CHCl_3$/HFIP, and tetrahydrofuran (THF), show a difference in miscibility behaviour. $CHCl_3$ is the most suitable solvent in this study, as it produced the greatest amount of miscible regions (Figure 5.9). The different solvents influence the crystallisation rate because they interact differently with the polymer chains and differ in evaporation rates.

Different substituent groups of cellulose polymers: cellulose acetate butyrate (CAB), cellulose acetate propionate (CAP), and cellulose propionate (CP), blended with PLLA and PCL were observed to have different effects on blend miscibility: CAB > CP > CAP (Figure 5.13). This is possibly influenced by the ability to form hydrogen-bonding interactions between their different substituent groups and other components.

- **Novel PLLA/PCL/TPU blends**

Thermoplastic polyurethane (Estane 5706 P from B.F.Godrich Co., Ltd) is another successful polymer used as a third component in the PLLA/PCL blend to produce a miscibile blend. TPU has an interesting chemical structure with hydrogen donor groups (-NH) and also their chains have both flexible and hard segments (Figure 5.16). The miscible and partially miscible blends of PLLA1/PCL1/TPU were observed when using a very small amount of PCL1 (less than 10 % (w/v)) (Figure 5.17). PLLA1 was observed to be miscible with TPU, while PCL1 was observed to be immiscible with TPU.

These results are similar to what is predicted from the Coleman-Painter approach; $\Delta\delta$ $(\text{cal.cm}^{-3})^{0.5}$ of PLLA/TPU = 0.3 (miscible), while that of PCL/TPU = 2.1 (immiscible). However, the miscibility of polymer blends depends on the composition of polymer used in the blends which cannot be predicted from critical solubility parameter ($(\Delta\delta)^{o}_{Crit}$) but from the free energy of mixing. PLLA1 chains might be able to interpenetrate the TPU chains and some H-bonding interactions thus occur between the -C=O group in PLLA and the – N-H group in TPU. The difference in molecular polarity between PCL1 (small polarity from dispersive forces) and TPU (strong polarity from H-bonding) leads PCL/TPU blends to be immiscible, and PCL1 chains prefer to crystallise with each other.

Higher molecular weight PLLA2 and PCL2 (slower crystallisation rates) were observed to improve blend miscibility (Figure 5.20):

PLLA2/PCL2/TPU > PLLA1/PCL2/TPU >>PLLA1/PCL1/TPU

The WAXS traces showed that the crystalline peaks of PCL1 and PCL2 cause the blend to be less miscible. Thus, the miscibility of PLLA/PCL/TPU blends is affected not only by the crystallisation rates of PLLA and PCL but also by the molecular interactions between

PLLA, PCL, and TPU (TPU/PLLA > TPU/PCL > PLLA/PCL), which associated with the structural conformations of PLLA (a helical structure) and PCL (a planar zig-zag structure).

It was observed that PLLA1 behaves differently in PCL2/CAB and in PCL2/TPU blends. The WAXS trace shows strong crystalline peaks of PLLA1 in the PLLA1/PCL2/CAB blend (Figure 6.7), but very small peaks in PLLA1/PCL2/TPU (Figure 6.12 - strong crystalline peaks of PCL2 were observed). Therefore, it can be said that PLLA1 causes the PLLA1/PCL2/CAB blend to be less miscible. On the other hand, PCL2 causes the PLLA1/PCL2/CAB blend to be less miscible. The compositions used to observe the crystallinity by WAXS analysis were 40/45/15 for the PLLA1/PCL2/CAB blend and 20/70/10 for the PLLA1/PCL2/CAB blend. Both films were opaque, however, theirs WAXS traces were noticeably different.

In summary, solvent blending is a good first step to observe the miscibility of polymer blends on a laboratory scale, using small qualities of polymer and solvent. A solvent study helps with the identification of compositional ranges for the subsequent melt blending. The cost would be large if solvent blending were used on an industrial scale and unpleasant for the environment from the evaporation of large quantities of solvent. Equally, melt blending would not enable such an extensive set of miscibility experiment to be carried out. Therefore, since both solvent blending and melt blending have advantages, it is logical to start with solvent and compare certain compositions subsequently with melt blending. Melt blending was therefore used to observe and compare the miscibility of PLLA1/PCL1/CAB blends.

- **Melt blending of PLLA/PCL/CAB**

Three different compositions of PLLA1/PCL1/CAB blends chosen from solvent blending; 40/10/50 (clear), 40/25/35 (translucent), and 40/45/15 (opaque) were melt blended. The results from hot-stage microscope analysis show that the crystallinity growth rate of PCL1 in the solvent blend of 40/45/15 PLLA1/PCL1/CAB was observed to occur faster than in the melt blend and showed a higher degree of crystallinity (Figures 8.5 and 8.6). However, PCL1 was observed to restrict blend miscibility by recrystallisation with itself in both blending techniques.

The FT-IR spectra of 40/10/50 and 40/25/35 PLLA1/PCL1/CAB blends of both solvent and melt blending showed the vibration region of the intermolecular and weakly hydrogen bonded –OH at 3520-3530 cm^{-1} and detectable "interaction" when the spectrum of the blend is compared to the individual spectra of PLLA1, PCL1, and CAB. This suggests that both blends are miscible. However, samples from solvent blending seem to show more miscibility than from melt blending as a higher value of percent transmittance can be observed in solvent blending samples.

The FT-IR spectra of 40/45/15 PLLA1/PCL1/CAB blends of both solvent and melt blending were very similar, as was the percentage transmittance together with the presence of the spectral sum of the three polymers. The vibration modes of the –C=O groups of the crystallisation process of PLLA at 1720-1760 cm^{-1} were observed in the melt blended sample more than in the solvent blended sample. This indicates that 40/45/15 PLLA1/PCL1/CAB blends with both blending technique are immiscible, but the degree crystallisation of PLLA1 in melt blending was more than in solvent blending.

The miscibility of PLLA1/PCL1/CAB blends using solvent and melt blending seems to show similar results in this thesis in terms of miscibility regions. However, melt blending samples might be capable of enhanced compatibility and toughness in the polymer blends produced.

In summary, the work described in this thesis has revealed a great deal about the formulation of miscible poly(lactic acid) or poly(lactide) (PLA) blends with other polymers. As a basis for the design of the novel biodegradable blends based on PLA, factors affecting their miscibility were studied. Two approaches were used to study the miscibility, the approach of Coleman and Painter and an experimental miscibility comparison between solvent blending and melt blending. It can be concluded that there are three novel approaches achieved from this work:

1. A novel solvent blending technique referred to as the rapid screening method.
2. The study of novel pre-synthesised α-ester homologues of PLA and their blends.
3. The investigation and development of novel three component blends, e.g. PLLA/PCL/CAB, PLLA/PCL/TPU.

9.2 Future Work

1. The pre-synthesised α-ester homologues of PLA; α4(cyclohexyl) and α6(chloromethyl-methyl), showed greater miscibility with PLA than any other member of the poly(α-ester) series. Therefore, it is logical to choose these two and undertake the synthesis of a larger quantity of higher molecular weight polymers and study blends more extensively (i.e. three components with PLA and PCL).

2. They are several experiments that will help to support the hypothesis that crystallisation is an important driver of immiscibility: for example, PDLLA should be blended with: pre-synthesised poly(α-ester) homologues, PLLA, TPU. Additionally, PDLLA blends with pre-synthesised poly(α-ester) homologues will be very useful to understand the limits of the Coleman and Painter approach.

3. Novel three-component blends of PLA/PCL/CAB and PLA/PCL/TPU should be used in studies of their mechanical, surface, and transport properties to find the compositions that can be used to improve the applicability of PLA. The fact that different polyurethanes (PU) show different miscibilities suggested that some more optimal PU structures can be found for further examination of three component blends. Therefore, PU miscibility as a function of structure could usefully be studied as a means of producing versatile and useful products.

4. The melt blending samples should be analysed by WAXS analysis to observe blend miscibility and compare their results with the results from solvent blending.

5. Different melt blending techniques, such as internal mixer and extrusion, should be investigated for homogeneous mixing instead of the two-roll mill. This is because the two-roll mill is too limited to produce homogeneous mixing of a wide range of components because of limited temperature control, polymer adhesion to the roll, polymer manipulation in the mixing process, etc.

6. Biodegradation studies involving both strong translucent crystalline material and extensible optically clear materials will be an important research target.

7. Novel PLLA/PCL/CAB and PLLA/PCL/TPU blends are interesting for fabrication of nano- to micron-scale fibres for biomedical use by Electrospinning. The fibres may have potential use in biomedical applications, such as connective tissue ingrowths, blood vessel ingrowths, and tissue engineering scaffolds.

8. The samples of the novel three-component blends based on PLLA, with different clarities of films (clear, translucent, and opaque), are good candidates for food packaging films, although their gas permeability (i.e. oxygen permeability) needs to be analysed.

REFERENCES

1. Coleman, M., Graf, J., and Painter, P., *Specific Interactions and the Miscibility of Polymer Blends*. 1991, Lancaster, Pennsylvania: Technomic Publishing AG.
2. Albertsson, A.-C., ed. *Degradable Aliphatic Polyesters*. Advances in Polymer Science. 2002, Springer-Verlag Berlin heidelberg New York: Berlin. 179.
3. Amass, W., Amass, A., and Tighe, B. J., *A review of biodegradable polymers: Uses, current developments in the synthesis and characterization of biodegradable polyesters, blends of biodegradable polymers and recent advances in biodegradation studies.* Polymer International, 1998. **47**(2): p. 89-144.
4. Fried, J.R., *Polymer Science and Technology*. 1995, New Jersey: Prentice-Hall International, Inc.
5. Blackbourn, G.P., *Some aspects of the synthesis and polymerisation of 1, 3, 2-dioxathiolan-4-one-2-oxides*, in *Chemical Engineering and Science*. 1970, Aston University: Birmingham. p. 150.
6. Crowe, A.J., *Ring opening reactions of some dialkyl substituted 1, 3, 2-dioxathiolan-4-one-2-oxides*, in *Department of Chemistry*. 1975, The University of Aston in Birmingham. p. 257.
7. Lunt, J., *Large-scale production, properties and commercial applications of polylactic acid polymers.* Polymer Degradation and Stability, 1998. **59**: p. 145-152.
8. Blumm, E., and Owen, A. J., *Miscibility, crystallization and melting of poly(3-hydroxybutyrate)/poly(L-lactide) blends.* Polymer, 1995. **36**(21): p. 4077-4081.
9. Moore, G.F., and Saunders, S. M. *Advances in Biodegradable Polymer*. Rapra Review Reports 1997.
10. Work, W.J., Horie, K., Hess, M., and Stepto, R. F. T., *Definitions of terms related to polymer blends, composites, and multiphase polymeric materials. (IUPAC Recommendations 2004). Pure and Applied Chemistry*, 2004. **76**: p. 1985-2007.
11. Paul, D.R., and Bucknall, C. B., *Polymer Blends Volume 1: Formulation*. 2000: John Wiley & Sons, Inc.
12. http://pslc.ws/macrog/blend.htm. 2010, 30th April.
13. Garlotta, D., et al., *Mechanical and thermal properties of starch-filled poly(D,L-lactic acid)/poly(hydroxy ester ether) biodegradable blends.* Journal of Applied Polymer Science, 2003. **88**(7): p. 1775-1786.
14. Gong, Q.X., Wang, L. O., and Tu, K. H., *In situ polymerization of starch with lactic acid in aqueous solution and the microstructure characterization.* Carbohydrate Polymers, 2006. **64**(4): p. 501-509.
15. Ke, T., and Sun, X., *Thermal and mechanical properties of poly(lactic acid) and starch blends with various plasticizers.* Transactions of the Asae, 2001. **44**(4): p. 945-953.
16. Willett, J.L., and Shogren, R. L., *Processing and properties of extruded starch/polymer foams.* Polymer, 2002. **43**(22): p. 5935-5947.
17. http://pslc.ws/mactest/blend.htm. 2010, 30th April.
18. Madhavan Nampoothiri, K., Nair, N.R., and John, R.P, *An overview of the recent developments in polylactide (PLA) research.* Bioresour Technol, 2010. **101**(22): p. 8493-501.
19. Hirao, K., Ohara, H. et al, *Hydrolysis of poly(L-lactic acid) using microwave irradiation.* Polymer Degradation and Stability, 2010. **95**: p. 86-88.
20. Harada, M., et al., *Reactive compatibilization of biodegradable poly(lactic acid)/poly(epsilon-caprolactone) blends with reactive processing agents.* Polymer Engineering and Science, 2008. **48**(7): p. 1359-1368.

21. Todo, M., et al., *Fracture micromechanisms of bioabsorbable PLLA/PCL polymer blends.* Engineering Fracture Mechanics, 2007. **74**(12): p. 1872-1883.
22. Dell'Erba, R., et al., *Immiscible polymer blends of semicrystalline biocompatible components: thermal properties and phase morphology analysis of PLLA/PCL blends.* Polymer, 2001. **42**: p. 7831-7840.
23. Wang, L., et al., *Reactive compatibilization of biodegradable blends of poly(lactic acid) and poly(epsilon-caprolactone).* Polymer Degradation and Stability, 1998. **59**(1-3): p. 161-168.
24. Noda, I., et al, *Polymer alloys of Nodax copolymers and poly(lactic acid).* Macromolecular Bioscience, 2004. **4**: p. 269-275.
25. Domb, A.J., *Degradable polymer blends .1. Screening of miscible polymers.* Journal of Polymer Science Part a-Polymer Chemistry, 1993. **31**(8): p. 1973-1981.
26. Zeng, J.B., et al., *A novel biodegradable multiblock poly(ester urethane) containing poly(L-lactic acid) and poly(butylene succinate) blocks.* Polymer, 2009. **50**: p. 1178-1186.
27. Lee, S., and Lee, J.W., *Characterization and processing of biodegradable polymer blends of poly(lactic acid) with poly(butylene succinate adipate).* Korea-Australia Rheology Journal, 2005. **17**(2): p. 71-77.
28. Chen, H., Pyda, M., and Cebe, P., *Non-isothermal crystallisation of PET/PLA blends.* Thermochimica Acta, 2009. **492**: p. 61-66.
29. Kozlowski, M., et al., *Biodegradable blends of poly(L-lactide) and starch.* Journal of Applied Polymer Science, 2007. **105**(1): p. 269-277.
30. Zhang, J.F., and Sun, X.Z., *Mechanical and thermal properties of poly(lactic acid)/starch blends with dioctyl maleate.* Journal of Applied Polymer Science, 2004. **94**(4): p. 1697-1704.
31. Ke, T.Y., Sun, S. X. Z., and Seib, P., *Blending of poly(lactic acid) and starches containing varying amylose content.* Journal of Applied Polymer Science, 2003. **89**(13): p. 3639-3646.
32. Wang, Y., and Hillmyer, M.A., *Polyethylene-poly(L-lactide) diblock copolymers: Synthesis and compatibilization of poly(L-lactide)/polyethylene blends.* Journal Polymer Science Part A: Polymer Chemistry, 2001. **39**: p. 2755.
33. Li, Y.J., and Shimizu, H., *Toughening of polylactide by melt blending with a biodegradable poly(ether)urethane elastomer.* Macromolecular Bioscience, 2007. **7**(7): p. 921-928.
34. Yuan, Y.M., and Ruckenstein, E., *Polyurethane toughened polylactide.* Polymer Bulletin, 1998. **40**(4-5): p. 485-490.
35. Lemmouchi, Y., Amass, A. J., et al, *Plasticization of poly(lactide) with blends of tributyl citrate and low molecular weight poly(D,L-lactide)-b-poly(ethylene glycol) copolymers.* European Polymer Journal, 2009. **45**: p. 2839-2848.
36. Lai, W.C., and Liau, W.B., *Thermo-oxidative degradation of poly(ethylene glycol)/poly(L-lactic acid) blends.* Polymer, 2003. **44**(26): p. 8103-8109.
37. Martin, O., and Averous, L., *Poly(lactic acid): plasticization and properties of biodegradable multiphase systems.* Polymer, 2001. **42**(14): p. 6209-6219.
38. Bechtold, K., Hillmyer, M. A., and Tolman, W.B., *Perfectly alternating copolymer of lactic acid and ethylene oxide as a plasticizing agent for polylactide.* Macromolecules, 2001. **34**(25): p. 8641-8648.
39. Chen, C.C., et al., *Preparation and characterization of biodegradable PLA polymeric blends.* Biomaterials, 2003. **24**(7): p. 1167-1173.

40. Piorkowska, E., et al., *Plasticization of semicrystalline poly(L-lactide) with poly(propylene glycol).* Polymer, 2006. **47**(20): p. 7178-7188.
41. Labrecque, L.V., et al., *Citrate esters as plasticizers for poly(lactic acid).* Journal of Applied Polymer Science, 1997. **66**(8): p. 1507-1513.
42. Labrecque, L.V., et al., *Citrate esters as biodegradable plasticizers for poly(lactic acid).* Antec 95 - the Plastics Challenger: A Revolution in Education, Conference Proceedings, Vols I-Iii, 1995: p. 1819-1823.
43. Papageorgiou, G.Z., et al, *PLA nanocomposites: Effect of filler type on non-isothermal crystallization.* Thermochimica Acta, 2010. **511**: p. 129-139.
44. Wang, L.S., et al., *Preparation and characterization of biodegradable thermoplastic elastomers (PLCA/PLGA blends).* Journal of Polymer Research, 2010. **17**(1): p. 77-82.
45. Cohn, D., and Salomon, A. H., *Designing biodegradable multiblock PCL/PLA thermoplastic elastomers.* Biomaterials, 2005. **26**: p. 2297-2305.
46. Tanaka, T., et al., *Microfiltration membrane of polymer blend of poly(L-lactic acid) and poly(epsilon-caprolactone).* Desalination, 2006. **193**(1-3): p. 367-374.
47. Bouapao, L., Tsuji, H., et al., *Crystallization, spherulite growth, and structure of blends of crystalline and amorphous poly(lactide)s.* Polymer, 2009. **50**: p. 4007-4017.
48. Mohamed, A.A., Gordon, S.H., et. al, *Thermal characteristics of polylactic acid/wheat gluten blends.* Journal of Food Quality, 2006. **29**: p. 266-281.
49. Ke, T.Y., and Sun, X. Z. S., *Thermal and mechanical properties of poly(lactic acid)/starch/methylenediphenyl diisocyanate blending with triethyl citrate.* Journal of Applied Polymer Science, 2003. **88**(13): p. 2947-2955.
50. Preechawong, D., et al., *Preparation and characterization of starch/poly(L-lactic acid) hybrid foams.* Carbohydrate Polymers, 2005. **59**(3): p. 329-337.
51. Anderson, K.S., Lim, S. H., and Hillmyer, M. A., *Toughening of polylactide by melt blending with linear low-density polyethylene.* Journal of Applied Polymer Science, 2003. **89**(14): p. 3757-3768.
52. Li, Y., and Shimizu, H., *Improvement in toughness of poly(L-lactide) (PLLA) through reactive blending with acrylonitrile–butadiene–styrene copolymer (ABS): Morphology and properties.* European Polymer Journal, 2009. **45**: p. 738-746.
53. Hailin, Z., Xinxing, F. et. al, *Structural characteristics and properties of silk fibroin/poly(lactic acid) blend films.* Jornal of Biomaterials Science, 2009. **20 No. 9**: p. 1259-1274(16).
54. Sebastien, F., et al., *Novel biodegradable films made from chitosan and poly(lactic acid) with antifungal properties against mycotoxinogen strains.* Carbohydrate Polymers, 2006. **65**(2): p. 185-193.
55. Peesan, M., Supaphol, P., et. al., *Preparation and characterization of hexanoyl chitosan/polylactide blend films.* Carbohydrate Polymers, 2005. **60**(3): p. 343-350.
56. Peesan, M., Supaphol, P., et. al., *Effect of casting solvent on characteristics of hexanoyl chitosan/polylactide blend films.* Journal of Applied Polymer Science, 2007. **105**(4): p. 1844-1852.
57. Feng, K., Sun, H. et al, *Novel antibacterial nanofibrous PLLA scaffolds.* Journal of Controlled Release, 2010. **146**: p. 363-369.

58. Kuo, Y.-C., Yeh, C-F, *Effect of surface-modified collagen on the adhesion, biocompatibility and differentiation of bone marrow stromal cells in poly(lactide-co-glycolide)/chitosan scaffolds.* Colloids and Surfaces B: Biointerfaces, 2011. **82**: p. 624-631.
59. Cui, W., et al., *Evaluation of electrospun fibrous scaffolds of poly(DL-lactide) and poly(ethylene glycol) for skin tissue engineering.* Materials Science and Engineering C, 2009. **29**: p. 1869-1876.
60. Gu, S.-Y., Wang, Z-M., Ren, J., and Zhang, C-Y, *Electrospinning of gelatin and gelatin/poly(L-lactide) blend and its characteristics for wound dressing.* Materials Science and Engineering C, 2009. **29**: p. 1822-1828.
61. Tanoue, S., et al., *Preparation of poly(lactic acid)/poly(ethylene glycol)/organoclay nanocomposites by melt compounding.* Polymer Composites, 2006. **27**(3): p. 256-263.
62. Fukushima, K., et al., *Biodegradation of poly(lactic acid) and its nanocomposites.* Polymer Degradation and Stability, 2009. **94**: p. 1646-1655.
63. Bordes, P., Pollet, E., and Averous, L., *Nano-biocomposites: Biodegradable polyester/nanoclay systems.* Progress in Polymer Science, 2009. **34**: p. 125-155.
64. Oyama, H.T., *Super-tough poly(lactic acid) materials: Reactive blending with ethylene copolymer.* Polymer, 2009. **50**: p. 747-751.
65. Bledzki, A.K., and Jaszkiewicz, A., *Mechanical performance of biocomposites based on PLA and PHBV reinforced with natural fibres – A comparative study to PP.* Composite Science and Technology, 2010. **70**: p. 1687-1696.
66. Tsuneizumi, Y., et. al., *Chemical recycling of poly(lactic acid)-based polymer blends using environmentally benign catalysts.* Polymer Degradation and Stability, 2010. **95**: p. 1387-1393.
67. Kosolsumollamas, N., *Synthesis and properties of fluorine-containing poly α-esters*, in *Chemical engineering and science*. 1976, Aston University: Birmingham. p. 211.
68. Http://www.moleculardevices.com. 2009, 20th May.
69. Sanders, E.K.M., and Hunter, B. K., *Modern NMR spectroscopy (a guide for chemists)*, ed. 2nd. 1993, Oxford: Oxford University Press.
70. Homer, J., and Perry, M., *New method for NMR signal enhancement by polarization transfer, and attached nucleus testing.* J. of Chemical Society. Chemical Communication, 1994: p. 373-374.
71. Homer, J., and Perry, M., *Enhancement of the NMR spectra of insensitive nuclei using PENDANT with long coupling constants.* J. of Chemical Society, 1995. **2**: p. 533-536.
72. http://www.thermoscientific.com/ecomm/servlet/home?storeId=11152. 2009, 20th June.
73. Http://las.perkinelmer.com. 2009, 23rd May.
74. Http://www.purdurdue.edu/REMrs/graphics/sem2.gif. 2009, 22nd April.
75. Cowie, J.M.G., and Arrighi, V., *Polymers: Chemistry and Physics of Modern Materials*. third ed. 2007: CRC Press.
76. Miyata, T., and Masuko, T., *Crystallization behavior of poly(L-lactide).* Polymer, 1998. **39**(22): p. 5515-5521.
77. Yasin, M., Amass, A. J., and Tighe, B. J., *Biodegradable polymer blends.* Polymer and Other Advanced Materials, 1995: p. 169-176.

78. Yoon, J.S., Lee, W. S., Kim, K. S., et al., *Effect of poly(ethylene glycol)-block-poly(L-lactide) on the poly[(R)-3-hydroxybutyrate]/poly(L-lactide) blends.* European Polymer Journal, 2000. **36**(2): p. 435-442.
79. Perego, G., Cella, G. D., and Bastioli, C., *Effect of molecular weight and crystallinity on poly(lactic acid) mechanical properties.* Journal of Applied Polymer Science, 1996. **59**(1): p. 37-43.
80. Garlotta, D., *A literature review of poly(lactic acid).* Journal of Polymers and the Environment, 2001. **9**(2): p. 63-84.
81. He, A.H., Han, C. C., and Yang, G. S., *Preparation and characterization of PLLA/P(CL-b-LLA) blends by an in situ ring-opening polymerization.* Polymer, 2004. **45**(24): p. 8231-8237.
82. Furukawa, T., et al., *Comparison of miscibility and structure of poly (3-hydroxybutyrate-co-3-hydroxyhexanoate)/poly(L-lactic acid) blends with those of poly (3-hydroxybutyrate)/poly(L-lactic acid) blends studied by wide angle X-ray diffraction, differential scanning calorimetry, and FTIR microspectroscopy.* Polymer, 2007. **48**(6): p. 1749-1755.
83. Nakafuku, C., and Takehisa, S. Y., *Glass transition and mechanical properties of PLLA and PDLLA-PGA copolymer blends.* Journal of Applied Polymer Science, 2004. **93**(5): p. 2164-2173.
84. Shibata, M., Inoue, Y., and Miyoshi, M., *Mechanical properties, morphology, and crystallization behavior of blends of poly(L-lactide) with poly(butylene succinate-co-L-lactate) and poly(butylene succinate).* Polymer, 2006. **47**(10): p. 3557-3564.
85. Sheth, M., et al., *Biodegradable polymer blends of poly(lactic acid) and poly(ethylene glycol).* Journal of Applied Polymer Science, 1997. **66**(8): p. 1495-1505.
86. Chen, H.L., Li, L. J., and Lin, T. L., *Formation of segregation morphology in crystalline/amorphous polymer blends: Molecular weight effect.* Macromolecules, 1998. **31**(7): p. 2255-2264.
87. Li, J.C., He, Y., and Inoue, Y., *Thermal and mechanical properties of biodegradable blends of poly(L-lactic acid) and lignin.* Polymer International, 2003. **52**(6): p. 949-955.
88. Shibata, M., Teramoto, N., and Inoue, Y., *Mechanical properties, morphologies, and crystallization behavior of plasticized poly(L-lactide)/poly(butylene succinate-co-L-lactate) blends.* Polymer, 2007. **48**(9): p. 2768-2777.
89. Yoon, J.S., Oh, S. H., Kim, M. N., et al., *Thermal and mechanical properties of poly(L-lactic acid)/poly(ethylene-co-vinyl acetate) blends.* Polymer, 1999. **40**(9): p. 2303-2312.
90. Shuai, X., et al., *Miscibility and phase structure of binary blends of poly(L-lactide) and poly(vinyl alcohol).* Journal of Applied Polymer Science, 2001. **81**(3): p. 762-772.
91. Kokturk, G., et al., *Evolution of phase behavior and orientation in uniaxially deformed polylactic acid films.* Polymer Engineering and Science, 2002. **42**(8): p. 1619-1628.
92. Wong, Y.S., Stachurski, Z. H., and Venkatraman, S. S., *Orientation and structure development in poly(lactide) under uniaxial deformation.* Acta Materialia, 2008. **56**(18): p. 5083-5090.
93. Jacobsen, S., and Fritz, H. G., *Plasticizing polylactide - The effect of different plasticizers on the mechanical properties.* Polymer Engineering and Science, 1999. **39**(7): p. 1303-1310.

94. Tighe, B.J., Amass, A. J., and Yasin, M., *Novel biodegradable ester-based polymer blends.* Macromolecular Symposia, 1997. **123**: p. 133-145.
95. www.wag.caltech.edu/msc99/talks/e5/. 2009, 2nd July.
96. Bradsnaw, *Polymeric compositions containing inorganic fillers and use thereof*, in *U.S.Patent*. 1995: U.S.A.
97. Zia, K.M., Barikani, M., et al., *Morphological studies of polyurethane elastomers extended with α, ω alkane diols.* Iranian Polymer Journal, 2008. **17**(1): p. 61-72.
98. Krikorian, V., and Pochan, D. J., *Poly (L-lactic acid)/layered silicate nanocomposite: Fabrication, characterization, and properties.* Chemistry of Materials, 2003. **15**: p. 4317-4324.
99. Komatsuka, T., Kusakabe, A., and Nagai, K., *Characterization and gas transport properties of poly (lactic acid) blend membranes.* Desalination, 2008. **234**: p. 212-220.
100. Mano, J., et al., *Cold crystallization of PLLA studied by simultaneous SAXS and WAXS.* Macromolecular Materials and Engineering, 2004. **289**: p. 910-915.
101. Cabedo, L., et al, *Optimization of biodegradable nanocomposites based on aPLA/PCL blends for food packaging appications.* Macromolecular Symposia, 2006. **233**: p. 191-197.
102. Ajili, S.H., and Ebrahimi, N. G., *Miscibility of TPU(PCL diol)/PCL blend and its effect on PCL crystallinity.* Macromolecular Symposia, 2007. **249-250**: p. 623-627.
103. Tripathy, A.R., MacKnight, W. J., and Kukureka, S. N., *In-situ copolymerization of cyclic poly(butylene terephthalate) oligomers and epsilon-caprolactone.* Macromolecules, 2004. **37**: p. 6793-6800.
104. Espi, E., Fernandezberridi, M. J., and Iruin, J. J., *An extension of the Painter-Coleman miscibility guide to ternary polymer blends.* Polymer Engineering and Science, 1994. **34**(17): p. 1314-1318.
105. Flory, P.J., *Thermodynamics of high polymer solutions.* Journal of Chemical Physics, 1941. **9**: p. 660.
106. Huggins, M.L., *Solutions of long chain compounds.* Journal of Chemical Physics, 1941. **9**: p. 440.
107. Hilderbrand, J.H., and Scott, R. L., *The Solubility of Noneelectrolytes*. Third ed. 1950.
108. Espi, E., Alberdi, M., and Iruin, J.J., *On the application of an association model to blends containing poly(hydroxy ether of bisphenol A).* Macromolecules, 1993. **26**: p. 4586-4590.
109. Koenig, J.L., *Spectroscopy of Polymers*, ed. 2nd. 1999, New York, USA: Elsevier.
110. Kodama, Y., Machado, L.D.B., Giovedi, C., and Nakayama, K., *FTIR investigation of irradiated biodegradable blends*, in *17 Congresso Brasileiro de Engenharia e Ciencia dos Materials*. 2006: Brasil. p. 8212-8220.
111. Zhang, J., Duan, Y., et al., *Crystal modifications and thermal behavior of poly(L-lactic acid) revealed by infrared spectroscopy.* Macromolecules, 2005. **38**: p. 8012-8021.
112. Agrawal, A., et al., *Constrained nonlinear optimization for solubility parameters of poly(lactic acid) and poly(glycolic acid) - validation and comparison.* Polymer, 2004. **45**(25): p. 8603-8612.
113. Tsuji, H., et al., *Polyglycolide as a biodegradable nucleating agent for poly(L-lactide).* Macromolecular Materials and Engineering, 2008. **293**: p. 947-951.